Discovery of circulating DMARD response biomarkers in rheumatoid arthritis

Amanda Jayne Eakin
BSc. (Hons)

Supervisors: Dr David S. Gibson and Professor Anthony J. Bjourson

Northern Ireland Centre for Stratified Medicine

School of Biomedical Sciences

Faculty of Life and Health Sciences

Ulster University

This thesis is presented for the degree of Doctor of Philosophy

January 2018

I confirm the word count of this thesis is less than 100,000 words.

Contents

Acknowledgements

Firstly, I'd like to thank my supervisors for all their help over the last 3 years. David, I can't thank you enough for your guidance and advice throughout. You've taught me that there is no such thing as a bad result and that every mistake is a learning experience! Tony, I am extremely grateful for all the advice in each Friday meeting, and I will always admire your enthusiasm for science!

I'd also like to thank all of the staff at CTRIC for guiding me in some way through the PhD. Particularly Denis, I appreciate the time you have given to advising me and your words of wisdom not only for the science world but for life in general.

My fellow students, what can I say? A huge thank you for all of the memories! From panicking in the office to each other about deadlines and lab disasters, to late afternoon coffee breaks in the tea room. I wouldn't have survived the stressful times without the laughs we have all shared. Thanks guys!

I would like to give a huge thank you to my friends and family for the continued support throughout the years. In particular, my mum and dad. I could never thank you enough for the amazing example you have set for me, the encouragement you have given me, and the never-ending support you have provided. Also, I can't forget my brother and sisters, who probably don't realise it but have each inspired me in their own way. Finally, I would like to thank my fiancé, Paul. I would split this achievement with you if I could because I truly couldn't have done any of it without your constant support. Thanks for everything!

For Katelyn, my inspiration throughout.

Declaration

I hereby declare that with effect from the date on which the thesis is deposited in Ulster University Doctoral College, I permit:

1. The Librarian of the University to allow the thesis to be copied in whole or in part without reference to me on the understanding that such authority applies to the provision of single copies made for study purposes or for inclusion within the stock of another library.

2. The thesis to be made available through the Ulster Institutional Repository and/or EThOS under the terms of the Ulster eTheses Deposit Agreement which I have signed.

Abstract

Current clinical methods for determining disease activity and treatment response in rheumatoid arthritis (RA) are inadequate. The aim of this thesis was to discover accessible circulating biomarkers of disease activity and thus treatment response in RA. This has the potential to aid clinical decision making at an earlier time point and improve long-term patient outcome.

This study has established that the ratio between relative numbers of $CD169^+$ monocytes and $CD43^+$ Tregs, two key cells in inflammation, are positively associated with disease activity in RA patients. Furthermore, RA patients who have not responded to cDMARD treatment exhibited circulating Tregs with a lower activation state compared to those who have responded. Subsequent cell culture experiments used sialic acid (Sia) as a surrogate of CD169, because it binds to CD169 before ligation. Sia was found to suppress Treg activity, reducing intracellular activation markers FoxP3 and NFκB, and secretion of inflammatory cytokines. Thus, changes in levels of circulating $CD169^+$ monocytes may be the cause of defective Treg activity in RA non-responders, potentially via the CD43 Treg cell surface marker.

A range of circulating plasma proteins were identified to be associated with RA disease activity as well as treatment response. With further validation, a biomarker panel of specific plasma proteins could prove to be a reliable method of determining treatment response earlier than currently possible. Such a panel may also improve knowledge of RA pathogenesis.

In summary, this thesis provides compelling evidence of the potential of how treatment response can be determined by analysing key cells and proteins in peripheral blood. It is postulated that with further validation, these markers could enable RA treatment response to be determined earlier than the current timeline of 3-6 months, which would be advantageous to both the clinician and the patient.

Abbreviations

AB serum = Human serum from AB donors

ACPAs = Anti-citrullinated peptide antibodies

ACR = American College of Rheumatology

AGP = Alpha-1 glycoprotein

ANG-1 = Angiopoietin-1

ANOVA = Analysis of variance

APC = Antigen presenting cell

BHSCT = Belfast Health and Social Care Trust

CASP-3 = Caspase-3

CK2 = Casein kinase 2

CD40-L = CD40 ligand

cDMARDs = Conventional disease modifying anti-rheumatic drugs

cDNA = Complementary DNA

COX = Cyclooxygenase

CRP = C-reactive protein

Ct = Cycle threshold

CTLA-4 = Cytotoxic T lymphocyte protein-4

CVD = Cardiovascular disease

CXCL = C-X-C motif chemokine

DCTN1 = Dynactin subunit-1

DECR1 = Mitochondrial 2,4-dienoyl-CoA reductase

DGB = Density gradient buffer

dH2O = Deionized water

Dkk-1 = Dickkopf-related protein 1

DMARDs = Disease modifying anti-rheumatic drugs

DNA = Deoxyribonucleic acid

EDTA = Ethylene diamine tetra acetic acid

ELISA = Enzyme-linked immunosorbent assay

ESR = Erythrocyte sedimentation rate

EULAR = European League against Rheumatism

FABP2 = Intestinal fatty acid binding protein

FBC = Full blood count

FDR = False discovery rate

FLS = Fibroblast-like synoviocyte

FoxP3 = Forkhead box P3

Gal-9 = Galectin-9

GCs = Glucocorticoids

HBEGF = Proheparin-binding EGF-like growth factor

HCQ = Hydroxychloroquine

HLA = Human leukocyte antigen

Hp = Haptoglobin

HRP = Horseradish peroxidase

HSP-27 = Heat shock 27kDa protein

IFN-γ = Interferon gamma

IFN = Interferon

IgG = Immunoglobulin G

IgG0 = Agalactosylated IgG

IKK = IκB kinase

IL = Interleukin

IL-6 = Interleukin-6

IL-6RA = Interleukin-6 receptor subunit alpha

IL17RA = Interleukin-17 receptor A

IO = Ionomycin

IRAK = Interleukin-1 receptor-associated kinase

ITAM = Immunoreceptor tyrosine-based activation motif

ITGB1BP2 = Melusin

ITIM = Immunoreceptor tyrosine-based inhibitory motif

JAM-A = Junctional adhesion molecule-A

JIA = Juvenile idiopathic arthritis

JUN = Transcription factor AP-1

LAG3 = Lymphocyte activation gene 3 protein

LC-MS/MS = Liquid chromatography – Tandem mass spectrometry

LFN = Leflunomide

LFTs = Liver function tests

LPS = Lipopolysaccharide

MACS = Magnetic-activated cell sorting

MAPK = Mitogen-activated protein kinases

MB = Myoglobin

MCP = Monocyte chemotactic protein

MDE = Major depressive episodes

MFI = Median fluorescence intensity

MHC = Major histocompatibility complex

MMPs = Matrix Metalloproteinases

mPER = Mammalian Protein Extraction Reagent

MRP = Myeloid related protein

MS = Multiple sclerosis

MTX = Methotrexate

MYD88 = Myeloid differentiation primary response 88

NBD = NEMO-binding domain peptide

NEMO = NFκB essential modulator

NICE = National institute for health and care excellence

NFAT = Nuclear factor of activated cells

NFκB = Nuclear factor kappa B

NPX = Normalised protein expression

NSAIDS = Non-steroidal anti-inflammatory drugs

NTRK2 = BDNF/NT-3 growth factors receptor

OD = Optical density

PADI4 = Peptidyl arginine deiminase-type 4

PAI/serpine1 = Plasminogen activator/inhibitor-1

PBMC = Peripheral blood mononuclear cell

PBS = Phosphate buffered saline

PD = Periodontitis

PDGF = Platelet derived growth factor

PEA = Proximity extension assay

PI3K/AKT = Phosphoinositide 3-kinase/protein kinase B

PKC = Protein kinase C

PMA = Phorbol 12-myristate 13-acetate

PRSS8 = Prostasin

PTPN22 = Protein tyrosine phosphatase-non-receptor type 22

qPCR = Quantitative polymerase chain reaction

RBC = Red blood cell

rcf= Relative centrifugal force

RCL = Red cell lysis

RF = Rheumatoid factor

RIP1 = Receptor interacting protein 1

RNA = Ribonucleic acid

ROC = Receiver operating characteristic

rpm = Revolutions per minute

RT-PCR = Reverse-transcription polymerase chain reaction

SAA = Serum amyloid A

SD = Standard deviation

SELP = P-selectin

SEM = Standard error of the mean

Sia = Sialic acid

Siglec = Sialic acid-binding immunoglobulin-like lectin

SLE = Systemic lupus erythematosus

SLZ = Sulfasalazine

SNP = Single nucleotide polymorphism

STK4 = Serine/threonine-protein kinase 4

TCR = T cell receptor

TCZ = Tocilizumab

TGF-β = Transforming growth factor - Beta

Th = T helper

TICORA = Tight control of RA

TIR = Toll/interleukin-1 receptor

TLR = Toll-like receptor

TMB = Tetramethylbenzidine

TNF = Tumor necrosis factor

TNFα = Tumor necrosis factor-alpha

TNFRSF14 = Tumor necrosis factor receptor superfamily member 14

TRAF6 = TNF receptor-associated factor 6

TRAIL = TNF-related apoptosis-inducing ligand

TRAM = TRIF-related adaptor molecule

Treg = Regulatory T cells

TRIF = TIR domain-containing adaptor inducing IFN-β

U+E = Urea and electrolytes

WHSCT = Western Health and Social Care Trust

Chapter 1

General Introduction

1.0 Rheumatoid Arthritis

Rheumatoid arthritis (RA) is a chronic, autoimmune condition that involves inflammation of the synovial membrane surrounding joints. Physical symptoms of RA vary depending on disease severity, but typically include swelling, tenderness and pain in affected joints. The joint pain and stiffness experienced during RA is a consequence of the actions of various immune cells within the synovial membrane. These immune cells contribute to cartilage breakdown via secretion of specific proteins and enzymes. As the cartilage surrounds and protects the underlying bone, its destruction causes the bone to become exposed and susceptible to erosion (Miller *et al.* 2009; Jung *et al.* 2014). Therefore, in severe cases patients may develop long term disabilities due to the irreversible damage caused.

As joint damage can rapidly occur in RA, clinicians need to make robust decisions in prescribing an effective treatment regimen in order to dampen disease activity in a timely fashion. Currently however, clinicians are unable to pre-determine treatment efficacy for individual patients, thus it may take an extensive amount of time to reach remission. Additionally, current measures of disease activity are considered to be unreliable (Smolen *et al.* 2010a; Ormseth *et al.* 2015; Jensen Hansen *et al.* 2017). This chapter discusses current clinical measures of disease activity in RA and common treatment strategies. Furthermore, this thesis postulates that the action of key immune cells in RA may be a better representation of disease activity than current measures, and may therefore be more effective in determining treatment response. Sensitive biological markers of disease activity would vastly benefit both the patient and clinician as they could assist in determining treatment response earlier than

currently possible. Therefore, this could prevent long term damage in patients who do not respond to initial treatments, enabling them to move to a more effective treatment at an earlier time point.

1.0.1 Prevalence of Rheumatoid Arthritis

RA affects between 0.5% and 1% of the entire adult population (Gabriel and Michaud 2009), increasing to 6% in people aged above 65 years (Davis and Matteson 2012). Women are approximately 3 times more likely to suffer from RA than men (The Arthritis Foundation 2015), which may be due to a number of factors at play as discussed below. Increased levels of specific female hormones may contribute, however conflicting evidence from previous studies suggest further work needs to be carried out (Pikwer *et al.* 2012; Beydoun *et al.* 2013; Alpizar-Rodriguez *et al.* 2017). Environmental factors may also play a role in RA prevalence, with trends observed across particular geographical populations. For example, lower prevalence is reported in China and Japan, whereas increased prevalence is observed in Pima Indians (Jacobsson *et al.* 1994; Shichikawa *et al.* 1999).

Research to date also suggests diet and infections could play a role (Karlson and Deane 2012). Additionally, the human microbiome has been associated with RA prevalence and pathogenesis. For example, the gut microbiome in RA patients was previously found to contain a different bacterial composition compared to the control group, including a lower percentage of *Bifidobacteria (*Vaahtovuo *et a*l. 2008*)*. This is of importance because bacterial composition in the gut can produce butyric acid, leading to the differentiation of regulatory T cells (Tregs) which play a pivotal role in RA (Furusawa *et al.* 2013). Periodontal disease, caused by the oral bacteria

Porphyromonas gingivalis, has also been associated with RA prevalence where as many as 60% of RA patients exhibit symptoms (Mobini *et al.* 2017).

Overall, the prevalence of RA can be a combination of many factors, not least the influence of predisposing genes. Interestingly, a genetic study of monozygotic twins demonstrates a low concordance rate of approximately 15%, which suggests a number of additional factors impact upon RA risk (Silman *et al.* 1993). However, more recent advances have shown a number of differences in gene expression in disease discordant monozygotic twins, including upregulation of laeverin and osteoclast stimulating factor-1 in RA (Haas *et al.* 2006).

The predisposing genetics of RA has been the focus of many research efforts over the last decade. The human leukocyte antigen (HLA) genes in particular are associated with increased risk of RA (Stastny 1976). Specifically, various risk alleles that share a unique amino acid sequence within HLADRB1 have been associated with RA risk (Gregersen *et al.* 1987). For example, HLADR4 is linked to increased prevalence of the disease (Pratt *et al.* 2009), and has been shown to increase in RA patients compared to healthy controls (Stastny 1978). Further studies have associated the involvement of these 'shared epitope' HLA molecules with the production of autoantibodies such as anti-citrullinated peptide antibodes (ACPAs) (Arend and Firestein 2012; Viatte *et al.* 2013). Interestingly, environmental factors such as smoking have been associated with HLADRB1 as well as autoantibody production, thus indicating RA prevalence may be a combination of genetic and environmental factors (Boechat Nde *et al.* 2012; Fisher *et al.* 2014).

Advances in the ability to detect single nucleotide polymorphisms (SNPs) have greatly accelerated the unearthing of variants associated with RA. For example, polymorphisms of cytotoxic T lymphocyte protein-4 (CTLA-4), an important factor in T cell co-stimulation, have been related to RA risk (de Vries 2011). Further SNPs associated with risk include peptidyl arginine deiminase-type 4 (PADI4) and protein tyrosine phosphatase-non-receptor type 22 (PTPN22), the latter being one of the most strongly RA associated SNPs to date (Suzuki *et al.* 2003; Begovich *et al.* 2004).

Epigenetic studies of RA have also added to the knowledge base of how the disease develops. DNA methylation, which can modulate gene expression, is extremely important due to its downstream impacts on key pathways. For example, global hypomethylation in T cells was previously unveiled in RA patients compared to healthy subjects (Richardson *et al.* 1990), stressing the importance of methylation in autoimmune responses. More recent studies observed methylation differences in RA patients compared to control groups, including within fibroblast-like synoviocytes (FLS) which are key cells involved in disease pathogenesis within the synovial membrane (Nile *et al.* 2008; Nakano *et al.* 2013). This type of analysis may provide more insight into the cellular pathology in RA patients.

1.0.2 Diagnosis of RA

When a patient is referred to a rheumatologist, a series of tests must be carried out before the patient is formally diagnosed. A physical examination of the joints is carried out to detect any swelling or tenderness. Blood tests are also used to check for common biological markers that can indicate whether inflammation is present.

Additionally, radiographic tests may be carried out to assess any damage or inflammation of the joints (NICE 2009).

The American College of Rheumatology (ACR) and the European League Against Rheumatism (EULAR) provide classification criteria guidelines to aid clinical diagnosis of RA. The 2010 ACR/EULAR guidelines describe a scoring system that takes into account the number of swollen and tender joints, the presence of autoantibodies in serum, the duration of symptoms and elevation of acute phase reactants (American College of Rheumatology and European League Against Rheumatism 2010). If a patient has a final score of more than six, they can then be diagnosed with RA (**Figure 1.1**).

JOINT DISTRIBUTION (0-5)	SCORE
1 large joint	0
2-10 large joints	1
1-3 small joints (large joints not counted)	2
4-10 small joints (large joints not counted)	3
>10 joints (at least one small joint)	5
SEROLOGY (0-3)	
Negative RF AND negative ACPA	0
Low positive RF OR low positive ACPA	2
High positive RF OR high positive ACPA	3
SYMPTOM DURATION (0-1)	
<6 weeks	0
≥6 weeks	1
ACUTE PHASE REACTANTS (0-1)	
Normal CRP AND normal ESR	0
Abnormal CRP OR abnormal ESR	1

Figure 1.1: Scoring system detailed in ACR/EULAR 2010 guidelines (American College of Rheumatology and European League Against Rheumatism, 2010)

The guidelines from the National Institute for Health and Care Excellence (NICE), published in 2009, suggest that a patient should be urgently referred for treatment if synovitis persists for 3 months (NICE 2009). In order to confirm diagnosis, NICE also recommends testing levels of autoantibodies in the blood, as well as performing X-Rays for patients with early onset of symptoms.

1.0.2.1 Autoantibodies in RA

Autoantibodies are self-reactive antibodies, produced by plasma B cells in autoimmune conditions. Rheumatoid factor (RF) and anti-citrullinated peptide antibodies (ACPAs) are most commonly tested in RA and are associated with increased disease severity and therefore poorer outcome (Pai *et al.* 1998). ACPAs are more specific to RA than RF with approximately 65% of patients exhibiting high levels in the blood (Charpin *et al.* 2013). Patients who contain high concentrations of RF autoantibodies are diagnosed as sero-positive, however an RA diagnosis can still be made for sero-negative patients. Sero-positive patients can exhibit high concentrations of autoantibodies years before the onset of symptoms, which are associated with a poorer clinical outcome (Nielen *et al.* 2006). Several studies point to the potential role of autoantibodies in the pathogenesis of RA (Bax *et al.* 2014).

1.0.3 Treatment of RA

As there is no cure for RA, the aim of treatment for patients is to reach remission or reduce disease activity in order to prevent permanent damage to joints and keep symptoms under control (Smolen *et al.* 2014b). The treatment pathway of RA patients is case dependent, however the 2009 NICE guidelines outline how to manage symptoms and indicate the most suitable treatments (NICE 2009). The

guidelines for currently available treatments are summarised in the below subsections.

1.0.3.1 Symptom control

Milder treatments are often recommended to control symptoms of RA. Examples include analgesics such as paracetamol and non-steroidal anti-inflammatory drugs (NSAIDS). NSAIDs work by inhibiting cyclooxygenase (COX), an enzyme that leads to prostaglandin production (Vane 1971). The COX enzyme has different isoforms including COX-1 and COX-2. COX-1 has been linked to homeostatic functions (Crofford 2013), whereas COX-2 is involved in inflammation (Crofford *et al.* 2000). COX-2 inhibitors work to prevent this process and are recommended to treat RA symptoms (NICE 2009).

The most common side effect associated with NSAIDs is gastrointestinal problems (Lanas 2009). Additionally, COX inhibitors have been linked to increased cardiac risk (Mukherjee *et al.* 2001). However, side effects of these drugs are less common compared to disease-modifying anti-rheumatic drugs (DMARDs). NICE guidelines suggest DMARD treatment should be considered if the milder treatments are ineffective in controlling symptoms (NICE 2009).

1.0.3.2 Disease-modifying anti-rheumatic drugs (DMARDs)

DMARDs are generally immunosuppressive and anti-inflammatory in nature, however the particular mode of action is drug dependent, as detailed in subsequent paragraphs. In cases where milder treatments are deemed ineffective, DMARDs are recommended as the first-line therapy for newly diagnosed patients. They can be

used as a monotherapy or in combination, depending on each patient's condition. Drug dosage is usually increased gradually, however the guidelines recommend decreasing dosage if a patient is responding well (NICE 2009). Conventional DMARDs (cDMARDs) include drugs such as Methotrexate (MTX), Sulfasalazine (SLZ), Leflunomide (LFN) and Hydroxychloroquine (HCQ).

MTX prevents folic acid metabolism by inhibiting dihydrofolate, which subsequently reduces tetrahydrofolate (White and Goldman 1976; Johnston *et al.* 1995). Previous studies have also shown MTX inhibits purine and pyrimidine metabolism (Eleff *et al.* 1985; Tian and Cronstein 2007), prevents cell proliferation and increases T cell apoptosis (Cronstein 2005; Klak *et al.* 2016). Therefore it is suggested that these mechanisms are responsible for the anti-inflammatory effects of MTX (Klak *et al.* 2016).

SLZ is generally used as a substitute for MTX when clinicians decide MTX is ineffective or intolerable for patients. However, SLZ can also be used in combination with MTX to increase efficacy of treatment (Ogrendik 2013). The mechanism of action of SLZ is not as well known as MTX, however previous studies have shown it inhibits cell growth by autophagy (Guo *et al.* 2011). Additionally it inhibits the expression of tumor necrosis factor-alpha (TNFα), a key pro-inflammatory cytokine involved in RA pathogenesis (Rodenburg *et al.* 2000).

LFN or HCQ can be used to treat RA patients when MTX and SLZ have shown no efficacy. LFN blocks dihydroorotate dehydrogenase, therefore inhibiting pyrimidines (Greene *et al.* 1995). Subsequently the proliferation of T cells and antibody production by B cells is reduced (Klak *et al.* 2016). HCQ has previously been used to

treat malaria (ter Kuile *et al.* 1993), but can also be effective in treating RA (Wiacek *et al.* 2012). The mechanism of HCQ includes inhibition of Toll-like receptor (TLR) signalling and antigen presentation to T cells, which are key steps in the immune response (Ziegler and Unanue 1982; Kyburz *et al.* 2006). It has also been described as an immunomodulatory drug because it inhibits pro-inflammatory cytokines such as interleukin-6 (IL-6) and TNFα (Wozniacka *et al.* 2008).

Unfortunately, cDMARDs are commonly associated with side effects, which can depend on the drug prescribed, dosage, pharmacokinetics and response of the individual patient. Undesirable side effects include toxicity of the lungs and liver (Lee *et al.* 2012; Conway *et al.* 2015), as well as nausea and vomiting (Patil *et al.* 2014). If the side effects are severe, it is classed as an adverse reaction and the drug type is switched. A long-term study found approximately 50% of RA patients on DMARD medication will experience an adverse event or non-response after 2-5 years, depending on drug type (Grove *et al.* 2000). However the number of patients that experience adverse events alone is unclear due to the different time frames between longitudinal studies. For example, MTX was previously found to be less associated with adverse events compared to SLZ, however contraindications are more common with MTX when patients are followed for a longer time (Grove *et al.* 2000). This observation may be due to the drug accumulating over time. Further to the negative impact experienced by patients, adverse events also pose additional cost problems for health care providers due to the need of extra resources in order to accommodate additional monitoring.

Despite the risk of severe side effects, cDMARDs have been shown to improve symptoms in 60-70% of patients, depending on drug type. For example, previous studies have shown on average 67% of patients have clinical improvement when on MTX (Willkens *et al.* 1980; Willkens and Watson 1982; Hoffmeister 1983), approximately 60% have improvement of symptoms on SLZ (McWilliams *et al.* 2013), and 68% of patients were shown to have a reduction of disease activity after 1 year on LFN (Wiacek *et al.* 2012). Although the majority of patients show improvement on cDMARD treatment, 30-40% will not respond therefore clinicians must seek alternative treatment options.

The tight control of RA (TICORA) study assessed whether intensive patient management during cDMARD therapy would improve overall clinical outcome (Grigor *et al.* 2004). The study identified a tightly monitored dosage escalation programme that reduced disease activity and improved remission rates in study patients compared with routine management (Appendix A). In agreement with these findings, a further systematic review identified that 65% of TICORA study patients achieved remission compared to 16% of control patients (Bakker *et al.* 2007). This relatively new concept is promising in guiding clinician's dose escalation decisions and improving clinical efficacy of cDMARDs.

1.0.3.3 Glucocorticoids

Glucocorticoids (GCs) are a type of steroid hormone of which the mechanism is not fully understood. They are considered anti-inflammatory and have been shown to inhibit inflammatory gene expression (Newton 2014). The 2013 EULAR guidelines

recommend GCs for use in the treatment of RA in combination with one or more DMARD (Smolen *et al.* 2014b).

Previous studies have demonstrated the benefits of GCs in combination therapy to treat RA. For example, supplementing with GCs reduces progression of joint damage (Svensson *et al.* 2005). In agreement with this finding, a more recent study demonstrated that use of GCs in combination therapy was more beneficial in reducing joint damage, compared to monotherapy (Goekoop-Ruiterman *et al.* 2008).

However, GCs are also associated with adverse events including cataracts, fractures and weight gain, with the latter being the most common (Curtis *et al.* 2006). GCs are only recommended as a short-term treatment with the aim being rapid reduction of inflammation (Smolen *et al.* 2014b). Long-term treatment may be considered when all other treatment options have been exhausted.

1.0.3.4 Biological DMARDs

Biological DMARDs are designed to inhibit cells and cytokines involved in the immune response, and are therefore anti-inflammatory and immunosuppressive. However, as the name would suggest biologic DMARDS are high purity recombinant proteins such as receptors, antibody fragments and chimeras and are therefore more expensive to produce than cDMARDs. For example, adalimumab costs an estimated £9,295 per patient per year and is one of the top grossing drugs worldwide alongside other biologics including etanercept, rituximab and infliximab (Malottki *et al.* 2011). In order to be eligible to receive biologic DMARD treatment, patients must have failed at least two cDMARDs and have a disease activity score (DAS) of ≥5.1 on two

occasions that are 1 month apart (National rheumatoid arthritis society (NRAS) 2013). The use of DAS will be discussed in more detail in section 1.0.4.

The biologic drugs approved by NICE include tumor necrosis factor (TNF) inhibitors known as anti-TNFs, tocilizumab (TCZ), rituximab and abatacept (NICE 2009). Anti-TNFs are one of the first choice biologics for clinicians as they inhibit TNFα, a key pro-inflammatory cytokine involved in RA pathogenesis (Jin *et al.* 2010). There are many anti-TNF biologics available, each with different physical attributes, including adalimumab, certolizumab, etanercept, infliximab and golimumab. Choice of drug is usually agreed between the patient and rheumatologist, and often is decided based on how the drug is administered and risk of side effects (Smolen *et al.* 2014b). The efficacy of anti-TNFs ranges from approximately 60-70% depending on the type of drug used, and whether or not it is combined with a cDMARD (Hirabara *et al.* 2014; Keystone *et al.* 2014; Takeuchi *et al.* 2014; Smolen *et al.* 2014a). Many studies suggest combination therapy improves clinical outcome compared to anti-TNF monotherapy (Keystone *et al.* 2014; Smolen *et al.* 2014a). However, specific combination treatments display a variety of responses in individual patients.

In recent years, TCZ has been one of the first biologics considered by clinicians to treat RA. The reason is because it targets IL-6, one of the most important pro-inflammatory cytokines present in the joint (Alves *et al.* 2011). Along with TNFα, IL-6 is involved in T helper cell-17 (Th17) differentiation which has been directly associated with RA pathogenesis (Jovanovic *et al.* 1998). Additionally, IL-6 production leads to the secretion of C-reactive protein (CRP) from the liver, which is an inflammatory marker that can be included in the calculation of disease activity in RA

(section 1.0.4). The clinical efficacy of TCZ is slightly higher than other biologics, where approximately 80% of patients display a clinical response, however remission is only achieved in 50-60% of patients after 24 weeks (Ogata *et al.* 2014).

Rituximab is a B cell inhibitor that targets CD20 specifically. This mechanism is important because of the key involvement of B cells in RA pathogenesis (Marston *et al.* 2010). Rituximab has proven to be clinically effective in improving RA symptoms for approximately 70% of RA patients (Edwards *et al.* 2004; Wendler *et al.* 2014). Interestingly some patients may not benefit from rituximab initially, but later show good response with further doses (National rheumatoid arthritis society (NRAS) 2013).

Abatacept inhibits the activation of T cells, thereby inhibiting one of the key cells involved in the immune response (Moreland *et al.* 2002). It has been shown to reduce the progression of RA after one year of treatment (Kremer *et al.* 2005). Additionally, approximately 60% of abatacept treated patients had reduced swollen and tender joints after 1 year of treatment compared to a placebo control group.

Although biologic response differs between drug type, these drugs are generally associated with a response rate of 60-70%, with efficacy considered to be similar across each drug type (Smolen *et al.* 2014a). Although less common than cDMARDs, biological DMARDs are also associated with severe side effects, and therefore symptoms must be carefully monitored. Severe side effects include increased risk of infection (Singh *et al.* 2015; Curtis *et al.* 2015; Yun *et al.* 2015), and therefore increased risk of infectious diseases such as Hepatitis B and tuberculosis (Keane *et al.* 2001; Chen *et al.* 2017).

1.0.4 Monitoring RA

The NICE guidelines state that patients with recent-onset active RA should be subject to a composite scoring system, such as the disease activity score in 28 joints (DAS28) (NICE 2009). The DAS28 is an equation (**Figure 1.2**) that takes into account physical symptoms of the disease, a blood-based marker of inflammation, and the general well-being of the patient. It is used to assess levels of disease activity in a consistent manner and guide clinicians in drug dosage as patients show response or non-response to treatment.

$$DAS28 = 0.56 * \sqrt{(tender28)} + 0.28 * \sqrt{(swollen28)} + 0.70 * \ln(ESR \text{ or } CRP) + 0.014 * GH$$

Figure 1.2: DAS28 equation taking into account swollen and tender joints, a blood based marker of inflammation and the general health of the patient. ESR = erythrocyte sedimentation rate, CRP = C-reactive protein, GH = General health or visual analogue scale (VAS).

Review appointments are recommended to assess disease activity and damage (NICE 2009). The EULAR guidelines recommend frequent monitoring for up to 3 months after commencing treatment (Smolen *et al.* 2014b). Improvement, as measured by a reduction in DAS28, must be achieved within the first 3 months. A reduction in DAS28 score of more than 1.2 is deemed a good response, and a reduction of more than 0.6, but less than 1.2 is considered a moderate response (NICE 2009; Smolen *et al.* 2014b). Furthermore, clinical remission in RA is when a patient achieves a DAS28 score of less than 2.6. If a patient has not reached remission or low disease activity

within the first 6 months of cDMARD treatment, alternative options must be visited, such as the use of biological DMARDs.

The 2010 EULAR guidelines define remission as a DAS28 score of less than 2.6 (Smolen *et al.* 2010b), however the 2013 update also includes the need to account for maximum functional improvement and prevention of further damage (Smolen *et al.* 2009; Aletaha and Smolen 2011; Smolen *et al.* 2014b). The patient perspective can therefore be taken into account during treatment monitoring by use of a visual analogue scale (VAS) and health assessment questionnaire (HAQ). These disease scoring tools focus on pain levels and ability to carry out everyday tasks. For long term remission, the drug dosage should be cautiously lowered with regular monitoring until both the patient and clinician are satisfied that a lower and stable disease activity has been achieved.

As detailed in section 1.0.5, comorbidities must be taken into account during treatment and monitoring of RA. Comorbidities are commonly associated with high disease activity. For example, a recent study found that RA patients with comorbidities such as osteoporosis and depression exhibited a higher DAS score than those without (Garip *et al.* 2016). Additionally, effective treatment may prevent comorbidities from developing (Westlake *et al.* 2010). NICE recommend regular monitoring of inflammatory markers including CRP and erythrocyte sedimentation rate (ESR), which can assist in assessing elevated risk of comorbidities (NICE 2009). If a comorbidity is detected, appropriate referrals must be made within the multidisciplinary team, and the treatment strategy may need to be revised depending on each case.

Other blood tests may be carried out during treatment to detect adverse effects of the medication. For example liver function tests (LFTs) and urea and electrolytes testing (U+E) check for liver and kidney damage. This is particularly important during cDMARD treatment, as some drugs have been linked specifically to organ damage (Dahl *et al.* 1971; Salliot and van der Heijde 2009).

1.0.5 Comorbidities

RA has been associated with a range of comorbidities which may contribute to increased risk of mortality (Wolfe *et al.* 1994; Gabriel and Michaud 2009). A recent study has established that depression is the most common comorbidity associated with RA (Dougados *et al.* 2014), with an average of 15% of RA patients affected, depending on geographical location. A separate study found that as many as 31% of RA patients suffer from major depressive episodes (MDE) (Cabrera-Marroquin *et al.* 2014), and these patients had a poorer outcome compared to non-MDE patients. Similar to RA, depression is now considered an inflammatory condition (Berk *et al.* 2013; Kiecolt-Glaser *et al.* 2015), however it is unclear in many cases whether depression manifests as a consequence of RA.

Cardiovascular disease (CVD) is also strongly associated with RA. For example, a recent study found 6% of RA patients also suffer from ischaemic CVD (Dougados *et al.* 2014). Further studies suggest chronic inflammation such as RA can lead to the development or increased risk of CVD such as myocardial infarction and stroke (Solomon *et al.* 2010), and may subsequently reduce the lifespan of patients (Avina-Zubieta *et al.* 2008). EULAR recommendations suggest clinicians should take a

multidisciplinary approach when treating such patients, for example involving cardiologists when making clinical decisions. (Peters *et al.* 2010).

RA is associated with a high risk of infection (Doran *et al.* 2002), which could be a consequence of immunosuppressive drugs used to reduce symptoms. One example is periodontitis (PD), an inflammatory condition caused by a bacterial infection in the mouth. Many studies have associated RA with an increased prevalence of PD compared to controls (de Pablo *et al.* 2008; Dissick *et al.* 2010; Scher *et al.* 2012). It has also been found that infection in RA may contribute to poorer clinical outcome (Wolfe *et al.* 1994; Bjornadal *et al.* 2002; Perez-Sola *et al.* 2011).

RA patients also have an increased prevalence of other conditions including diabetes. Approximately 12% of patients are more likely to be diabetic if they have RA compared to non-RA controls (Liao *et al.* 2009; Dubreuil *et al.* 2014). Additionally, ophthalmological manifestations such as Sjögren's syndrome have been linked to RA in approximately 25% of patients (Antero *et al.* 2011; Artifoni *et al.* 2014). With all of the evidence presented to date, it seems that in the case of some patients, RA may be part of a multi-morbidity rather than just one condition. However, the pathogenesis behind this phenomenon is unclear, therefore clinicians must carefully consider each condition before beginning a treatment regimen.

1.1 Cellular pathology of RA and loss of tolerance

The physical manifestations of RA are a result of cells involved in the adaptive and innate immune responses, which migrate into the synovial membrane (**Figure 1.3**). This leads to various changes within the joint, one of the earliest being the formation of a thin layer of tissue called pannus. Pannus can be considered an aberrant transformation of the synovial tissue toward a tumour-like, invasive and hyper-proliferative state. Within pannus there is a high density of migrated immune cells including B cells, T cells, macrophages and neutrophils (Wright *et al.* 2014). As described in subsequent sections, these cells are responsible for the production of various cytokines and chemokines, which can lead to the development and activation of osteoclasts. Osteoclasts are responsible for irreversible bone destruction (Jung *et al.* 2014), evident in severe cases of RA.

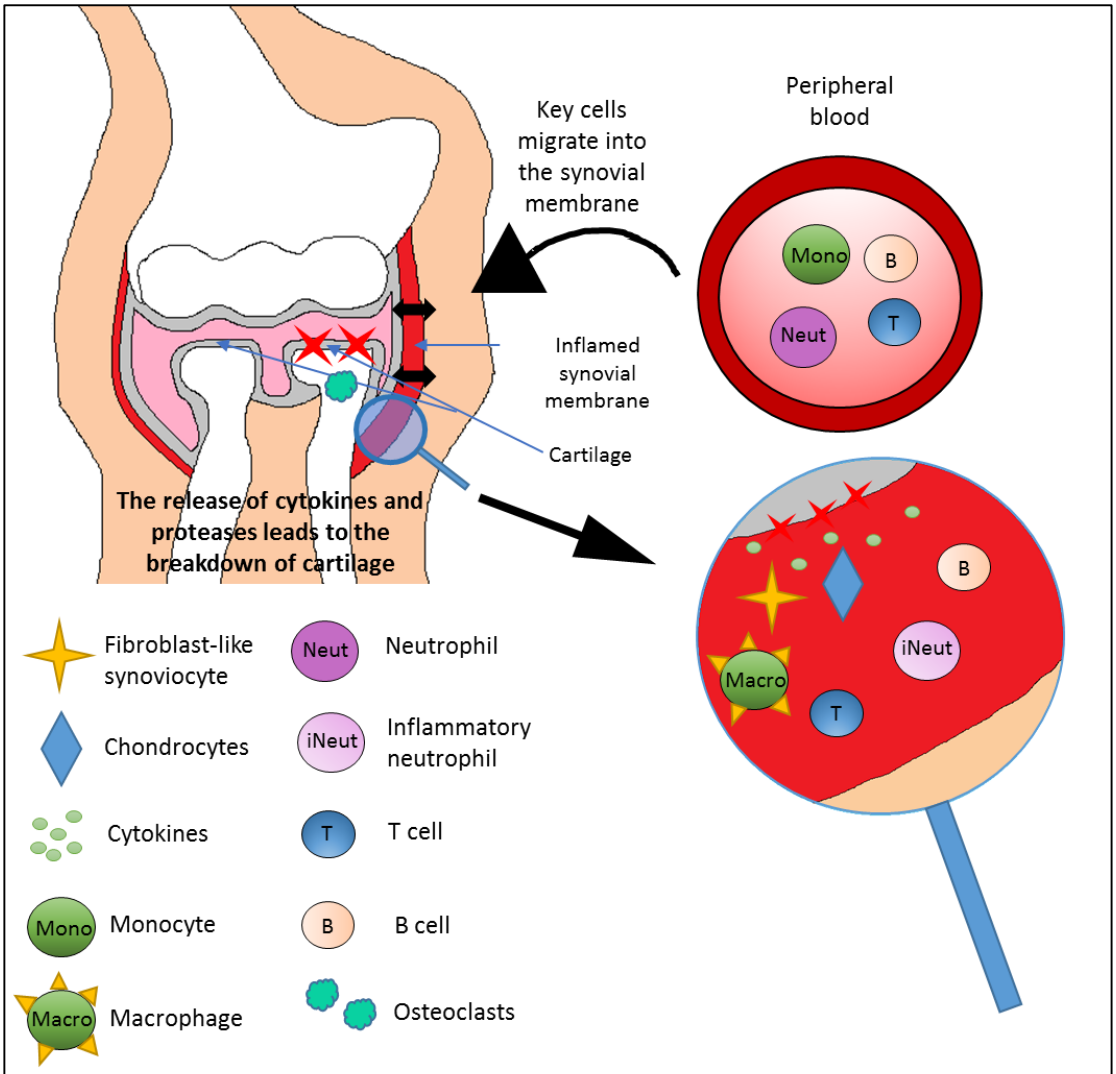

Figure 1.3: The key cells involved in inflammation of the synovial membrane in RA

Fibroblast-like synoviocytes (FLS) are specific cells within the synovium that also play a role in RA pathogenesis. Following activation from specific cytokines including IL-1 and TNFα, FLS and chrondrocytes are responsible for cartilage degradation by mobilisation of matrix metalloproteinase enzymes (MMPs) (Miller *et al.* 2009; Sabeh *et al.* 2010). This increases risk of disability and long term damage in RA as the bone becomes exposed and susceptible to further erosion.

1.1.1 Neutrophils

Neutrophils are the most abundant leukocyte in peripheral blood and are one of the first cells recruited to inflammatory sites, such as the synovium in RA (Wright *et al.* 2014). In RA, they become activated within the joint following interaction with vascular endothelial cells (Yang *et al.* 2005). Activation of these inflammatory neutrophils leads to production of cytokines and chemokines including IL1a, IL1b and IL-8, which subsequently triggers the activation of other inflammatory cells (Beaulieu and McColl 1994; Wright *et al.* 2013). For example, secretion of chemokine IL-8 causes further neutrophils to migrate to the joint and continue the inflammatory process (Fujishima *et al.* 1993). Inflammatory neutrophils within the pannus also contribute to physical joint damage in RA through release of various cartilage-degrading enzymes, including MMP-8 and MMP-9 (Murphy and Nagase 2008).

1.1.2 Monocytes and macrophages

Monocytes are phagocytic cells that circulate in blood. They migrate into tissue in response to ongoing inflammation, before differentiating into mature macrophages. As discussed in further detail in chapter 3, monocytes and macrophages are highly significant in RA pathogenesis. Peripheral monocytes have been shown to be present at higher densities in RA circulating blood (Huang *et al.* 2007; Chara *et al.* 2015). Macrophages are also found in large numbers within the cartilage-pannus junction of RA patients. They display signs of activation such as the expression of the major histocompatibility complex class II (MHC-II), which enables them to function as antigen presenting cells (APCs), leading to T cell activation. Macrophages also produce cytokines, both pro-inflammatory and regulatory (Bresnihan 1999; Kinne *et*

al. 2000). TNFα, IL-6 and IL-1 are examples of pro-inflammatory cytokines produced by macrophages (Kinne *et al.* 2000). They lead to chondrocyte activation, which subsequently results in secretion of cartilage degrading enzymes, including MMPs (Bresnihan 1999).

Macrophage activation correlates with progression of joint destruction, as evidenced by radiological examination (Mulherin *et al.* 1996). Previous studies have shown synovial macrophages can differentiate into distinct subpopulations, which can trigger the activation of T-cells and pro-inflammatory cytokines, leading to more damage and further progression of the disease (Klareskog *et al.* 1982; Miossec and van den Berg 1997).

1.1.3 Lymphocytes

Lymphocytes are important cells in maintaining immune tolerance. They are exposed to two types of tolerance, recessive and dominant. Briefly, recessive or central tolerance involves exposure of self-antigens to early lymphocytes before they further mature. In cases where lymphocytes 'self-react', they can be subject to higher rates of apoptosis (Sakaguchi *et al.* 2008). Dominant or peripheral tolerance is mediated by Tregs following maturation. Tregs, discussed further in section 1.1.3.1 are suppressor cells that ensure over-reactive lymphocytes do not survive in the periphery. In autoimmune disease (AD) such as RA, tolerance is lost allowing self-reactive cells to rapidly lose control and participate in tissue and organ damage.

1.1.3.1 T cells

Although the exact aetiology of RA remains elusive, the pathogenesis is largely believed to be T cell driven. T cells play a primary role in cellular mediated immunity

through interaction with MHC molecules. This interaction leads to a variety of inflammatory responses including production of cytokines, recruitment and activation of other immune cells to the inflammatory site, and production of memory cells and cytotoxic killer T cells (Alberts and Johnson 2002). HLA-DRB1 is a specific human MHC involved in antigen presentation to T cells, and is widely studied in relation to RA due to its association with increased prevalence (Gregersen *et al.* 1987; Amos *et al.* 2007; Mohan *et al.* 2014).

During inflammation in RA, $CD4^+$ T helper (Th) and $CD8^+$ cytotoxic T cells migrate into the synovial membrane following recruitment from other inflammatory cells (Smeets *et al.* 2001; Lundy *et al.* 2007; Wehrens *et al.* 2013). $CD4^+$ cells are associated with RA initiation and autoantibody production (Kadowaki *et al.* 1994; Petrow *et al.* 1996; Wong *et al.* 2006; Alzabin and Williams 2011). Furthermore, $CD4^+$ and $CD8^+$ cells contribute to disease severity, initiated by IL-6 production which subsequently leads to bone resorption by osteoclasts (Wong *et al.* 2006).

Specific Th cells including pro-inflammatory Th-1 and Th-17 are associated with RA pathogenesis and joint damage (Alzabin and Williams 2011). These cell subsets produce further inflammatory molecules including IL-17 (van den Berg and Miossec 2009), which triggers the release of cytokines such as IL-6 and TNFα, chemokines such as C-X-C ligand 1 and 2, and MMPs leading to bone degradation (Chabaud *et al.* 2000; Onishi and Gaffen 2010).

Further to Th-1 and Th-17, Tregs are also considered major players in RA pathogenesis (Mellado *et al.* 2015). The function of Tregs is widely researched in relation to AD because of their association with self-tolerance (Eakin *et al.* 2016).

They work to suppress the functions of effector T-cells (Teffs), thus keeping the immune response under control by limiting damage (Wu *et al.* 2009). However, their suppressive function is compromised during an autoimmune response, allowing loss of control of damage-causing Teffs, and in the case of RA this damage is targeted to the joints.

The suppressor function of Tregs depends on cell-cell interactions between Tregs, Teffs and APCs. A number of studies report negative regulation of Tregs in RA (van Amelsfort *et al.* 2007; Bonelli *et al.* 2016), as well as other autoimmune conditions (Morita *et al.* 2016; Schloder *et al.* 2017). Consequently, Tregs are unable to suppress damage-causing Teffs. However, several studies report conflicting levels of active Tregs in autoimmune diseases, possibly due to contamination of non-regulatory T cells during immunophenotyping (Ehrenstein *et al.* 2004; van Amelsfort *et al.* 2004; Mottonen *et al.* 2005).

Forkhead box P3 (Foxp3) is a Treg cell transcription factor which activates genes including TNF-related apoptosis-inducing ligand (TRAIL) and CTLA4 which are required for the suppressor function (Gavin *et al.* 2007). Previous studies have associated FoxP3 expression with impaired Treg activity (Kennedy *et al.* 2014; Cribbs *et al.* 2015). For example, one study analysed the Treg cell-specific demethylated region (TSDR), which is located in the FoxP3 locus and relates to regulation of its expression (Polansky *et al.* 2008).

Additional to the uncertainty surrounding levels of active Tregs in RA, there are conflicting reports of FoxP3 expression levels. A recent study reported an increase in FoxP3 expression by circulating Tregs in RA (Walter *et al.* 2016), strongly suggesting

peripheral Tregs are in an active state before entering the joint. Additionally, FoxP3$^+$ Treg levels are increased in synovial fluid compared to peripheral blood in matched RA samples (Shalini P. *et al.* 2015). However, a number of studies have reported no difference in the percentage of FoxP3$^+$ T cells in peripheral blood of RA patients (Cao *et al.* 2003; Mottonen *et al.* 2005). Conversely, the percentage of FoxP3$^+$ Tregs reduce in mouse models in association with increased autoimmunity (Sakaguchi *et al.* 2006). Furthermore, in other autoimmune conditions such as multiple sclerosis (MS), separate studies have reported circulating FoxP3$^+$ Tregs both increase and decrease compared to healthy controls (Kumar *et al.* 2006; Venken *et al.* 2008).

The reason for the discrepancies between studies is unclear. One suggestion is that results may be dependent on the treatment pathway of individual patients. For example, an increase in FoxP3 expression, thus Treg suppressive activity, was found in patients who were treated with MTX compared to cDMARD naïve patients (Cribbs *et al.* 2015). Additionally, RA patients exhibited an increase in FoxP3 expression after response to anti-TNFs, suggesting restoration of Treg function (Nie *et al.* 2013). Furthermore, the immunophenotypic classification of Treg cells differs between studies, with the potential of contaminating Teff cells contributing to the results (Appendix D).

1.1.3.2 B cells

B cells are involved in the humoral response as part of the adaptive immune system. In healthy individuals, they differentiate into plasma cells which produce antibodies that bind to specific foreign antigens. In AD conditions such as RA, B cell central and peripheral tolerance is lost. Loss of tolerance at each checkpoint has been observed

by production of self-reactive autoantibodies from defective B cells in RA patients (Samuels *et al.* 2005). As previously mentioned, RF and ACPAs are the most commonly studied autoantibodies in RA, and are generally used in diagnosis of the disease (NICE 2009).

B cells also influence other inflammatory cells during the immune response. For example, they can act as APCs in order to activate T cells. Previous studies have demonstrated this role of B cells in T cell stimulation within the synovial membrane in RA (Takemura *et al.* 2001). T cell activation subsequently leads to the release of pro-inflammatory cytokines, which in turn triggers the activation of other immune cells, thereby continuing this inflammatory process (Bugatti *et al.* 2014). Cytokines produced by B cells have been studied in RA, including IL-6 and IL-17 (Barr *et al.* 2012; Schlegel *et al.* 2013). In particular, IL-6 has been found to lead to further activation of pathogenic T cells (Barr *et al.* 2012).

As B cells are considered central to RA pathogenesis, many studies have confirmed the benefits of targeting B cells using specific biological DMARD rituximab. (Caporali *et al.* 2009).

1.1.3.3 Glycosylation in immune cell function

Immune cells contain sugar structures known as glycans on their surface (Alavi and Axford 2006). An increasing number of studies have analysed the role of glycans in health and disease because of their pivotal role in cell function (Alavi and Axford 2008). For example, glycans are involved in maintaining protein structure, and importantly immunogenicity (Caramelo and Parodi 2007; Li *et al.* 2008). During disease, because of the vast changes in cell biology as discussed, glycan alterations

are also observed (Alavi and Axford 2008). Analysis of cellular glycosylation changes has enabled researchers to understand functions of the monocyte cell-surface marker CD14, including cell trafficking (Meng *et al.* 2008). Additionally, researchers have studied glycosylation changes of the B cell receptor in multiple myeloma, and further studies have shown a role of glycosylation in Teff cells in regulating cell death (Toscano *et al.* 2007; Ilic *et al.* 2008). The importance of glycosylation in relation to RA is discussed in further detail in section 1.2.2.

1.1.4 Siglecs as master regulators of immune response

Lectins are a type of protein that will bind to glycans on the surface of a cell, which is an important process in regulating specific cell functions during the immune response (Toscano *et al.* 2007; Meng *et al.* 2008; Alavi and Axford 2008). Sialic acid-binding immunoglobulin-like lectins (Siglecs) are a family of trans-membrane proteins that are present on a variety of immune cells and are involved in determining immune tolerance. There are many subtypes of siglec, differing in function and structure. The general function of siglecs is to modulate the immune response, participating in cell adhesion, signalling and endocytosis (Crocker 2002; Nitschke 2005; Varki and Angata 2006; Crocker *et al.* 2007).

The structure of siglecs comprises of one ligand binding V-set domain, and a varying number of C2-set domains (**Figure 1.4**) (Crocker *et al.* 2007). The extracellular structure of siglecs can facilitate specific functions. For example siglec-1, also known as sialoadhesin or CD169, contains a large number of C2-set domains, which extend the V2-set binding domain away from the surface of the cell (Crocker *et al.* 1994). This elongation may overcome ‘masking’ of the binding site, caused by cis

interactions with alternative glycans (Razi and Varki 1999). CD22 (siglec-2) is also thought to overcome 'masking', due to the competitive binding of its sialylated glycans with same-cell *cis* ligands (Collins *et al.* 2006).

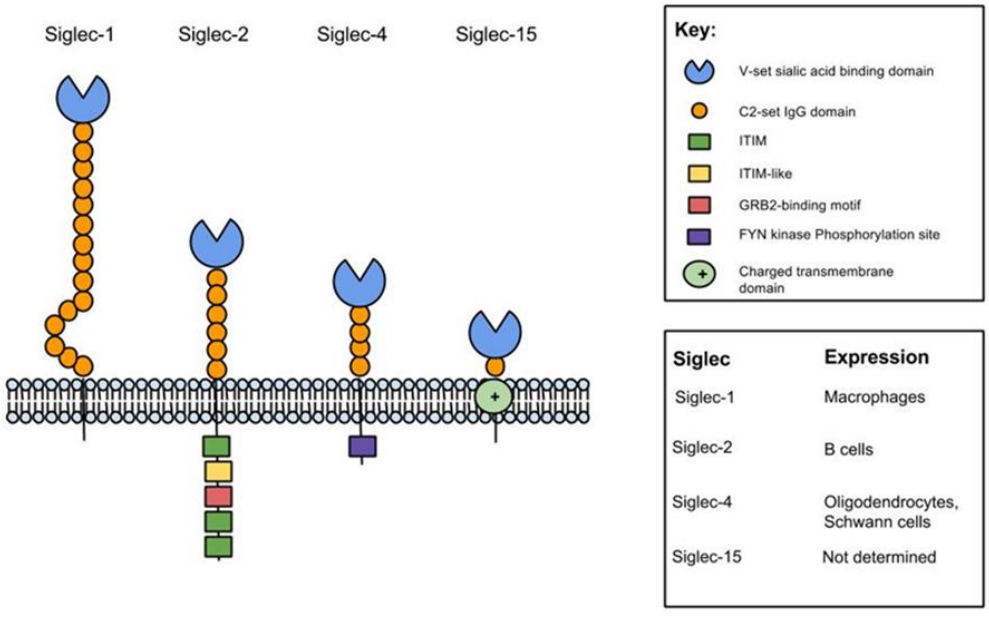

Figure 1.4: Structural differences between a select number of siglecs (Eakin et al., 2016*)

*Note: Refer to Appendix B for published review paper on the role of Siglec-1 and -2 in autoimmune disease (Proteomics Clinical Applications).

Additionally, intracellular characteristics of the cytoplasmic tail contributes to the function of siglecs. For example CD22 and some CD33 (siglec-3) subtypes contain immunoreceptor tyrosine-based inhibitory motifs (ITIMs) within the cytoplasmic tail (Ravetch and Lanier 2000). These regions facilitate an inhibitory siglec function, suppressing activation signals to the cell. Conversely, siglec-14 and siglec-15 lack ITIMs and are associated with immunoreceptor tyrosine-based activation motifs (ITAMs). Siglec-14 in particular functions as both an inhibitor and activator of cellular signals (Angata *et al.* 2006; Hamerman and Lanier 2006). Siglec-1 and siglec-4,

however do not contain tyrosine-based motifs, which suggests their primary function is to enable cell-cell interactions (Hartnell *et al.* 2001; Pillai *et al.* 2012).

Siglecs also possess specific binding affinities for sialylated glycans. Siglec-2 displays a binding preference for α2-6 glycosidic linkage (Powell *et al.* 1993; Kelm *et al.* 1994), whereas siglec-7 and siglec-11 bind in an α2-8 manner (Yamaji *et al.* 2002). Siglec-1 preferentially binds α2-3 linked sialic acid and weakly binds α2-8 linked residues (Ohtsubo and Marth 2006; Crocker *et al.* 2007). This binding preference is important in facilitating the function of the siglec, and subsequently the immune cell to which it is bound. Siglec-1 is one of the most studied siglecs in relation to RA. The subsequent section will detail the involvement of siglec-1 in RA pathogenesis.

1.1.4.1 Siglec-1

Siglec-1 is a cell surface protein present on monocytes, macrophages and dendritic cells. Its expression is associated with pro-inflammatory mechanisms in the immune response, displaying involvement in Teff cell induction as well as secretion of cytokines such as interferon-gamma (IFN-γ) (Jiang *et al.* 2006). Additional to a subset of $CD8^+$ T cells, siglec-1 can bind to granulocytes, B-cells and erythrocytes (Hartnell *et al.* 2001).

Siglec-1 has been shown to possess many roles, such as cell adhesion, accommodated by the elongation of the C2-set domains (**Figure 1.4**) (Munday *et al.* 1999). Common highly conserved siglec-1 regions exist within mouse and man, especially in the extra-cellular region, which confirms its role in cell-cell interactions (Hartnell *et al.* 2001). Siglec-1 is regulated as a result of type I and type II IFN induction, which suggests a role in anti-viral and anti-bacterial activity (O'Neill *et al.*

2013). Furthermore, it has been suggested that it contributes to the internalization of sialic acid (Sia) carrying pathogens by acting as an endocytic receptor (Delputte *et al.* 2011).

Siglec-1 has been described as a putative biomarker for RA due to its increased expression in patients with the disease, relative to patients with osteoarthritis (OA) or normal controls (Xiong *et al.* 2014). In RA patients, the increase in the relative number of siglec-1 positive cells, as measured by flow cytometry, positively correlates with clinical measures including DAS28, ESR, RF and CRP levels (Xiong *et al.* 2014). Furthermore, the average relative number of siglec-1 positive monocytes decrease after DMARD treatment response (Xiong *et al.* 2014). However, siglec-1 expression is not specific to RA as it has also been associated with other inflammatory diseases, including systemic lupus erythematosus (SLE). A strong correlation has been observed between siglec-1 positive monocytes and clinical parameters for SLE patients (Biesen *et al.* 2008).

The phosphorylation sites of siglec-1 responsible for intracellular signal transduction are poorly understood, however two potential sites that lack ITIMs have previously been investigated (Crocker *et al.* 1994). The cytoplasmic domain contains a Protein kinase C (PKC) motif and Casein kinase 2 (CK2) phosphorylation sites, which strengthens the suggestion that extracellular interactions potentiate intracellular signal transduction. The CK2 site is involved in signal transduction, transcriptional control, apoptosis and cell regulation (Malik and Clements 2004), therefore allowing for the normal functions of siglec-1.

It is thought that siglec-1 can bind ligands on the surface of Tregs, and that direct cell-cell binding could contribute to their suppression (Wu *et al.* 2009). A recent study presented data showing the induction of siglec-1 ligand expression on both Tregs and a subset of Teffs after TCR (T-cell receptor) activation in a murine model of SLE, with the exposure of siglec-1 being linked to cell death (Kidder *et al.* 2013). Furthermore, there was an association found between siglec-1 ligand expression and increased sialylation. (Kidder *et al.* 2013). This further suggests siglec-1 could be acting in a pro-inflammatory manner during the immune response.

CD43 (Sialophorin) is a sialoglycoprotein expressed on, but not restricted to Tregs. It is a T cell 'counter receptor' of ligands presented by siglec-1 (van den Berg *et al.* 2001), however a recent study suggested the induction of siglec-1 ligands can occur independent of CD43 (Kidder *et al.* 2013). In summary, although it is suggested that siglec-1 plays a role in Treg suppression, Teff activation, and therefore disease pathogenesis, the specific mechanisms behind these functions remain elusive. Furthermore, the nature and downstream effects of the siglec-1/CD43 balance is unclear. The interaction between siglec-1 (CD169) and CD43 is one of the key focusses of this thesis.

1.2 Systemic effects due to loss of immune system tolerance

The acute phase response (APR) is a process by which plasma proteins synthesised by the liver change in concentration as a result of inflammation in the body. The release of cytokines from various immune cells triggers and modulates the APR (Heinrich *et al.* 1990; van Miert 1995; Heinrich *et al.* 1998). For example IFN-γ, interleukin-1β (IL-1 β) and TNFα are essential for induction of the APR, as well as further recruitment of inflammatory cytokines such as IL-6 and IL-8 (van Miert 1995; Gruys *et al.* 2005).

Due to the inflammation present in the joint in RA, some studies have investigated APR proteins as a potential biomarker of disease (Ortea *et al.* 2012). Negative APR proteins which decrease during inflammation include transthyretin, retinol binding protein, transferrin and albumin (Kushner *et al.* 1981; Blackburn 1994; Ingenbleek and Young 1994). Positive APR proteins which increase in concentration during inflammation include CRP, serum amyloid A (SAA) and Haptoglobin (Hp) (Heinrich *et al.* 1990; Heinrich *et al.* 1998). The positive APR proteins are more commonly studied in relation to rheumatic disease, as discussed below.

MRPs (myeloid related proteins) 8 and 14 are heterodimeric structures situated in the cytosol of leukocytes and monocytes (Hessian and Fisher 2001). Both MRP-8 and MRP-14 promote the pathogenesis of RA by triggering the activation of neutrophils and monocytes (Frosch *et al.* 2000). Additionally, they are markers of differentiation on tissue infiltrating macrophages (Chen *et al.* 2009), where their function is to recruit further macrophages to the inflamed tissue (Pouliot *et al.* 2008).

SAA is also a widely studied APR protein due to its increase in concentration during inflammation (O'Hara *et al.* 2000). It is secreted by the liver following production of cytokines including IL-1, IL-6 and TNFα. C-reactive protein is also increased during the APR and correlates strongly with SAA levels during inflammation in RA (Chambers *et al.* 1983).

In summary, the complex proteomic environment in RA is potentially a promising target for biomarker discovery. These proteins have a direct impact on immune cells and vice versa, and therefore may be representative of disease activity. As discussed in chapter 5, the profiling of various proteins has the potential to improve understanding of RA pathogenesis and enables the analysis of differences between treatment responders and non-responders.

1.2.1 CRP and ESR

CRP and ESR are blood-based measures of non-specific inflammation. The NICE guidelines encourage monitoring of both markers during RA treatment (NICE 2009). CRP is one of the positive APR proteins, secreted from the liver following induction of IL-6 during inflammation (Sokka and Pincus 2009; Doyle *et al.* 2013). CRP has been shown to increase years before the onset of symptoms, along with autoantibodies RF and ACPAs (Nielen *et al.* 2006). Previous literature provides conflicting evidence of CRP as a reliable marker of inflammation. For example, a recent study described CRP as a useful biomarker of flare-ups in SLE (Eudy *et al.* 2014). Furthermore, normal CRP levels have been associated with better clinical outcome in RA (Kojima *et al.* 2013). However, other studies have found CRP is not representative of disease

activity in RA, with up to 45% of patients exhibiting normal levels (Sokka and Pincus 2009).

ESR is also a non-specific marker of inflammation, however it has previously shown no correlation with CRP levels in RA (Sbong and Feldman 2014). The increase of ESR is caused by the upregulation of the APR reactant fibrinogen. Therefore it is somewhat representative of the APR during inflammation (Gruys *et al.* 2005). A previous study suggested ESR is a sensitive measure of disease activity in RA, compared to CRP levels (Ward 2004). However, either marker may be used in the DAS28 equation during RA treatment.

1.2.2 Glycosylation of APR proteins

Glycosylation is an essential protein modification that is important to the structure and function of over 70% of proteins (Apweiler *et al.* 1999). Alteration of glycans is important because it can sterically disrupt interactions, for example between lectins and glycoproteins, which can in turn prevent normal receptor signalling (Collins *et al.* 2013). Glycosyltransferase and glycosidase enzymes can lead to abnormal glycosylation (Ohtsubo and Marth 2006). Numerous studies have highlighted their potential role in the pathogenesis of rheumatic diseases (Raghav *et al.* 2006).

Changes in glycosylation patterns of serum IgG have been associated with the progression of RA (Parkkinen 1989). Patients with RA express a higher concentration of agalactosylated IgG (IgG0), which correlates with disease severity in RA patients, suggesting a potential role in disease pathogenesis (Carson *et al.* 1987). Furthermore decreased galactosylation of IgG correlates with inflammatory markers IL-6 and CRP (Troelsen *et al.* 2012). Previous studies have suggested the use of IgG0 as a marker

for severity and duration of RA. For example IgG0 levels were shown to return to normal in RA patients following treatment with anti-TNF (Pasek *et al.* 2006; Van Beneden *et al.* 2009). Furthermore, treatment with MTX and infliximab decreased levels of IgG0 in RA responder patients (Croce *et al.* 2007).

The glycosylation patterns of several non-IgG proteins have also been widely studied in relation to RA inflammation. For example, increased numbers of bi-antennary and alpha 1, 3-fucosylated glycans were found at glycosylation sites of alpha-1 glycoprotein (AGP) in patients with acute inflammation compared to healthy individuals (Higai *et al.* 2005). AGP is important in RA due to its increase in plasma during acute inflammation (Hrycaj *et al.* 1993). Additionally, fucosylation is abnormally elevated in the sera of RA patients (Mann *et al.* 1994). A recent study also reported a unique monosaccharide pattern of AGP and Hp in RA patients (Saroha *et al.* 2011), which is suggested to play a role in disease pathogenesis.

1.2.2.1 Sialylation of APR proteins

Several studies have highlighted the role of Sia and its residues in inflammation. IgG is a serum glycoprotein involved in inflammatory events by the binding of its Fc region. Glycosylation changes in IgG can lead to changes in antibody activity. Sialylation of the Fc region decreases the affinity of the antibody to its receptor, and increases inflammatory activity of IgG (Kaneko *et al.* 2006; Anthony *et al.* 2008; Chrostek *et al.* 2014).

Sialylation of other APR glycoproteins have also been implicated in rheumatic disease pathogenesis (Chrostek *et al.* 2014), such as fibronectin, transferrin, Hp and AGP (Feelders *et al.* 1992; Przybysz *et al.* 2007; Saroha *et al.* 2011). Furthermore, these

changes in sialylation have been implicated as a potential biomarker for disease activity in RA (Cylwik *et al.* 2010). Previous studies have analysed levels of bound or unbound Sia to measure both APR activity and changes in sialylation of glycoproteins during disease (Paul and Rotzsch 1989; Alturfan *et al.* 2007). A recent study found increased levels of Sia in RA patients compared to healthy controls, which correlated with levels of positive APR proteins (Chrostek *et al.* 2014). Furthermore, levels of Sia in RA had a positive association with DAS28. Therefore, changes in Sia present in the sera of RA patients may be representative of sialylation patterns of APR glycoproteins, which could a play a role in disease pathogenesis.

In summary, previous literature has stressed the importance of siglec-1 in relation to pivotal immune cells including Tregs and Teffs, and additionally has shown the association of siglec-1 with increased sialylation (Kidder *et al.* 2013). CD43, a known counter receptor of siglec-1 is not as well known in relation to RA, however some studies have demonstrated its downregulation in diseased subjects (Humbria *et al.* 1994; Lopez *et al.* 1995). This thesis postulates that CD43 may be responsible for Treg function following binding of Sia ligands.

1.3 Conclusion

In summary, evidence to date suggests there is need for a more robust measurement of disease activity in RA, with various studies demonstrating the potential of new biomarkers for the disease. The time between diagnosis and a successful treatment

program for RA patients is quite extensive. Additionally, 30-40% of RA patients are unresponsive to treatment, thus allowing the disease to rapidly worsen.

On a cellular level there is strong evidence suggesting that siglec-1 could be a useful biomarker that is indicative of response or non-response to DMARD therapy. Research to date has also shown an association between siglec-1 positive monocytes and Tregs, where siglec-1 leads to Treg suppression. Specifically, siglec-1 interacts with CD43, however little is known about the nature or consequences of this interaction. It is also unclear whether this cellular interplay could be indicative of response or non-response to treatment of RA patients in relation to DAS28ESR. Further knowledge may assist in determining response at an earlier stage, thus improving the clinical outcome of patients, as non-responders could switch to a more effective treatment sooner than currently possible.

APR proteins have been of significant interest in RA patients, with some being described as potential biomarkers for the disease due to their aberrant glycosylation patterns during RA inflammation. Specifically, the role of Sia, which is involved in the interaction between siglec-1 and CD43, has been implicated in RA pathogenesis. However, information is lacking in whether these protein patterns reflect on clinical measures of the disease.

In summary, there is great need for sensitive biomarkers that are more representative of disease activity in RA than current clinical measures. This study aims to investigate the involvement of key immune cells and proteins present in peripheral blood in RA patients, their association with disease activity, and their potential in discriminating between responders and non-responders to treatment.

This could lead to the stratification of patients into clinically relevant groupings, subsequently assisting clinicians in providing an efficient treatment regimen. The knowledge gained from this study has the potential to prevent irreversible joint damage and poor quality of life in RA patients by improving overall clinical outcome.

1.4 Hypothesis

The immunophenotype of circulating siglec-1 positive monocytes and CD43 positive Tregs, and the surrounding plasma proteome, act as sources of potential disease activity and treatment response biomarkers in RA.

1.5 Aims and objectives

1.5.1 Aim 1 (Chapter 3): To determine the relationship between siglec-1 (CD169) positive monocytes and CD43 positive Tregs in RA.

Siglecs are of interest in RA due to their involvement in determining immune tolerance. Specifically, siglec-1 (CD169) has been widely studied due to its increased expression in RA in association with clinical measures of disease activity. Chapter 3 aims to assess the ratio between CD169 positive monocytes and CD43 positive Tregs in circulating blood of RA patients who are DMARD naïve, DMARD responders and DMARD non-responders. This data will be compared to clinical measures of disease activity in order to assess their potential as circulating biomarkers.

1.5.2 Aim 2 (Chapter 4): To assess the activation state of Tregs in RA.

The intracellular activation of Tregs will initially be assessed in each patient group described in aim 1.5.1. This will be carried out by using FoxP3 as a surrogate measure of Treg activation. Additionally, co-culture experiments with CD169 positive monocytes will be carried out in order to assess their effects on specific Treg intracellular signalling pathways as well as activation state.

1.5.3 Aim 3 (Chapter 5): To discover circulating protein biomarkers indicative of treatment response in RA.

Plasma samples from each patient group will be analysed for various proteins associated with inflammatory and immune response pathways. This data will be compared to clinical measures of response, as well as cell data obtained from the same immunophenotyped samples from previous aims.

Chapter 2

Materials and methods

2.0 Participant recruitment and sampling

2.0.1 Study Design

Office for Research Ethics Committees Northern Ireland (ORECNI) approval (11/NI/0188), Ulster University Research Ethics Committee (UREC) approval (REC/14/0053) and Integrated Research Application System (IRAS) approval (88730) were obtained for the study. The research team at Ulster University (UU) collaborated with rheumatologists from the Western Health and Social Care Trust (WHSCT) and the Belfast Health and Social Care Trust (BHSCT) to design and conduct the study. All RA patients were recruited from either the WHSCT or the BHSCT. Healthy control subjects recruited to the study were staff or student members from either the WHSCT or UU.

2.0.2 Sampling and participant demographics

Venepuncture was used to extract peripheral blood from each participant. Vacutainer collection tubes (Aquilant Scientific) were used to obtain blood for either serum extraction (red topped tubes) or plasma and cell extraction (purple topped tubes). Sampling was carried out by a nurse during routine bloods were being taken, or by a trained member of the research team.

Consent to participate was obtained from all patients and healthy controls. Diagnosis for all patients fulfilled the 2010 American college of rheumatology (ACR) criteria. Patients were classed as cDMARD ‘responders’ or ‘non-responders’ according to ACR/EULAR guidelines. Non-responders were due to commence biological DMARD

treatment on the day of sampling. Clinical data from the day of sampling was retrieved from patient notes retrospectively (Table 2.1). Healthy controls were also recruited to the study, excluding individuals with any chronic inflammatory or autoimmune disorder.

The cDMARD non-responder patient numbers needed were estimated initially using previously determined potential genetic biomarkers of DMARD response. Flow cytometry analysis of this patient cohort was used to determine a suitable sample number needed based on relative numbers of $FOXP3^+$ Tregs in healthy controls (mean = 45.86, n=24) compared to RA patients (mean = 29.74, n=24). The PWR package in R [http://cran.r-project.org/] was used to calculate a power of 0.81 with a sample number of n=24 in each group. This calculation assumes a significance level of 0.05 and a medium Cohen's effect size of 0.67.

Table 2.1: Demographics of patients treated with (A) cDMARD and (B) biological DMARDs

(A)

	Healthy Controls (n=21)	RA: cDMARD naïve (n=6)	RA: cDMARD responder (n=24)	RA: cDMARD non-responder (n=32)
Female, *n* (%)	16 (76.2)	5 (83.3)	22 (91.7)	27 (81.8)
Age, mean (SD), years	35.9 (9.2)	42.5 (16.7)	59.7 (12.2)	57.7 (10.1)
Disease duration, mean (SD), years	N/A	N/A	5.0 (3.8)	10.8 (12.1)
Full Blood Count				
Lymphocytes, mean (SD), 10^9/L	1.9 (0.4), n=19	1.6 (0.5), n=6	1.7 (0.3), n=24	1.6 (0.5), n=26
Monocytes, mean (SD), 10^9/L	0.5 (0.3), n=19	0.6 (0.2), n=6	0.5 (0.1), n=24	0.6 (0.3), n=26
Erythrocyte Sedimentation Rate (ESR), mean (SD), mm/hr	N/A	23.5 (15.2), n=6	12.2 (7.9), n=24	24.1 (20.0), n=29
C-reactive Protein (CRP), mean (SD), mg/L	N/A	6.1 (2.9), n=6	5.3 (7.3), n=22	10.6 (9.4), n=28
Disease Activity Score in 28 joints (DAS28-ESR), mean (SD)	N/A	4.3 (0.4), n=4	2.6 (1.0), n=24	4.9 (1.1), n=19

(B)

		Biologic DMARD responder (n=8)	Biologic DMARD non-responder (n=6)	Biologic DMARD adverse event (n=2)
Female, *n* (%)		6 (75.0)	4 (66.7)	2 (100.0)
Age, mean (SD), years		56.0 (10.5)	57.2 (6.7)	46.5 (14.8)
Disease duration at baseline appointment, mean (SD), years		12.6 (11.7)	14.8 (16.3)	1.75 (0.3)
Drug commenced, *n* (%):	Adalimumab	7 (87.5)	3 (37.5)	2 (100.0)
	Etanercept	1 (12.5)	1 (12.5)	N/A
	Tocilizumab	N/A	1 (12.5)	N/A
	Golimumab	N/A	1 (12.5)	N/A

2.1 Blood processing

2.1.1 Density gradient separation for isolation of peripheral blood mononuclear cells (PBMCs)

Density gradient separation is a well-established technique that allows for separation of whole blood into distinct layers. **Figure 2.1** shows the isolation of peripheral blood mononuclear cells (PBMCs).

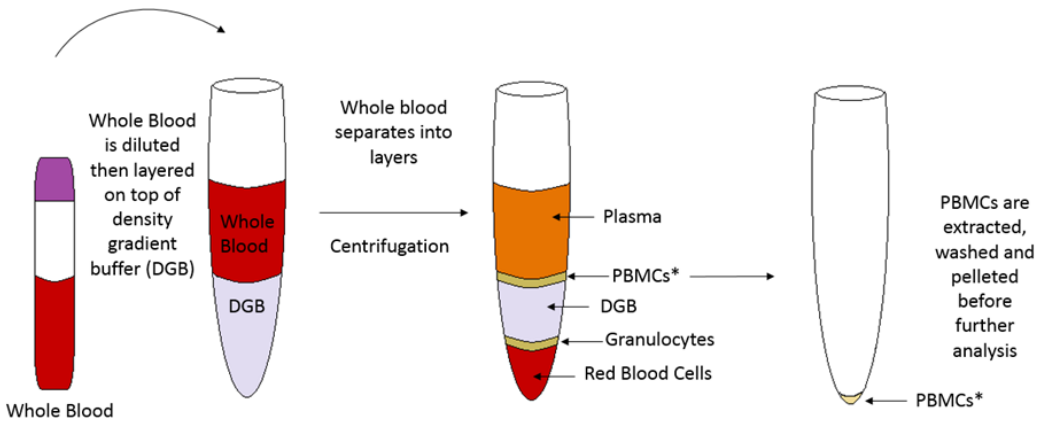

Figure 2.1: Density gradient separation of whole blood showing extraction of peripheral blood mononuclear cells (PBMCs).

Peripheral whole blood used for PBMC isolation was collected in an ethylene diamine tetra acetic acid (EDTA) coated tube (Aquilant Scientific) using a venepuncture technique. Blood tubes were stored at 18 ˚C until processing. Histopaque-1077 (Sigma-Aldrich, UK) was used to isolate PBMCs. Prior to separation, whole blood was diluted 1:1 in BD Cell wash (Becton Dickinson). Then, 8 mL of diluted blood was carefully layered onto 5 mL Histopaque-1077 in a 15 mL Falcon. Ratios remained the same when the volume of blood was scaled up or down. The 15 mL falcon tube was centrifuged at 400 rcf for 30 minutes at 18 ˚C. This speed is sufficient for pelleting

cells with minimal damage. After centrifugation, the majority of the upper plasma layer was discarded, leaving approximately 0.5 mL above the PBMC layer. The PBMC layer was dispensed into a clean 15 mL falcon tube along with the remaining plasma layer and approximately half of the Histopaque layer. Extraction of all of the Histopaque layer would decrease the final cell yield because the density of this buffer is higher than standard wash buffer. BD Cell wash (Becton Dickinson), a sterile PBS buffer, was added to the crude extracted PBMCs up to the 15 mL mark. The tube was inverted 3-4 times to ensure sufficient mixing. The tube was centrifuged at 300 rcf for 10 minutes at 18 ˚C. After centrifugation, the supernatant was discarded and the cell pellet was resuspended in 10 mL BD Cell wash (Becton Dickinson). The tube was centrifuged again at 300 rcf for 10 minutes at 18 ˚C. After centrifugation, the supernatant was discarded and the cell pellet was resuspended in 5 mL BD Cell wash (Becton Dickinson). The tube was centrifuged again at 300 rcf for 10 minutes at 18 ˚C, followed by final resuspension in 0.5-3.0 mL BD Cell wash (Becton Dickinson).

2.1.2 Buffy coat and plasma extraction from whole blood

The extraction of the 'buffy coat' layer from whole blood allows for isolation of leukocytes and platelets (Mathay *et al.* 2012). It is commonly used prior to DNA extraction and analysis (Ip *et al.* 2015).

Peripheral whole blood used for buffy coat extraction was collected in an EDTA coated tube (Aquilant Scientific) using a venepuncture technique. Blood tubes were stored at 4 ˚C until processing. The blood tube was centrifuged at 300 rcf for 10 minutes at 18 ˚C. The centrifugation allows for the separation of layers, as shown in **Figure 2.2**.

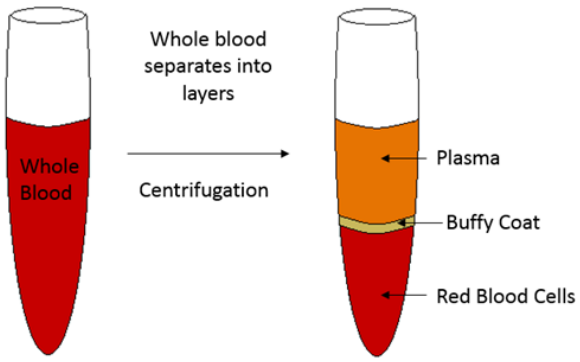

Figure 2.2. Centrifugation of whole blood, allowing separation of plasma, buffy coat and red blood cells.

The majority of the plasma layer was removed leaving approximately 0.5 mL above the buffy coat. If required by the study protocol, the plasma layer was aliquoted and stored at -80 ˚C for later analysis. The remaining plasma along with the buffy coat and up to 1 mL of the RBC layer was removed and placed into a clean 1.5 mL Eppendorf tube. The remaining red blood cells in the blood tube were stored at -80 ˚C if required for future DNA analysis. The crude buffy coat sample was mixed gently using a pipette and divided appropriately for RNA and protein analysis. Then, 250 µL of Mammalian Protein Extraction Reagent (mPER) (Ambion) was added to tubes destined for protein analysis, and 500 µL of RNALater (Thermo Scientific) was added to those needed for RNA analysis. Samples were labelled and stored at -80 ˚C until future analysis.

2.1.3 Serum extraction from whole blood

Peripheral whole blood used for serum extraction was collected in a serum clot activator tube (Aquilant Scientific) using a venepuncture technique. The blood tube was kept upright at 18 ˚C for 30 minutes to allow clotting to occur, then stored at 4

˚C until processing. The tube was then centrifuged at 3500 rcf for 10 minutes at 18 ˚C. After centrifugation, the top serum layer was aliquoted (up to 5 x 500 µl) into 1.5-2 mL screw-top vials and stored at -80 ˚C until further analysis.

2.2 Magnetic-activated cell sorting (MACS)

2.2.1 Pan Monocyte Isolation

PBMCs were separated from whole blood as described in section 2.1.1. Then, 10 µl of the cell suspension was diluted with 90 µl autoMACS buffer (section 2.2.1.1) to make a 1 in 10 dilution. After pipetting up and down to ensure sufficient mixing, 20 µl was added to a haemocytometer for counting. The cell number was determined and the original cell suspension was centrifuged at 300 rcf for 10 minutes at 4˚C. The supernatant was aspirated and the cell pellet was resuspended in 30 µl autoMACS buffer per 10^7 cells. The Pan Monocyte Isolation kit (Miltenyi Biotec) was used on the autoMACS Pro separator for all monocyte cell separations. Then, 10 µl of Fragment crystallisable region (FcR) blocking reagent was added per 10^7 total cells followed by 10 µl biotin-antibody cocktail per 10^7 total cells. The cell suspension was vortexed gently and incubated for 5 minutes at 2-8˚C. Then, 30 µl of autoMACS buffer was added per 10^7 cells followed by 20 µl anti-biotin microbeads per 10^7 cells. The cell suspension was mixed well and incubated for an additional 10 minutes at 2-8˚C. If required for analysis, staining antibodies were then added at the optimized concentration (Appendix D). The cell suspension was gently vortexed followed by a final incubation at 2-8˚C for 15-30 minutes with protection from light. Cells were

washed by addition of 1-2 mL autoMACS buffer followed by centrifugation at 300 rcf for 10 minutes at 4˚C. After removing the supernatant, the wash step was repeated followed by final resuspension of the cell pellet in 500 µl autoMACS buffer per 10^8 cells.

The autoMACS Pro separator used to deplete the monocyte cell population. This automated instrument contains a magnetic column. When a magnetic field is applied to the column, it enables it to pull out the ferrite-containing anti-biotin microbeads. As these beads have now bound with the antibody-antigen complex, it enables specific cells to also be pulled out. This is a 'negative selection', which means the monocyte cells are not pulled out, so are depleted and eluted in the first flow-through. The cell sample was placed in row A of the tube rack and empty tubes were placed in rows B and C. The tube rack was placed on the instrument stand and the 'Deplete' program was selected. The monocyte cells were collected in row B.

2.2.1.1 Preparation of autoMACS buffer (PBS + 2 mM EDTA + 0.5% BSA)

Ten PBS tablets (Thermo Scientific) were dissolved in 1L dH_2O and autoclaved to sterilise. Then, 5g BSA (Sigma-Aldrich) and 0.74 g EDTA (Sigma-Aldrich) were dissolved in the PBS. This solution was stored for no longer than 2 weeks at 2-8˚C.

2.3 Fluorescence-activated cell sorting (FACS)

FACS is a technique that utilizes lasers to detect specific cell phenotypes via an antibody-fluorophore conjugate. It is coupled with highly specialized software that

allows for simultaneous analysis and isolation of cells of interest. Once cells have been isolated, they can be stored until downstream analysis.

2.3.1 Sample preparation and extracellular antibody-fluorophore labelling

PBMCs were separated from whole blood as described in section 2.1.1. Then, 10 µl of the resulting cell suspension was diluted with 90 µl autoMACS buffer (section 2.2.1.1) to make a 1 in 10 dilution. After pipette mixing, 20 µl was added to a haemocytometer for counting. The cell number was determined and the original cell suspension was centrifuged at 300 rcf for 10 minutes at 4˚C. The supernatant was discarded and the remaining cell pellet was resuspended in 100 µl BD Stain Buffer per $1x10^6$ cells. Each required antibody-fluorophore conjugate was added according to the optimised concentration per $1x10^6$ cells (Appendix D). The cell suspension was gently passed up and down through a pipette to ensure sufficient mixing. The sample was then incubated at 4 ˚C with protection from light for 15-30 minutes. After incubation, the cell suspension was made up to 4 mL with BD Stain buffer. This was centrifuged at 400 rcf for 10 minutes at 18 ˚C. The supernatant was discarded and the pellet was resuspended in 4 mL autoMACS buffer (section 2.2.1.1). The cell suspension was centrifuged again at 400 rcf for 10 minutes at 18 ˚C. The supernatant was discarded and the cell pellet was resuspended in 0.5-2.0 mL autoMACS buffer. The sample was then analysed using the FACS Aria III within 4 hours of processing.

When analysing each sample using FACS, dot plots were drawn depending on the panel of antibodies used. A negative control was used (section 2.3.3) to determine a suitable gating strategy for the labelled sample. Once the gating strategy was established, the labelled sample was loaded onto the Aria III, and up to 100,000

events were recorded. If cells were to be sorted, a sort layout was prepared depending on the cell population of interest. Cells were either sorted into cold PBS or 20% human serum from AB donors (AB serum) (Sigma Aldrich) in PBS, depending on downstream analysis. The latter would be used in cases of downstream cell culture experiments, as detailed in section 2.4.

When analysing cell populations for results chapter 3, the first part of the sample was used for monocyte analysis and was labelled with antibodies targeting CD14, CD16, CD32, CD64 and CD169 (Becton Dickinson) following use of the Pan Monocyte isolation kit (Miltenyi Biotec) for magnetic-activated cell sorting (MACS), as detailed in section 2.2.1 (**Figure 2.3**) (Appendix D). The autoMACS Pro Separator was used for this monocyte enrichment step (Miltenyi Biotec). Immunophenotyping and counts of enriched monocytes were carried out using an Aria III FACS (Section 2.3).

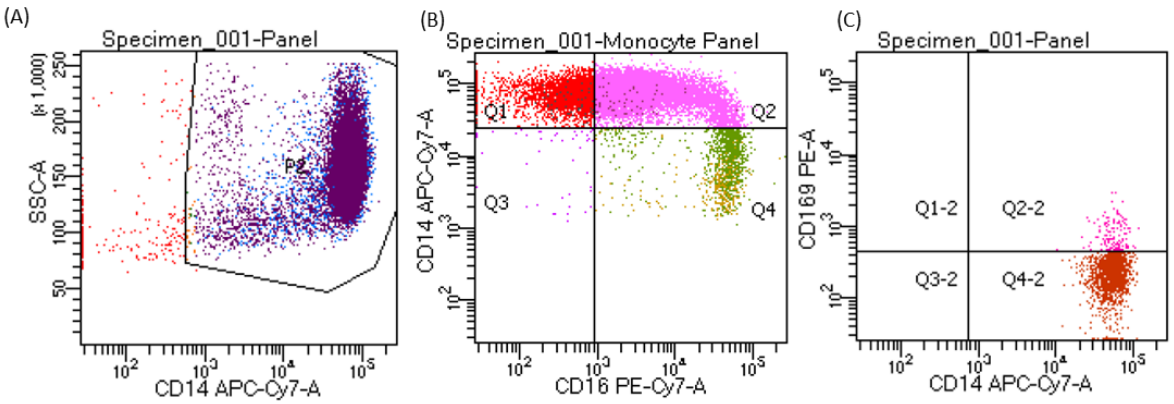

Figure 2.3: (A) $CD14^{+}$ cells were gated, where the positioning was based on negative controls. (B) A subsequent dot plot was used to subdivide monocyte subsets into $CD14^{++}CD16^{-}$ classical (A, Q1), $CD14^{++}CD16^{+}$ intermediate (A, Q2) and $CD14^{+}CD16^{++}$ non-classical (A, Q4). (C) A subsequent dot plot of (A) and (B) was used to analyse CD169 positivity (B, Q2-2).

The second part of the sample was used for Treg analysis and labelled with antibodies targeting CD3, CD4, CD45, CD45Ra, CD127, CD25 and CD43 (**Figure 2.4**) (Appendix D). The Treg phenotype was selected based on markers used in recent literature (Appel *et al.* 2011; Walter *et al.* 2016).

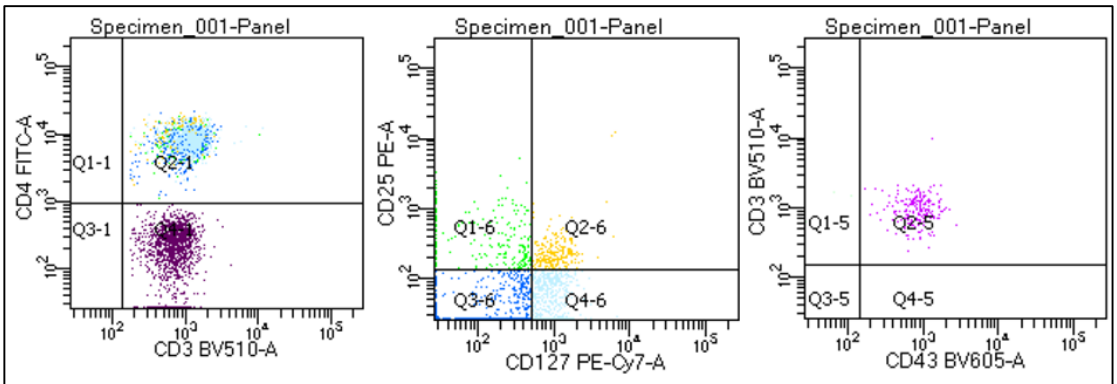

Figure 2.4: CD43 positivity (Q2-5) was analysed in a subsequent dot plot of $CD3^{+}CD4^{+}$ (Q2-1) cells, further subdivided according to the phenotype $CD25^{+}CD127^{-}$ (Q1-6).

2.3.2 Intracellular antibody-fluorophore labelling

After cells were labelled extracellularly (section 2.3.1) for 15-30 minutes, the cell suspension was made up to 4 mL with BD stain buffer. This was centrifuged at 400 rcf for 10 minutes at 18 ˚C. The supernatant was discarded and the cell pellet was resuspended in 500 µl 1X BD Permeabilizing Solution 2 (Becton Dickinson), a buffer containing <15% formaldehyde and <50% diethylene glycol. The cell suspension was incubated at 18 ˚C for 10 minutes. Following incubation, the cell suspension was made up to 4 mL with autoMACS buffer. The tube was inverted slowly a few times to ensure sufficient mixing. The cell suspension was then centrifuged at 400 rcf for 10 minutes at 18 ˚C. The supernatant was discarded and the cell pellet was resuspended in 100 µl BD Stain Buffer per $1x10^{6}$ cells. Each required antibody-fluorophore

conjugate was added according to the optimised concentration per $1x10^6$ cells. The cell suspension was gently passed up and down through a pipette to ensure sufficient mixing. The sample was incubated at 18 ˚C with protection from light for 15-30 minutes. Following incubation, the sample volume was made up to 4 mL with BD Stain Buffer and the tube was inverted a few times to ensure sufficient mixing. The cell suspension was centrifuged at 400 rcf for 10 minutes at 18 ˚C. After discarding the supernatant, the cell pellet was resuspended in 500 µl of 1X BD CellFix (Becton Dickinson). The sample was kept at 4 ˚C and analysed using the FACS Aria III within 4 hours of processing.

When analysing cell populations for chapter 4, extracellular antibody labelling was initially carried out according to section 2.3.1. The antibody panel used for extracellular staining included CD45-BV421, CD4-FITC, CD3-BV510, CD45RA-APCR700, CD127-PE-Cy7, CD25-PE and CD43-BV605 (Becton Dickinson). Following extracellular staining, intracellular staining of FoxP3-APC and NFκB-PerCP-eFluor710 (Thermo Fisher) was carried out.

2.3.3 Preparation of negative controls

Negative controls were used each time a sample was analysed on the FACS Aria III in order to determine the gating strategy that differentiates a positive and negative population.

2.3.3.1 Unstained PBMC negative controls

Unstained PBMCs were prepared according to section 2.3.1, however autoMACS buffer was added in substitution for antibody-fluorophore conjugates. This sample

was carried through the same process as the labelled samples in order to ensure it is a fair negative control. These controls were run with every sample to rule out differences in auto-fluorescence between runs.

2.3.3.2 Isotype negative controls

Isotype control samples were prepared according to section 2.3.1, however isotype matched antibody-fluorophore conjugates were added in substitution for the specific panel antibody-fluorophore conjugates. *Note: Isotype controls are antibody-fluorophore conjugates of the same class of antibody, however the antibody has not been raised against the specific cell marker of interest.* Isotype controls were also carried through the same process as the labelled samples in order to ensure it is a fair negative control. These controls were run every 6 months to ensure the gating strategy did not deter from batch to batch of antibody-fluorophore conjugates.

2.3.4 Data analysis and statistical methods

BD FACSDiva software was used to run and analyse all samples. Following recording of cell events and sorting, data was extracted from Diva software and stored on an encrypted hard drive. The positivity of a specific cell surface marker in labelled samples compared to the negative control was analysed as a percentage of the parent population, as detailed further in subsequent results chapters. The median fluorescence intensity (MFI), which gives an indication of cell surface density of a specific marker, was also noted for various cell populations.

The mean percentage of positive cells and standard deviation (SD) or standard error of the mean (SEM) were recorded for healthy controls and RA patients, with 95%

confidence interval (CI). Unpaired T tests or non-parametric Mann Whitney tests were used to assess significant differences between sample groups, depending on normality of distribution. The normality of distribution was tested using IBM SPSS statistics software using the 'explore' command. Two-tailed P values and R squared values were recorded. The mean and standard deviation was noted for all data in the format *mean ± standard deviation*, however when a Mann Whitney test was used, graphs depict the median value with error bars representing the interquartile range.

Linear regression analysis was used to assess any correlation within the RA patient group, as well as association with clinical data using 95% CI. R squared and P values were also recorded.

2.4 Cell culture

All cells were sorted as detailed in sections 2.2 and 2.3, depending on the specific cell population of interest. Cell were cultured in TexsMACS^{TM} medium (Miltenyi Biotec), supplemented with 5% AB serum (Sigma Aldrich), 1% Penicillin-Streptomycin (Gibco) and human IL-2 (Miltenyi Biotec). During culture, cells were stored in a temperature controlled incubator (Galaxy 170 S, New Brunswick) at 37 ˚C with 5% CO_2. Counting and viability tests were carried at specific time points throughout culture. Images of cells were also taken during culture using an inverted microscope (Zeiss Primovert). This was to observe any physical differences of the cells.

PBMCs were obtained from anonymous healthy participants for the purpose of cell culture. As detailed in section 2.1.1, PBMCs were separated using Ficoll density

gradient buffer and labelled with extracellular antibodies depending on the cell populations of interest. Tregs used in results chapter 4 were labelled using antibodies CD4, CD25 and CD127. Tregs were then sorted into PBS containing 20% AB serum (Sigma Aldrich) using the phenotype $CD4^{+}CD25^{+}CD127^{-}$, and were expanded as detailed in section 2.4.2.

Monocytes used for co-culture experiments were obtained from healthy participants. Following isolation of PBMCs using Ficoll, cells were extracellularly labelled with antibodies CD14-APCCy7, CD16-PECy7 and CD169-PE. Monocytes were initially enriched using the Miltenyi Biotec Pan monocyte isolation kit, as detailed in section 2.2.1. The enriched monocytes were then analysed by FACS and sorted into 20% AB serum according to the phenotype $CD14^{+}CD169^{+}$.

Following cell sorting of Tregs or monocytes into 20% AB serum, cells were washed twice in TexsMACS^{TM} medium (Miltenyi Biotec), supplemented with 5% AB serum (Sigma Aldrich), 1% Penicillin-Streptomycin (Gibco) and human IL-2 (Miltenyi Biotec).

2.4.1 Cell viability

The cell viability test was carried out using Trypan Blue solution (Sigma). Trypan blue allows for the differentiation between live and dead cells as it will penetrate the cell membrane of non-viable cells, causing them to stain blue. The cell suspension was added at an equal volume to Trypan blue, for example 25 µL cells + 25 µL Trypan blue. The solution was pipetted up and down gently to ensure sufficient mixing, then incubated for 5 minutes at 18 ˚C. Following incubation, the live and dead cells were

counted on a standard haemocytometer. The percentage of viable cells was calculated using the following equation:

No. Live cells / (No. Live cells + No. Dead cells) * 100

2.4.2 Human Treg expansion

Following Treg cell sorting and wash steps, cell were resuspended in 1 mL of media per $1x10^6$ cells. 100 µL ($1x10^5$ cells) was added to each well of a round-bottom 96-well plate (Sarstedt). The Miltenyi Biotec human Treg expansion kit was used to induce Treg proliferation in order to expand the cell population for sufficient cell numbers prior to stimulation experiments. CD3/CD28 particles were resuspended thoroughly before taking 100 µL into a fresh tube. Then 500 µL of fresh media was added, and the particles were centrifuged at 300 rcf for 5 minutes at 18˚C. The supernatant was discarded and the particles were resuspended in 100 µL fresh media. Then 20 µL of the particle suspension was added per well containing $1x10^5$ cells. Then 100 µL of media was added to each well on Day 1 of expansion. On Day 3-5, depending on cell counts and viability, cells were either split between wells to allow further expansion, or media was exchanged in each well. These checks were carried out carefully every other day until Day 14. On Day 14, if further expansion was needed, the particles were removed using a DynaMAG™ spin magnet (Invitrogen). In order to successfully remove particles, cells were placed in a 1.5 mL eppendorf and held on the magnet for 1-2 minutes. The supernatant was carefully placed in a fresh tube, and replaced on the magnet for a further 1-2 minutes. The cells in the supernatant could then be re-stimulated with fresh CD3/CD28 particles as before, if necessary.

Sorted Tregs were expanded for a no longer than 14 days. Cell stimulation experiments were carried out in a 24-well plate at a density of 3-5x10^5 cells per well. At each time point, counting and viability testing was carried out as described in section 2.4.1. Additionally, at relevant time points during stimulation, cells were centrifuged at 1600 rcf for 5 minutes at 18 ˚C and the supernatant was stored at -80 ˚C if required for ELISA analysis of secreted cytokines. The cells were resuspended in 1 mL of sterile PBS and centrifuged at 400 rcf for 10 minutes at 18 ˚C. The supernatant was discarded, and cells were either resuspended in 1 mL Trizol if required for RNA extraction and qPCR (storage at -80 ˚C until RNA extraction), or staining buffer if required for flow cytometry (processed immediately at 18 ˚C).

2.4.3 Phorbol 12-myristate 13-acetate/Ionomycin (PMA/IO) and Lipopolysaccharide (LPS) optimisation

LPS was reconstituted in media to make a stock solution of 1 µg/ml (Sigma Aldrich). The stock solution was diluted as required using media. PMA (Abcam) was reconstituted in 99.8% ethanol (Sigma Aldrich) to make a stock solution of 1 mg/ml. The stock solution was diluted as required using media. PMA was used in combination with IO (Invitrogen). IO was reconstituted in dH_2O to make a stock solution of 1 mg/ml. The stock solution was further diluted to 500 ng/ml using media. The expanded Tregs were initially exposed to a range of each stimulant, based on quantities reported in previous literature papers (Yu *et al.* 2012). In preliminary experiments aimed at optimising the concentration of each stimulant, cells were stored for subsequent RNA extraction and qPCR at time points 0, 24hrs and 48hrs after exposure to the appropriate stimulant. On repeating the experiment with

optimal conditions subsequent to these preliminary experiments, cell supernatants were analysed for cytokine secretion by ELISA.

2.4.4 Sialic acid (Sia) stimulation of Tregs

Expanded Tregs (3-5x10^5 cells per well of 24-well plate) were stimulated with 10 ng/ml PMA and 500 ng/ml IO as these conditions were found to be optimal primarily in increasing TNFα and IL-10 cytokine secretion (Chapter 4). Tregs were also stimulated with 10 mM Sia either with or without PMA/IO. Monomeric Sia was reconstituted in dH_2O to make a stock solution of 50 mg/ml (Sigma Aldrich). Then 10 mM of Sia was added directly to each well as required from the stock solution. The effects of adding Sia after 1 day of PMA/IO stimulation were assessed. A vehicle control was also included in the experiment to ensure the dH_2O in which Sia was resuspended did not have any effect on the Treg cells. At time points Day 0, Day 1 and Day 2, cells were removed from culture and labelled for FACS analysis with extracellular staining antibodies CD4, CD25, CD127 and CD43, as well as intracellular staining antibodies NFκB and FoxP3. The cell culture supernatants were also analysed for secreted cytokine levels as before.

2.4.5 Monocyte/Treg co-culture

Sorted monocytes were used in culture on the same day of sampling. The ratio of monocytes to Tregs in co-culture was approximately 1:2 i.e. 1.5-2.5x10^5 monocytes: 3-5x10^5 Tregs per well of a 24-well plate. Blocking antibodies were used in co-culture experiments of Tregs and monocytes. CD169 blocking antibody was reconstituted in PBS and used at a concentration of 4 µg/ml (AF5197, R&D systems). CD43 blocking antibody was reconstituted in PBS and used at a concentration of 1 µg/ml (AF2038,

R&D systems). CD169 was incubated with monocytes in TexsMACS™ medium (Miltenyi Biotec), supplemented with 5% AB serum (Sigma Aldrich), 1% Penicillin-Streptomycin (Gibco) and human IL-2 (Miltenyi Biotec) at 37 ˚C for 30 minutes prior to addition of Tregs. Similarly, CD43 was incubated with Tregs in the supplemented TexsMACS™ medium at 37 ˚C for 30 minutes prior to addition of monocytes. Following co-culture, cells were gently scraped with a sterile scraper (Thermo Fisher) into suspension before placing into a 1.5 mL eppendorf tube prior to antibody labelling for FACS analysis

2.5 Molecular methods

2.5.1 RNA extraction

Total RNA was extracted from human cells using TRIzol® (Invitrogen). Cells were resuspended in 1 mL TRIzol® in a 1.5 mL eppendorf and mixed vigorously up and down using a pipette. Cell samples were then frozen at -80 ˚C prior to continuing the extraction. The homogenized cell samples were thawed to room temperature then vortexed thoroughly. Then 200 µL chloroform (Sigma Aldrich) was added to each sample in a fume hood. The Eppendorfs were capped and shaken well for 15-20 seconds. The mixture was allowed to settle at room temperature for 2-3 minutes to allow layers to separate, then each sample was centrifuged at 12,000 rcf for 15 minutes at 4 ˚C. Following centrifugation, the mixture separates into 3 layers; an upper aqueous layer where RNA is contained, a cloudy interphase and a lower phenol layer. RNA was pipetted from the upper layer and into a clean 1.5 mL Eppendorf,

being careful not to disturb the interphase. 5 µg of Glycogen (Invitrogen) was added to the wall of each Eppendorf. Glycogen is a carrier protein that is co-precipitated with the RNA. The aim of adding a carrier is to improve yield of RNA. 500 µL of 100% propan-2-ol (Sigma Aldrich) was added to each sample, ensuring to flood the small quantity of Glycogen to the bottom of the Eppendorf. The sample was mixed gently up and down using a pipette, then incubated at room temperature for ten minutes. Following incubation, the samples were centrifuged at 12,000 rcf for 10 minutes at 4 ˚C. During centrifugation, the hinge of the Eppendorf was pointed upwards to ensure the RNA pellet would fall on the same side of the Eppendorf. The supernatant was carefully removed as the pellet is often not visible. The pellet was resuspended in 1 mL 75% ethanol (Sigma Aldrich) and pipetted up and down gently to ensure sufficient mixing. The suspension was then centrifuged at 7500 rcf for 5 minutes at 4 ˚C. After discarding the supernatant, the pellet was again resuspended in 75% ethanol. At this point, the suspension was placed at -80 ˚C for 1 hour to overnight. The centrifugation step was repeated and the supernatant was discarded, ensuring not to leave any liquid behind. The lid of the Eppendorf was left open and the pellet was allowed to air-dry for 10 minutes, ensuring not to completely dry the pellet as it would cause difficulty when resuspending. RNase-free water (20 µl – 50 µl) (Roche) was added to the pellet followed by gently pipetting up and down to ensure sufficient mixing. The sample was placed on a heat block at 55 ˚C for 10-15 minutes then cooled on ice for 5 minutes before quantifying. Samples were stored at -80 ˚C prior to downstream applications.

2.5.1.1 RNA Quantification

RNA was quantified using a NanoDrop 1000 spectrophotometer (Thermo Scientific). The NanoDrop was blanked using 2 µL of RNase-free water (Roche). Following instrument blanking, 2 µL of sample was added for quantification. The NanoDrop software provides RNA quantities in ng/µl as well as absorbance ratios A_{260}/A_{280} and A_{260}/A_{230} for an estimation of purity.

2.5.2 Reverse Transcription Polymerase Chain Reaction (RT-PCR)

Reverse transcription is a process where RNA is used as a template to produce complementary DNA (cDNA), a reaction that is enabled by a reverse transcriptase (RT) enzyme (**Figure 2.5**).

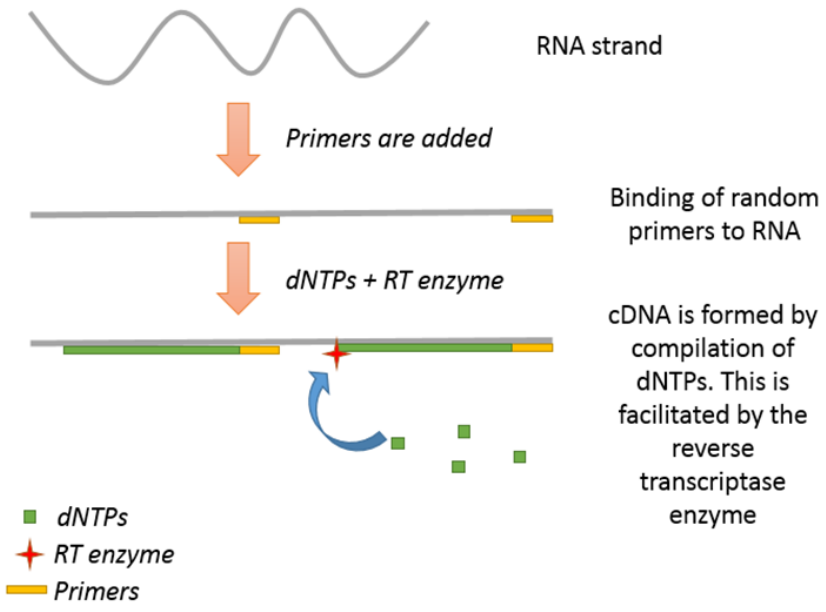

Figure 2.5: Formation of complementary DNA (cDNA) strand using reverse transcriptase (RT) enzyme.

All RT-PCR reactions were facilitated by the Transcriptor First Strand cDNA Synthesis kit (Roche Diagnostics). Following RNA quantification (section 2.5.1.1), the concentration of RNA to be used for RT-PCR was calculated. The volume of RNA to satisfy this concentration could not exceed 11 µl, and if required, PCR grade water (as supplied in kit) was added to the RNA to make up the volume. Throughout preparation of RNA/water, samples were kept on ice to prevent degradation of the RNA. Then 2 µl of random hexamer primers (as supplied in kit) was added to each sample. The tube was then capped and briefly spun in a microcentrifuge in order to ensure all of the sample was at the bottom of the tube. Each sample was then placed in a thermocycler (Techno) at 65 ˚C for 10 minutes to allow the primers to bind to the RNA. During this incubation, a master mix was prepared as detailed in Table 2.2. It is important to compensate for pipetting losses when calculating master mix volumes. Generally, a 10% increase is recommended, for example if there were 20 samples, enough master mix was prepared for 22 samples.

Table 2.2: Preparation guide for RT-PCR master mix following addition of primers to RNA/water samples.

Kit component	Volume per sample (µl)	Number of samples	Total volume of component (µl)
RT Reaction Buffer	4	N	(4 x N)
RNase Inhibitors	0.5	N	(0.5 x N)
dNTPs	2	N	(2 x N)
RT enzyme	0.5	N	(0.5 x N)
		Total Volume of Master Mix = (7 x N)	

Once all the relevant kit components were added, the master mix was vortexed gently and briefly spun in a microcentrifuge to pull the entire volume to the bottom of the tube. The samples were removed from the Thermocycler and 7 µl of master mix was added to each sample. The samples were mixed by gently flicking the capped tube, and briefly spun to pull all of the liquid to the bottom of the tube. They were then placed back in the thermocycler at 25 ˚C for 10 minutes, 50 ˚C for 60 minutes, 85 ˚C for 5 minutes and finally 4 ˚C for up to 2 hours. The samples could be stored at -20 ˚C until PCR, or if using immediately they were kept on ice.

2.5.2.1 Negative controls in RT-PCR

Negative controls are introduced into RT-PCR to ensure reliability of results. The first negative control used for every PCR experiment is called ‘no RT’. This is when PCR grade water is used as a substitute of RT enzyme during master mix preparation. Usually the sample with the highest amount of RNA is prepared twice, only with no RT added for the duplicate tube. This will give confidence to PCR results following amplification of cDNA because it eliminates the possibility that DNA has been introduced accidently into the reaction.

The second negative control introduced at this stage of PCR is called ‘no RNA’. This is simply an extra tube that has been carried through RT-PCR, however at the start of the reaction 11 µl of water is added with no RNA. This type of control also gives confidence to results by confirming that DNA has not been introduced to the reaction.

2.5.3 Quantitative Polymerase Chain Reaction (qPCR)

Quantitative PCR (qPCR) is a molecular technique used to amplify and obtain a relative quantity of DNA. This amplification is measured in real-time, which is why this method is often referred to as real-time qPCR (RT-qPCR). All qPCR reactions were carried out using sequence-specific probe sets (Roche, RealTime ready) that are compatible with the LightCycler 480 Probes Master kit (Roche Diagnostics). The kit comprises of a ready to use master mix which utilizes Taq DNA polymerase, the enzyme that drives the reaction.

Following RT-PCR, samples were thawed and tubes were placed in a microcentrifuge briefly to allow all contents to be recovered. All qPCR reagents were kept on ice throughout to avoid degradation. The qPCR master mix was prepared on ice using quantities described in Table 2.3, where the final volume depended on the number of wells needed. Pipetting losses were compensated for by increasing the required sample number by 10% before calculating the final master mix volume.

Table 2.3: Preparation guide for qPCR master mix.

Component	Volume per sample (µl)	Number of samples	Total volume of component (µl)
Water, PCR grade (Vial 2)	2	N	(2 x N)
Kit Master Mix (Vial 1)	5	N	(5 x N)
Probe (RealTime Ready)	1	N	(1 x N)
		Total Volume of final Master Mix = (8 x N)	

The final master mix was pipetted up and down gently to ensure sufficient mixing. The master mix preparation was repeated for each probe set required. *Note: Each sample was also run with a* β*-actin probe as the housekeeping gene.* Then 2 µL of each sample was pipetted into the relevant well, followed by 8 µL of final master mix. The plate was covered with plastic film and centrifuged for 2 minutes at 1500 rcf, 4 ˚C to ensure all contents are pulled to the bottom of the well. A LightCycler 480 PCR machine (Roche) was used to read the plate. The plate was read under the Roche template programme 'Monocolour Hydrolysis Probes', with an annealing temperature of 60 ˚C.

Results displayed in chapter 4 use probe sets obtained from Roche including TNF, IL-6 and IL-10. βactin was used as the housekeeping gene to calculate ΔCt values for each probe as it was found exhibit stable Ct values when tested with unstimulated and stimulated expanded Tregs (Appendix P).

Table 2.4: Roche probe sets used for qPCR experiments

Gene Name	Gene Symbol	Assay ID	Accession ID	Transcript length	Amplicon length
β actin	ACTB	143636	ENST00000331789	1917 bps	127 bps
Tumor Necrosis Factor	TNF	147880	ENST00000443707	1676 bps	76 bps
Interleukin-6	IL6	144013	ENST00000404625	1527 bps	88 bps
Interleukin-10	IL10	137154	ENST00000423557	1630 bps	65 bps

2.5.3.1 Negative controls in qPCR

Negative controls are introduced into qPCR to ensure reliability of results. The first negative control used for every qPCR experiment is called a 'no probe control'. This

is when PCR grade water is substituted for the probe during master mix preparation. Usually, the sample with the highest amount of RNA is prepared with double the quantity at the RT-PCR stage. This is to ensure there is enough leftover sample for the 'no probe' control. Inclusion of the 'no probe' control gives confidence that any signal produced when a probe is present is true signal.

The second negative control used in qPCR is called a 'no cDNA control'. This is simply when the sample is substituted for PCR grade water supplied in the kit. The 'no cDNA control' alongside the 'no RNA control' from the RT-PCR reaction gives confidence that no contaminating DNA has been introduced into the process. If one of the negative controls gives a signal at the PCR stage, the presence of both helps to determine the reagent in which the contaminant was introduced. However, any probes used were exon spanning in order to reduce measurement of genomic DNA.

2.5.4 Data analysis

Following RT-PCR and qPCR, plates were run on the LightCycler 480 using LightCycler 480 Software (release 1.5.0 SP4). The cycler threshold (Ct), which is the number of amplification cycles it has taken for the fluorescent signal to be detected, was recorded for each well. The ΔCt value was calculated by subtracting the Ct value of the housekeeping gene β-actin from that of the gene of interest. This value was then inverted by using the equation (1/ΔCt) *100, and the results were plotted and analysed.

2.6 Proteomic Methods

2.6.1 Proseek multiplex

Plasma from each patient, extracted as described in section 2.1.2, was thawed and a small volume of ~40 µl was sent to OLINK (Analysis service Uppsala, Sweden). Each sample was analysed across OLINK's CVD II, CVD III, immune response and inflammatory panels (Appendix F). Each high throughput multiplex immunoassay consists of 92 proteins. The technology used is known as 'Proximity Extension Assay' (PEA), where matched antibody pairs containing unique DNA sequences are incubated with the sample. Sequences that are exactly matched will hybridize and are extended using DNA polymerase. The elongated DNA can then be amplified and a qPCR readout using Fluidigm® BioMARK™ is used to determine the results of each protein target. The assay includes internal controls at each stage of the reaction, negative controls to determine background values, and inter-plate controls to account for variability between plates. ΔCt values are log normalised to what is called 'normalised protein expression' values or NPX.

2.6.1.1 PEA analysis: Statistical methods

Perseus software (version 1.6.0.7) was used to analyse the vast range of NPX values across patient groups (Tyanova *et al.* 2016). A Z-score was performed across the entire data set in order to standardise the NPX values. The order in which each analysis was carried out is summarised in **Figure 2.6**. To visualise significant changes in protein expression between groups, initially a volcano plot was drawn using a two sided t-test. In order to filter data based on significance of differentially expressed

proteins across all patient groups, an analysis of variance (ANOVA) test was carried out. These proteins were expressed in a heat map with unsupervised clustering. The ANOVA test was carried out either with or without permutation-based false discovery rate (FDR) depending on the analysis required, as detailed in section 2.6.1.2. Following this statistical analysis, bioinformatic analysis was carried out using online pathway programmes including STRING (Szklarczyk *et al.* 2017), Enrichr (Kuleshov *et al.* 2016), and Reactome (Fabregat *et al.* 2017). These programmes were used to assess the association of significant proteins with various immune pathways.

Diagram	Method used	Comments
Volcano Plot	Two-tailed t-test	The volcano plot was used as an initial visualisation of the variation of data between patient groups. However, at this step the data was not filtered. The y axis represents the -Log10(p value), and the x-axis represents the difference between the Z scored NPX value in each patient group. The significance threshold was set when the p value was less than 0.05 (-Log10(0.05) = 1.3), and the fold change in protein expression was ≥2.
Heat Map	Analysis of variance (ANOVA)	Initially, the ANOVA test was used to assess the significant changes in protein expression when considering all patient groups. The analysis was adjusted to include permutation-based false discovery rate (FDR), where significance was determined based on a q value of less the 0.05. The proteins calculated to be significantlly differentially expressed across all patient groups were plotted as a heatmap. Unsupervised clustering was plotted in a hierarchical manner, determined based on the euclidean distance between data points.
Protein pathways (Literature mining)	STRING	STRING was used to visualise interactions between the proteins that are significantly differentially expressed between patient groups, as calculated by the ANOVA test.
	Enrichr	Enrichr was used to obtain information initially on diseases associated with the proteins of interest. This analysis calculates significance of literature evidence based on a p-value of less than 0.05. Enrichr then combines p-value with Z-score to calculate an adjusted overall score ranking the significance of association of the inputed proteins with disease. Additionally, Enrichr provides information regarding immune pathways that the proteins are associated with. Reactome is one of many programmes used by Enrichr for this analysis.
	Reactome	Reactome determines the involvement of the inputed proteins in various immune pathways. Pathways are ranked by significance of literature evidence based on a p value of less than 0.05. Reactome was used to highlight the most significant pathways with which multiple proteins of interest are associated.

Figure 2.6: Flow chart showing the order of which OLINK data was analysed, and the rationale for each step.

2.6.1.2 Comparisons of OLINK data to clinical and cellular data

The patient subgroup comparisons made with PEA data are broken into 4 sections as detailed below. On analysing A and B, the more stringent ANOVA test with permutation based FDR was used. However, on analysing sections C and D, the less stringent ANOVA test without FDR was used due to the low patient number present

in the group (C) or in due to the lack of significance observed using the more stringent test (D).

A) cDMARD response: (Section 5.1.1) Initially, the aim was to determine whether a subset of circulating proteins distinguish cDMARD treatment response in RA. Patients were grouped according to EULAR response criteria, and data was analysed as detailed in section 2.6.1.1.

B) Disease activity: (Section 5.1.2) The above analysis was repeated when patients were grouped by DAS28-ESR score according to EULAR disease activity criteria, recorded on the day of sampling. A score of ≥5.1 was classified as 'high' disease activity, >3.2 and ≤5.1 was 'moderate', >2.6 and ≤3.2 was 'low', and <2.6 was classified as 'remission'. The aim was to determine whether the circulating proteome is associated with disease activity in RA, thus discovering which proteins may be involved in disease pathogenesis and subsequently treatment response.

C) Biologic DMARD Response: (Section 5.1.3) The last comparison involved patients treated with biological DMARDs who were sampled before treatment and after 6 months. These patients were grouped according to response to treatment. The aim of this analysis was to determine whether circulating proteins correlate with biological DMARD treatment response, and if so whether these proteins are the same as those representative of cDMARD treatment response.

D) Immunophenotype: (Section 5.1.4) Additionally, a comparison was made between the OLINK data and previous immunophenotype and flow cytometry data (chapter 3 and 4). The aim of this analysis was to determine associations between pathologically relevant cells in circulating blood and changes in circulating proteins.

2.6.2 Enzyme-linked immunosorbent assay (ELISA)

2.6.2.1 DuoSet ELISAs

Following cell culture experiments (section 2.4), cell supernatants were analysed by DuoSet ELISA for quantification of human TNFα, human IL-10 and human IFN-γ (R&D systems). Before beginning, the kit contents were brought to room temperature. The capture antibody was prepared according to the instructions for each specific kit (Table 2.5). The wells of a 96-well plate were then coated with 100 µL of the diluted antibody. The plate was sealed and incubated overnight at 18 ˚C with gentle shaking of 300 rpm.

Table 2.5: Preparation of capture antibody for DuoSet ELISAs

Capture Antibody	Quantity supplied (µg)	Reconstitution	Working concentration (µg/ml)	Dilution required from stock
TNFα	240	500 mL PBS	4	1/120
IL-10	120	500 mL PBS	2	1/120
IFN-γ	240	500 mL PBS	4	1/120

Following overnight incubation, the contents of each well was discarded and washed 3 times with 1x wash buffer. After the last wash, any remaining wash buffer was removed by inverting the plate and blotting against dry paper towels. Each well was then blocked with 300 µL block buffer and incubated for 1 hour at 18 ˚C on a shaker at 300 rpm. Following blocking, the wash step was repeated and the plate was blotted dry on tissue paper as before. Standards were prepared as detailed in Table 2.6, and samples were diluted 1:1 with reagent diluent. Then 100 µL of each standard

or sample was added to wells in replicates of 2, and the plate was covered and incubated for 2 hours at 18 ˚C on a shaker at 300 rpm.

Table 2.6: Preparation of highest standard for DuoSet ELISAs. This highest standard was diluted 1:1 with reagent diluent to produce the next level standard. This dilution series was repeated until there was a range of 7 standards.

Standard	Quantity supplied (ng)	Reconstitution in reagent diluent	Working concentration of highest standard (pg/ml)	Dilution required from stock
TNFα	67.5	500 mL	1000	1/135
IL-10	75	500 mL	2000	1/75
IFN-γ	55	500 mL	1000	1/110

Following incubation of standards and samples, the wash step was repeated. The plate was blotted dry as before and 100 µL of detection antibody was added to each well (Table 2.7). The plate was incubated with detection antibody for 2 hours at 18 ˚C on a shaker at 300 rpm.

Table 2.7: Preparation of detection antibody for DuoSet ELISAs.

Detection Antibody	Quantity supplied (µg)	Reconstitution in reagent diluent	Working concentration (ng/ml)	Dilution required from stock
TNFα	18	1 mL	300	1/60
IL-10	4.5	1 mL	75	1/60
IFN-γ	12	1 mL	200	1/60

The plate was then washed and blotted dry as before. Then 100 µL of streptavidin-horseradish peroxidase (HRP) was added to each well and the plate was covered with foil to protect from light. The plate was incubated for 20 minutes at 18 ˚C on a shaker at 300 rpm. The wash step was repeated as before and the plate was blotted dry. Then 100 µL of substrate solution was added to each well and the plate was covered in foil to protect it from light. The plate was then incubated for 20 minutes at 18 ˚C on a shaker at 300 rpm. Then 50 µL of stop solution was added to each well and the plate was gently tapped to ensure sufficient mixing. The optical density (OD) was determined using an EPOCH plate reader (Biotek) with Gen5^{TM} software. The plate was read at a wavelength of 450 nm and 540 nm. The OD values at 540 nm were subtracted from those at 450 nm in order to account for wavelength correction. A standard curve was plotted using the ODs and known concentrations from the standards. Using the y=mx+c equation produced by the standard curve, the concentrations of the unknown samples were then calculated.

2.6.2.2 Proximity extension assay validation by ELISA

In order to validate the changes in protein expression observed from the OLINK data set, two of the proteins of interest were selected to be quantified by ELISA.

2.6.2.2.1 Caspase-3

The first protein quantified by ELISA was Caspase-3 (CASP-3), using the Human CASP3/Caspase 3 ELISA kit (sandwich ELISA) sourced from LifeSpan BioSciences, Inc. The kit was brought to room temperature (18 ˚C) before preparation of the standard. The CASP-3 standard was reconstituted in 1 mL of sample diluent to make a stock concentration of 20 ng/ml. Then 500 µL of the stock solution was pipetted into an

Eppendorf as the highest concentration standard. Then 250 µL of the highest standard was pipetted into a fresh Eppendorf and diluted 1:1 with sample diluent in order to make the next standard. This was repeated until there was a total of 7 standards, with the lowest concentration of 0.313 ng/mL. A blank of only sample diluent was included as the lowest standard. The plasma samples were thawed on ice and diluted 1:1 with sample diluent. Then 100 µL of standard or sample was pipetted in duplicate into corresponding wells of the provided 96-well plate. The plate was covered with a provided sealer and incubated for 90 minutes at 37 ˚C on a shaker at 150 rpm. Following incubation, the liquid of each well was removed and discarded using a multi-channel pipette. Then 100 µL of biotinylated detection antibody was added to each well and the plate was recovered with a fresh plate sealer. The plate was incubated for 1 hour at 37 ˚C on a shaker at 200 rpm. Following incubation, the liquid was aspirated and the wells were flooded with wash buffer using a squirt bottle. The plate was allowed to sit for 1-2 minutes before aspirating the liquid and repeating this wash step 3 times. Following the last wash, the liquid was aspirated and the plate was inverted and gently blotted on paper towels to remove any excess liquid. Then 100 µL of HRP conjugate working solution was added to each well and the plate was covered with a sealer. The plate was incubated for 30 minutes at 37 ˚C on a shaker at 150 rpm. Following incubation, the liquid was discarded and the wells were washed a total of 4 times as before. The plate was blotted onto paper towels to dry and 90 µL tetramethylbenzidine (TMB) substrate solution was added to each well. A plate sealer was added and the plate was incubated for 15 minutes at 37 ˚C on a shaker at 150 rpm. During this incubation step, the plate was covered with aluminium foil to protect from light. Then 50 µL stop

solution was added to each well following development and the ODs for each well were determined using an EPOCH plate reader (Biotek) with Gen5^{TM} software. The plate was read at a wavelength of 450 nm and 540 nm. The OD values at 540 nm were subtracted from those at 450 nm in order to account for wavelength correction. A standard curve was plotted using the ODs and known concentrations from the standards. Using the y=mx+c equation produced by the standard curve, the concentrations of the unknown samples were then calculated.

2.6.2.2.2 CD40 Ligand

CD40 Ligand (CD40-L) was also quantified by ELISA, using the Human CD40 Ligand/TNFSF5 Quantikine®ELISA kit (R&D systems). The kit was brought to room temperature (18 ˚C) prior to use. 100 µL of assay diluent as supplied in the kit was added to each well. CD40-L standard was reconstituted in 1 mL of ddH_2O to make a stock concentration of 40,000 pg/mL. Then 100 µL of standard was added to 900 µL calibrator diluent to make the highest standard at a concentration of 4000 pg/mL. Then 500 µL was taken out of the top standard into a fresh tube and diluted 1:1 with diluent. This was repeated until there were a total of 7 standards. A blank containing only calibrator diluent was also included as the lowest standard. Plasma samples were thawed on ice and diluted 1:1 with calibrator diluent. Then 100 µL of standard or sample was added in duplicate to corresponding wells. The plate was covered with a sealer and incubated for 2 hours at 18 ˚C on a shaker at 450 rpm. Following incubation, the liquid of each well was discarded and the wells were flooded using a squirt bottle containing 1x wash buffer. This was repeated 3 times and the plate was blotted onto tissue paper to remove excess liquid. Then 200 µL of Human CD40

Ligand Conjugate, as supplied in the kit, was added to each well. A new plate sealer was added and the plate was incubated at 18 ˚C for 2 hours on a shaker at 450 rpm. Following incubation, the liquid was discarded from each well and the wash step was repeated 4 times as before. The plate was blotted dry on paper towels and 200 µL of substrate solution was added to each well. The plate was incubated for 30 minutes at 18 ˚C and covered with aluminium foil to protect from light. Then 50 µL stop solution was added to each well to stop the development. ODs for each well were determined using an EPOCH plate reader (Biotek) with Gen5^{TM} software. The plate was read at a wavelength of 450 nm and 540 nm. The OD values at 540 nm were subtracted from those at 450 nm in order to account for wavelength correction. A standard curve was plotted using the ODs and known concentrations from the standards. Using the y=mx+c equation produced by the standard curve, the concentrations of the unknown samples were then calculated.

Chapter 3

Monocytes and Tregs, the key cells in RA

3.0 Introduction

Rheumatologists commonly use the disease activity score across 28 joints (DAS28) to determine whether a patient has responded to treatment. The DAS28 is assessed before and during DMARD therapy, however response is frequently not determined until 3-6 months after commencing treatment. Many studies have highlighted weaknesses with DAS28, especially due to the use of CRP or ESR in the composite score. Additional to being non-specific markers of inflammation, environmental and lifestyle factors may play a role in the elevation of CRP and ESR (Kushner *et al.* 2006; Kushner *et al.* 2010). Several studies indicate that ESR and CRP can be poor markers of inflammation, namely due to their lack of correlation with disease activity, and therefore their elevation can be misleading (Sheehan *et al.* 1986; Ruof and Stucki 1999; Baum *et al.* 2008). Thus there is a strong clinical need for more specific biomarkers that are directly associated with disease activity in RA. Such markers would ideally enable treatment response to be determined at an early stage, enabling non-responders to switch to an alternative DMARD medication sooner than currently possible. Furthermore, identifying those with highly active or potentially subclinical disease would be extremely useful for clinicians to direct DMARD treatment. Finding the correct treatment for individual patients soon after diagnosis could potentially improve clinical outcome. This chapter investigates how the immunophenotype of pathologically relevant circulating cells relates to clinical measures of disease activity.

3.0.1 Monocyte subsets

As mentioned in section 1.1.2, monocytes and macrophages are key mediators of the inflammatory response, and have been widely studied in RA patients due to their increase during active disease (Huang *et al.* 2007; Chara *et al.* 2015). Furthermore, an increasing number of studies have emerged that subdivide CD14 positive monocytes into resident or inflammatory subsets, depending on the presence or absence of CD16, respectively (Passlick *et al.* 1989; Auffray *et al.* 2009). Inflammatory $CD14^{++}CD16^{-}$ monocytes are also termed classical M1 type monocytes, whereas resident M2 type monocytes can be further subdivided into $CD14^{++}CD16^{+}$ intermediate and $CD14^{+}CD16^{++}$ non-classical.

Previous studies have highlighted the differences between these subsets in relation to RA. Resident $CD16^{+}$ monocytes have been shown to increase during active RA (Kawanaka *et al.* 2002; Cairns *et al.* 2002), whereas $CD16^{-}$ classical monocytes are reduced in RA peripheral blood compared to healthy controls (Lacerte *et al.* 2016). However, classical and intermediate dominate over non-classical macrophages in RA synovial fluid (Lacerte *et al.* 2016). Additionally, a previous study demonstrated an increase in intermediate, but not classical or non-classical monocytes and macrophages in RA peripheral blood and synovial fluid compared to healthy controls (Yoon *et al.* 2014). This increased expression of CD16 on synovial macrophages was shown to be induced by inflammatory cytokine transforming growth factor-beta (TGF-β) (Yoon *et al.* 2014). Furthermore, although the main function of classical monocytes has previously been believed to be phagocytic (Ziegler-Heitbrock 2000), a recent study demonstrated their ability to produce pro-inflammatory cytokines

including IL-6 and TNFα following *in vitro* stimulation with TLR2 and TLR9 agonists (Lacerte *et al.* 2016).

The number of circulating monocyte subsets has been linked to treatment response in RA patients. A previous prospective study by Chara *et al*. demonstrated the role of the absolute count of monocytes, as well as each monocyte subset in predicting anti-TNF treatment response (Chara *et al.* 2012). More recently, the group analysed monocyte differences in RA responders and non-responders to MTX both before and during treatment. They found that the numbers of each subset were increased in non-responders compared to responders and healthy controls. Furthermore, the number of classical and intermediate monocytes had predictive value in determining response to MTX before starting the drug (Chara *et al.* 2015).

3.0.2 The monocyte-Treg interplay in RA

Evidence to date implies monocytes play a role in RA pathogenesis and may be clinically useful in determining treatment response. However, additional studies have highlighted the need to consider the interplay between monocytes and T cells. Localisation of macrophages and T cell clusters have been identified within the inflamed synovium, suggesting they may interact at the inflamed site (Fonseca *et al.* 2002). *In vitro* studies have demonstrated the ability of synovial macrophages to promote Th1 and Th17 responses in $CD4^+$ T cells (Yoon *et al.* 2014), for example the induction of pro-inflammatory cytokines which in turn releases damage-causing enzymes.

Additional studies have found an association between RA monocytes and Tregs, and the potential effects monocytes exhibit on Treg activation. An increase in IL-6 and IL-

23 secretion was observed from monocyte derived dendritic cells, which was associated with the induction of Th17 cells and Tregs in RA (Estrada-Capetillo *et al.* 2013). Similarly, activated monocytes were shown to increase the percentage of Tregs possessing intracellular inflammatory cytokines IL-17, IFN-γ, TNFα and IL-10 (Walter *et al.* 2013). Interestingly, the increase in Treg cells was induced by monocyte derived cytokines, including IL-6 and TNFα (Walter *et al.* 2013).

3.0.3 CD169 (Siglec-1) interacts with CD43

CD169 (Siglec-1) is a cell surface protein present on monocytes and macrophages. CD169 expression is associated with pro-inflammatory mechanisms in the immune response, displaying involvement in effector T cell induction as well as secretion of cytokines such as IFN-γ from activated T cells (Jiang *et al.* 2006). As detailed in section 1.1.4.1, previous studies have shown an association between increased levels of $CD169^{+}$ monocytes and RA (Hartnell *et al.* 2001; Xiong *et al.* 2014). Furthermore, a number of studies have highlighted the direct involvement of CD169 expression with disease pathogenesis in RA among other autoimmune conditions (York *et al.* 2007; Xiong *et al.* 2014). Circulating relative numbers of $CD169^{+}$ monocytes also show correlation with clinical measures of disease activity in RA, and significantly reduce as a result of treatment response (Xiong *et al.* 2014).

It is thought that CD169 can bind to ligands on the surface of Tregs, and that direct cell-cell binding could contribute to Treg suppression (Wu *et al.* 2009), which further suggests the function of CD169 to be pro-inflammatory. Previous studies have uncovered CD169 ligands on the surface of Tregs that may play a role in Treg activity, including CD43 (van den Berg *et al.* 2001). CD43 is a sialoglycoprotein expressed on

nucleated cells. It has been associated with T cell activation, where proliferation is observed following CD43 stimulation *in vitro* (Higashi *et al.* 2001). Importantly, CD43 was previously shown to partake in the activation of monocytes and Tregs (Axelsson *et al.* 1988; Nong *et al.* 1989; Piller *et al.* 1989; Park *et al.* 1991). Furthermore, a more recent finding demonstrated direct binding between CD169 and CD43 using immunostaining, suggesting CD169 and CD43 are involved in the interaction of monocytes and T cells (Ohnishi *et al.* 2013).

CD43 expression is increased during inflammation on synovial cells including lymphocytes and neutrophils in an adjuvant induced arthritis model (Volin *et al.* 1999). However, conflicting results show CD43 is downregulated in synovial neutrophils of RA patients (Humbria *et al.* 1994; Lopez *et al.* 1995). Other intriguing studies have demonstrated a role for CD43 in relation to HIV. CD43-directed autoantibodies have been observed in HIV infected patients (Ardman *et al.* 1990), which on further investigation are related to differential patterns of CD43 glycosylation (Lefebvre *et al.* 1994). Additional studies have linked CD43 to Wiskott-Aldrich syndrome, which further suggests it plays role in autoimmunity (Remold-O'Donnell *et al.* 1984).

In summary, the interaction between monocytes and Tregs plays an important role in RA pathogenesis. This thesis postulates that CD169 is involved in Treg suppression via CD43 interaction, however the balance between these two cell types is unclear. This study focuses on establishing the relationship between disease activity in RA and the balance of $CD169^{+}$ monocytes and $CD43^{+}$ Tregs in peripheral blood. This chapter specifically addresses the objective to identify circulating biomarkers of RA disease

activity in order to aid clinical decision making and subsequently improve overall patient outcome.

3.1 Results

3.1.1 Decreased absolute numbers of circulating monocytes in DMARD responders compared to non-responders

As part of routine blood testing, full blood counts (FBCs) were carried out on the same day as sampling. The absolute number of monocytes present in each sample was obtained retrospectively from the online electronic care record of the sampling date. Healthy control samples were anonymously analysed for FBC in Altnagelvin Hospital (WHSCT), and results were obtained on the same day. The absolute number of circulating monocytes in DMARD responders ($0.527x10^9$/l ± 0.097, n=23) and non-responders ($0.670\ x10^9$/l ± 0.229, n=30) were significantly increased compared to healthy controls ($0.452\ x10^9$/l ± 0.097, n=19, p=0.019 and 0.0003 respectively) (**Figure 3.1**). There was no statistically significant difference between healthy controls and DMARD naïve patients ($0.552\ x10^9$/l ± 0.223, n=6, p=0.407). Additionally, the absolute number of monocytes in responders was significantly lower than non-responders (p=0.041).

3.1.2 Relative number of $CD16^+$ monocytes increase and $CD16^-$ monocytes decrease in RA compared to health

FACS analysis was used to assess the relative numbers of circulating $CD14^+$ monocytes in RA patients and healthy controls. In order to isolate monocytes,

samples were initially enriched using the pan monocyte isolation kit (Miltenyi Biotec) and the autoMACS Pro separator, as detailed in section 2.2. The relative number of $CD14^{++}CD16^{-}$ classical monocytes was significantly decreased in RA responders (21.37% ± 9.68, n=24) and non-responders (22.09% ± 15.03, n=32) to DMARD treatment, compared to healthy controls (45.03% ± 20.33, n=19, p<0.001) (**Figure 3.1**). However, the relative number of $CD14^{+}CD16^{++}$ non-classical monocytes was increased in RA patients compared to healthy controls (7.595% ± 2.606, n=19), reaching statistical significance in DMARD responders (10.93% ± 4.978, n=24, p=0.017). Furthermore, the relative number of $CD14^{++}CD16^{+}$ intermediate monocytes was significantly increased in both responders (66.37% ± 10.31, n=24, p=0.004) and non-responders (66.90% ± 13.90, n=32, p=0.001) compared to healthy controls (45.83% ± 21.31, n=19). However, no statistically significant difference was observed between responders and non-responders across any of the monocyte subsets.

3.1.3 Increased $CD169^{+}$ monocytes in RA patients compared to healthy controls

The percentage of CD169 was analysed in classical, non-classical and intermediate monocytes by FACS. Overall, CD169 percentage was increased in RA patients compared to healthy controls when considering each patient subgroup (**Figure 3.2**). RA patients who are DMARD naïve (21.83% ± 22.80, n=6, p=0.039) and DMARD responders (21.89% ± 26.31, n=24, p=0.014) have a significantly increased relative number of $CD169^{+}$ classical monocytes compared to healthy controls (9.426% ± 5.890, n=19), however the difference was not statistically significant in DMARD non-responders (19.83% ± 26.40, n=32, p=0.185) compared to healthy controls. A similar

observation was made in non-classical monocytes, where CD169 percentage was increased in DMARD naïve (30.10% ± 18.41, 0.014), DMARD responder (30.95% ± 16.73, p<0.001) and DMARD non-responder (30.68% ± 15.05, p<0.001) RA patients compared to healthy controls (12.15% ± 8.392). Additionally, CD169 percentage was increased in intermediate monocytes for each patient group compared to healthy controls (13.87% ± 9.778), however only with statistical significance in DMARD naïve patients (30.02% ± 23.00, p=0.011). Furthermore, the MFI of CD169 on the surface of classical and intermediate monocytes was increased in DMARD non-responders compared to other patient groups and healthy controls, however without reaching statistical significance.

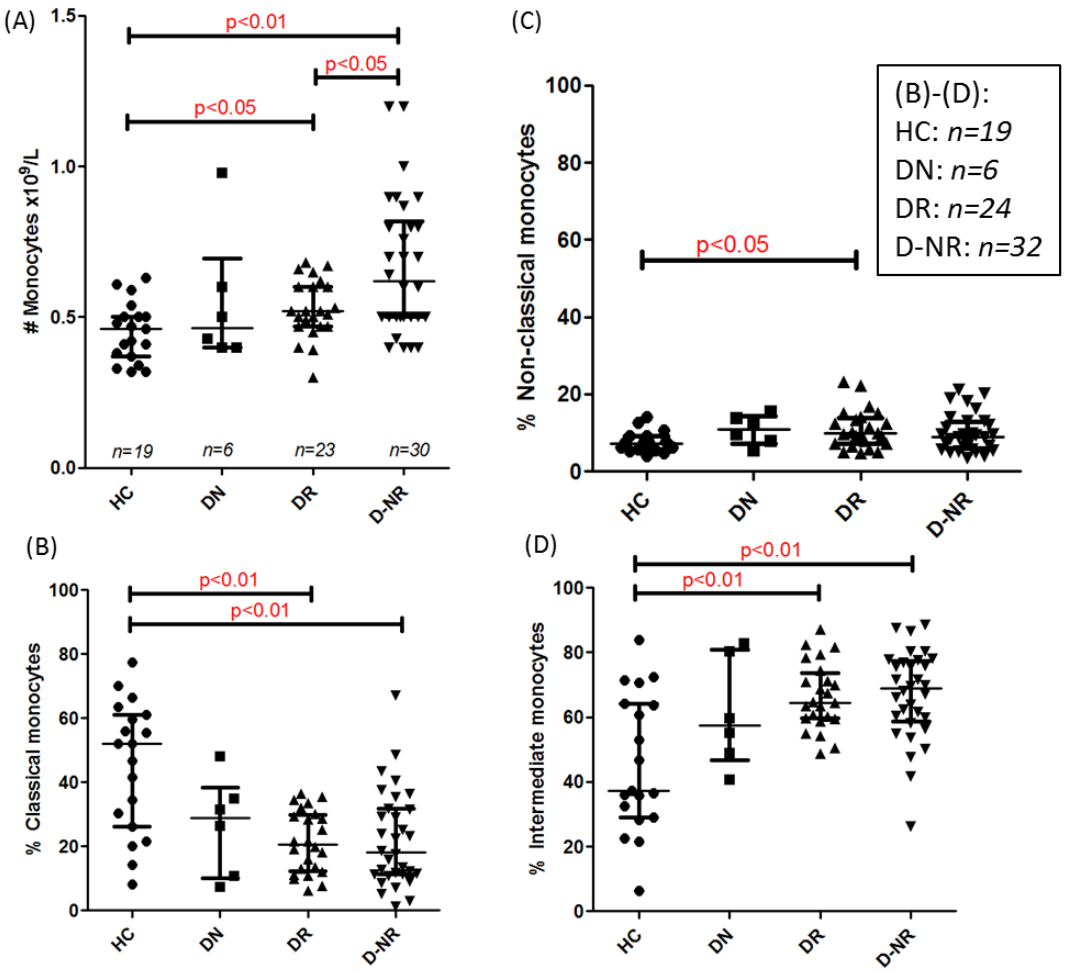

Figure 3.1: (A) The absolute number of monocytes as measured by FBC in healthy controls and RA patients. The percentage of classical (B), non-classical (C) and intermediate (D) monocytes in healthy controls and RA patients. P values shown were obtained using unpaired t-tests or Mann Whitney tests depending on normality of distribution. Error bars represent interquartile range. HC=healthy controls, DN=DMARD naïve, DR=DMARD responder, D-NR= DMARD non-responder.

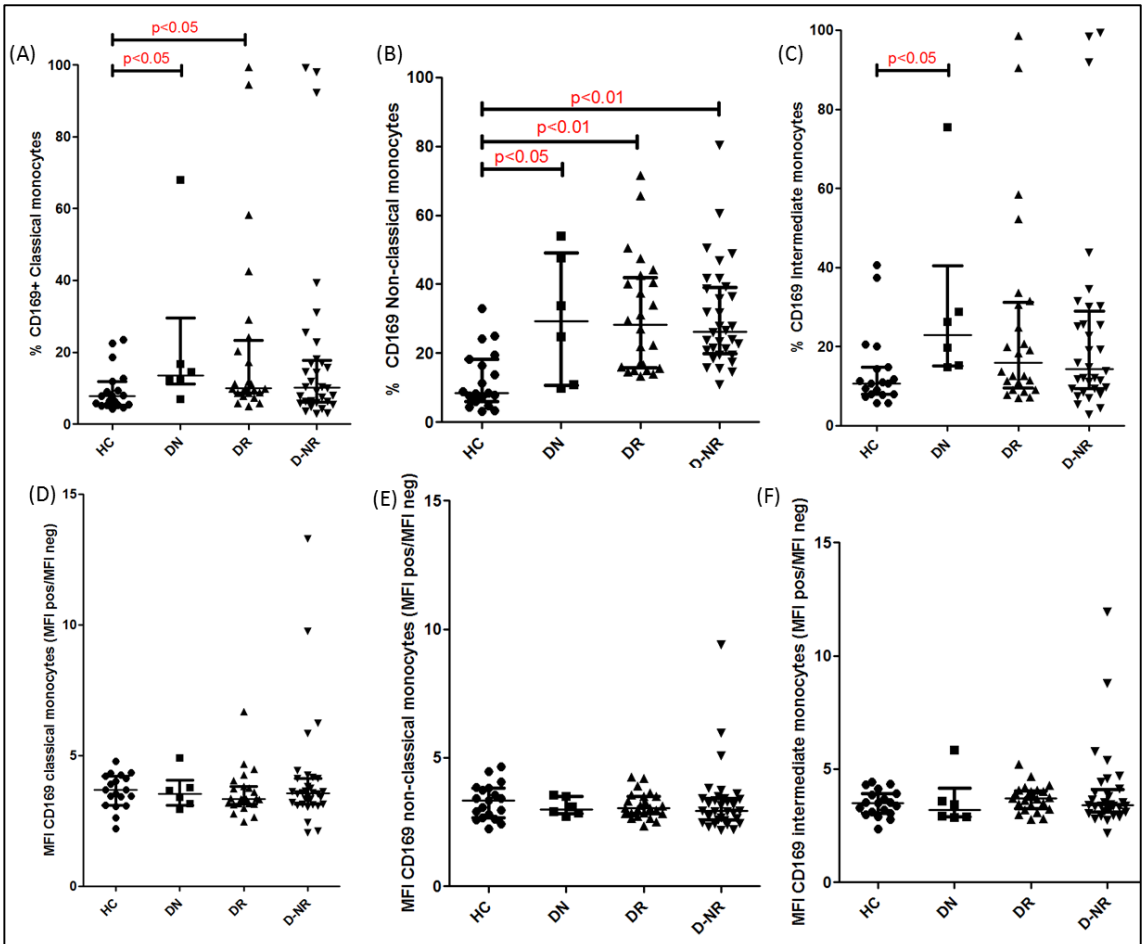

Figure 3.2: (A-C) The relative number of CD169^{+} classical (A), non-classical (B) and intermediate (C) monocytes in healthy controls and RA patients. (D-F) CD169 MFI levels of classical (D), non-classical (E) and intermediate (F) monocytes in healthy controls and RA patients. P values shown were obtained using Mann Whitney tests. Error bars represent interquartile range. HC=healthy controls (n=19), DN=DMARD naïve (n=6), DR=DMARD responder (n=24), D-NR= DMARD non-responder (n=32), MFI = Median fluorescence intensity.

3.1.4 Decreased CD43^{+} Tregs in RA compared to health

CD43 positivity was analysed as a percentage of CD4^{+}CD25^{+}CD127^{-} Tregs using FACS. The relative number of CD43^{+} Tregs was reduced in each patient group compared to

healthy controls (96.94% ± 2.434, n=19), however only with statistical significance in DMARD responders (94.37% ± 2.698, n=24, p=0.001) (**Figure 3.3**). Furthermore, the relative number of CD43^{+} Tregs was significantly reduced in DMARD responders compared to DMARD naïve (96.37% ± 2.524, n=6, p=0.049) and non-responder patients (95.41% ± 4.647, n=32, p=0.024). Additionally, the MFI of CD43 on the surface of Tregs was reduced in each RA patient group compared to healthy controls (23.44MFI ± 27.96), however significance was only observed in non-responders (10.34MFI ± 11.55, p=<0.001).

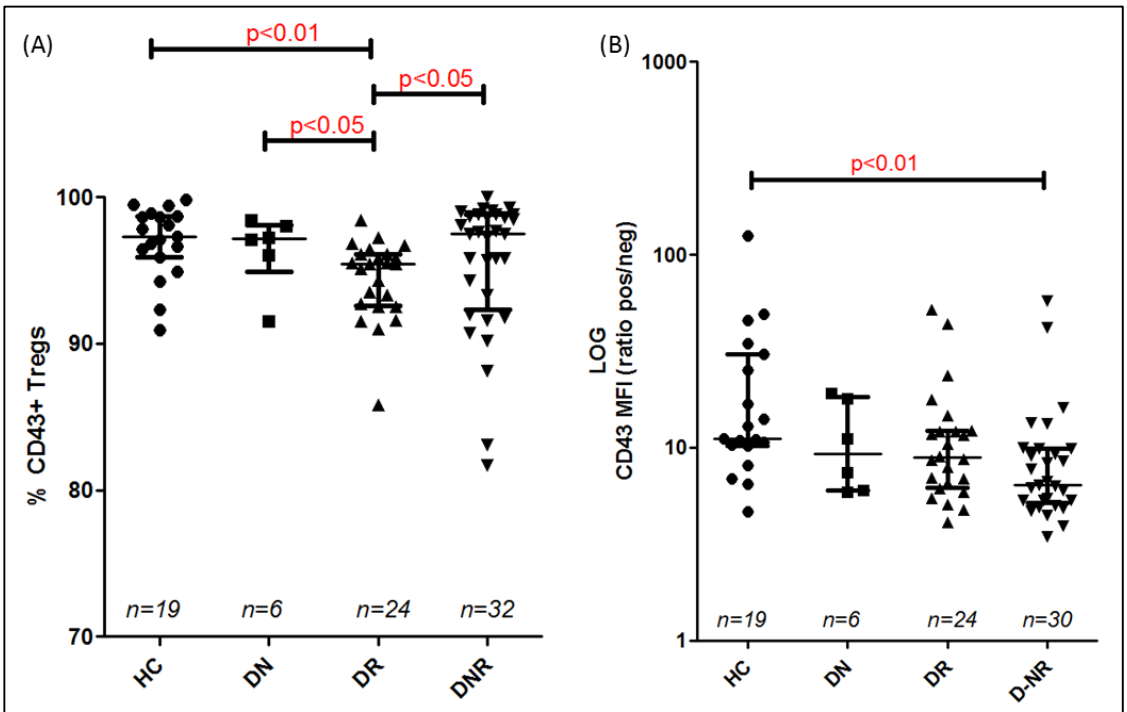

Figure 3.3: (A) The relative number of CD43^{+} Tregs in healthy controls and RA patients. (B) The LOG of CD43 MFI in Tregs of healthy controls and RA patients. P values shown were obtained using Mann Whitney tests. Error bars represent interquartile range. HC=healthy controls, DN=DMARD naïve, DR=DMARD responder, D-NR= DMARD non-responder, MFI = Median fluorescence intensity.

3.1.5 The balance between CD169 and CD43 may be related to disease activity

The DAS28-ESR score was assessed on the day of sampling and recorded. A significant positive association was observed between DAS28-ESR and the percentage of CD169 on classical (p=0.022, r=0.424, n=29), non-classical (p=0.012, r=0.459, n=29) and intermediate (p=0.017, r=0.440, n=29) monocytes (**Figure 3.4**). However, the relative number of $CD169^+$ non-classical monocytes showed the most significance. The relative number of $CD43^+$ Tregs had no significant association with DAS28-ESR (p=0.868, r=0.032, n=29).

Additionally, the CD169 MFI of monocytes was compared to DAS28-ESR (**Figure 3.5**). A weak positive association was observed between DAS28-ESR and the CD169 MFI of classical monocytes (p=0.156, r=0.271, n=29), however without statistical significance. No significant association was observed between DAS28-ESR and the CD169 MFI of non-classical monocytes (p=0.920, r=0.019, n=29). However, a significant positive association was observed between DAS28-ESR and the CD169 MFI of intermediate monocytes (p=0.024, r=0.420, n=29).

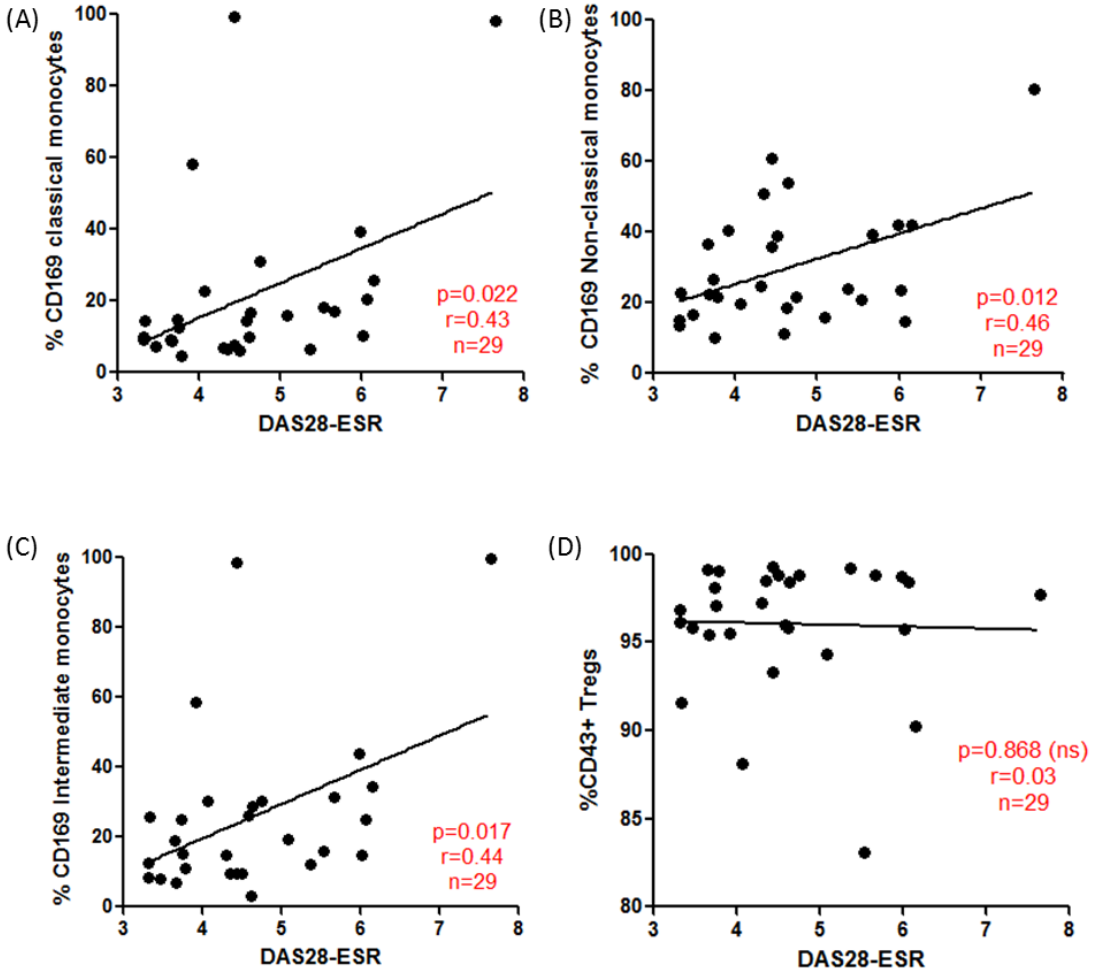

Figure 3.4: (A-C) The association between the relative number of CD169^{+} classical (A), non-classical (B) and intermediate (C) monocytes and DAS28-ESR. (D) The association between CD43^{+} Tregs and DAS28-ESR. Linear regression was used to assess significance, with 95% CI. Data points were included if DAS28-ESR was available and patients has a moderate or high disease activity, as defined by EULAR criteria.

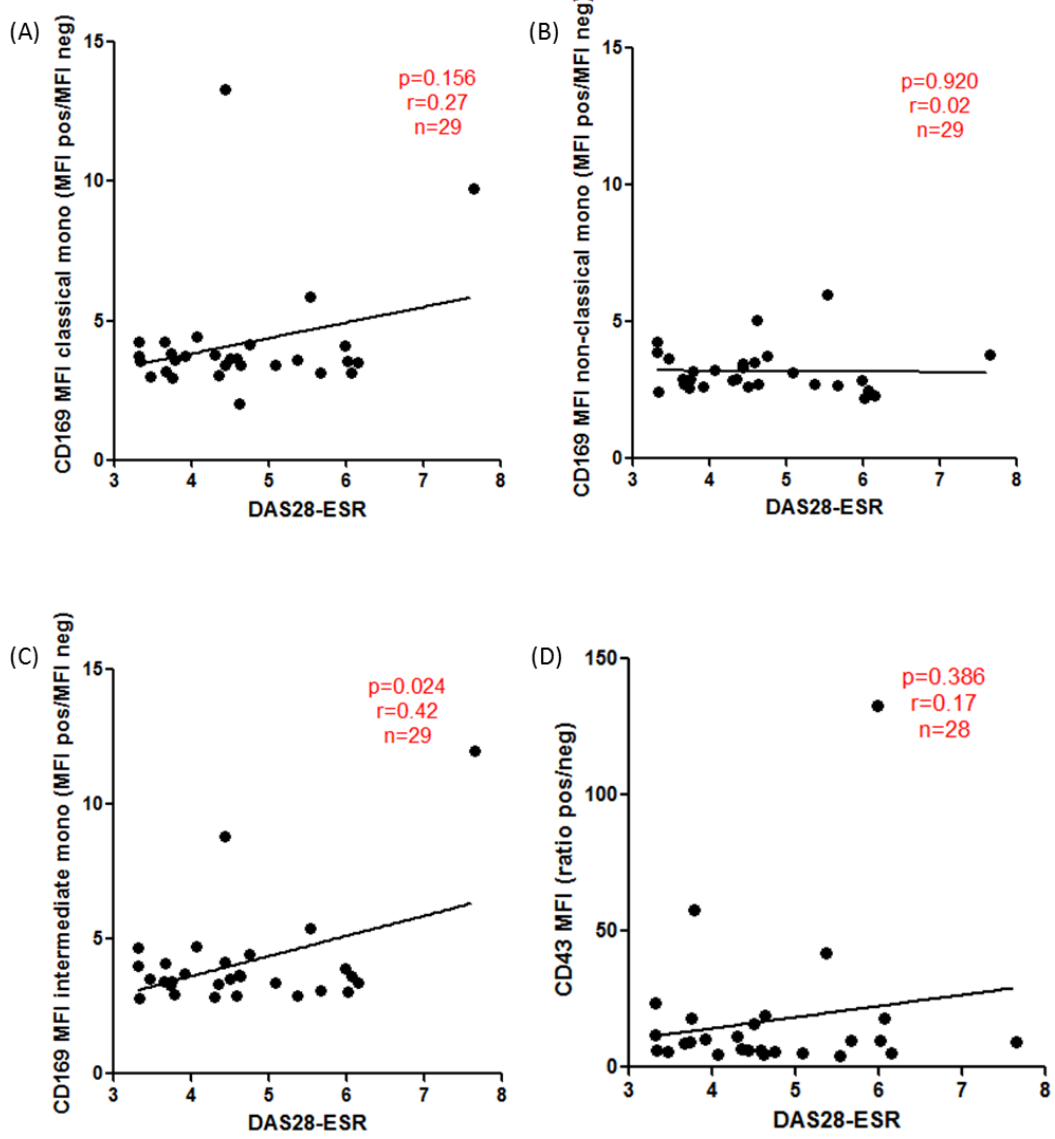

Figure 3.5: (A-C) The association between the MFI of CD169 on classical (A), non-classical (B) and intermediate (C) monocytes and DAS28-ESR. (D) The association between the MFI of CD43 on Tregs and DAS28-ESR. Linear regression was used to assess significance, with 95% CI. The analysis included patients with a high or moderate disease activity as determined by EULAR criteria.

Before a comparison was made of the combination of CD169 and CD43 to clinical data, the ratio between relative numbers of $CD169^{+}$ monocytes and $CD43^{+}$ Tregs was assessed in healthy controls and each patient group (**Figure 3.6**). Initially, the ratio of

the percentage of CD169 to CD43 was analysed when considering each of the three monocyte subsets. The %CD169/%CD43 ratio was significantly increased in DMARD naïve (0.232±0.252, n=6, p=0.039) and DMARD responders (0.232±0.280, n=24, p=0.009) compared to healthy controls (0.098±0.062, n=19) when considering classical monocytes. The same observation was made when analysing non-classical monocytes, where DMARD naïve (0.313±0.194, p=0.017) and DMARD responders (0.328±0.177, p<0.001) exhibited a significantly increased %CD169/%CD43 ratio compared to healthy controls (0.125±0.086). Similarly, in intermediate monocytes the ratio was significantly increased in DMARD naïve (0.317±0.256, p=0.010) and DMARD responders (0.273±0.267, p=0.044) compared to healthy controls (0.144±0.104). However, in the case of non-classical monocytes, DMARD non-responders also had a significantly increased ratio (0.321±0.155) compared to healthy controls.

The ratio between CD169 MFI on monocytes and CD43 MFI on Tregs was also analysed and compared between healthy controls and RA patient groups. The CD169/CD43 MFI ratio was significantly increased in DMARD non-responders compared to healthy controls when considering classical (0.571±0.430 vs 0.295±0.187, p=0.005), non-classical (0.463±0.316 vs 0.261±0.163, p=0.012) and intermediate monocytes (0.572±0.378 vs 0.281±0.177, p=0.003). Additionally, the CD169/CD43 MFI ratio when considering intermediate monocytes was significantly higher in DMARD responders (0.430±0.219, p=0.022) compared to healthy controls.

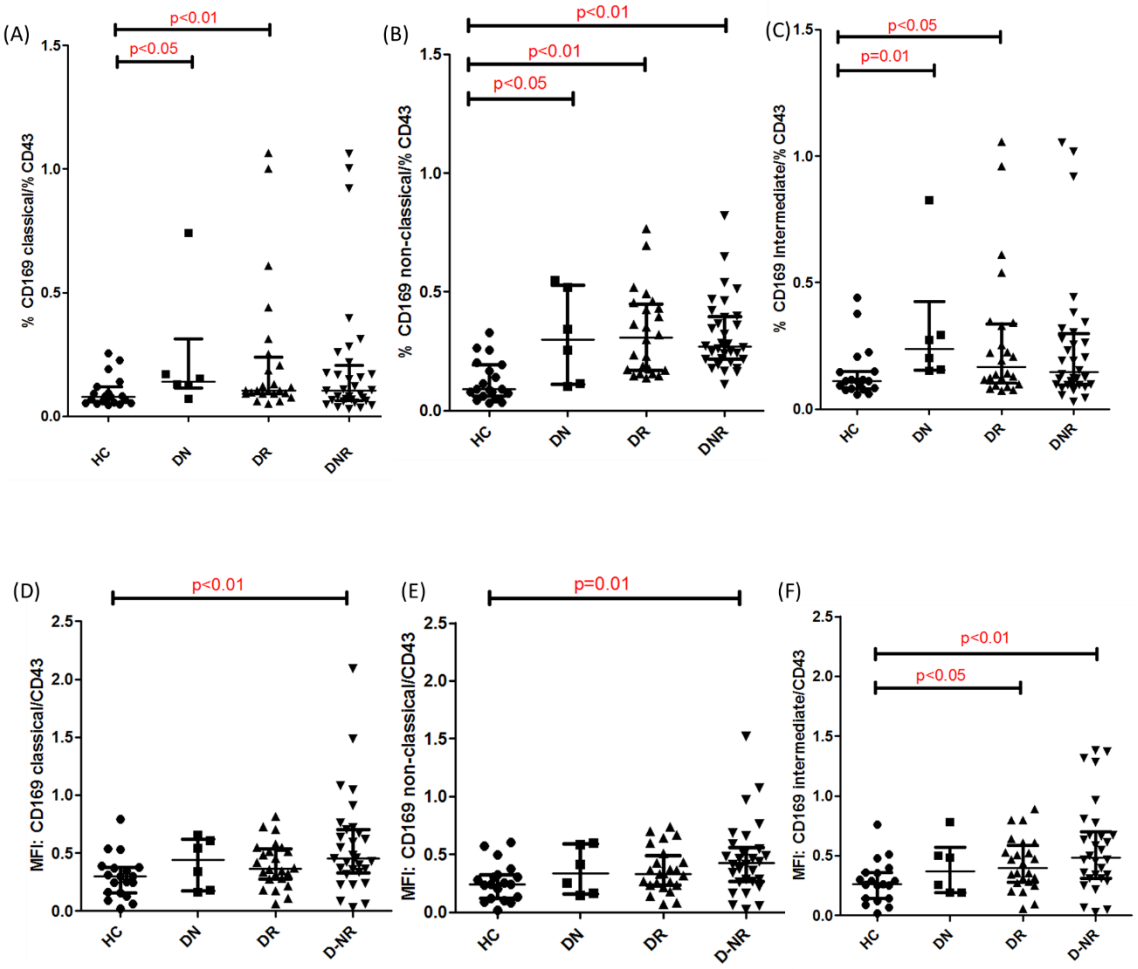

Figure 3.6: (A-C) The ratio between the relative number of CD169⁺ classical (A), non-classical (B) and intermediate (C) monocytes and the relative number of CD43⁺ Tregs in healthy controls and RA patients. (D-F) The ratio of CD169 to CD43 MFI in healthy controls and RA patients when considering classical (D), non-classical (E) and intermediate (F) monocytes. Error bars represent interquartile range. HC=healthy controls (n=19), DN=DMARD naïve (n=6), DR=DMARD responder (n=24, D-NR= DMARD non-responder (n=29), MFI = Median fluorescence intensity.

The ratio of CD169 to CD43 was also compared to DAS28-ESR (**Figure 3.7**). Initially the comparison was made using the ratio between the relative numbers of CD169 and CD43 positive cells. A significant positive correlation was observed between DAS28-ESR and the %CD169/%CD43 ratio when considering classical (p=0.025,

r=0.415, n=29), non-classical (p=0.01, r=0.464), n=29) and intermediate monocytes (p=0.020, r=0.429, n=29). Additionally, DAS28-ESR was compared to the ratio between CD169 MFI and CD43 MFI. The results show no significant association between DAS28-ESR and CD169/CD43 MFI ratio when considering classical (p=0.398, r=0.166, n=28), non-classical (p=0.818, r=0.046, n=28) and intermediate monocytes (p=0.204, r=0.247, n=28).

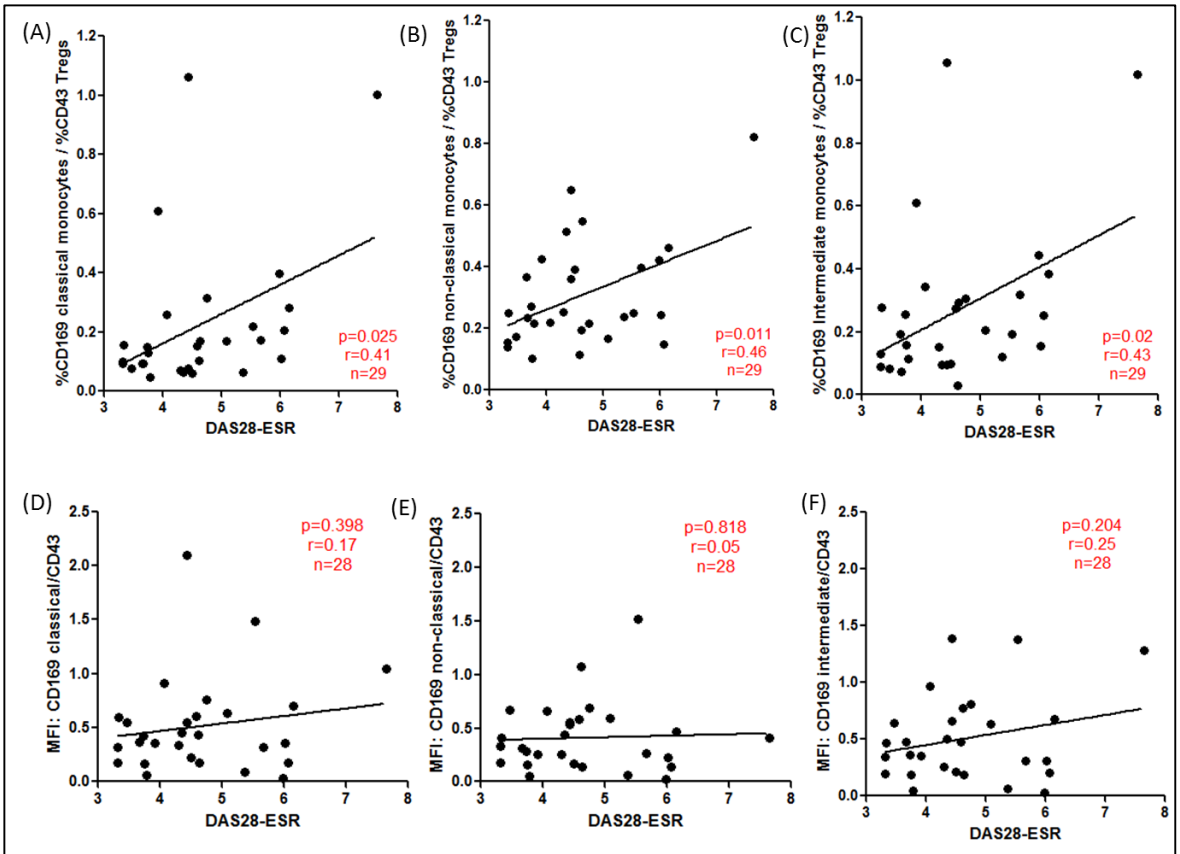

Figure 3.7: (A-C) The association between the ratio of the relative number of $CD169^+$ monocytes to $CD43^+$ Tregs and DAS28-ESR when considering classical (A), non-classical (B) and intermediate (C) monocytes. (D-F) The association between the ratio of CD169 to CD43 MFI and DAS28-ESR when considering classical (D), non-classical (E) and intermediate (F) monocytes. Linear regression was used to assess significance, with 95% CI. The analysis included patients with a high or moderate disease activity as determined by EULAR criteria.

Due to the finding that the percentage ratio between CD169^{+} non-classical monocytes and CD43^{+} Tregs had the strongest positive association with DAS28-ESR, these values were also compared to SJC (**Figure 3.8**). A weak positive association was observed when comparing ESR to SJC (p=0.409, r=0.163) and when comparing the ratio of %CD169(non-classical)/%CD43 to SJC (p=0.377, r=0.174, n=28), however with a lower p value for the latter, and without reaching statistical significance in either comparison.

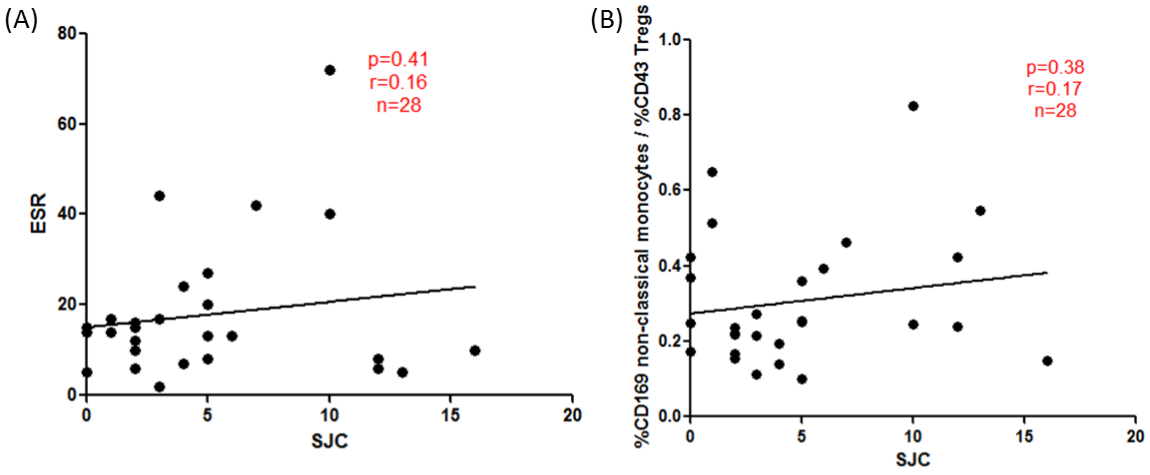

Figure 3.8: The association between the number of swollen joints (SJC) in RA patients with high or moderate disease activity to (A) ESR and (B) the ratio between the percentage of CD169^{+} non-classical monocytes and CD43^{+} Tregs. Linear regression was used to assess significance, with 95% CI. ESR = Erythrocyte sedimentation rate.

3.1.6 Potential role of CD169 in determining biological DMARD treatment response

A number of patients who had failed cDMARD treatment were sampled before commencing biological DMARDs and 6 months after (Table 2.1b). Treatment response was determined by EULAR criteria. Changes in cellular levels of CD169 and

CD43 were assessed at baseline and 6 months, and the difference between the two time points was calculated (**Figure 3.9**). A previous study highlighted the potential predictive role of circulating monocytes in determining Adalimumab treatment response (Chara *et al.* 2012). In order to test this finding, only patients treated with Adalimumab were included in the analysis. If patients experienced an adverse event to the drug, this was not classified as non-response, and therefore these samples were excluded. Overall, of the 16 patients sampled at baseline and 6 months following biologic treatment, 7 were classed as responders and 3 were non-responders. Although patient numbers were low in the current study, CD169 MFI was shown to decrease in 6 out of the 7 responders to Adalimumab at 6 months compared to baseline (**Figure 3.9**). Furthermore, CD169 MFI increased in non-responders at 6 months compared to baseline. However, no clear pattern was observed when comparing baseline and 6 month CD43 MFI levels.

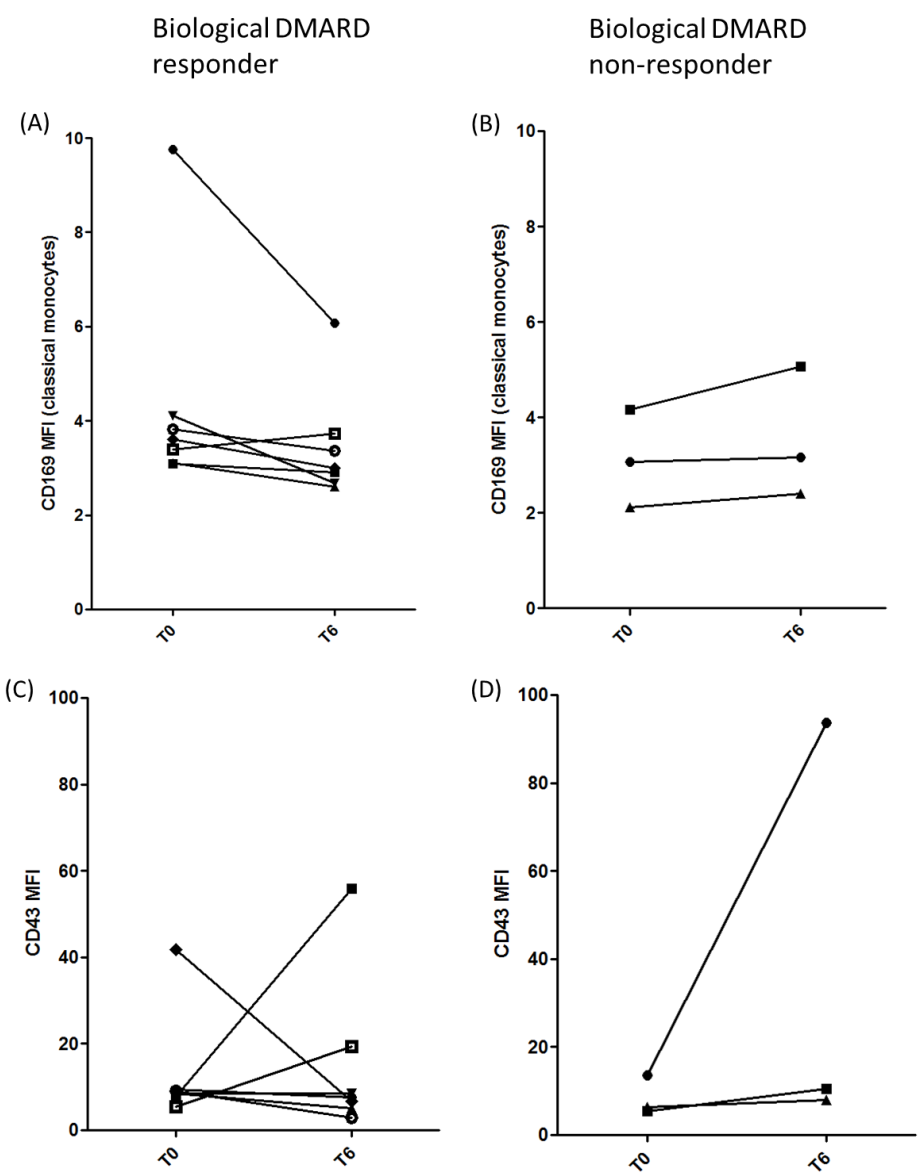

Figure 3.9: (A, B) The MFI of CD169 on classical monocytes in Adalimumab responders (n=7) (A) and non-responders (n=3) (B). (C, D) The MFI of CD43 on Tregs in Adalimumab responders (n=7) (C) and non-responders (n=3) (D). Patients were excluded if they were not treated with Adalimumab or if they experienced an adverse reaction while on the drug. T0 = Baseline sample before commencing drug, T6 = 6 month follow up sample. MFI = Median fluorescence intensity.

3.2 Discussion

The objective of this chapter was to investigate the relationship between disease activity in RA and the balance between circulating relative numbers of $CD169^+$ monocytes and $CD43^+$ Tregs. The data presented in relation to circulating monocytes and their subsets is in agreement with previous findings. Increased absolute monocyte numbers were observed from FBC results of RA patients compared to healthy controls, which confirms that inflammatory recruitment of monocytes can be detected even in peripheral blood. Similar to Chara *et al*., the absolute number of monocytes were significantly reduced in DMARD responders compared to non-responders (Chara *et al.* 2012). This is in agreement with a more recent study by Chara *et al.*, which describes how monocytes were found to increase in number during active disease (Chara *et al.* 2015). This explains why in the current study monocytes are found in higher numbers in non-responders to treatment who are inclined to have a greater disease activity.

In agreement with previous studies, the relative number of $CD16^+$ monocytes was observed to be increased in RA (Kawanaka *et al.* 2002; Cairns *et al.* 2002), whereas $CD16^-$ classical monocytes were reduced (Lacerte *et al.* 2016). A previous study also found an increase in $CD16^+$ intermediate monocytes in patients with longer disease duration compared to those with less than 2 years duration (Radwan *et al.* 2015), however this observation was not made when the group analysed $CD16^+$ non-classical monocytes. Possibly due to the low number of early RA DMARD naïve patients, this observation was not confirmed in the current study. However, a similar

pattern was observed where DMARD responders and non-responders had higher intermediate monocytes compared to healthy controls. Additionally, intermediate monocytes, which seem to represent a middle state between classical and non-classical, adopted a similar pattern to non-classical monocytes with increased percentage noted in RA compared to healthy controls. This indicates that $CD16^+$ monocytes may have more impact on RA pathogenesis than previously considered. $CD16^+$ monocytes are more likely to differentiate into dendritic cells (Ancuta *et al.* 2003), which are believed to play a pivotal role in RA progression and have been suggested as a potential target for therapy (Khan *et al.* 2009). However, despite the recent finding that classical and intermediate monocytes had predictive value in determining treatment response (Chara *et al.* 2015), the data presented in the current study demonstrates no significant difference between responders and non-responders for any of the monocyte subsets. This may be due to modest patient numbers in the current study.

Despite the differences observed in the relative number of each monocyte subset, the relative number of CD169 positive classical, non-classical and intermediate monocytes was increased in RA compared to healthy controls. This is similar to findings by Xiong *et al.* (Xiong *et al.* 2014), however the relative number of $CD169^+$ non-classical monocytes in the current study were found at significantly increased levels in RA compared to health. To our knowledge this observation has not been previously made and therefore represents a novel finding. This result further suggests $CD16^+$ monocytes perhaps have a more important role in RA pathogenesis compared to $CD16^-$ monocytes, due to the previous suggestions of CD169 playing a pivotal role in progression of the disease (York *et al.* 2007; Xiong *et al.* 2014).

Additionally, no significant difference was observed between healthy controls or any of the RA groups and the MFI of CD169 across the monocyte subsets. This suggests that although CD169 positivity as a percentage of monocytes is increased in RA, the number of CD169 cell surface markers remains constant.

The cell surface density of CD43 (MFI) on circulating Tregs, as well as the relative number of $CD43^+$ Tregs, was found to be reduced in RA compared to health. There is limited knowledge of CD43 as a Treg transmembrane sialoglycoprotein, however previous studies have demonstrated its involvement in T cell activation and proliferation (Sperling *et al.* 1995; Cruz-Munoz *et al.* 2003). Therefore, the reduction in CD43 density and percentage observed in this study may be related to the reduced activation observed in Tregs (Bonelli *et al.* 2016). However, in disagreement with this theory, DMARD responders have a significantly lower relative number of $CD43^+$ Tregs compared to non-responders. Conversely, although no significance is observed, the MFI of CD43 is increased in responders compared to non-responders. This means that although there may be lower CD43 as a percentage of Tregs in responders compared to non-responders, there is perhaps increased CD43 cell surface density per $CD43^+$ Treg cell in responders. Therefore the increase in CD43 per cell in responders may be related to increased T cell activation, as previously suggested (Sperling *et al.* 1995; Cruz-Munoz *et al.* 2003), however further investigation is needed to confirm this. Although the CD43 profile may be difficult to interpret in this preliminary study, the difference in percentage between responders and non-responders would suggest CD43 has the potential as a surrogate marker of treatment response.

In addition to analysing CD169 and CD43 as individual cell surface markers, a possible association between the combined markers and disease activity was also assessed. The relative number of $CD169^+$ monocytes when considering each subset had a significant association with DAS28-ESR. Interestingly, $CD169^+$ non-classical monocytes had a stronger association with DAS28-ESR, whereas $CD169^+$ classical monocytes had the weakest of the three subsets. This implies $CD16^+$ monocytes are more closely associated with disease activity than $CD16^-$ monocytes. Additionally, in comparing CD169 MFI to DAS28-ESR, significance was only observed in $CD16^+$ intermediate monocytes. Therefore, contrary to previous findings of the current study where CD169 MFI was not significantly differentially expressed between patient groups, it appears to be associated with disease activity in a subset of monocytes.

When analysing the ratio of the relative numbers of $CD169^+$ classical monocytes to $CD43^+$ Tregs, an increase was found in RA compared to healthy controls. However, no significant difference was observed between responders and non-responders. Additionally, the ratio of the percentage of CD169 to CD43 had a significant positive association with DAS28-ESR when each monocyte subset was considered. Similar to before, the strongest association was observed when only non-classical monocytes were considered in the CD169 to CD43 ratio. Despite the lack of association between the relative number of $CD43^+$ Tregs and DAS28-ESR, a slightly stronger positive association was observed when accounting for the relationship between the ratio of the relative number of $CD43^+$ Tregs to $CD169^+$ non-classical monocytes and DAS28-ESR. This implies that the ratio of %CD169/%CD43 may be a useful surrogate measure of disease activity. The lack of difference in these markers between responders and

non-responders may be due to various factors. For example, comorbidities may account for a change in DAS28-ESR, or perhaps a flare of disease in a responder would emulate the cell profile of a non-responder at the time of sampling. One way of taking these factors into consideration would be to increase the patient cohort and subdivide depending on confounding factors.

As the strongest positive association between DAS28-ESR and the ratio of CD169 to CD43 positive cells was observed when accounting for non-classical monocytes only, this data was also compared to SJC. Swollen joints is one of the main symptoms of RA, therefore this comparison was made to determine whether the balance of these key cells contribute to this physical manifestation of the disease. A weak positive association was observed between SJC and the ratio of %CD169/%CD43, as well as ESR. Due to the lack of statistical significance in each association it is difficult to say whether the cellular ratio or ESR has any influence on SJC. The association with %CD169/%CD43 ratio was slightly stronger, indicated by a lower p value, however further investigation with increased patient numbers would be useful in verifying these findings. Overall, the potential involvement of changes in the ratio of %CD169/%CD43 with disease activity appears to be mainly driven by CD169. This suggestion is made based on the evidence of the relative number of $CD169^{+}$ monocytes as being more strongly associated with DAS28-ESR.

The MFI of CD169 on monocytes and CD43 on Tregs was also assessed in RA patients before and after 6 months of Adalimumab therapy. In order to robustly compare responders to genuine non-responders, any patients who experienced an adverse event were excluded from the analysis. Six out of the seven patients who responded

at 6 months had a reduction in CD169 MFI compared to baseline. Conversely, non-responders did not have a reduction in CD169 MFI, but rather a modest increase. These preliminary results further suggest CD169 MFI could be a potential marker of response in individual patients. However, patient numbers are small and this analysis would need to be repeated on a larger cohort, and perhaps compared across different drug types.

In summary, these results strongly suggest that relative numbers of $CD169^+$ monocytes and $CD43^+$ Tregs mirror disease activity in RA, and can be measured in peripheral blood, coincident with synovial inflammation. Although inconclusive in the current study, it can be postulated that with further investigation, these markers have the potential to determine treatment response in RA. Future work could demonstrate treatment response may be determined at an earlier time point than currently possible, thus improving overall patient outcome. For example, introducing early sampling time points and analysing these cellular levels before the clinical 3-6 month assessment could verify this.

3.3 Conclusion

The key findings of this study highlight the need to consider $CD16^+$ as well as classical $CD16^-$ monocytes. Although the increased relative number of $CD169^+$ classical monocytes with RA disease activity has been previously highlighted in other studies, it is demonstrated here that $CD169^+$ non-classical monocytes may have a more pronounced role. This is mainly shown by the increased association of $CD169^+$ non-

classical monocytes with DAS28-ESR compared to $CD169^+$ classical monocytes. Furthermore, these results provide preliminary evidence of an association between the balance of $CD169^+$ monocytes and $CD43^+$ Tregs in peripheral blood, and disease activity in RA. Although CD169 plays a role in the negative regulation of Tregs (Wu *et al.* 2009), further investigation is required to determine whether CD169 and CD43 positive cells interact, and if this interaction directly contributes to this function. The results of this study allows postulation that the balance of these cells is key in the immune response and could be a surrogate measure of disease activity, and subsequently treatment response in RA. With further investigation, these markers could enable response to be determined at an earlier stage, thus improving clinical outcome.

Chapter 4

Activation state of Tregs in RA

4.0 Introduction

4.0.1 Tregs in RA

As discussed in section 1.1.3.1, Tregs are associated with self-tolerance and therefore are believed to play a pivotal role in AD. In health, Tregs function by suppressing over-reactive Teff cells, which maintains balance in the immune response by preventing unnecessary inflammation that can precipitate tissue damage (Wu *et al.* 2009). However, in autoimmune conditions such as RA, this function is inhibited. Previous studies report conflicting Treg numbers and activation state in RA, likely due to lack of clarity of patient characteristics, such as disease activity, disease duration and treatment pathway at the point of sampling. For example, one study reported reduced suppressive capabilities of $CD4^+CD25^+$ Tregs from RA patients when co-cultured *in vitro* with autologous monocytes (van Amelsfort *et al.* 2007). However, a recent study reported that although there were increased relative numbers of $CD4^+CD25^+FoxP3^+$ Tregs in RA patients following abatacept treatment, they had reduced activity as measured by activation markers CD69 and CD71 (Bonelli *et al.* 2016). The latter study did not specify whether patients were responding to the treatment, and furthermore used an alternative phenotype to assess Tregs and their activation state. A separate study did however classify patients by response to anti-TNF therapy, and found increased relative numbers of $CD4^+CD25^+$ Tregs in peripheral blood of responder RA patients (Ehrenstein *et al.* 2004). Importantly, this observation was shown to be associated with a reduction in CRP levels, suggesting circulating Treg

numbers may be a useful surrogate measure of, and may play a role in, RA disease activity.

Further studies have compared the relative number of Tregs in RA synovial fluid to circulating peripheral blood. RA patients have been shown to exhibit an increased relative number of $CD4^+CD25^+$ Tregs in synovial fluid compared to peripheral blood, and increased Tregs in peripheral blood compared to that of healthy controls (van Amelsfort *et al.* 2004; Mottonen *et al.* 2005). Additionally, synovial fluid Tregs were in an active state as measured by activation markers including FoxP3 and CTLA-4 (van Amelsfort *et al.* 2004; Mottonen *et al.* 2005). For such studies, it is difficult to obtain synovial fluid from healthy controls due to the invasive sampling procedure. Therefore, the 'normal' range and activation state of synovial Tregs in health is unclear.

4.0.2 Forkhead box P3 (FoxP3)

FoxP3 is an intracellular transcription factor of Tregs. As described in section 1.1.3.1, it can be used as a marker of Treg activation as it has been shown to regulate the suppressor function (Gavin *et al.* 2007). Furthermore, increased FoxP3 expression leads to decreased activity of Teff cells, and subsequent reduction of pro-inflammatory cytokines including IL-2 and IFN-γ (Bettelli *et al.* 2005). Some researchers have suggested that FoxP3 is a phenotypic marker of Tregs because of this association with suppressive activity (Hori *et al.* 2003; Fontenot *et al.* 2005). The involvement of FoxP3 in relation to AD has been widely studied, where reduced FoxP3 expression is related to increased autoimmune susceptibility (Ulmanen *et al.*

2005). This may be due to the association of FoxP3 with impaired Treg activity in autoimmune conditions such as RA (Kennedy *et al.* 2014; Cribbs *et al.* 2014).

The development of FoxP3$^+$ Tregs in the thymus is dependent on c-REL, which is a transcription factor of the NFκB family (Isomura *et al.* 2009). Additionally, NFκB activity is increased in FoxP3 KO mice, adding further weight to the concept of a relationship between the two transcription factors (Bettelli *et al.* 2005; Le Bras and Geha 2006). NFκB is associated with an increased inflammatory response in RA. This has previously been observed primarily with CD45RA$^-$ memory Tregs (Nagar *et al.* 2010). Furthermore, a reduced inflammatory response as measured by osteoclast activity is associated with NFκB inhibition (Aya *et al.* 2005).

NFκB activation is controlled by the enzyme complex IκB kinase (IKK). IKK phosphorylates IκBα, subsequently releasing NFκB (**Figure 4.1**) (Li and Verma 2002). The NFκB essential modulator (NEMO) plays a pivotal role in NFκB activation as it can inhibit the actions of the IKK complex. Various studies have investigated the potential therapeutic effects of targeting NFκB responses via the NEMO pathway in inflammatory arthritis (May *et al.* 2000; Dai *et al.* 2004; Min *et al.* 2013). Specifically, NEMO-binding domain peptide (NBD) therapy can prevent NFκB activity, thus reducing the severity of inflammation via reduced osteoclastogenesis and bone erosion (May *et al.* 2000; Dai *et al.* 2004). More recently, NBD therapy was shown to prevent IκBα phosphorylation thus reducing NFκB activity in inflammatory arthritis (Min *et al.* 2013). Furthermore, this observation was associated with an increase in relative numbers of FoxP3$^+$ Tregs as well as restored Treg suppressor function. Anti-TNF treatment is also believed to combat the inflammatory role of NFκB in RA. On

binding to its receptor, TNF can activate the NFκB pathway, a response that is inhibited with anti-TNF treatment (Baud and Karin 2001; Nagar *et al.* 2010).

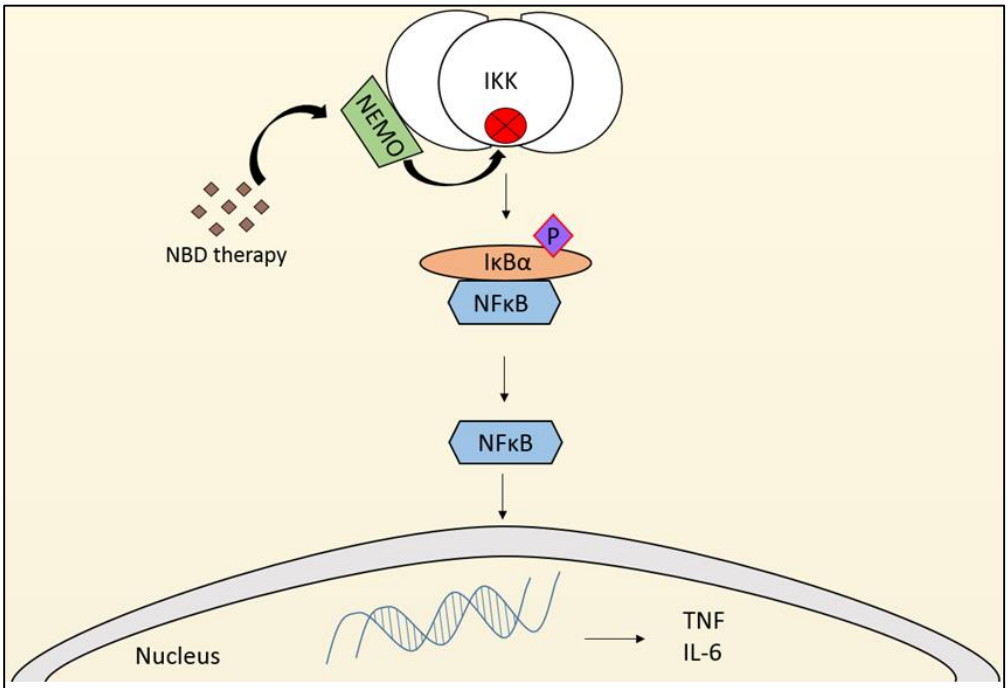

Figure 4.1: The IKK enzyme complex phosphorylates IκBα, subsequently releasing NFκB. Free NFκB translocates to the nucleus, which leads to the release of various inflammatory cytokines. NBD therapy targets the NEMO pathway, causing inhibition of the IKK complex, thus preventing the release of NFκB and reducing inflammatory responses.

4.0.3 The influence of monocytes on Tregs

As discussed in section 3.0.2, previous studies have uncovered the association of monocytes with Treg activity (Estrada-Capetillo *et al.* 2013; Walter *et al.* 2013). For example, CD169 binds to various ligands on the surface of Tregs, including CD43 (van den Berg *et al.* 2001). It has been found that through binding these ligands, monocyte-CD169 can suppress Treg activity (Wu *et al.* 2009). As explored in chapter 3, the balance between $CD169^{+}$ monocytes and $CD43^{+}$ Tregs may be associated with

disease activity in RA, as determined by the DAS28-ESR score. However, the impact of $CD169^+$ monocytes on $CD43^+$ Treg activity remains elusive. Furthermore, although a previous study has demonstrated direct binding of these two cell surface markers via immunocytochemistry, the function of this interaction is unclear (Ohnishi *et al.* 2013).

4.0.4 *In vitro* stimulation of Tregs

One of the aims of the experiments within this chapter is to assess the effect of peripheral $CD169^+$ monocytes and their sialic acid (Sia) motifs on Tregs in an *in vitro* inflammatory model of RA. The effects of $C169^+$ monocyte co-culture and Sia incubation upon Tregs will be quantified by measuring intracellular Treg percentages of NFκB and FoxP3, as well as secreted cytokines from both cell types. In order to create a state of inflammation in cultured Tregs, they must first be exposed to a suitable stimulant that will induce an inflammatory response similar to that present in RA patients.

Previous studies have investigated the ability of lipopolysaccharides (LPS) to induce an inflammatory response in human immune cells, such as $CD4^+$ cells (McAleer and Vella 2008). LPS is a component of the membrane of Gram-negative bacteria, mainly functioning to maintain structural support of the bacteria (Ramachandran 2014). It binds to Toll-like receptor-4 (TLR4) assisted by CD14, a cell surface receptor present on monocytes and dendritic cells (**Figure 4.2**) (Kawai and Akira 2006; Kagan and Medzhitov 2006; McAleer and Vella 2008). TLR4 contains an intracellular Toll/interleukin-1 receptor (TIR) which initiates the signalling cascade. This includes recruitment of myeloid differentiation primary response 88 (MYD88) by the TLR

adaptor TIRAP. The MyD88 pathway involves phosphorylation of IL-1 receptor-associated kinase -1 and -4 (IRAK-1/4), which subsequently activates TNF receptor-associated factor 6 (TRAF6) and transforming growth factor-β-activated protein kinase 1 (TAK1). TAK1 activates the IKK complex (**Figure 4.1**), ultimately leading to the release of NFκB and thus upregulation of inflammatory cytokines including TNF and IL-6. Additional to the MyD88 pathway, LPS also induces TIR domain-containing adaptor inducing IFN-β (TRIF) through the TRIF-related adaptor molecule (TRAM). The induction of TRIF leads to activation of receptor interacting protein 1 (RIP1) as well as TRAF6, which both contribute to the release of NFκB (Kagan and Medzhitov 2006; Kawai and Akira 2006; McAleer and Vella 2008).

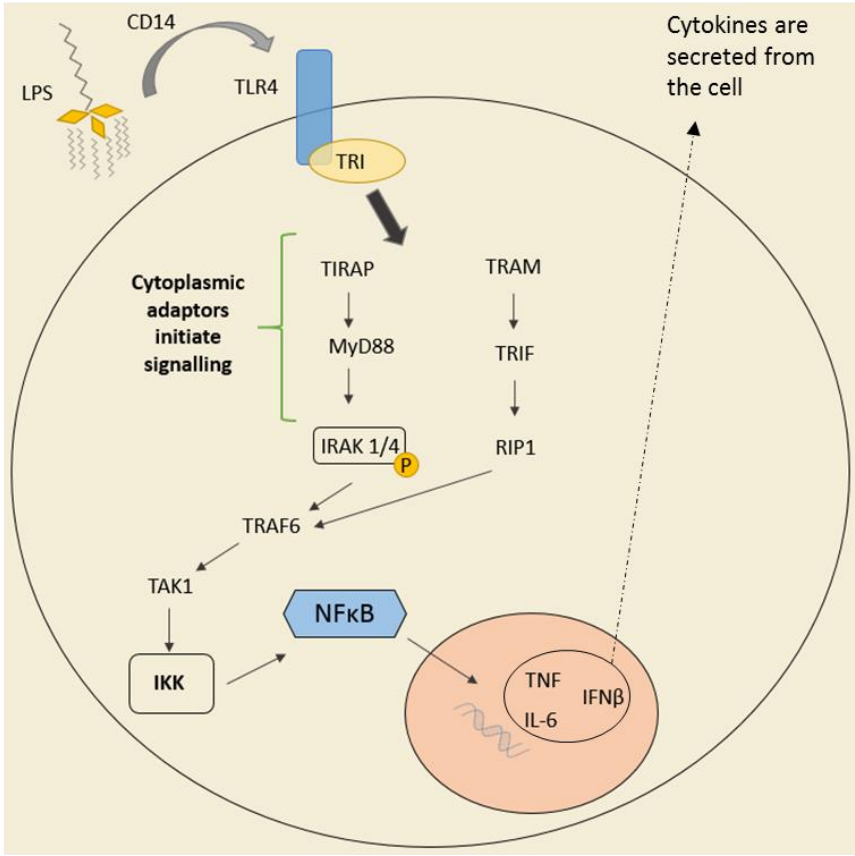

Figure 4.2: LPS binds to TLR4 via CD14, which leads to activation of NFκB via MyD88 and TRIF pathways. This consequently upregulates proinflammatory cytokines including TNF, IL-6 and IFNβ.

Previous studies have also demonstrated the activation of Tregs by LPS stimulation. For example, LPS has been shown to increase the suppressive function of $CD4^+CD25^+$ Tregs in mice (Caramalho *et al.* 2003). Additionally, this suppressive function was previously suggested to be IL-10 dependent (Lewkowicz *et al.* 2006). More recently, Lewkowicz *et al.* demonstrated the role of LPS-stimulated Tregs in IL-10 production by neutrophils, which was not observed when Tregs were unstimulated (Lewkowicz *et al.* 2016). IL-10 plays an important anti-inflammatory role as it promotes Treg production as well as reduces the pathogenic effects of Th17 cells (Heo *et al.* 2010). Furthermore, a previous study showed an upregulation of $FoxP3^+$ Tregs upon LPS and

IL-2 stimulation (Milkova *et al.* 2010). This effect was not observed following NFκB pathway inhibition, suggesting FoxP3 expression is dependent on NFκB.

Other studies have demonstrated a role of phorbol 12-myristate 13-acetate (PMA) in combination with ionomycin (IO) in inducing cytokine production from T cells (Wang *et al.* 2013). PMA, along with TCR/CD28 co-stimulation, increases T cell activation pathways including protein kinase-C (PKC), mitogen-activated protein kinases (MAPK) and IKK (**Figure 4.3**) (Macian *et al.* 2002). IO is often used in combination with PMA as it is required for the calcium ion dependent nuclear factor of activated cells (NFAT) signalling pathway (Schwartz 1996). The upregulation of these signalling pathways from PMA/IO stimulation ultimately leads to increased transcription factors NFAT, AP-1 and NFκB, which subsequently upregulates inflammatory cytokines including IFNγ and TNF (Macian *et al.* 2002; Ai *et al.* 2013). In a similar mechanism, anti-CD3/CD28 antibodies are often used to induce proliferation of T cells through TCR/CD28 co-stimulatory signalling (Li and Kurlander 2010).

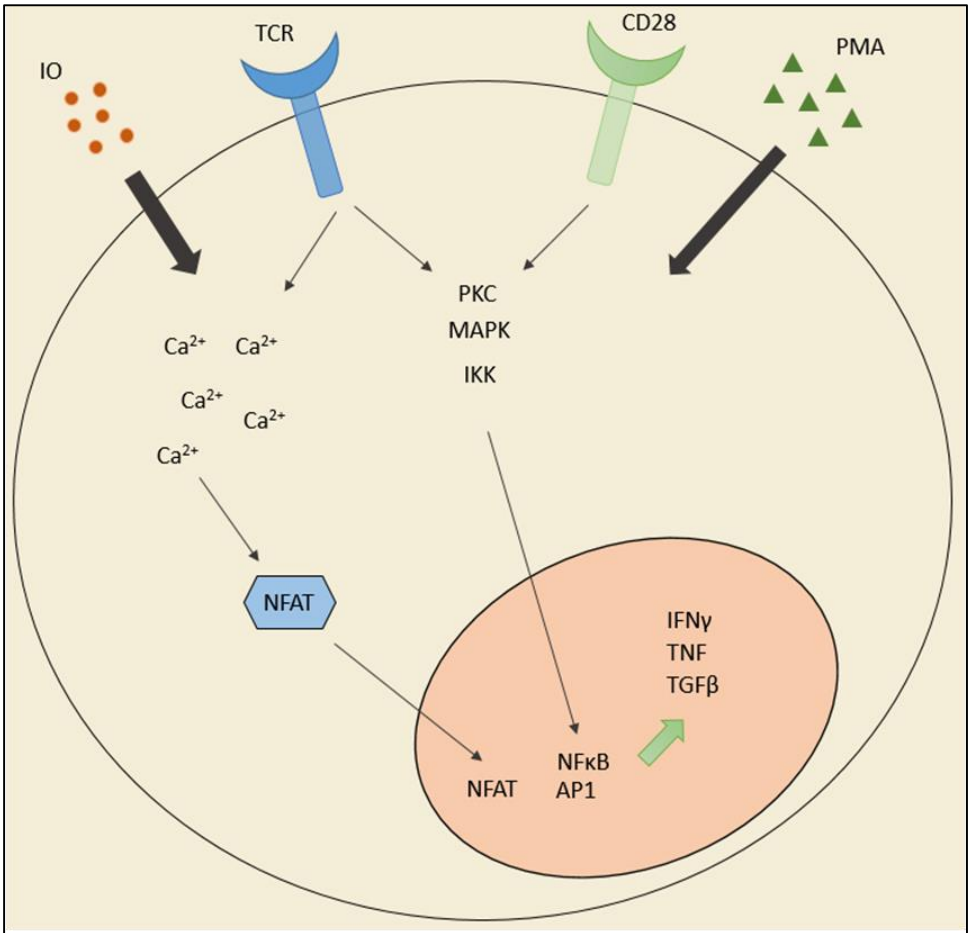

Figure 4.3: PMA and IO stimulation of T cells leads to activation of various intracellular signalling pathways, subsequently leading to secretion of inflammatory cytokines.

In summary, this chapter initially aims to define the activation state of Tregs in peripheral blood of RA patients, by analysing relative numbers of FoxP3^{+} Tregs. Specifically, this chapter focusses on relative numbers of FoxP3 positive CD45RA$^{+/-}$ Tregs, where CD45RA is used as a marker of naïve Tregs. Furthermore, this chapter will assess both intracellular and extracellular consequences of Sia or CD169 binding to Tregs, and whether CD43 is necessary for this interaction. Induction of NFκB and FoxP3 will be the core readouts used to define effects caused by the interaction between monocytes and Tregs.

4.1 Results

4.1.1 Relative numbers of circulating Tregs in RA

Tregs from PBMCs of healthy control participants and RA patients were analysed by flow cytometry using the phenotype $CD4^{+}CD25^{+}CD127^{-}$. Relative Treg numbers were expressed as a percentage of $CD3^{+}CD45^{+}$ T cells (**Figure 4.4**). Circulating relative Treg numbers were significantly increased in DMARD naïve and DMARD responder RA patients compared to healthy controls. Furthermore, RA patients who have not responded to DMARD treatment had a significantly lower percentage of circulating Tregs compared to those who have responded.

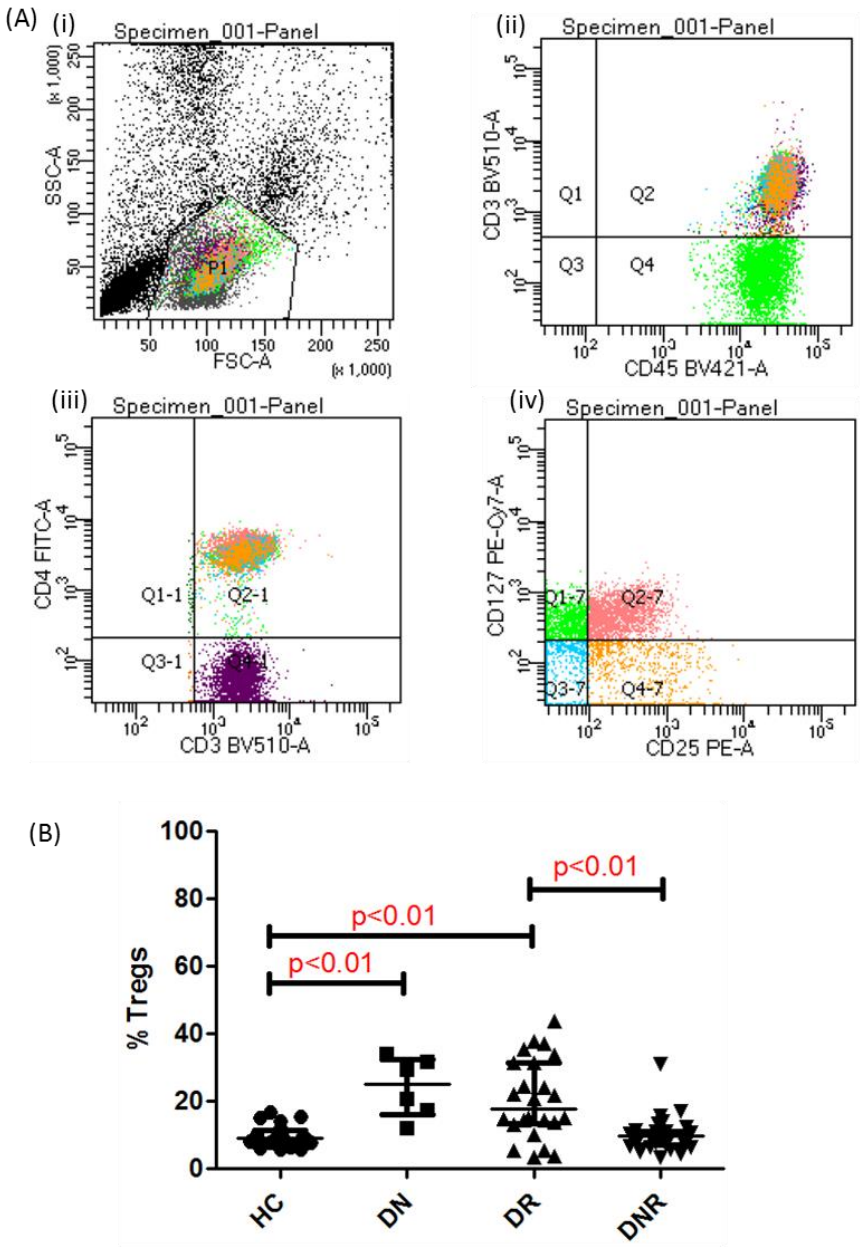

Figure 4.4: (A) FACS dot plot showing gating of (i) lymphocyte population and subsequent $CD3^{+}CD45^{+}CD4^{+}CD25^{+}CD127^{-}$ Tregs ((ii)-(iv)). (B) The relative number of $CD4^{+}CD25^{+}CD127^{-}$ Tregs in healthy controls and RA patients. P values shown were obtained using Mann Whitney tests. Error bars represent interquartile range. HC = healthy controls (n=21), DN = DMARD naïve (n=6), DR = DMARD responders (n=24) and DNR = DMARD non-responders (n=31).

4.1.2 Treg activation state in RA (FoxP3 and CD45Ra)

The relative numbers of $CD45RA^+$ and activated $FoxP3^+$ Tregs were analysed in healthy controls and RA patients (**Figure 4.5 (A, B)**). Furthermore, CD45RA and FoxP3 were analysed specifically in $CD43^+$ Tregs (**Figure 4.5 (C, D)**). The results for Tregs and $CD43^+$ Tregs showed similar patterns between patient groups (**Figure 4.6**). The relative number of $CD45RA^+FoxP3^-$ Tregs was significantly higher in DMARD non-responders, compared to healthy controls, DMARD naïve and DMARD responder patients. The same result was shown in $CD43^+$ Tregs. Alternatively, the relative number of $CD45RA^+FoxP3^+$ Tregs was significantly reduced in DMARD non-responders compared to healthy controls, however the same observation was made of DMARD responders. This result was also shown in $CD43^+$ Tregs. The relative number of $CD45RA^-FoxP3^+$ Tregs was significantly elevated in DMARD naïve, DMARD responder and DMARD non-responder patients, in comparison to healthy controls. However, DMARD non-responders exhibited a significantly lower relative number of $CD45RA^-FoxP3^+$ Tregs compared to DMARD naïve and DMARD responder patients. A similar result was observed in $CD43^+$ Tregs.

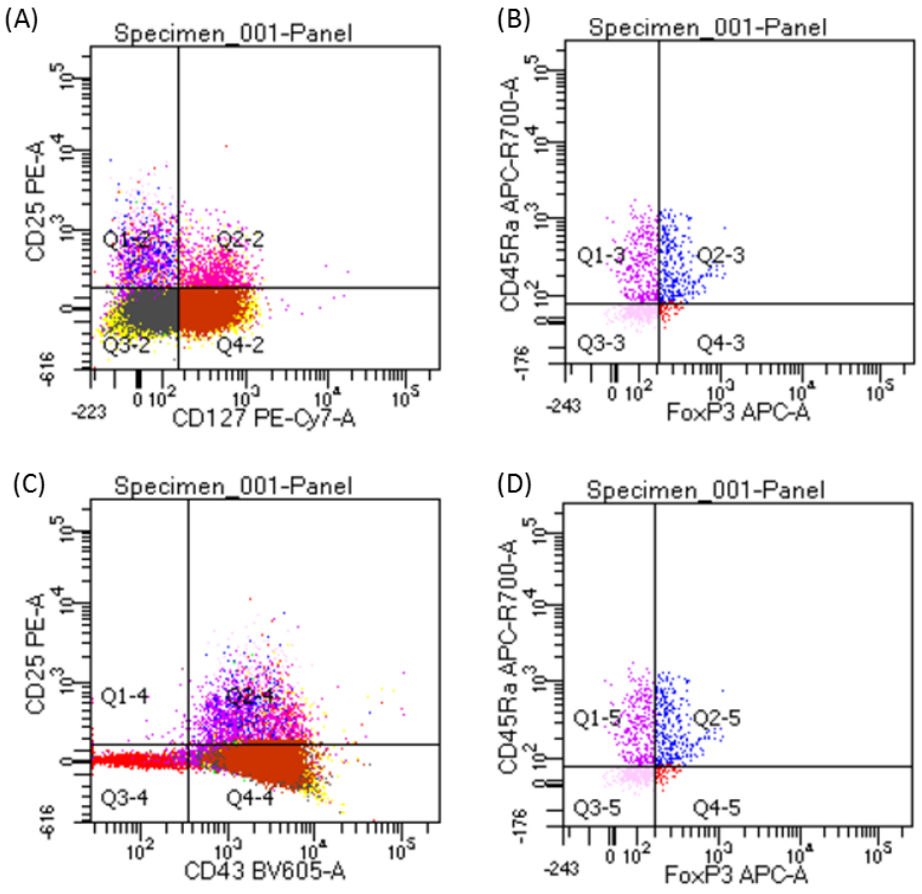

Figure 4.5: (B, D) CD45RA/FoxP3 percentages were analysed in subsequent dot plots of either (A) $CD4^+CD3^+CD25^+CD127^-$ Tregs, or (C) $CD4^+CD3^+CD25^+CD127^-CD43^+$ Tregs.

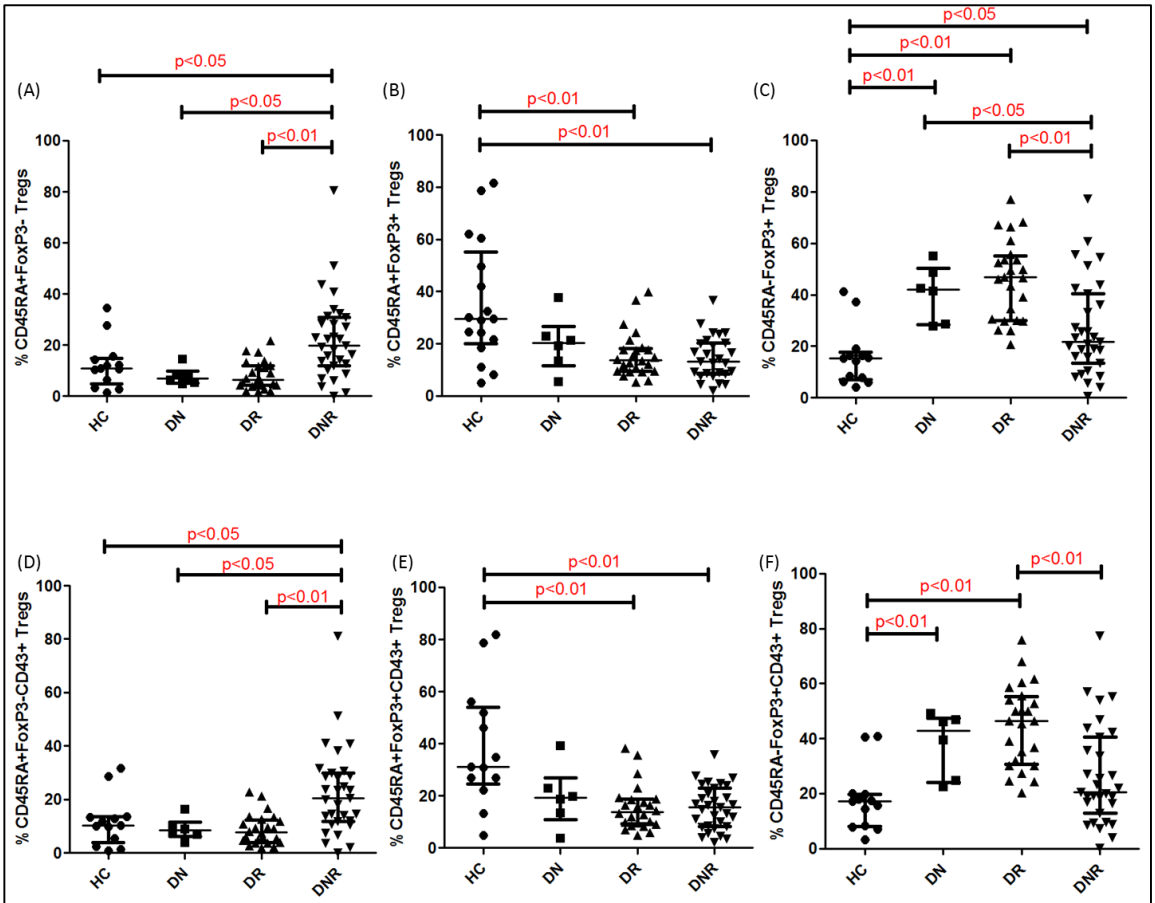

Figure 4.6: (A-C) Relative numbers of CD45RA/FoxP3 subsets analysed in circulating Tregs and in (D-F) specific CD43^{+} circulating Tregs. P values shown were obtained using Mann Whitney tests. Error bars represent interquartile range. HC=healthy controls (n=13), DN=DMARD naïve (n=6), DR=DMARD responder (n=24), D-NR= DMARD non-responder (n=31).

4.1.3 Effect of PMA and LPS on *in vitro* Tregs

Sorted CD4^{+}CD25^{+}CD127^{-} Tregs were expanded in culture with CD3/CD28 microbeads as described in section 2.4.2, and incubated with varying concentrations of PMA/IO or LPS. At this preliminary stage, qPCR reactions were carried out as output measures of pro-inflammatory cytokines TNFα, IL-6 and IL-10. βactin was used as the housekeeping gene as it was shown to be stable using unstimulated and

stimulated expanded Tregs (Appendix P). The cell supernatants were not kept at this stage as the purpose of this experiment was to determine the optimal concentration of each stimulant in increasing cytokine production.

The cells increased in number on Day 1 and Day 2 when stimulated with LPS compared to control cells with no stimulant. However, the viability of the cells remained fairly stable throughout the experiment for both LPS stimulated and control cells (**Figure 4.7**). Cell counts of the PMA/IO stimulated cells were fairly similar to control cells, however the viability was slightly compromised on Day 1 compared to the control.

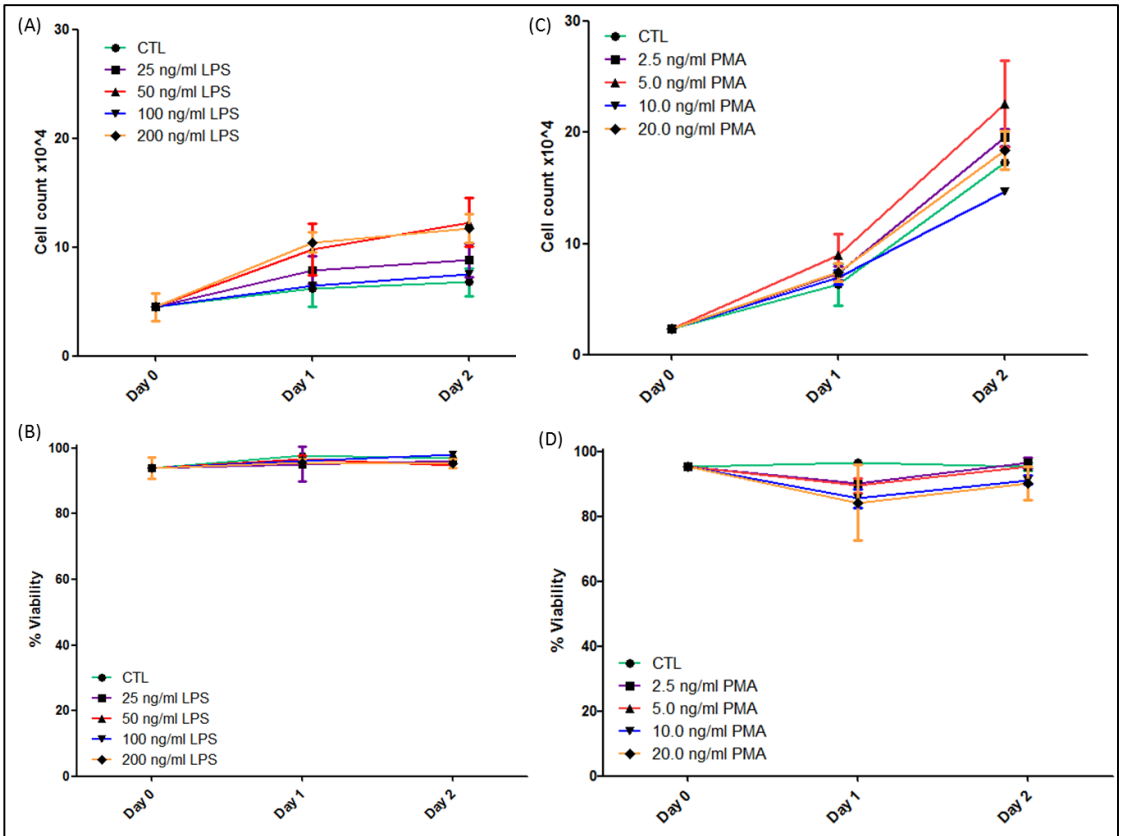

Figure 4.7: (A) and (B) cell counts and viability respectively of Tregs stimulated with increasing concentrations of LPS. (C) and (D) cell counts and viability respectively of Tregs stimulated with increasing concentrations of PMA and 500 ng/ml IO. Error bard represent standard deviation from the mean. Number of wells at each time point = 2.

At each time point, the cells were removed from wells and resuspended in Trizol for RNA extraction, followed by transcriptomic analysis by qPCR. The relative gene expression of TNF and IL-6 was obtained using β-actin as the reference housekeeping gene. Transcript levels of TNF were increased in Tregs that were stimulated for 2 days with PMA/IO, however no significant increase was observed when stimulated with LPS (**Figure 4.8**). Similarly, IL-6 gene expression was increased in Tregs that were stimulated for 2 days with 20 ng/ml PMA. 50 ng/ml of LPS was observed to increase IL-6 gene expression after stimulation for 1 day.

The experiment was subsequently repeated using just one concentration of each stimulant, i.e. 200 ng/ml LPS and 10 ng/ml PMA. At the transcript level, the results showed no detectable effect of LPS on expression of any of the genes tested (**Figure 4.9**). However, PMA stimulation decreased TNF expression after 2 days, and increased IL-10 expression. Similarly, the ELISA results showed no statistically significant difference in levels of any of the secreted cytokines levels after stimulation with LPS. However, an increase in TNFα and IL-10 cytokine levels was observed after cells were treated with PMA for 2 days. Conversely, PMA stimulation caused a reduction in levels of secreted IFNγ. Due to the detectable impact of PMA on cytokine production, and the success of its use in previous literature to stimulate an *in vitro* inflammatory model (Macian *et al.* 2002; Wang *et al.* 2013), going forward PMA was chosen at the most optimal stimulant.

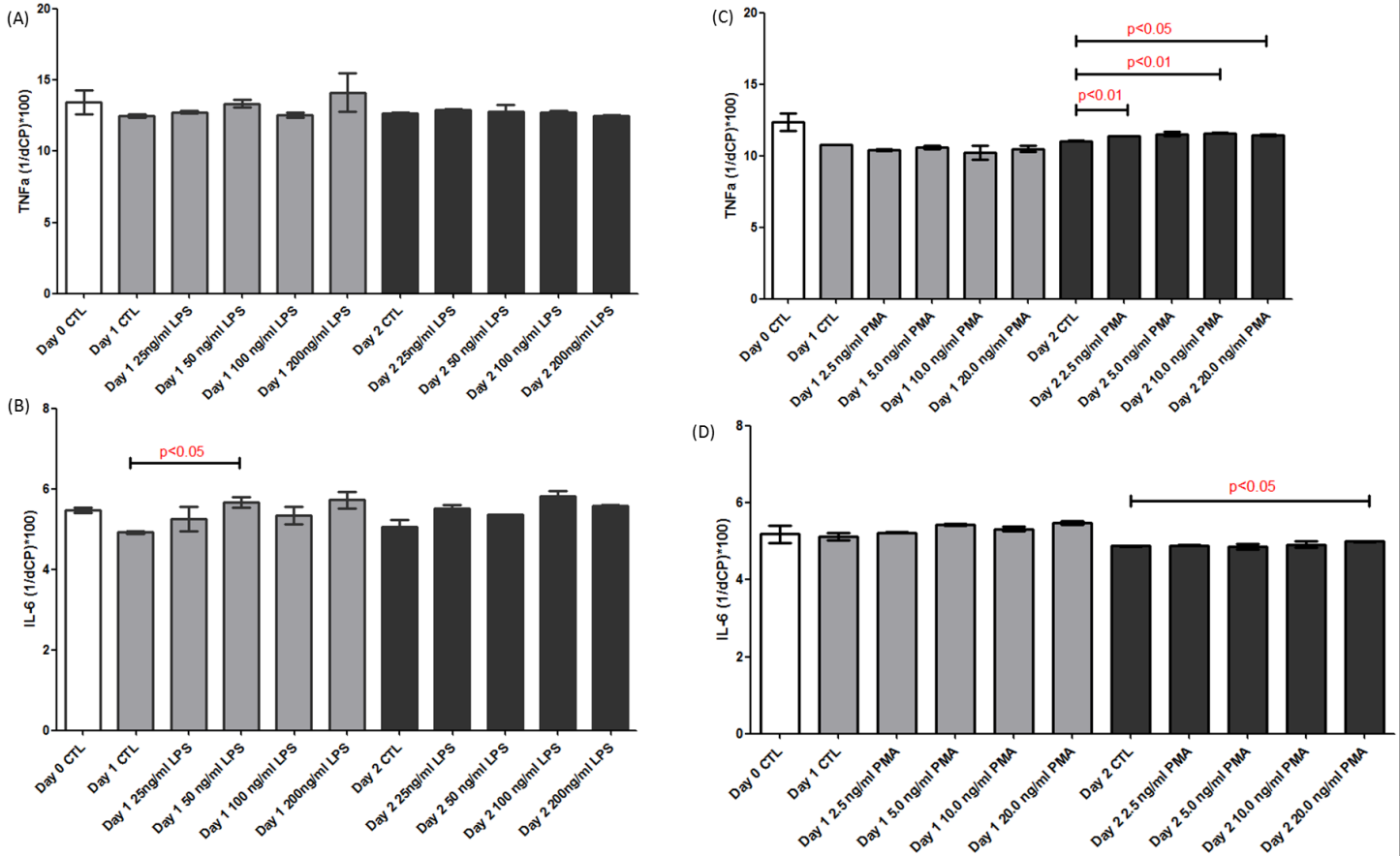

Figure 4.8: TNFα and IL-6 gene expression of Tregs when stimulated with increasing concentrations of (A, B) LPS or (C, D) PMA/IO. P values were obtained using Mann Whitney tests. Error bars represent interquartile range. Number of cell culture plate wells at each time point = 2. Each sample was run in duplicate wells of qPCR plate. CTL=Control, LPS=Lipopolysaccharides, PMA=Phorbol 12-myristate 13-acetate. White bars=Day 0, grey bars=Day 1, black bars=Day 2.

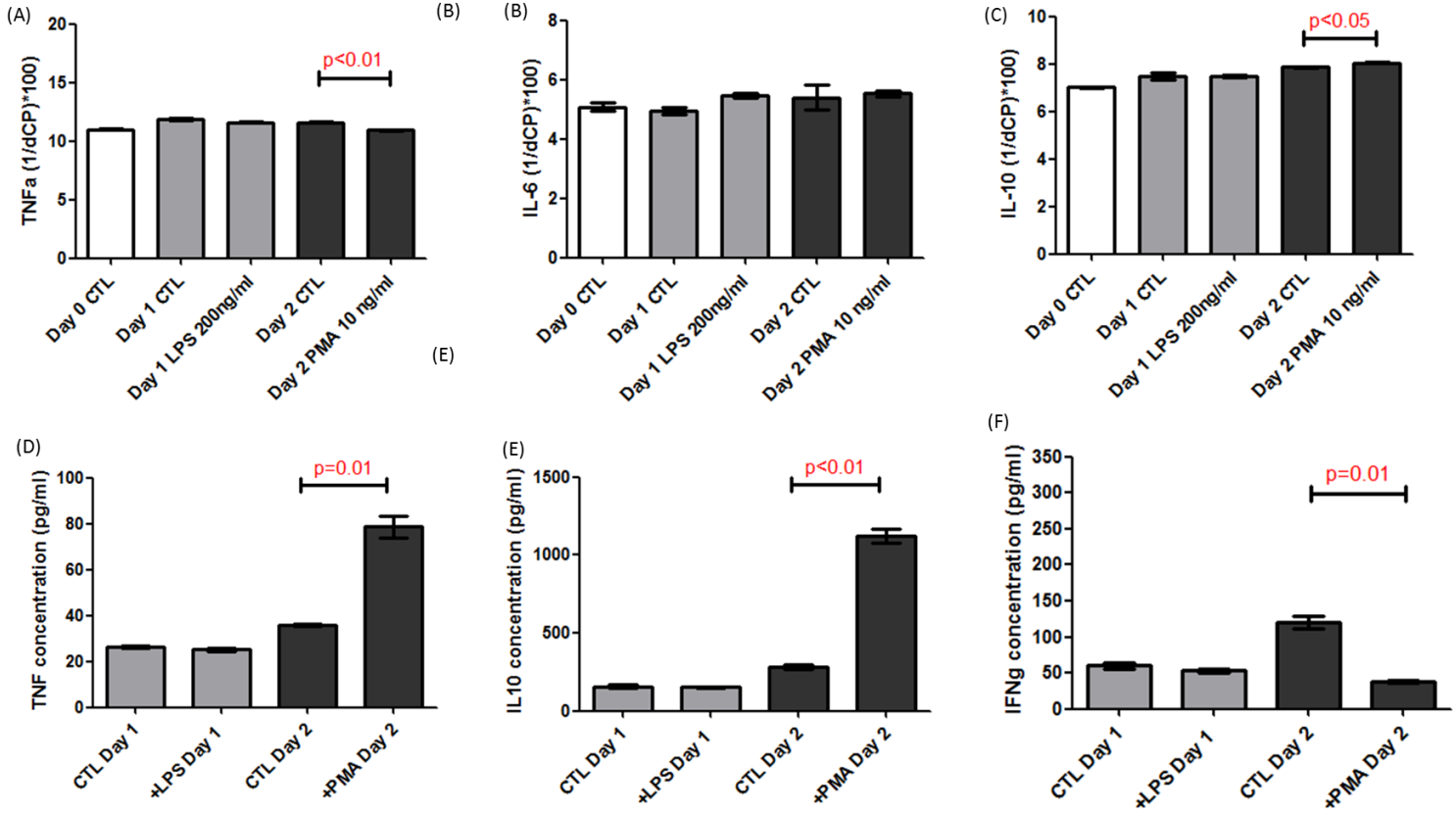

Figure 4.9: (A-C) qPCR data of TNFα, IL-6 and IL-10 gene expression respectively. (D-F) ELISA quantification data of TNFα, IL-10 and IFNγ cytokines respectively. P values were obtained using Mann Whitney tests. Error bars represent interquartile range. Number of cell culture plate wells at each time point = 2. Each sample was run in duplicate wells of qPCR or ELISA plate. CTL=Control, LPS=Lipopolysaccharides, PMA=Phorbol 12-myristate 13-acetate. Grey bars=Day 1, black bars=Day 2.

4.1.4 Effect of sialic acid on *in vitro* PMA stimulated Tregs

Upon stimulation with PMA, a reduction in CD4 cell-surface expression was observed (**Figure 4.11**). Additionally, percentage levels of CD43 was significantly lower across all Tregs following *in vitro* expansion, compared to that observed from fresh PBMCs analysed on the same day of sampling (chapter 3.0). NFκB and FoxP3 percentage positivity was assessed in $CD43^+$ and $CD43^-$ Tregs (**Figure 4.10**). Stimulation with PMA increased intracellular percentages of NFκB and FoxP3 in both $CD43^+$ and $CD43^-$ Tregs at each time point. After 1 day in culture, Sia reduced the relative numbers of $NF\kappa B^+$ and $FoxP3^+$ Tregs, where the latter displays a statistically significant reduction over time. The same effect was observed after 2 days in $CD43^-FoxP3^+$ Tregs but not in $CD43^+FoxP3^+$ Tregs. Furthermore, after 2 days, the addition of Sia had no significant effect on $NF\kappa B^+$ Tregs.

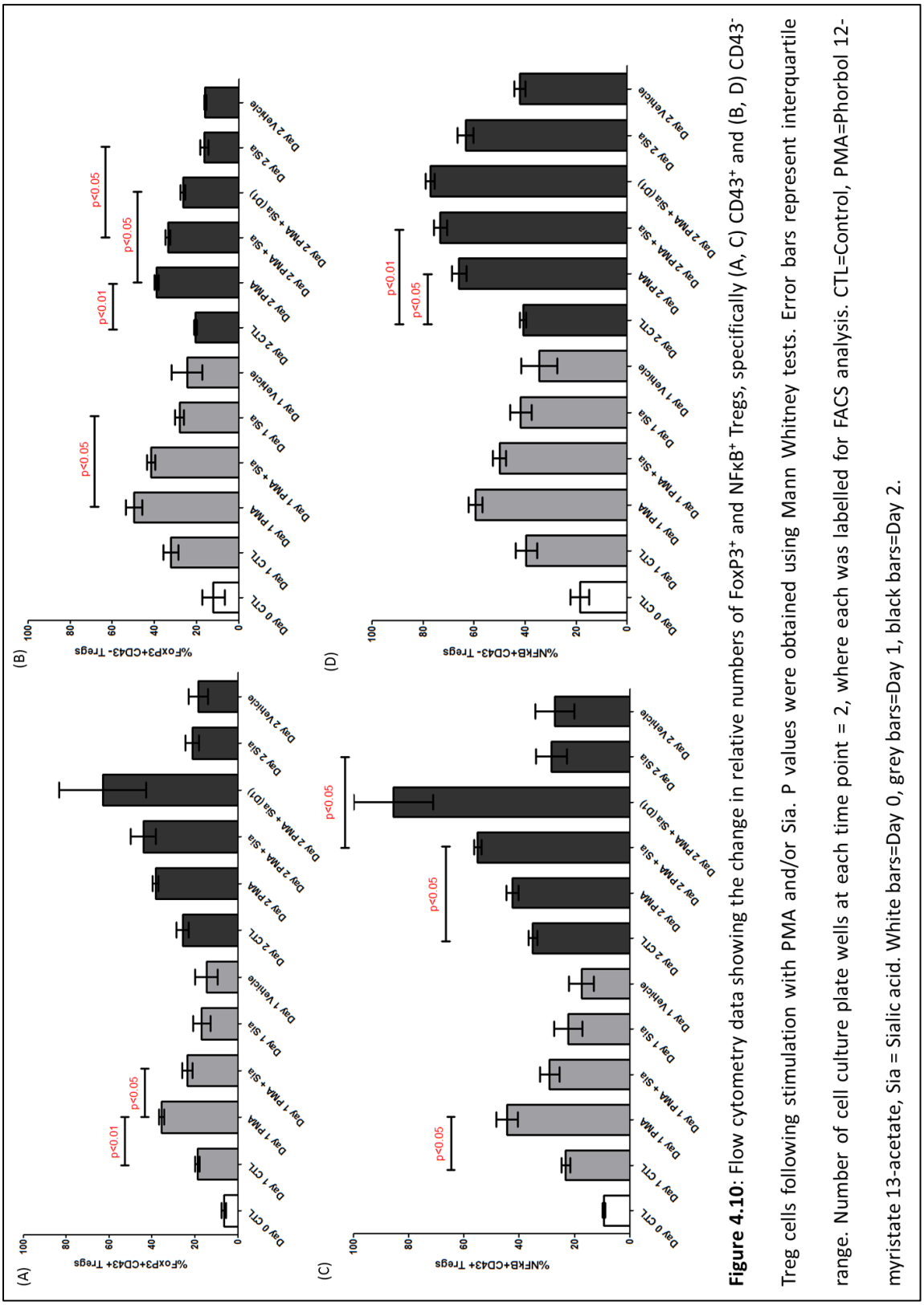

Figure 4.10: Flow cytometry data showing the change in relative numbers of FoxP3$^+$ and NFκB$^+$ Tregs, specifically (A, C) CD43$^+$ and (B, D) CD43$^-$ Treg cells following stimulation with PMA and/or Sia. P values were obtained using Mann Whitney tests. Error bars represent interquartile range. Number of cell culture plate wells at each time point = 2, where each was labelled for FACS analysis. CTL=Control, PMA=Phorbol 12-myristate 13-acetate, Sia = Sialic acid. White bars=Day 0, grey bars=Day 1, black bars=Day 2.

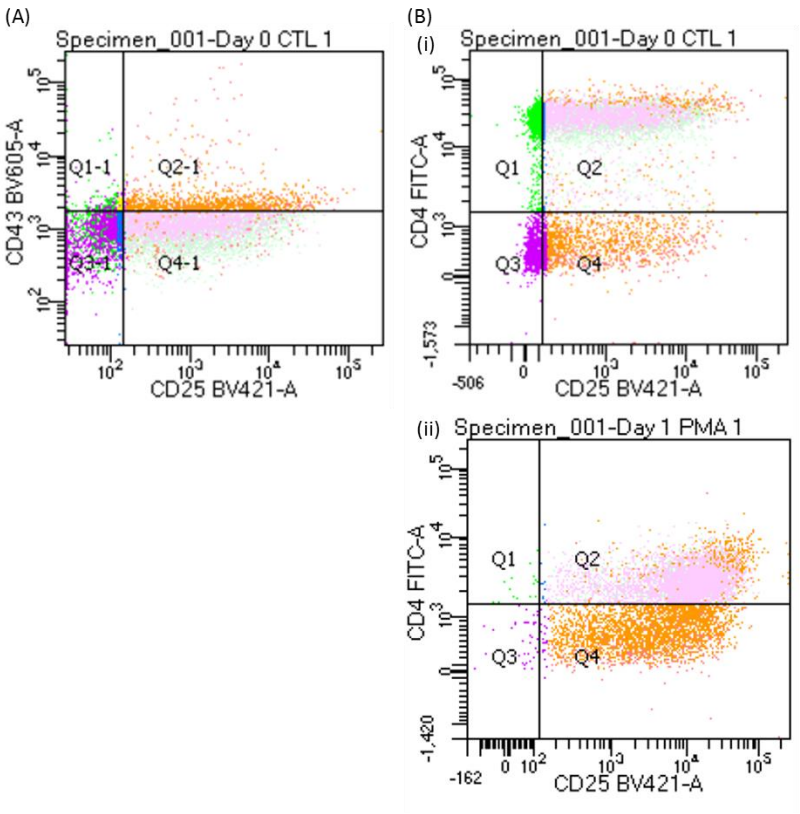

Figure 4.11: (A) The relative number of CD43⁺ Tregs (Q2-1) was reduced after being placed in culture for 14 days in comparison to PBMCs analysed on the day of sampling (Refer to chapter 3.0, Figure 3.2). (B) (ii) The percentage of CD4 positivity (Q2) was reduced following PMA stimulation, compared to (i) CTL cells without stimulation.

Additionally, the cell culture supernatants from the same experiment were analysed as before for levels of cytokines including TNFα, IL-10 and IFNγ (**Figure 4.12**). As shown previously, PMA increased levels of TNFα and IL-10 on both Day 1 and Day 2. IFNγ levels were also increased upon stimulation with PMA on Day 1, however contradictory to previous results, IFNγ levels remained similar in PMA stimulated and unstimulated cells. At each time point, addition of Sia caused a significant reduction in each of the cytokines tested. The experiment was repeated using Tregs expanded from a different source. On this occasion, only time points Day 0 and Day 1 were assessed, with similar results observed.

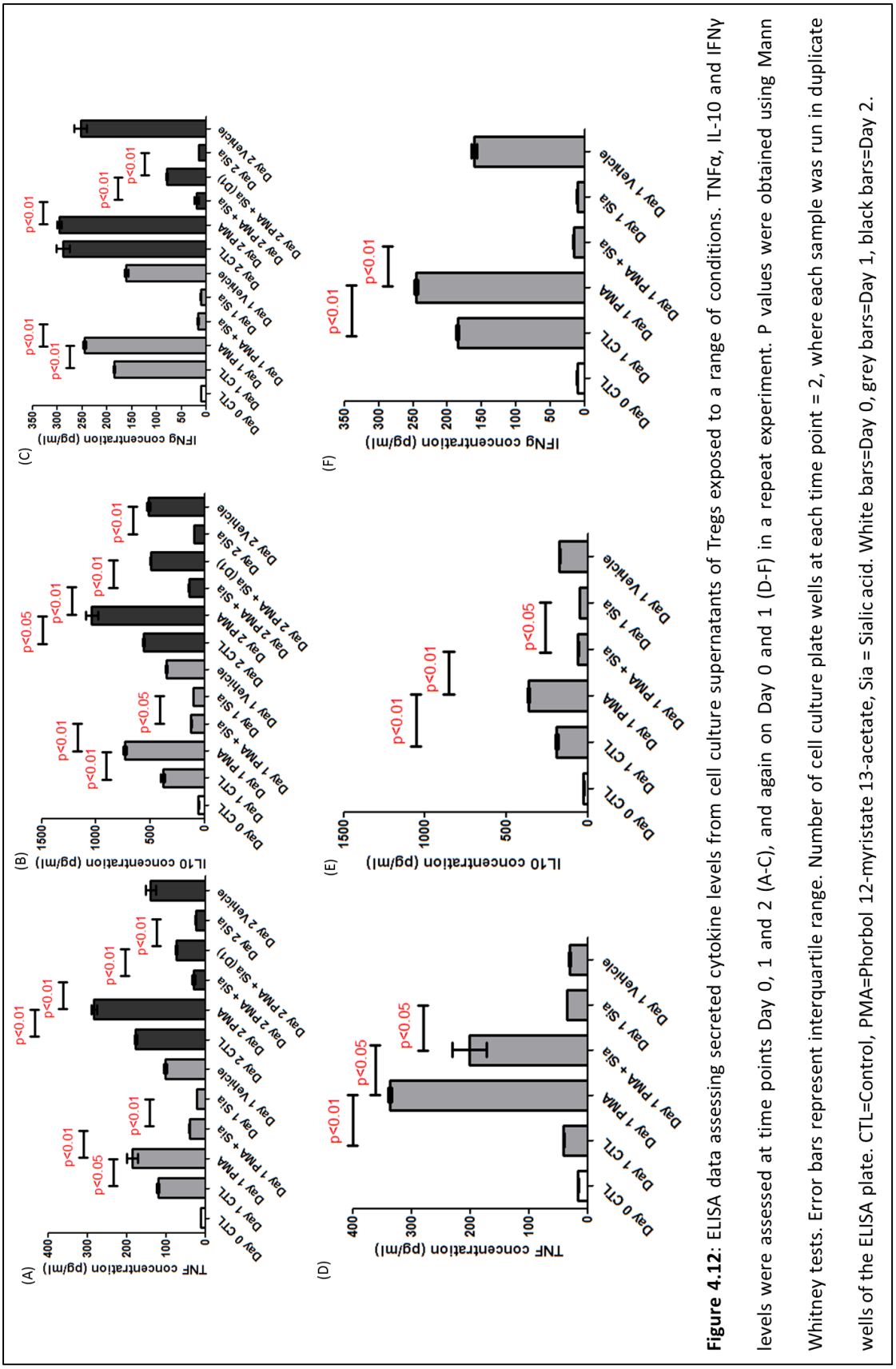

Figure 4.12: ELISA data assessing secreted cytokine levels from cell culture supernatants of Tregs exposed to a range of conditions. TNFα, IL-10 and IFNγ levels were assessed at time points Day 0, 1 and 2 (A-C), and again on Day 0 and 1 (D-F) in a repeat experiment. P values were obtained using Mann Whitney tests. Error bars represent interquartile range. Number of cell culture plate wells at each time point = 2, where each sample was run in duplicate wells of the ELISA plate. CTL=Control, PMA=Phorbol 12-myristate 13-acetate, Sia = Sialic acid. White bars=Day 0, grey bars=Day 1, black bars=Day 2.

4.1.5 Monocyte and Treg co-culture

Similar to the previous experiments, expanded Tregs were stimulated with PMA and exposed to a range of conditions. The Tregs were co-cultured for 1 day with $CD169^+$ monocytes that were sorted on Day 0 of the experiment. CD169 and CD43 blocking antibodies were also added in separate conditions in order to assess the downstream effects of preventing any interaction between these markers. As a control, Tregs not co-cultured with monocytes were also subjected to CD169 and CD43 blocking antibodies in order to test the effect of the antibodies alone on the Tregs. The experiment was carried out using expanded Tregs from two healthy individuals. As before, relative numbers of $NF\kappa B^+$ and $FoxP3^+$ Tregs were assessed by flow cytometry. Additionally, the media in which the cells were incubated was kept for cytokine analysis. For each biological replicate, an increase in relative number of $FoxP3^+$ Tregs was observed after CD43 blocking for Tregs with and without monocytes, however this was not statistically significant (**Figure 4.13**). A similar effect was observed in $NF\kappa B^+$ Tregs, however statistical significance was only observed in Tregs that were co-cultured with monocytes, and only in one of the two biological replicates. Additionally, $NF\kappa B^+$ Tregs were increased in PMA stimulated Tregs that were co-cultured with monocytes compared to those that were not, however significance was observed only with one of the two replicates.

The ELISA results show a significant increase in levels of TNFα when monocytes are co-cultured with Tregs compared to Tregs alone (**Figure 4.14**). Additionally, a decrease was observed when the co-cultured Tregs and monocytes were incubated with CD169 blocking antibody, however statistical significance was only observed in

one replicate. Similarly, a decrease in secreted TNFα was also observed when CD43 blocking antibody was added to Tregs both with and without monocyte co-culture. However, this was only significant for one replicate. IL-10 levels were significantly decreased when Tregs were incubated with CD43 antibody for one of the two replicates, however this observation was not made when monocytes were co-cultured with the Tregs. Furthermore, blocking with CD169 antibody increased IL-10 levels in Treg-monocyte co-culture, which was statistically significant in one of the biological replicates. Finally, IFNγ levels were increased when monocytes were co-cultured with Tregs compared to Tregs alone, with statistical significance observed in one of the biological replicates.

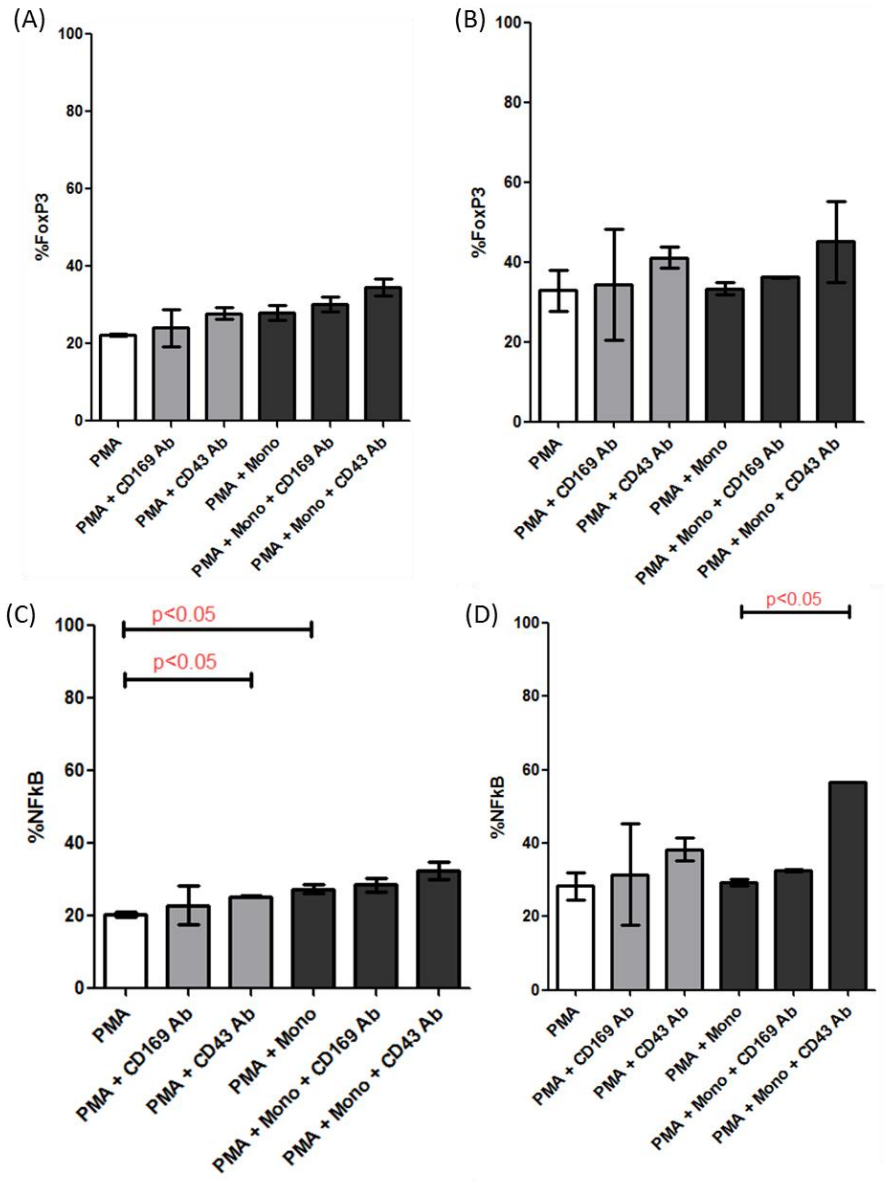

Figure 4.13: Flow cytometry data showing relative numbers of NFκB^{+} and FoxP3^{+} Tregs after being exposed to a range of different conditions. The experiment was carried out on Tregs from two separate individuals; (A,C) and (B,D). P values were obtained using Mann Whitney tests. Error bars represent interquartile range. Number of cell culture plate wells at each time point = 2, where each was labelled for FACS analysis. PMA=Phorbol 12-myristate 13-acetate, Sia = Sialic acid. White bars=PMA only, grey bars=PMA + Ab, black bars=PMA + monocytes with or without Ab.

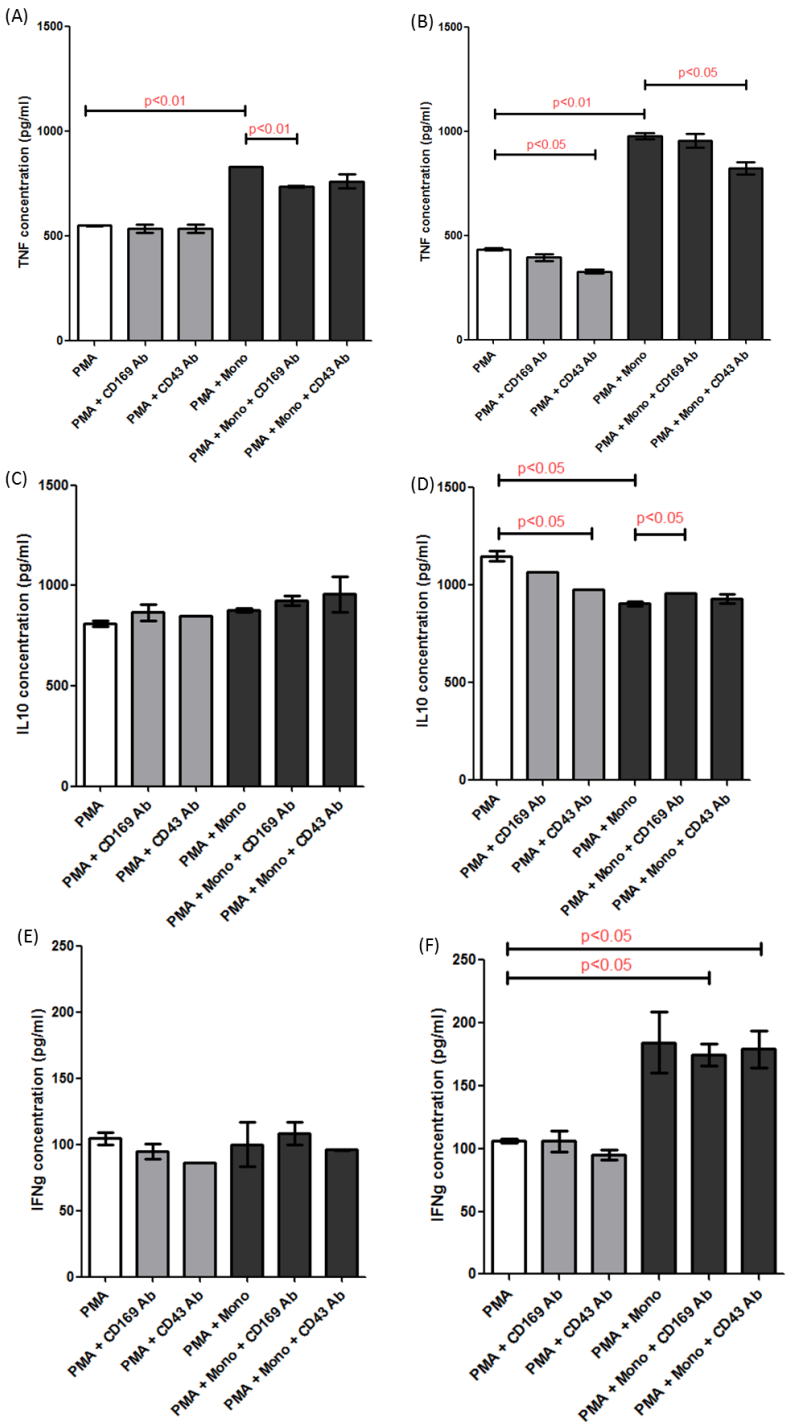

Figure 4.14: ELISA data showing extracellular levels of TNFα, IL-10 and IFNγ present in culture media when Tregs were exposed to a range of different conditions. The experiment was carried out on Tregs from two separate individuals; (A,C,E) and (B,D,F). P values were obtained using Mann Whitney tests. Error bars represent interquartile range. Number of cell culture plate wells at each time point = 2, where each was run in duplicate wells of the ELISA plate. PMA=Phorbol 12-myristate 13-acetate, Sia = Sialic acid. White bars=PMA only, grey bars=PMA + Ab, black bars=PMA + monocytes with or without Ab.

4.2 Discussion

This chapter is focused on an investigation of the activation state of circulating Tregs in RA patients as well as an *in vitro* model of RA. Furthermore, it investigates the role of Sia in potentiating Treg intracellular signalling pathways that are involved in cytokine production during an *in vitro* inflammatory response.

The initial studies defined the relative number of circulating Tregs in RA patients who were cDMARD naïve, responders and non-responders, with healthy participant samples as controls. cDMARD naïve and responder patients have an increased relative number of Tregs compared to healthy controls, however cDMARD non-responders exhibit reduced Tregs compared to responders. This is in agreement with previous data, where patients who responded to anti-TNF treatment had increased relative numbers of circulating Tregs compared to their own baseline samples, suggesting the downregulation of Tregs in RA may be reversed as a consequence of treatment response. (Ehrenstein *et al.* 2004). This is one explanation for the significant reduction in Tregs of cDMARD non-responders compared to responders in the current study. However, the current study did not find a significant difference in relative Treg numbers between cDMARD naïve patients and cDMARD responders, perhaps because of its cross-sectional rather than longitudinal nature. Also, there was a relatively small number of cDMARD naïve patients (n=6) sampled for the study compared to responders (n=24).

Intracellular levels of FoxP3 were determined in each patient subgroup as a surrogate measure of Treg activation, as summarised in **Figure 4.15**. $CD45RA^{+}$ Tregs were also

analysed, representing a naïve subset of Tregs that have not previously been exposed to activation by antigen encounter. Within the $CD45RA^+$ Tregs, the percentage of $FoxP3^-$ cells were increased in cDMARD non-responders compared to healthy controls, cDMARD naïve and cDMARD responder patients. Furthermore, the relative number of $FoxP3^+$ cells was decreased in cDMARD responders and non-responders compared to healthy controls. This suggests the activation state of naïve Tregs is reduced in circulating blood of RA patients, which concurs with previous findings, where $FoxP3^+$ Tregs from peripheral blood were reduced in RA patients compared to healthy controls (Matsuki *et al.* 2013). Interestingly, the relative number of $CD45RA^-$ $FoxP3^+$ Tregs was increased in RA patients compared to healthy controls, in agreement with a recent study (Walter *et al.* 2016). This data suggests there is an increase in activation of $CD45RA^-$ memory Tregs in RA peripheral blood compared to health. However, a significant decrease is observed in the relative number of $CD45RA^-FoxP3^+$ Tregs in cDMARD non-responders compared to cDMARD naïve and cDMARD responder patients. In summary, these findings suggest cDMARD non-responder RA patients exhibit reduced activity in both naïve and memory Tregs. Similar findings were observed in $CD43^+$ Tregs, suggesting there is no significant difference in the activity state of overall Tregs compared to the $CD43^+$ subset. However, as reported in chapter 3, the percentage of CD43 positive Tregs is >80% in RA and health.

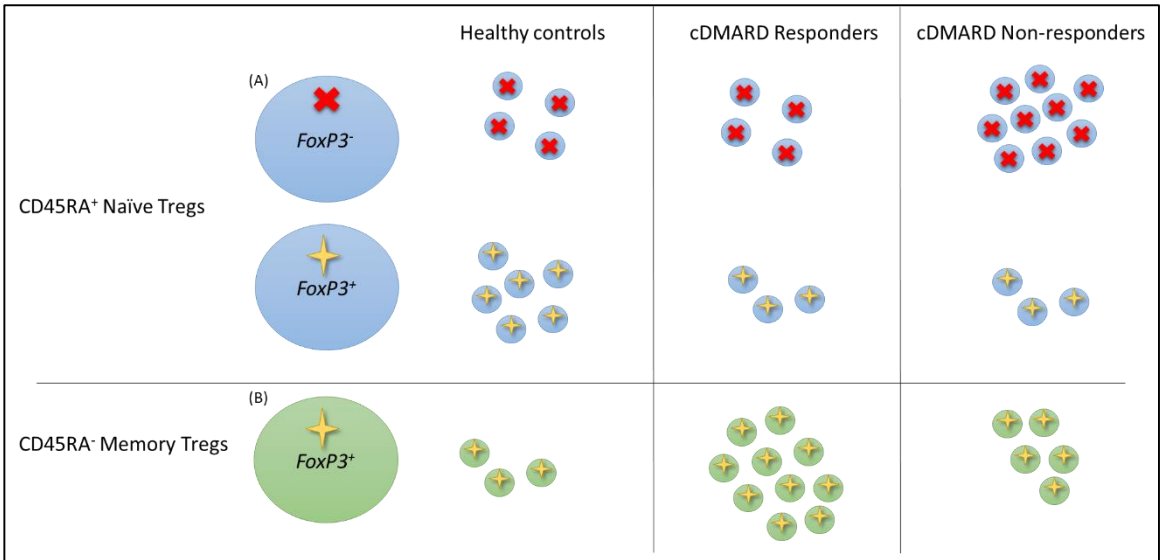

Figure 4.15: (A) The relative number of naïve Tregs with low activation (FoxP3$^-$) are significantly increased in cDMARD non-responders compared to healthy controls and responders. However, the relative number of naïve Tregs with high activation (FoxP3$^+$) are decreased in responders and non-responders compared to healthy controls. (B) The relative number of activated memory Tregs (FoxP3$^+$CD45RA$^-$) are significantly increased in RA patients compared to healthy controls, however with more effect in responders.

An *in vitro* model of inflammation was created in order to assess specific intracellular signalling pathways of Tregs and the subsequent cytokines produced. The aim of the inflammatory model was to induce an activation state in Tregs mimicking their phenotype in RA, as measured by production of pro-inflammatory cytokines including TNFα and IL-6. As described in section 4.0.4, LPS and PMA/IO are common stimulants used to activate Tregs. Transcript levels of TNFα and IL-6 were measured in preliminary experiments in order to firstly decide which stimulant was optimal, and secondly which concentration of the stimulant had the greatest effect on cytokine production. LPS stimulation had no effect on TNFα or IL-6 transcript levels, or on TNFα, IL-10 and IFNγ cytokine production. One possible explanation for this is that perhaps 48-hour stimulation was insufficient to observe a significant increase in TNFα or IL-6. Although 10 ng/ml PMA/IO increased TNFα transcript levels after 2 days

of stimulation, this was not reproducible when the experiment was repeated. A similar effect was observed in IL-6 transcript levels. However, PMA/IO reproducibly increased TNFα cytokine production of Tregs. An increase in TNFα transcript may be detected at an earlier time point than Day 1, and perhaps for this experiment this effect could have been missed. This would explain why secreted TNFα levels are higher in surrounding media when stimulated with PMA/IO, but transcript levels are not. Previous studies have used short incubation times of usually 5 hours during PMA/IO stimulation of Tregs (Duhen *et al.* 2012; Guo *et al.* 2016). Interestingly, PMA/IO stimulation increased IL-10 transcript levels as well as cytokine production. This effect was not observed with LPS stimulation. Conversely, PMA/IO reduced IFNγ cytokine levels after 2 days of stimulation, however later experiments demonstrate the opposite effect with a reduced stimulation time of just 1 day. This suggests there is an initial increase in IFNγ within 1 day of PMA/IO stimulation, however it is unclear why this is not detected between Day 1 and Day 2 of stimulation. It may be possible that IFNγ eventually binds to its receptors on the surface of Tregs and therefore is not detected by ELISA, however further experiments are needed to confirm this finding. Furthermore, it may reflect the fact that IFNɣ is unstable and has a relatively short half-life (Lortat-Jacob *et al.* 1996).

Sia was added to the activated Tregs in order to imitate the effect of CD169, which can bind to and present this residue. CD169 binds to Sia in order to carry out its functions, including binding to ligands on the surface of Tregs. A previous study showed Tregs contain many Sia ligands on their cell surface (Wu *et al.* 2009). Although the purpose of the experiment was to determine cytokine and intracellular pathway responses, it cannot be definitively stated that CD169 has the same effect.

This experiment concluded that the addition of Sia significantly reduced the activation state of Tregs, as measured by decreased levels of secreted cytokines TNFα, IL-10 and IFNγ, as well as decreased relative numbers of $NF\kappa B^+$ and $FoxP3^+$ Tregs (**Figure 4.16**). This agrees with previous findings, where Sia has been shown to reduce Treg activation as measured by a reduction of Treg suppressive function as well as activation markers including CD25 (Wu *et al.* 2009; Naito-Matsui *et al.* 2014). However, the impact on cytokine and transcription factors utilised in the current study has not previously been reported. This effect was observed in $NF\kappa B^+$ Tregs only when they were activated with PMA/IO for just 1 day. A similar effect was observed for $NF\kappa B^+CD43^+$ and $NF\kappa B^+CD43^-$ Tregs. However, after 2 days of stimulation Sia significantly reduced $FoxP3^+CD43^-$ Tregs, an effect which was not observed in $FoxP3^+CD43^+$ Tregs. However, although CD43 is present in on average >80% of Tregs in healthy individuals and RA patients (Chapter 3.0), Tregs that have been in culture exhibit a large reduction in CD43 levels. For this reason, $CD43^+$ and $CD43^-$ Tregs were analysed, primarily because $CD43^-$ cells were greater in number than $CD43^+$, and thus data analysis was more reliable.

Introducing Sia into Treg culture significantly reduced TNFα, IL-10 and IFNγ cytokine secretion, an effect that was observed on both Day 1 and Day 2 of culture (**Figure 4.16**). Perhaps the discrepancy between the relative number of $NF\kappa B^+$ and $FoxP3^+$ Tregs, and cytokine levels on Day 2 of culture is a result of an initial cytokine response within the first day of stimulation that is still detected in surrounding media on Day 2.

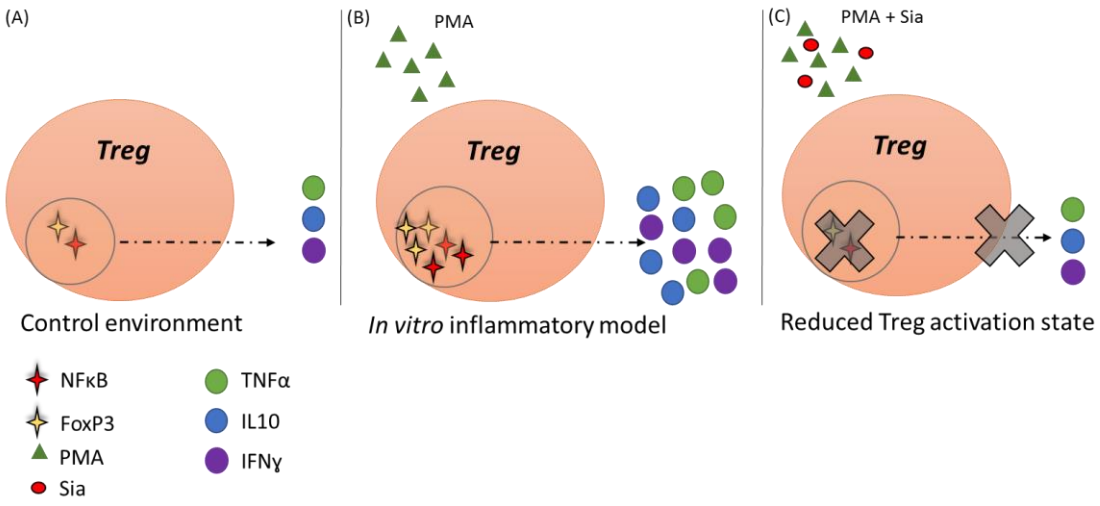

Figure 4.16: (B) In vitro Tregs stimulated with PMA exhibit increased percentages of FoxP3 and NFκB, as well as increased secreted cytokines compared to (A) control unstimulated cells. However, when Sia is added in addition to PMA (C), a reduction in NFκB and FoxP3 as well as secreted cytokines is observed.

In order to assess the direct impact of CD169^{+} monocytes on activated Tregs, and the CD169-CD43 interaction, the two cell types were co-cultured for one day and cytokine secretion as well as intracellular signalling pathways were analysed. The relative number of FoxP3^{+} Tregs were increased following CD43 blocking, an effect observed both when cells were co-cultured with monocytes and without co-culture. Similarly, NFκB^{+} Tregs were also increased with CD43 blocking. Although further experiments are needed to confirm this effect, these results suggest blocking CD43 increases the activation state of Tregs as measured by FoxP3 and NFκB. This contradicts previous findings that suggest CD43 activation leads to increased proliferation of T cells (Higashi *et al.* 2001). Furthermore, NFκB positivity was increased in PMA stimulated Tregs that were co-cultured with monocytes compared to those that were not. Overall, significant differences in these intracellular levels were not consistent across each biological replicate, therefore perhaps with further replicates the results would be more conclusive. However, despite the lack of

statistical significance, similarities are observed between relative numbers of $FoxP3^+$ and $NF\kappa B^+$ Tregs which is in agreement with previous studies.

TNFα cytokine levels in surrounding media are significantly increased when monocytes are co-cultured with Tregs compared to Tregs alone (**Figure 4.14**). Furthermore, TNFα was reduced when the co-cultured Tregs and monocytes were incubated with CD169 blocking antibody. This result suggests CD169 has a direct effect on TNFα secretion, however further replicate experiments would need to be carried out to strengthen this. Furthermore, it cannot be determined which cell type is producing the increased TNFα levels. However, as CD169 does not contain a cytoplasmic tail and is believed to partake primarily in cell-cell interactions, this suggests the blocking of CD169 is likely to have a direct effect on Tregs. Similarly, TNFα expression decreased when CD43 blocking antibody was added to Tregs both with and without monocyte co-culture. The similarity in results between CD169 blocking and CD43 blocking suggests their interaction may have a direct effect on TNFα, however again further replicates are needed to strengthen this result. IL-10 levels were decreased when Tregs were incubated with CD43 antibody, however this observation was not made when monocytes were co-cultured with the Tregs. Additionally, IFNγ levels were increased when monocytes were co-cultured with Tregs compared to Tregs alone. Previous studies have detected TNFα secretion from peripheral monocytes following LPS stimulation (Schildberger *et al.* 2013), however although macrophages have been shown to produce IFNγ *in vitro*, less is known about whether monocytes have the same capability (Darwich *et al.* 2009). Therefore it is not clear whether the increase in TNFα or IFNγ is a product of Tregs after monocyte stimulation, or whether the monocytes are secreting these cytokines.

4.3 Conclusion

In summary, despite the increase of circulating Tregs in peripheral blood of RA patients compared to healthy controls, their activation state is reduced as observed in the naïve CD45RA^{+}FoxP3^{+} Treg population. Furthermore, although RA patients who have responded to cDMARD treatment have an increased relative number of memory CD45RA^{-}FoxP3^{+} Tregs compared to healthy subjects, cDMARD non-responders have a significantly lower relative number of overall FoxP3^{+} Tregs, suggesting these patients contain peripheral Tregs with a lower activation state. Furthermore, this suggests memory Tregs are upregulated in activation state during cDMARD response thus enabling Tregs to carry out their regulatory function in suppressing Teff cells, therefore suppressing disease activity. However, cDMARD non-responders do not regain an activation state in memory Tregs, therefore the disease cannot be suppressed. Additionally, this data confirms the activity of Tregs can be measured in the peripheral blood of RA patients before they migrate into the synovium. Therefore, it may be possible to use activated Tregs as a surrogate measure of disease activity and treatment response.

Additionally, Sia has a negative effect on Treg activation as measured by a reduction in FoxP3 and NFκB intracellular levels, as well as TNFα, IL-10 and IFNγ cytokine secretion. However, in the present study it is inconclusive whether monocytes have an effect on Treg activity, as further replicates would be needed to provide evidence of this. Furthermore, although similarities are observed in TNFα secretion when CD169 and CD43 blocking antibodies are added to monocyte-Treg co-culture, further

evidence is needed to definitively decide whether the CD169-CD43 interaction has an effect on Treg activation. It is clear however that siglec-Sia mediated signalling is an important control mechanism governing Treg activation and response to inflammation. In the context of RA, the siglec-Sia axis could therefore have significant influence on immune system tolerance and suppression.

Chapter 5

Discovery of proteomic response biomarkers

5.0 Introduction

Many studies have highlighted the need for robust biomarkers in RA in order to assist with diagnosis, prognosis and determining treatment response. The human plasma proteome is of interest as it contains proteins secreted or shed by circulating cells and tissue (Wilkins *et al.* 1996). When the body is under stress, for example during chronic inflammation, the plasma proteome changes as part of the immune response (Lee *et al.* 2015). This chapter focusses on identifying and analysing levels of circulating plasma proteins, as it not only holds potential for discovering treatment response biomarkers, but can also improve our understanding of disease pathogenesis.

5.0.1 Current clinical assessment

Currently, clinicians consider CRP as a protein biomarker, which when combined with clinical observations into a composite score (ie. DAS28-CRP), can assist in the determination of treatment response in RA. Although NICE guidelines recommend CRP levels are regularly monitored throughout treatment (NICE 2009), some studies suggest it can be used as a substitute of ESR in the DAS28 composite score (Wells *et al.* 2009). The increase in circulating CRP levels is caused in part by the secretion of IL-6 from T cells and macrophages during inflammation. However, as discussed in section 1.2.1, the literature presents conflicting evidence of CRP as a reliable marker of joint inflammation or disease activity. (Sokka and Pincus 2009; Eudy *et al.* 2014). Furthermore, the lack of specificity of CRP to RA pathology may be one of the reasons for contradictory evidence (Sokka and Pincus 2009).

Numerous studies have analysed a vast range of proteins in order to more accurately reflect the multifactorial nature of RA pathology, and broaden knowledge of proteomic changes during drug responses in RA. Such studies have successfully identified protein signatures that may increase the reliability of disease activity measures and detection of treatment response in RA.

5.0.2 Proteomic studies in RA

The wide variety of proteomic techniques available has enabled research groups to robustly analyse a number of biological sample types. The most obvious proximal sample to study disease activity in RA patients is synovial fluid. For example, one study used chemical labelling of isobaric tags that react with peptides in order to analyse differentially expressed proteins in synovial fluid between RA and OA patients (Balakrishnan *et al.* 2014). Over 500 proteins were successfully identified as being differentially expressed between the two disease types. Therefore, there is potential with analysing the synovial proteome to better distinguish RA and OA, and thus improve clinical decisions and patient outcome. Cytosolic proteins can be isolated from synovial tissue by 2-dimensional gel electrophoresis. A study using this method found protein expression patterns which differentiate RA from spondyloarthropathy (Tilleman *et al.* 2005), therefore enabling earlier diagnosis. Similar studies have used the same method to analyse proteins from fibroblast-like synoviocyte (FLS) cells and have also identified potential novel diagnostic proteins for RA (Dasuri *et al.* 2004; Li *et al.* 2013). The analysis of proteins from synovial fluid or tissue may be useful in understanding disease pathogenesis, as this is the target of the autoimmune response in RA. However, this sampling method is rather invasive,

and it is impractical to sample comparator healthy control groups. Although the study of proteins from tissue-specific cells is advantageous in understanding the cell biology of RA, the lengthy laboratory procedures are somewhat impractical for regular determination of treatment response.

Other studies adopt a less invasive approach, by analysing alternative biological samples including urine, plasma and serum. A recent study used liquid chromatography – tandem mass spectrometry (LC-MS/MS) in order to quantify proteins in urine (Kang *et al.* 2014). The study resulted in identification of 134 differentially expressed proteins between RA and OA patients. Furthermore, they identified soluble CD14 as a potential biomarker of disease activity in RA, as it was shown to correlate to ESR, CRP and DAS28. These results are similar to a previous study which used the same method to analyse synovial fluid protein expression profiles in RA, which were found to be associated with serum CRP levels (Liao *et al.* 2004). However, urine proteome analysis demonstrates that less invasive sampling may prove useful in identifying RA biomarker candidates (Kang *et al.* 2014)

An increasing number of studies are analysing proteins in circulating blood. One study compared circulating serum and plasma proteins in RA patients treated with anti-TNFs, in order to identify the mechanism of action of an anti-TNF biologic (Sekigawa *et al.* 2008). They used LC-MS/MS in order to deplete abundant proteins and analyse low level protein peptides in each sample. Initial findings reported differences in protein expression between serum and plasma samples, for example S100 calcium-binding protein A9 could be detected in plasma but not serum. Additionally, they identified an increase in proteins related to NFκB activation

following anti-TNF treatment, suggested to be released as a result of the death of TNFα producing cells following treatment.

In summary, previous proteomic studies have demonstrated how global analyses has the potential to improve our knowledge on the association of the circulating proteome with RA pathogenesis. However, a compromise must be made when deciding on which biological sample type to use. The analysis of synovial fluid is ideal in increasing understanding of the disease, however the invasiveness of the procedure may be impractical for biomarker discovery that may eventually inform clinical decisions. Additionally, previous chapters have discussed the involvement of pathologically relevant cells in response and non-response to treatment in RA. Thus, it is important to consider the impact the balance and interactions these circulating cells may have on surrounding plasma. Thus, this chapter focuses on the plasma proteome in RA patients, as it is a potentially rich source of biomarker candidates to more accurately define disease activity and treatment response. Furthermore, it contributes to our knowledge of the circulating changes in secreted and shed cellular proteins, which are involved in systemic pathology.

5.1 Results

5.1.1 cDMARD response

NPX values from all four OLINK panels across each patient group were analysed using Perseus software. Initially, a volcano plot was drawn to observe significant differences between the protein expressions of responders and non-responders (**Figure 5.1A**). Several proteins are upregulated in DMARD non-responders compared to responders. Such proteins include caspase-3 (CASP-3), P-selectin (SELP), junctional adhesion molecule-A (JAM-A), melusin (ITGB1BP2), dickkopf-related protein 1 (Dkk-1), angiopoietin-1 (ANG-1) and CD40 ligand (CD40-L) among others. Furthermore, peroxiredoxin-1 (PRDX1) is significantly reduced in DMARD non-responders compared to responders.

Statistically significant differences in detected levels of plasma proteins were calculated between each patient group using an ANOVA test with permutation based FDR, where FDR = 0.05 (with the number of randomizations set at 250). A heat map was then drawn showing only the proteins that were significantly different between groups, having an FDR q value of <0.05 (**Figure 5.1B and 5.1C**).

Of the 42 proteins calculated as significantly different between patient groups, the majority were upregulated in DMARD non-responders, compared to responders and DMARD naïve patients. The unsupervised clustering of the heat map shows a split between a) DMARD non-responders and b) DMARD naïve and responders, where just one DMARD non-responder is clustered among the responders. Furthermore, one DMARD non-responder shows a reduced protein expression for the majority of the

42 proteins graphed, compared to all other patient samples. The reason for this outlier is unclear from available clinical data.

Volcano plots were also drawn to observe any significant differences in protein expression between DMARD naïve patients and other patient groups. No statistically significant differences between DMARD naïve and responder RA patients were observed. However, 5 proteins were found to be significantly increased in DMARD non-responders compared to DMARD naïve patients, including CASP-3, SELP, JAM-A, PDGF subunit A and ITGB1BP2 (**Figure 5.2**). Furthermore, PRDX1 was significantly decreased in DMARD non-responders compared to responders.

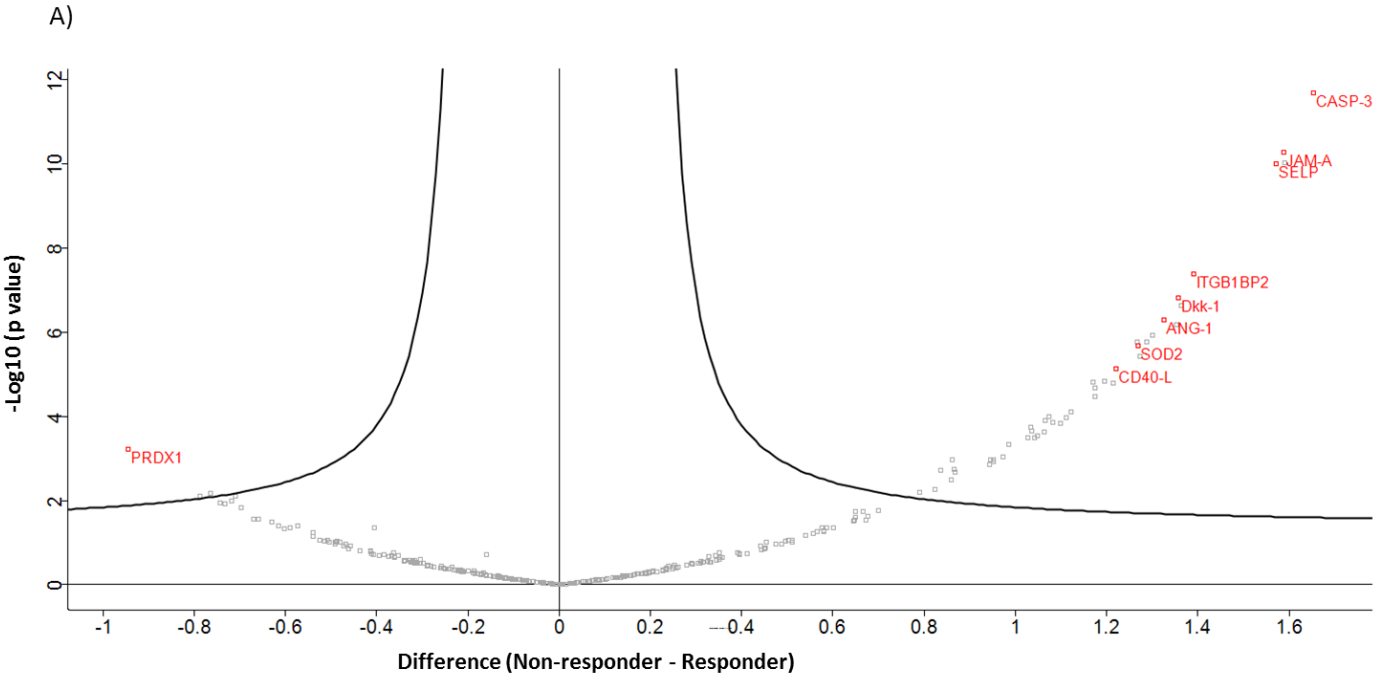

Figure 5.1A: Volcano plot showing the significance (-Log p) of the fold difference between DMARD non-responders (n=29) and responders (n=20). Red indicates proteins with the largest statistically significant differences in expression between groups. The y axis represents the -Log10(p value), and the x-axis represents the difference between the Z scored NPX value in each patient group. The significance threshold (bold black line) was set when the p value was less than 0.05 (-Log10(0.05) = 1.3), and the fold change in protein expression was ≥2.

B)

Protein	Difference (Non-responder - Responder)	- log ANOVA p value (all patient groups)	ANOVA p value	FDR q value
CASP-3	1.654	12.924	<0.0001	<0.001
SELP	1.571	11.523	<0.0001	<0.001
JAM-A	1.589	11.496	<0.0001	<0.001
PDGF subunit A	1.591	10.616	<0.0001	<0.001
ITGB1BP2	1.391	8.522	<0.0001	<0.001
Dkk-1	1.358	8.010	<0.0001	<0.001
PECAM-1	1.363	7.441	<0.0001	<0.001
ANG-1	1.326	7.229	<0.0001	<0.001
DECR1	1.267	6.782	<0.0001	<0.001
SOD2	1.269	6.529	<0.0001	<0.001
DAPP1	1.353	6.492	<0.0001	<0.001
DCTN1	1.288	6.278	<0.0001	<0.001
PAI	1.300	6.022	<0.0001	<0.001
CD40-L	1.220	5.899	<0.0001	<0.001
HB-EGF	1.169	5.446	<0.0001	0.001
HCLS1	1.273	5.285	<0.0001	0.002
IRAK4	1.173	5.008	<0.0001	0.002
STK4	1.214	4.892	<0.0001	0.002
SH2B3	1.196	4.743	<0.0001	0.002
NEMO	1.034	4.686	<0.0001	0.002
CD84	1.065	4.605	<0.0001	0.002
EIF4G1	1.175	4.584	<0.0001	0.002
PRDX1	-0.945	4.435	<0.0001	0.002
TANK	1.073	4.254	0.0001	0.004
CXCL1	1.036	4.251	0.0001	0.004
SIRT2	1.122	4.168	0.0001	0.005
ZBTB16	1.028	3.645	0.0002	0.010
NF2	1.112	3.639	0.0002	0.009
PDGF subunit B	1.042	3.536	0.0003	0.010
SPRY2	1.098	3.498	0.0003	0.011
HEXIM1	1.063	3.444	0.0004	0.011
PPP1R9B	1.048	3.424	0.0004	0.012
PRDX3	1.081	3.382	0.0004	0.013
PAR-1	0.866	3.241	0.0006	0.016
ICA1	0.985	3.217	0.0006	0.017
CCL17	0.837	3.183	0.0007	0.017
STAMPB	0.951	3.023	0.0009	0.021
MGMT	0.943	2.835	0.0015	0.026
SRPK2	0.972	2.757	0.0017	0.028
BLM hydrolase	0.945	2.678	0.0021	0.033
PLXNA4	0.951	2.630	0.0023	0.035
SORT1	0.790	2.612	0.0024	0.035

Protein is **upregulated** in non-responders compared to other patient groups

Protein is **downregulated** in non-responders compared to other patient groups

Figure 5.1B: Raw data showing proteins that are significantly differentially expressed between responders and non-responders, calculated by ANOVA with FDR q value of >0.05. The difference between the Z scored NPX values in non-responders and responders is also shown in correspondence with Figure 5.1A.

(C)

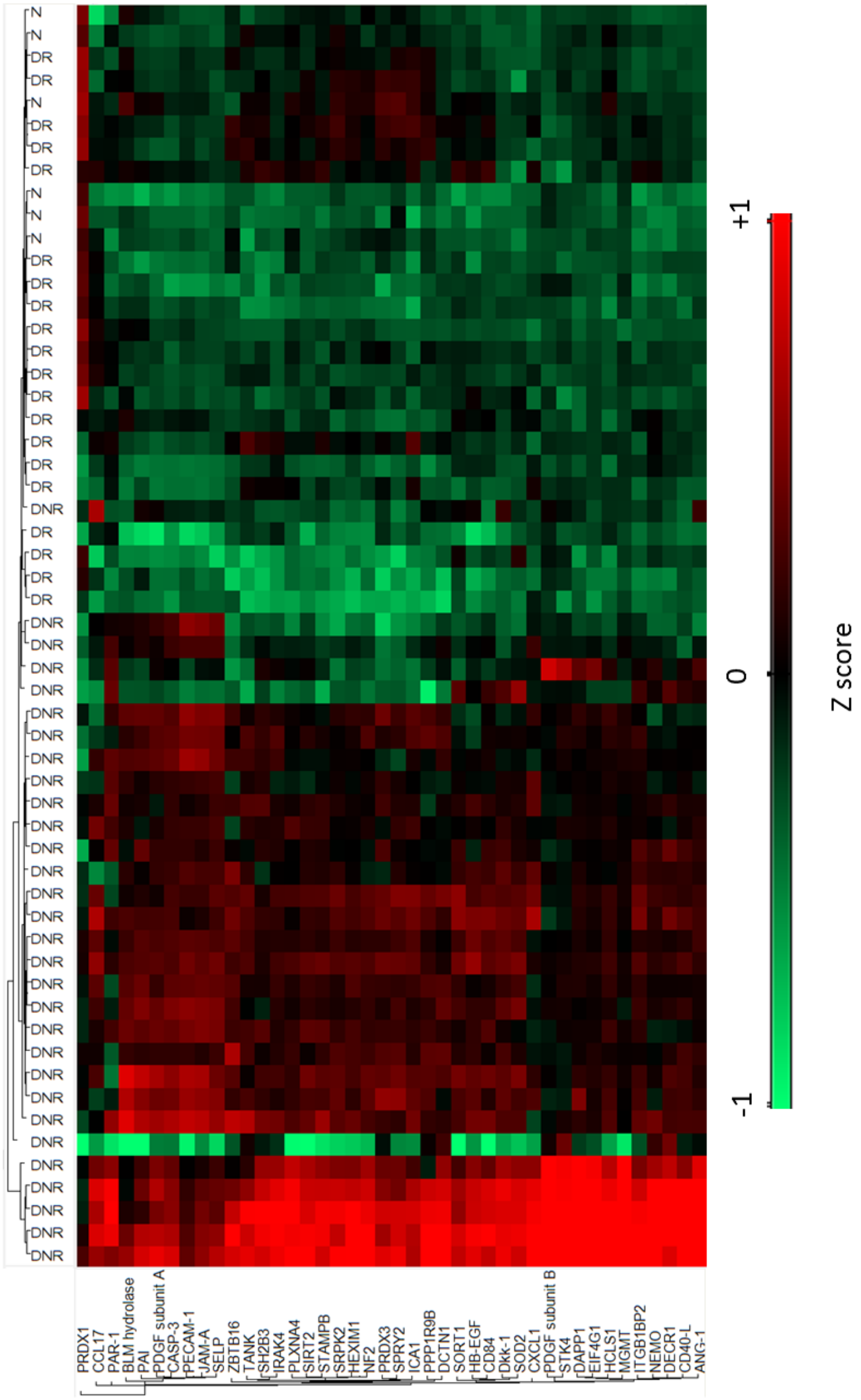

Figure 5.1C: Unsupervised clustering of proteins calculated to be significantly different between DMARD naïve (N), DMARD responder (DR) and DMARD non-responder (DNR) RA patients. Corresponding raw data is shown in Figure 5.1B.

(A)

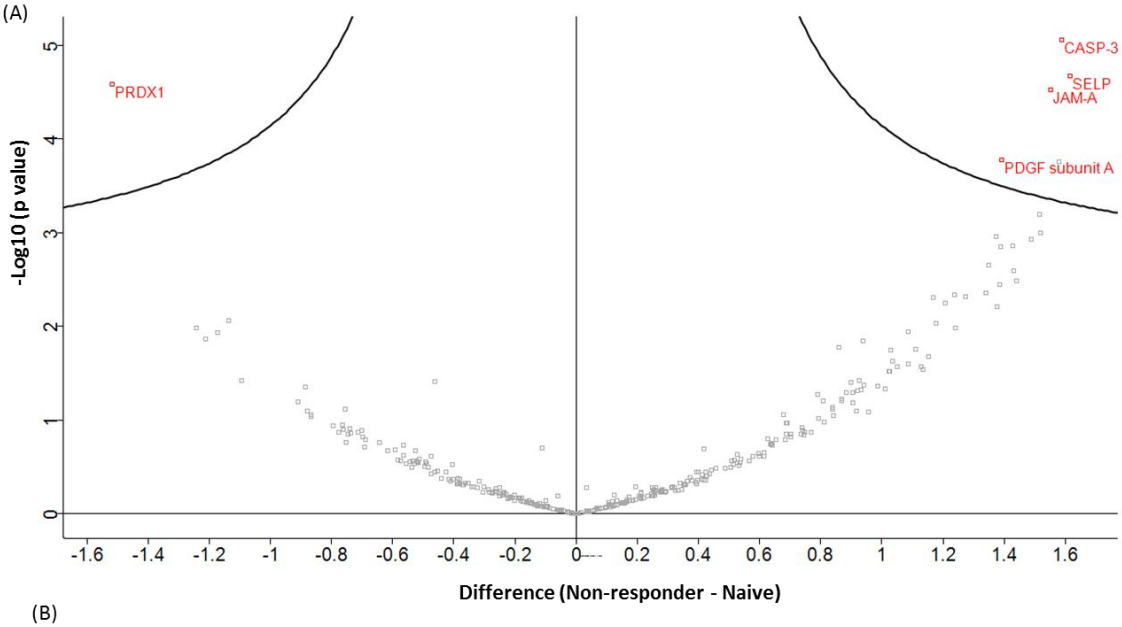

(B)

Protein	Difference (Non-responder - Naïve)	- log ANOVA p value (all patient groups)	ANOVA p value	FDR q value
CASP-3	1.589	12.924	<0.0001	<0.001
SELP	1.616	11.523	<0.0001	<0.001
JAM-A	1.553	11.496	<0.0001	<0.001
PDGF subunit A	1.393	10.616	<0.0001	<0.001
PRDX1	-1.518	4.435	<0.0001	0.002

Protein is **upregulated** in non-responders compared to other patient groups

Protein is **downregulated** in non-responders compared to other patient groups

Figure 5.2: (A) Volcano plot with (B) corresponding raw data showing the significance (-Log p) of the fold difference between cDMARD non-responders (n=29) and cDMARD naïve patients (n=6).Red indicates proteins with the largest statistically significant differences in expression between groups. The y axis represents the -Log10(p value), and the x-axis represents the difference between the Z scored NPX value in each patient group. The significance threshold (bold black line) was set when the p value was less than 0.05 (-Log10(0.05) = 1.3), and the fold change in protein expression was ≥2.

As detailed in **Figure 2.6** (section 2.6.1.1), in order to obtain information on the potential impact which these protein expression profiles may have within immune pathways, various online protein pathway programmes were used. Initially STRING was used to map any interaction between the 42 proteins of interest, and key pathways in which they are involved (**Figure 5.3**). The majority of proteins mapped

play a role in signal transduction. Additionally, a number of proteins are involved in MAPK and protein kinase activity, for example ANGPT1/ANG-1 and PDGF. Furthermore, a few of the proteins listed are associated with LPS induction through the TLR4 receptor, such as CASP-3, which has an unspecified reaction with serine/threonine-protein kinase 4 (STK4). Dkk-1 inhibits the plasminogen activator/inhibitor-1 (PAI/serpine1), which has a downstream effect on PDGFA and PDGFB. PDGFB is involved in ANG-1 activation, which subsequently regulates the transcription of proheparin-binding EGF-like growth factor (HBEGF).

Enrichr was also used to obtain further pathway information of the 42 significant proteins. Initially, the relevance of each protein to disease type was assessed. This data was plotted as a bar chart, where increasing length indicates a lower p value and therefore more significance in terms of evidence from current literature (**Figure 5.4**). The full table of associated diseases can be found in Appendix H. Among the 42 proteins analysed, the most statistically significant associated disease group was arthritis, involving proteins SELP, CASP-3, CXCL1 and Dkk-1.

The Enrichr programme was secondly used to obtain details about the pathways these proteins are involved in. One result, originating from Reactome, displayed several of these pathways (**Figure 5.5**). The full list of pathways obtained from the Reactome search can be found in Appendix I. The most significant resulting pathway in terms of evidence in literature from the Reactome search was regulation of phosphoinositide 3-kinase/protein kinase B (PI3K/AKT) signalling (Appendix J), which involves PDGF and interleukin-1 receptor-associated kinase-4 (IRAK4) proteins. Additionally, several proteins were found to be involved in various immune system

pathways, for example IL-10 downregulates CXCL1 among others (Appendix K). Furthermore, NEMO was found to be involved in interleukin-17 receptor A (IL17RA) signalling via the NFκB pathway (Appendix L).

In agreement with findings from STRING (**Figure 5.3**), the Reactome search also demonstrated an interaction between CASP-3 and STK4 (Appendix M). As part of the Hippo signalling pathway which regulates cell proliferation and apoptosis, CASP-3 is known to cleave STK4.

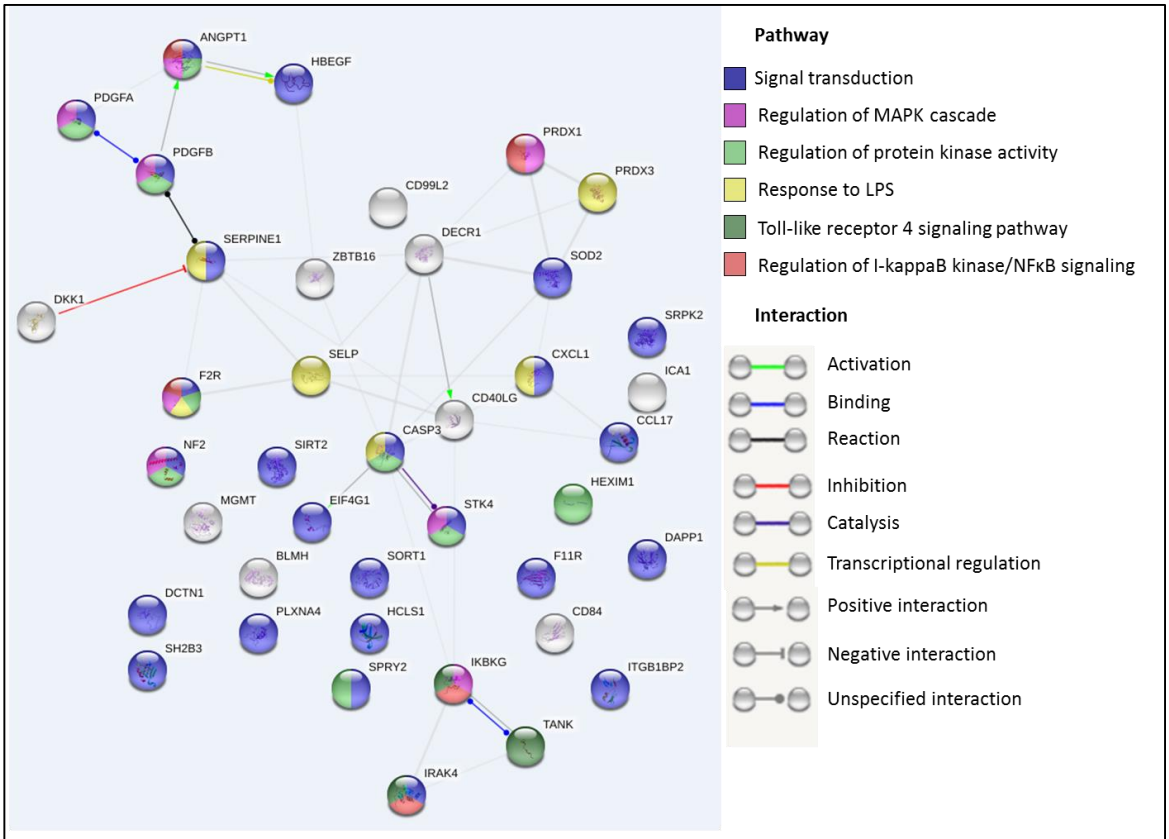

Figure 5.3: STRING mapping of 42 proteins that are significantly differentially expressed between cDMARD naïve, cDMARD responder and cDMARD non-responder RA patients.

Term	P-value	Adjusted P-value	Old P-value	Old Adjusted P-value	Z-score	Combined Score	Genes
Arthritis	0.000615	0.027062	0.000332	0.015781	-4.63612	34.2785932	SELP;CASP3;CXCL1;DKK1
Cerebrovascular_disease	0.011681	0.079781	0.007467	0.068107	-4.35705	19.3879556	SELP;CASP3;DECR1
Proliferative_vitreoretinopathy	0.000386	0.027062	0.000359	0.015781	-2.3334	18.3424629	PDGFB;PDGFA
Hypertension	0.022641	0.079781	0.014588	0.068107	-3.91028	14.8121752	SELP;CASP3;DECR1
Type_2_diabetes_mellitus	0.018776	0.079781	0.012063	0.068107	-3.70886	14.7433466	ZBTB16;ICA1;SPRY2
Huntington's_disease	0.011121	0.079781	0.008386	0.068107	-3.10014	13.9471358	CASP3;SIRT2
Cancer	0.024938	0.079781	0.016096	0.068107	-3.59353	13.2649758	ZBTB16;PDGFB;NF2
Neurodegenerative_disease	0.023462	0.079781	0.015127	0.068107	-3.30937	12.4179696	DCTN1;SIRT2;EIF4G1
Celiac_disease	0.014703	0.079781	0.011039	0.068107	-2.88628	12.1792403	SH2B3;PLXNA4
Hyperglycemia	0.021616	0.079781	0.016168	0.068107	-2.83262	10.8612144	CASP3;DECR1

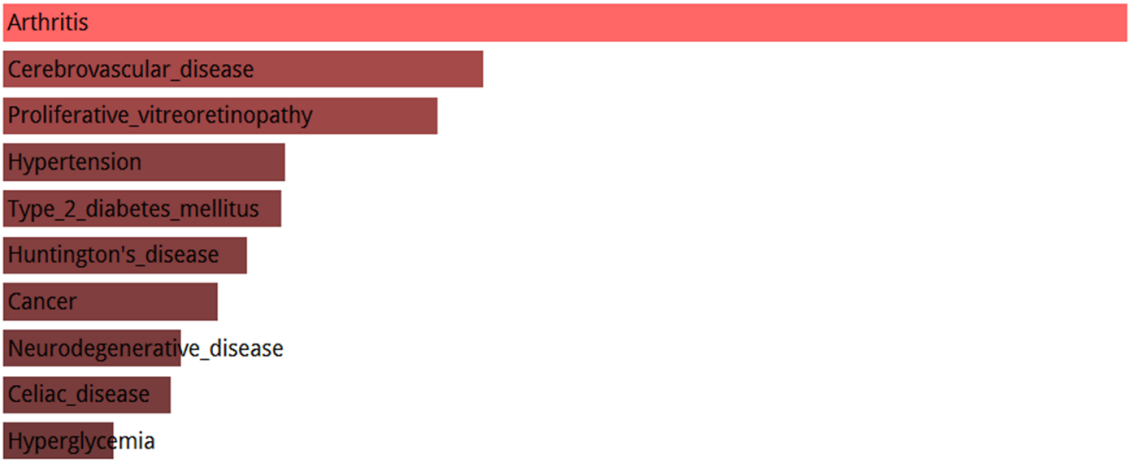

Figure 5.4: STRING mapping of 42 proteins that are significantly differentially expressed between cDMARD naïve, cDMARD responder and cDMARD non-responder RA patients.

Pathway name	#Entities found	#Entities total	Entities ratio	Entities pValue	Entities FDR	#Reactions found	#Reactions total	Reactions ratio	Species name	Submitted entities found
PI5P, PP2A and IER3 Regulate PI3K/AKT Signaling	5	112	0.00828831	1.05E-04	0.01621987	1	7	6.30E-04	Homo sapien	PDGFB;PDGFA;IRAK4;HBEGF
Negative regulation of the PI3K/AKT network	5	120	0.00888034	1.45E-04	0.01621987	1	10	9.00E-04	Homo sapien	PDGFB;PDGFA;IRAK4;HBEGF
Immune System	23	2643	0.19558943	1.79E-04	0.01621987	114	1444	0.13003152	Homo sapien	CD40L;DCTN1;ZBTB16;PDGFB;DAPP1;PDGFA;CXCL1;IRAK4;SOD2;TANK;SELP;CASP3;PECAM1;BLMH;NF2;NEMO;CCL17;EIF4G1;HBEGF
Platelet degranulation	5	137	0.01013839	2.66E-04	0.01621987	4	11	9.91E-04	Homo sapien	SELP;PDGFB;PECAM1;PDGFA
Neurodegenerative Diseases	3	31	0.00229409	3.06E-04	0.01621987	2	22	0.00198109	Homo sapien	PRDX1;SOD2
Deregulated CDK5 triggers multiple neurodegenerative pathways in Alzheimer's disease	3	31	0.00229409	3.06E-04	0.01621987	2	22	0.00198109	Homo sapien	PRDX1;SOD2
Response to elevated platelet cytosolic Ca2+	5	144	0.0106564	3.34E-04	0.01621987	4	14	0.00126069	Homo sapien	SELP;PDGFB;PECAM1;PDGFA
Signaling by Interleukins	11	793	0.05868423	3.60E-04	0.01621987	24	468	0.04214318	Homo sapien	CASP3;PDGFB;PDGFA;CXCL1;IRAK4;SOD2;NEMO;HBEGF
Downstream signal transduction	3	36	0.0026641	4.72E-04	0.01735625	16	16	0.00144079	Homo sapien	PDGFB;PDGFA
Cytokine Signaling in Immune system	13	1108	0.08199512	4.93E-04	0.01735625	31	601	0.05411977	Homo sapien	CD40L;CASP3;PDGFB;PDGFA;CXCL1;IRAK4;SOD2;NEMO;EIF4G1;HBEGF
Constitutive Signaling by Aberrant PI3K in Cancer	4	89	0.00658625	5.26E-04	0.01735625	1	2	1.80E-04	Homo sapien	PDGFB;PDGFA;HBEGF
PI3K/AKT Signaling in Cancer	4	120	0.00888034	0.00158116	0.04410302	1	21	0.00189104	Homo sapien	PDGFB;PDGFA;HBEGF
Platelet activation, signaling and aggregation	6	305	0.02257086	0.00163345	0.04410302	18	114	0.01026565	Homo sapien	SELP;PAR1;PDGFB;PECAM1;PDGFA
Detoxification of Reactive Oxygen Species	3	65	0.00481018	0.00255046	0.06332631	3	34	0.00306168	Homo sapien	PRDX3;PRDX1;SOD2
Signaling by Receptor Tyrosine Kinases	8	585	0.04329165	0.00273196	0.06332631	77	625	0.05628095	Homo sapien	CASP3;PDGFB;SPRY2;PDGFA;STK4;SH2B3;HBEGF
Sema3A PAK dependent Axon repulsion	2	19	0.00140605	0.00289467	0.06332631	3	6	5.40E-04	Homo sapien	STK4;PLXNA4
Signaling by PDGF	3	69	0.00510619	0.00301554	0.06332631	26	28	0.00252139	Homo sapien	PDGFB;PDGFA
Signaling by Hippo	2	22	0.00162806	0.00385023	0.0770046	7	30	0.00270149	Homo sapien	CASP3;STK4
Hemostasis	9	801	0.05927625	0.00541291	0.1028452	32	323	0.029086	Homo sapien	SELP;CD84;PAR1;PDGFB;PECAM1;PDGFA;SH2B3
RHO GTPases activate PAKs	2	27	0.00199808	0.005723	0.10301396	4	15	0.00135074	Homo sapien	NF2;STK4
MGMT-mediated DNA damage reversal	1	2	1.48E-04	0.00825467	0.13157922	2	2	1.80E-04	Homo sapien	MGMT
PIP3 activates AKT signaling	5	303	0.02242285	0.00839101	0.13157922	1	87	0.00783431	Homo sapien	PDGFB;PDGFA;IRAK4;HBEGF
Diseases of Immune System	2	34	0.0025161	0.00890891	0.13157922	9	14	0.00126069	Homo sapien	IRAK4;NEMO
Diseases associated with the TLR signaling cascade	2	34	0.0025161	0.00890891	0.13157922	9	14	0.00126069	Homo sapien	IRAK4;NEMO

Figure 5.5: Protein pathway list generated from Reactome online pathway browser after inputting 42 significantly differentially expressed proteins between DMARD naïve, DMARD responder and DMARD non-responder RA patients.

5.1.2 Disease activity

DAS28-ESR scores from clinical data recorded on the same day as sampling were classified according to EULAR criteria (NICE 2009; Smolen *et al.* 2014b). A DAS28-ESR score of ≥5.1 was classified as 'high' disease activity, >3.2 and ≤5.1 was 'moderate', >2.6 and ≤3.2 was 'low', and <2.6 was classified as 'remission'. As before, volcano plots were drawn to show the significant difference between patients grouped according to class of disease activity at the time of sampling.

No significant difference was observed in protein expression between RA patients with high or low disease activity, likely due to the low number of patients with low disease activity (n=2). However, numerous proteins were significantly different between patients with high disease activity and those in remission (**Figure 5.6**). These proteins include Dkk-1, CD40-L and CASP-3, which are upregulated in patients with high disease activity compared to remission. Furthermore, HSP-27 and MB are downregulated in patients with high disease activity compared to those in remission.

As before, each group was analysed by ANOVA with permutation based FDR. A heat map was then drawn with unsupervised clustering showing only the proteins that were significantly different between groups (**Figure 5.6C**). Of the four protein panels analysed, only ten were statistically significantly different in normalised levels between patient groups. Each of the ten proteins were also significantly different between patient groups when classified by response (section 5.1.1).

(A)

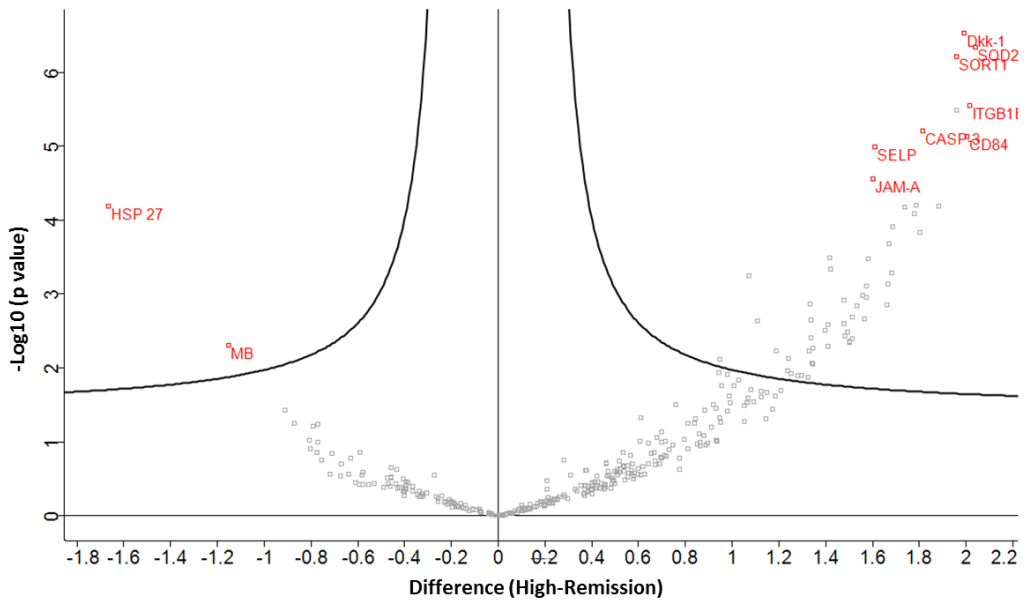

(B)

Protein	Difference (High disease activity - Remission)	- log ANOVA p value (all patient groups)	ANOVA p value	FDR q value
ITGB1BP2	2.015	5.514	<0.0001	0.200
CD84	2.005	5.375	<0.0001	0.110
Dkk-1	1.990	5.355	<0.0001	0.073
SOD2	2.039	5.200	<0.0001	0.057
SORT1	1.961	5.158	<0.0001	0.046
DECR1	1.959	4.988	<0.0001	0.051
CASP-3	1.813	4.985	<0.0001	0.044
CD40-L	1.882	4.724	<0.0001	0.044
PDGF subunit A	1.737	4.616	<0.0001	0.043
SELP	1.611	4.570	<0.0001	0.040

Figure 5.6A and 5.6B: (A) Volcano plot showing the significance (-Log p) of the fold difference between RA patients with disease activity classification of high (n=9) and remission (n=11). Red indicates proteins with the largest statistically significant differences in expression between groups. The y axis represents the -Log10(p value), and the x-axis represents the difference between the Z scored NPX value in each patient group. The significance threshold (bold black line) was set when the p value was less than 0.05 (-Log10(0.05) = 1.3), and the fold change in protein expression was ≥2. (B) Raw data showing proteins that are significantly differentially expressed between all patient groups, calculated by ANOVA with FDR q value of >0.05. The difference between the Z scored NPX values in patients with high disease activity and those in remission is also shown in correspondence with (A).

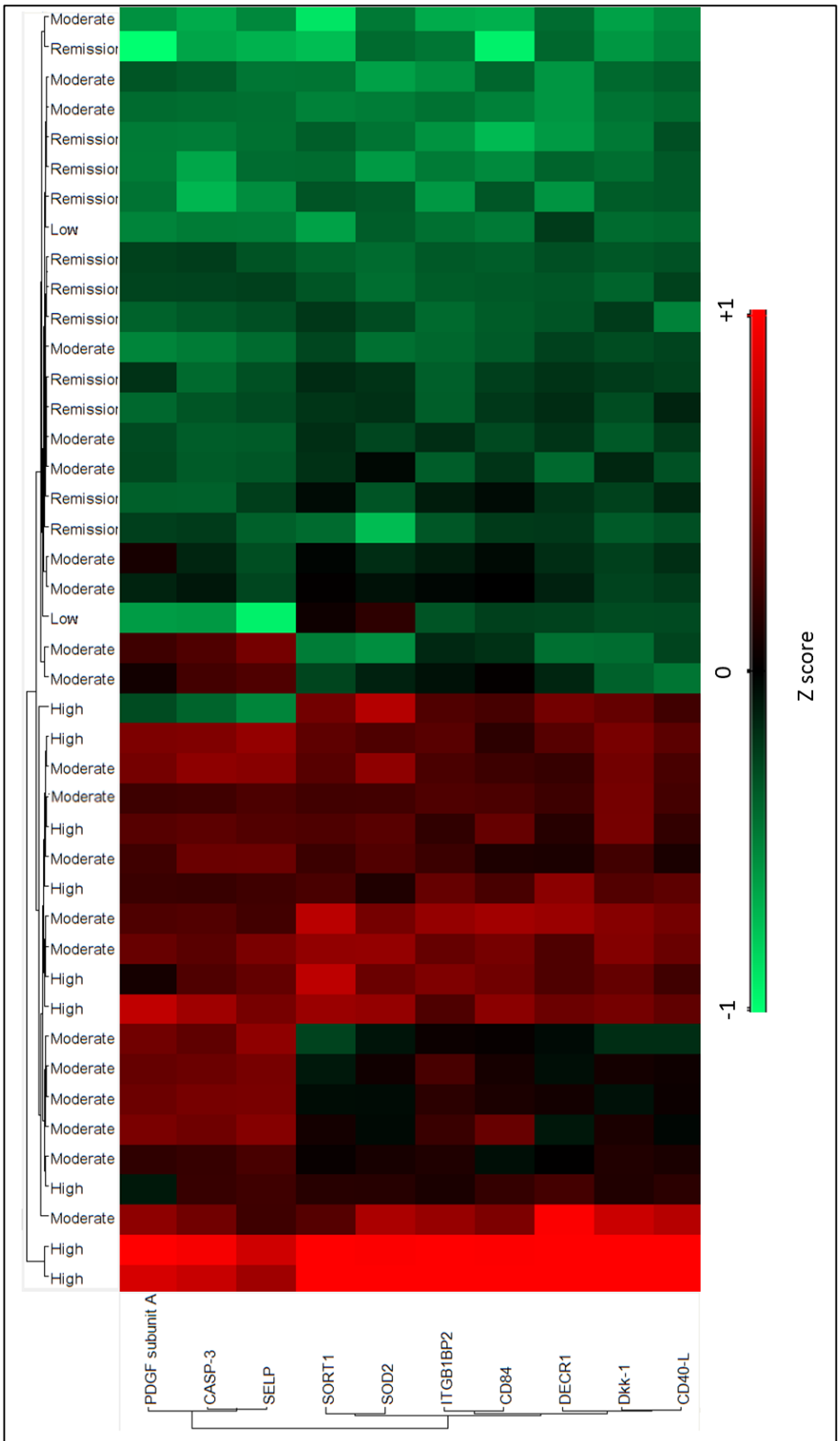

Figure 5.6C: Unsupervised clustering of proteins calculated to be significantly different between RA patients with high, moderate or low disease activity, or who are in remission. Disease activity classifications are based on EULAR guidelines.

5.1.3 Biologic DMARD response

A number of the cDMARD non-responders commenced biological DMARD treatment on the day of sampling. Thirteen of these patients were sampled again at their 6-month follow-up appointment, and their response was recorded according to clinical notes. The change in protein expression between these two time points was assessed in responders and non-responders to treatment by calculating the difference between the NPX value at baseline and 6 months. A volcano plot was drawn to observe the significant changes in expression between responders and non-responders (**Figure 5.7A and 5.7B**).

According to the volcano plot threshold, no significant difference was observed between each patient group when looking at the change in protein expression over time. However, several proteins highlighted in red display the highest change in expression between responders and non-responders. These include NEMO, CD40-L and mitochondrial 2,4-dienoyl-CoA reductase (DECR1), all of which were observed to be significantly different between cDMARD responders and non-responders.

An ANOVA test was carried out across all proteins using a p value threshold of 0.05. FDR was not included in the ANOVA test in order to reduce the stringency of the test parameters due to the low patient numbers. The results were plotted in a heat map using unsupervised clustering (**Figure 5.7C**). Of the 4 protein panels tested, 22 proteins were shown as statistically significantly different between responders and non-responders to biologics when considering the change in protein expression after 6 months of therapy. Although in this case patient numbers are small, similarities are observed with the differentially expressed proteins between cDMARD responders

and non-responders. For example, CD40-L and ANG-1 are upregulated in cDMARD non-responders compared to responders, and also in biologic DMARD non-responders compared to responders. However, patient numbers would need to be increased in the biologic DMARD cohort to confirm these findings.

Due to the low number of patient samples available and the use of the less stringent ANOVA test to carry out statistical analysis, protein mapping programmes were not used to assess bioinformatics of the significant proteins.

(A)

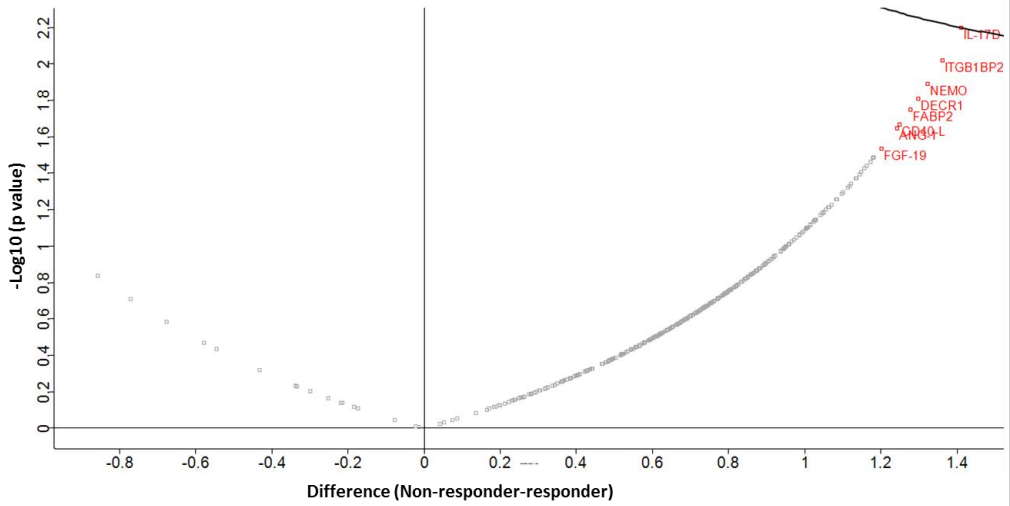

(B)

Protein	Difference (Non-responder - Responder)	- log ANOVA p value (all patient groups)	ANOVA p value
ANG-1	1.242	1.646	0.0226
CD40-L	1.249	1.667	0.0215
IL-17D	1.410	2.200	0.0063
CXCL1	1.148	1.404	0.0394
Gal-9	1.112	1.322	0.0476
DECR1	1.297	1.809	0.0155
VSIG2	1.163	1.441	0.0363
CCL17	1.157	1.426	0.0375
ITGB1BP2	1.361	2.019	0.0096
Dkk-1	1.149	1.407	0.0392
FABP2	1.277	1.749	0.0178
MMP12	1.133	1.370	0.0426
NEMO	1.323	1.892	0.0128
IRAK4	1.121	1.341	0.0456
FGF2	1.116	1.331	0.0466
TRIM5	1.181	1.486	0.0326
HEXIM1	1.135	1.374	0.0423
MGMT	1.121	1.343	0.0454
MCP-3	1.144	1.394	0.0403
MMP-1	1.172	1.463	0.0345
FGF-19	1.201	1.537	0.0290
TNFRSF9	1.180	1.482	0.0329

Figure 5.7A and 5.7B: (A) Volcano plot showing the significance (-Log p) of the fold difference of the change in protein expression at baseline and 6 months, between RA patients classed as responders (n=7) or non-responders (n=6) to biological DMARD treatment. Red indicates proteins with the largest statistically significant differences in expression between groups. The y axis represents the -Log10(p value), and the x-axis represents the difference between the Z scored NPX value in each patient group. The significance threshold (bold black line) was set when the p value was less than 0.05 (-Log10(0.05) = 1.3), and the fold change in protein expression was ≥2. (B) Raw data showing proteins that are significantly differentially expressed between all patient groups, calculated by ANOVA without FDR accounted for in the analysis. The difference between the Z scored NPX values in responders and non-responders is also shown in correspondence with (A).

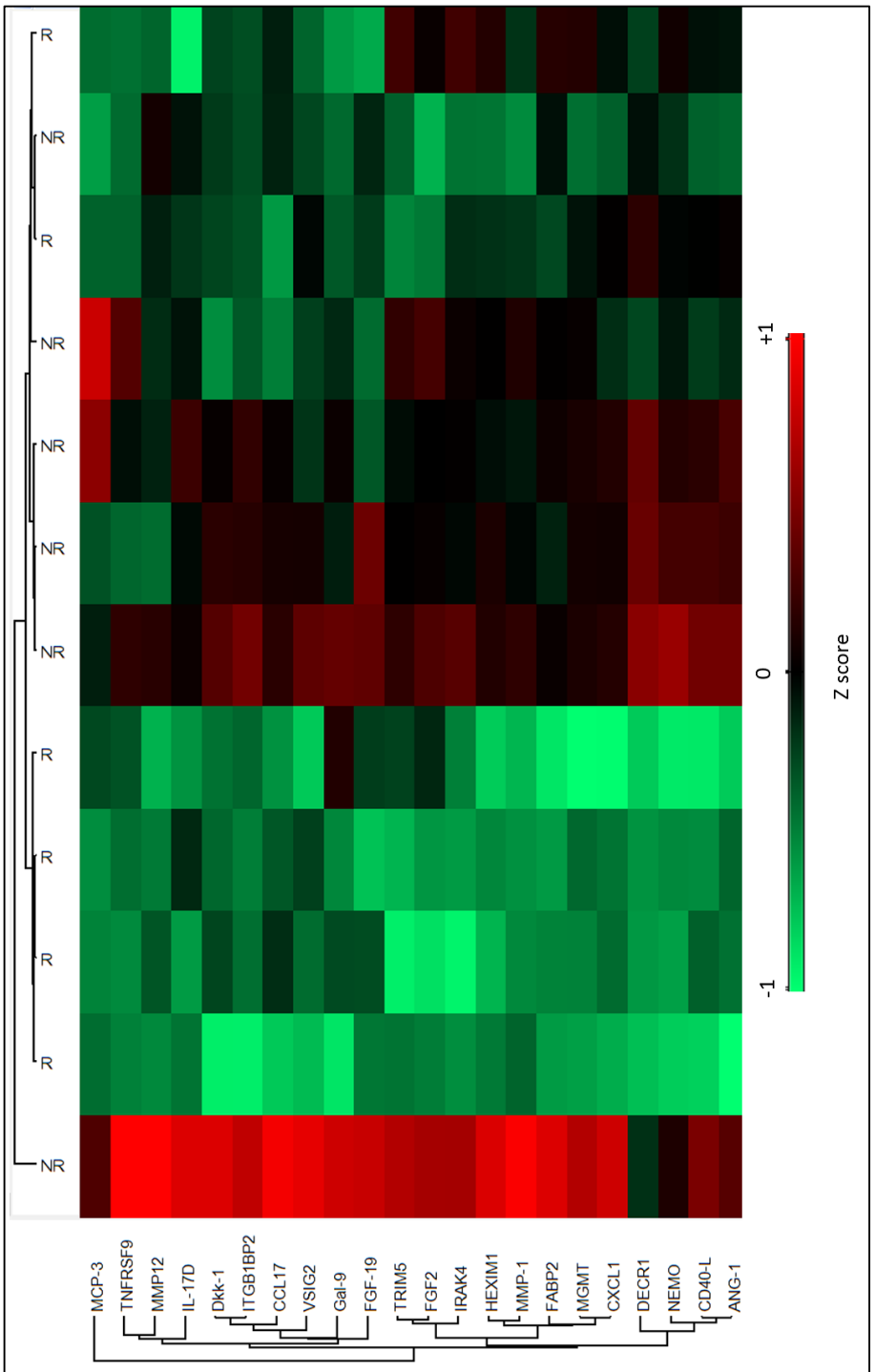

Figure 5.7C: Unsupervised clustering of the change in protein expression after 6 months of biological DMARD therapy in RA patients classed as responders (n=7) or non-responders (n=6) to treatment. Proteins listed were statistically significantly different between each patient group as calculated by ANOVA ($p<0.05$).

5.1.4 Comparison of cellular data

Cellular data from previous chapters obtained from FACS analysis was compared to proteomic data obtained from the OLINK analysis. The expression of each protein across all patients was initially compared to the relative of $CD169^+$ classical monocytes. The average was calculated and patients were grouped as having either 'above' or 'below' average relative numbers of $CD169^+$ monocytes. A volcano plot was then used to visually assess significant changes in protein expression between 'above' and 'below' patient groups (**Figure 5.8**).

Although no proteins were observed to be significantly differentially expressed between patient groups, those with the highest fold change between groups as well as the highest –Log p value are highlighted in red. For example, IL-5 is increased in patients with above average $CD169^+$ monocytes compared to those with below average. Furthermore, TNFRSF10C was found to be decreased in patients with above average $CD169^+$ monocytes compared to below average.

ANOVA tests were carried out across all proteins using a p value threshold of 0.05. When including FDR in the analysis, none of the proteins analysed were found to be significantly differentially expressed between patients with 'above' or 'below' relative numbers of $CD169^+$ monocytes. Therefore, the less stringent ANOVA was used without FDR to assess significance. The results were plotted as a heat map using unsupervised clustering (**Figure 5.8C**).

(A)

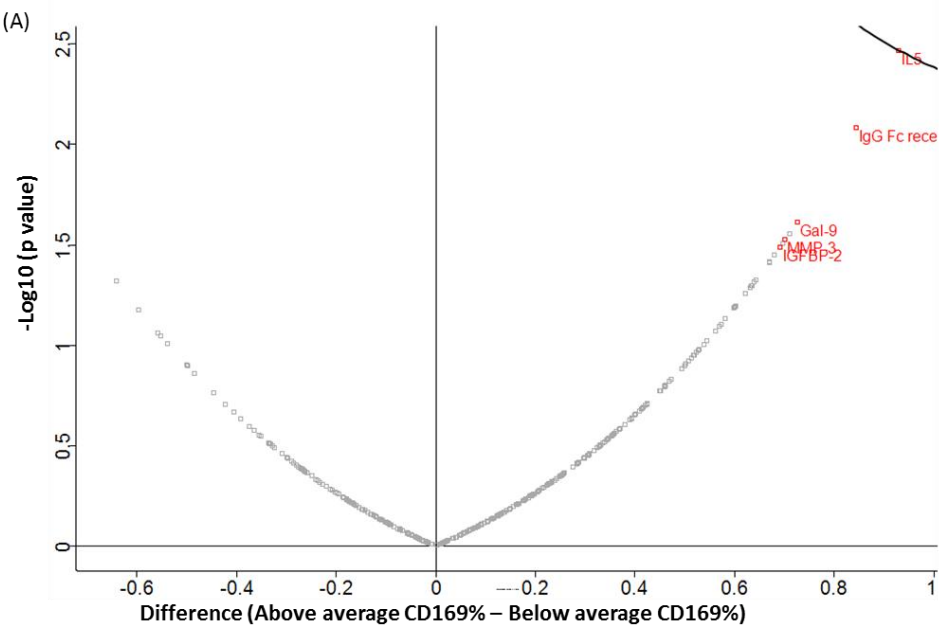

(B)

Protein	Difference (Above - below average CD169%)	- log ANOVA p value (all patient groups)	ANOVA p value
IL5	0.930	2.470	0.0034
IgG Fc receptor II-b	0.844	2.082	0.0083
Gal-9	0.726	1.615	0.0243
PGF	0.710	1.557	0.0278
MMP-3	0.702	1.525	0.0298
MARCO	0.697	1.508	0.0311
IGFBP-2	0.691	1.488	0.0325
CDCP1	0.680	1.448	0.0356
CHIT1	0.670	1.416	0.0384
CHI3L1	0.670	1.413	0.0386
FGF-21	0.643	1.325	0.0473
TNFRSF10C	-0.642	1.321	0.0477
MPO	0.640	1.313	0.0486

Protein is **upregulated** in 'above' compared to 'below' patient group.

Protein is **downregulated** in 'above' compared to 'below' patient group.

Figure 5.8A and 5.8B: A) Volcano plot showing the significance (-Log p) of the fold difference of the change in protein expression between RA patients classed as having an above (n=12) or below (n=43) average absolute number of CD169^{+} monocytes. Red indicates proteins with the largest statistically significant differences in expression between groups. The y axis represents the -Log10(p value), and the x-axis represents the difference between the Z scored NPX value in each patient group. The significance threshold (bold black line) was set when the p value was less than 0.05 (-Log10(0.05) = 1.3), and the fold change in protein expression was ≥2. (B) Raw data showing proteins that are significantly differentially expressed between all patient groups, calculated by ANOVA without FDR accounted for in the analysis. The difference between the Z scored NPX values in patient with 'above' or 'below' CD169^{+} monocytes is also shown in correspondence with (A).

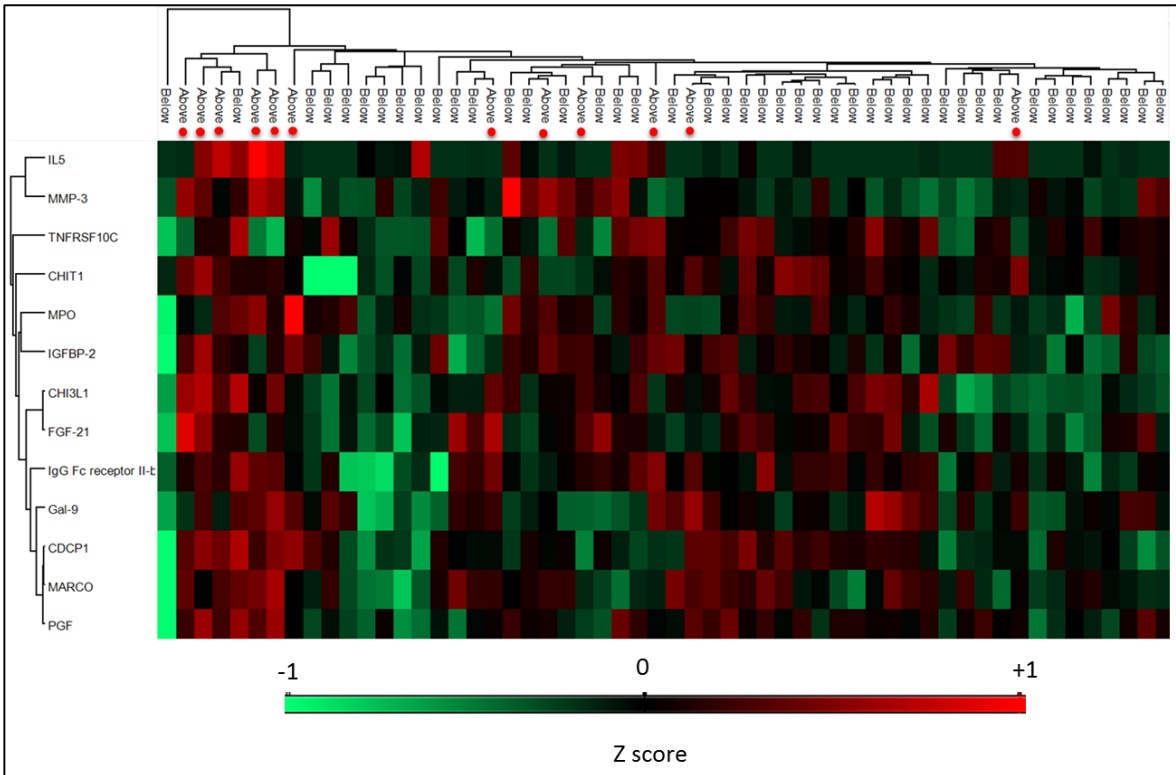

Figure 5.8C: Unsupervised clustering of proteins calculated to be statistically significantly different ($p<0.05$) between RA patients classed as having above or below average CD169$^+$ monocytes.

The same analysis was carried out when considering above and below average relative number of CD43$^+$ Tregs (**Figure 5.9**). Similar to the CD169 observation, none of the proteins were significantly different between patients who had above or below average CD43$^+$ Tregs. However, MCP-1 had the greatest fold difference between patients with above and below average CD43$^+$ Tregs, and the highest –Log p value. This protein was upregulated in patients with below average CD43$^+$ Tregs, compared to those with above average levels.

(A)

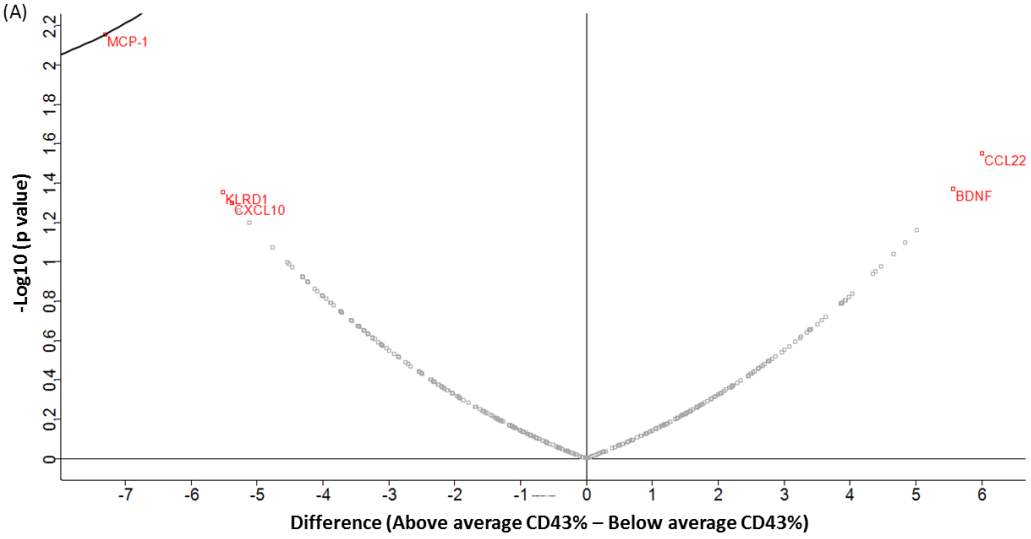

(B)

Protein	Difference (Above - below average CD43%)	- log ANOVA p value (all patient groups)	ANOVA p value
MCP-1	-0.730	2.156	0.0070
CCL22	0.600	1.549	0.0283
BDNF	0.557	1.371	0.0425
KLRD1	-0.552	1.353	0.0444

Protein is **upregulated** in 'above' compared to 'below' patient group.

Protein is **downregulated** in 'above' compared to 'below' patient group.

Figure 5.9A and 5.9B: A) Volcano plot showing the significance (-Log p) of the fold difference of the change in protein expression between RA patients classed as having an above (n=35) or below (n=21) average absolute number of $CD43^+$ Tregs. Red indicates proteins with the largest statistically significant differences in expression between groups. The y axis represents the -Log10(p value), and the x-axis represents the difference between the Z scored NPX value in each patient group. The significance threshold (bold black line) was set when the p value was less than 0.05 (-Log10(0.05) = 1.3), and the fold change in protein expression was ≥2. (B) Raw data showing proteins that are significantly differentially expressed between all patient groups, calculated by ANOVA without FDR accounted for in the analysis. The difference between the Z scored NPX values in patient with 'above' or 'below' $CD43^+$ Tregs is also shown in correspondence with (A).

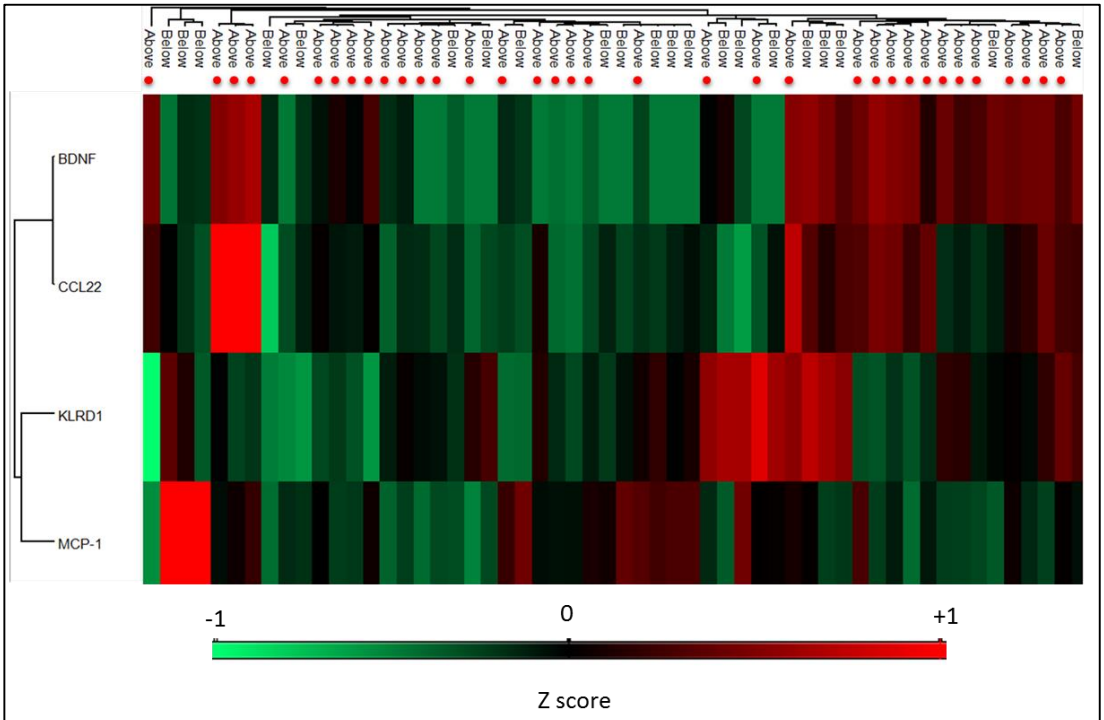

Figure 5.9C: Unsupervised clustering of proteins calculated to be significantly different ($p<0.05$) between RA patients classed as having above or below average $CD43^+$ Tregs.

The relative numbers of FoxP3$^+$ Tregs were also grouped into ‘above’ or ‘below’ average categories. As before differential protein expression was analysed across patient groups and observed as a volcano plot (**Figure 5.10**). Two of the proteins tested were shown to be significantly different in expression between patients with above and below average relative numbers of FoxP3$^+$ Tregs when the more stringent ANOVA test was used including FDR in the analysis. These proteins were CASP-3 and dynactin subunit-1 (DCTN1), which were observed to be increased in patients with below average FoxP3$^+$ Tregs, compared to those with above average levels. Furthermore, the less stringent ANOVA test was carried out in order to observe further significant differences between proteins. In this case SELP, JAM-A and ITGB1BP2 were among proteins that increased in patients with below average FoxP3$^+$ Tregs compared to those with above average levels. It is worth noting, these proteins were also among those that are significantly increased in cDMARD non-responders compared to cDMARD responders. Additionally, PRDX1 was shown to have the highest fold increase in patients with above average FoxP3$^+$ Tregs compared to those with below average. Similarly, this protein was previously observed to be significantly decreased in cDMARD non-responders compared to cDMARD responders.

(A)

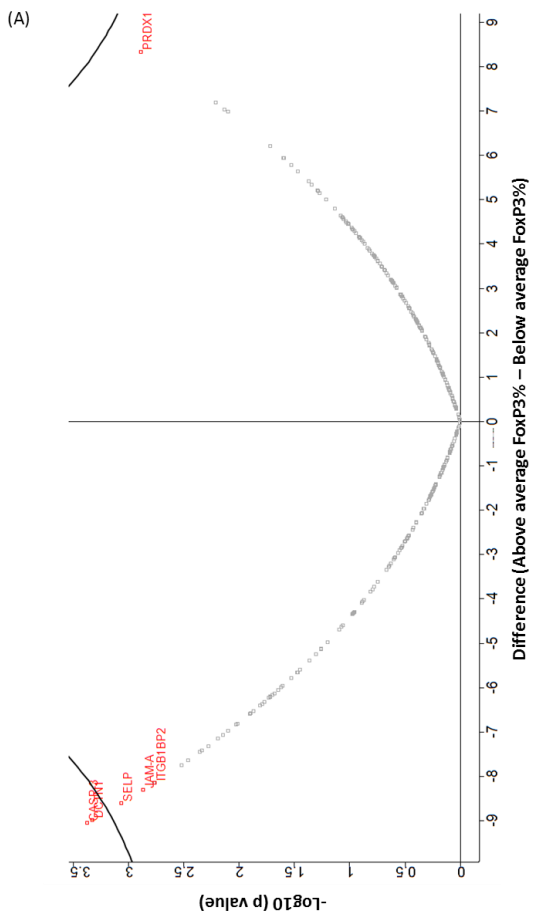

(B)

Protein	Difference (Above - below average FoxP3%)	- log ANOVA p value (all patient groups)	ANOVA p value	
*CASP-3	-0.905	3.375	0.0004	q = 0.084
*DCTN1	-0.898	3.327	0.0005	q = 0.046
SELP	-0.861	3.067	0.0009	
PRDX1	0.833	2.889	0.0013	
JAM-A	-0.830	2.869	0.0014	
DECR1	-0.814	2.766	0.0017	
ITGB1BP2	-0.814	2.763	0.0017	
ANG-1	-0.774	2.522	0.0030	
PDGF subunit A	-0.764	2.461	0.0035	
SH2B3	-0.745	2.357	0.0044	
IRAK4	-0.741	2.333	0.0046	
DAPP1	-0.731	2.278	0.0053	
FGF-21	0.719	2.214	0.0061	
Dkk-1	-0.715	2.191	0.0064	
TANK	-0.707	2.148	0.0071	
STK4	-0.707	2.148	0.0071	
PRSS8	0.704	2.132	0.0074	
ADAM-TS13	0.698	2.102	0.0079	
PAI	-0.697	2.096	0.0080	
ZBTB16	-0.683	2.025	0.0094	
PECAM-1	-0.681	2.012	0.0097	
PRDX3	-0.659	1.901	0.0126	
CD40-L	-0.657	1.894	0.0128	
HCLS1	-0.653	1.871	0.0135	
HEXIM1	-0.640	1.812	0.0154	
SPRY2	-0.636	1.793	0.0161	
CXCL1	-0.632	1.773	0.0169	
ITM2A	-0.623	1.731	0.0186	
NF2	-0.621	1.720	0.0191	
hOSCAR	0.621	1.718	0.0191	
NEMO	-0.620	1.716	0.0192	
PPP1R9B	-0.616	1.698	0.0200	
EIF4G1	-0.612	1.681	0.0208	
ICA1	-0.605	1.647	0.0225	
SOD2	-0.600	1.623	0.0238	
CD84	-0.596	1.609	0.0246	
IL-10RB	0.594	1.598	0.0253	
MMP-10	0.593	1.595	0.0254	
VEGFD	0.578	1.528	0.0297	
CCL22	-0.578	1.527	0.0297	
HB-EGF	-0.566	1.478	0.0332	
SIRT2	-0.565	1.472	0.0338	
PRELP	0.565	1.471	0.0338	
MGMT	-0.560	1.451	0.0354	
OPN	-0.559	1.448	0.0356	
SPON2	0.541	1.374	0.0423	
PAR-1	-0.539	1.367	0.0430	
CPA1	0.534	1.346	0.0451	
GT	-0.524	1.306	0.0494	

Figure 5.10A and 5.10B: A) Volcano plot showing the significance (-Log p) of the fold difference of the change in protein expression between RA patients classed as having above (n=30) or below (n=26) average FoxP3$^+$ Tregs. Red indicates proteins with the largest statistically significant differences in expression between groups. The y axis represents the -Log10(p value), and the x-axis represents the difference between the Z scored NPX value in each patient group. The significance threshold (bold black line) was set when the p value was less than 0.05 (-Log10(0.05) = 1.3), and the fold change in protein expression was ≥2. (B) Raw data showing proteins that are significantly differentially expressed between all patient groups, calculated by ANOVA without FDR accounted for in the analysis (* = significant with FDR included). The difference between the Z scored NPX values in patient with 'above' or 'below' average FoxP3$^+$ Tregs is also shown in correspondence with (A).

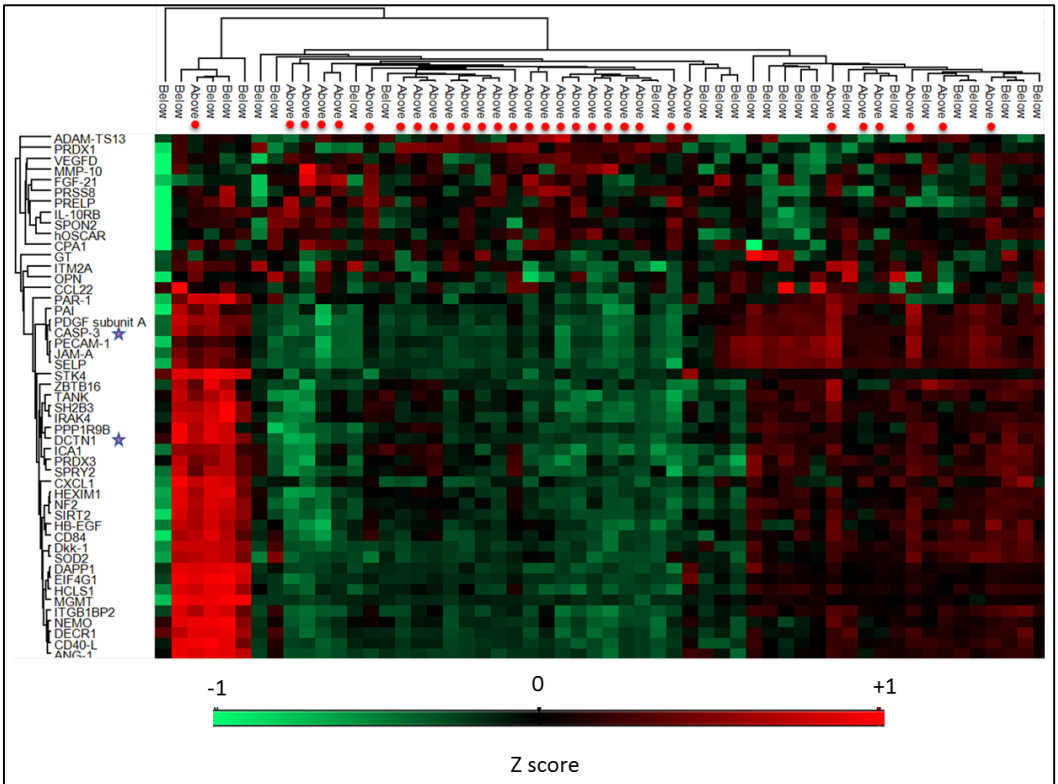

Figure 5.10C: Unsupervised clustering of proteins calculated to be statistically significantly different ($p<0.05$) between RA patients classed as having above or below average FoxP3^{+} Tregs. CASP-3 and DCTN1 as indicated by star symbol were also significantly differentially expressed when permutation based FDR was included in the analysis.

5.1.5 Quantification by ELISA

CASP-3 and CD40-L were quantified from the same plasma samples analysed by PEA, from DMARD naïve, DMARD responder and DMARD non-responder RA patients (**Figure 5.11 and 5.12**). The results from PEA show that CASP-3 is significantly increased in DMARD non-responders (11.91NPX±1.096, n=17) compared to DMARD naïve (9.104NPX±0.5961, n=6, $p<0.001$) and DMARD responder patients (8.964NPX±0.6093, n=17, $p<0.001$) (**Figure 5.11**). However, no significant differences were observed between patient groups when the same samples were analysed by ELISA. When plotting a receiver operating characteristic (ROC) curve on PEA CASP-3

results, a threshold can be set at 10.06 NPX to distinguish DMARD responders from non-responders, with 94.12% sensitivity and 94.12% specificity ($p<0.001$). Furthermore, the area under the curve is 0.955 which represents a strong classifier. However, a threshold cannot be set on the ELISA quantification of CASP-3 to significantly distinguish between patient groups ($p=0.142$), where the area under the curve is fair (AUC = 0.706). Although, a significant positive association was observed between PEA (NPX) and ELISA (ng/mL) results when all patient groups were included in the analysis ($p=0.049$, $r=0.314$, $n=40$).

CD40-L was found to be significantly increased in DMARD non-responders (9.637NPX±1.717, n=17) compared to DMARD naïve (6.713NPX±0.3653, n=6, $p<0.001$) and DMARD responder patients (6.971NPX±0.3778, n=17, $p<0.001$) when analysed by PEA (**Figure 5.12**). Furthermore, CD40-L was found to be significantly increased in DMARD non-responders (6.006ng/mL±3.077, n=17) compared to DMARD responders (4.044ng/mL±1.539, n=17, $p=0.025$) when analysed by ELISA. However, no significant difference was observed between DMARD naïve patients and DMARD responders. When plotting a ROC curve on PEA CD40-L results, a threshold can be set at 7.448 NPX to distinguish DMARD responders from non-responders, with 100% sensitivity and 94.12% specificity ($p<0.001$). This provides an excellent area under curve score of 1.000. Furthermore, if a threshold is set on ELISA CD40-L quantification results at 5.729 pg/mL, a 58.82% sensitivity and 88.24% specificity is achieved, $p=0.05$. However, the area under curve score is poor (AUC = 0.696). Additionally, a weak positive association was found between ELISA and PEA values when all patient groups were included in the analysis ($p=0.069$, $r=0.291$, $n=40$), however without significance.

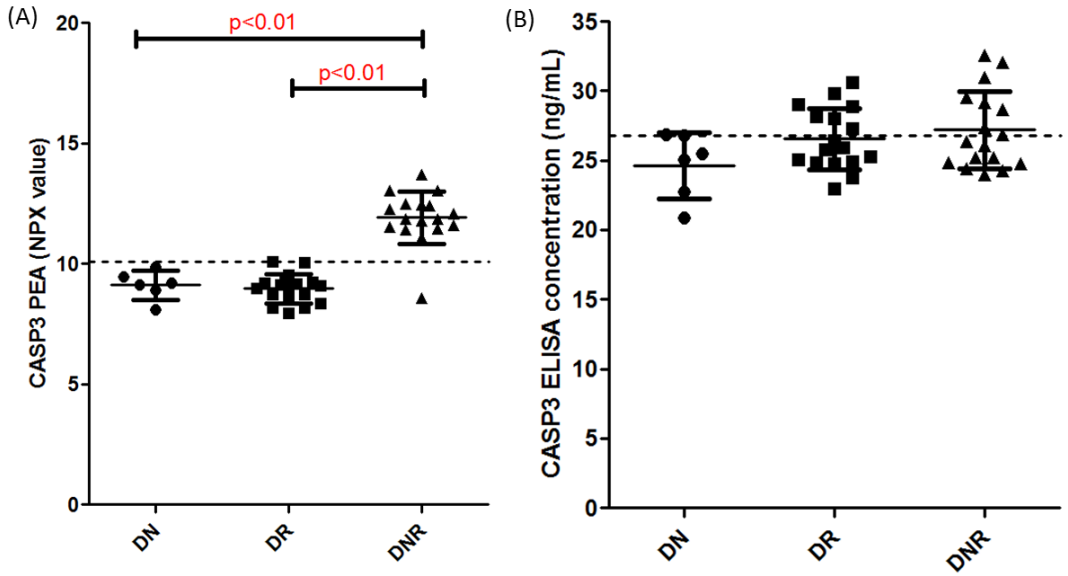

Analysis	Area	Standard error	P value	Y axis intercept	Sensitivity (%)	Specificity (%)
PEA: DR vs DNR	0.955	0.044	<0.001	10.06 NPX	94.12	94.12
ELISA: DN vs DNR	0.706	0.119	0.142	26.81 ng/mL	47.06	83.33

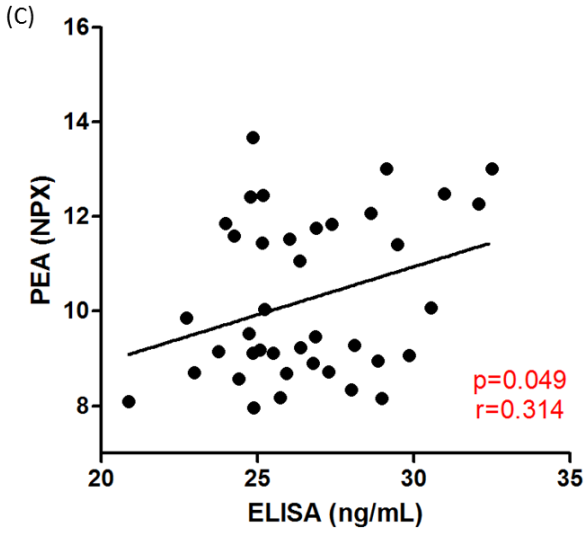

Figure 5.11: (A) CASP-3 in circulating plasma was found to be increased in DMARD non-responders (n=17) compared to DMARD naïve (n=6) and DMARD responder patients (n=17) when analysed by PEA. (B) However, no significant difference in CASP-3 protein quantity was observed between patient groups when the same samples were analysed by ELISA. (C) A significant positive association was observed between CASP-3 NPX values obtained by PEA and quantifications obtained by ELISA analysis of the same samples. Significant difference in protein expression across patient groups was assessed by unpaired t-tests. Sensitivity/specificity values were obtained by ROC curve analysis.

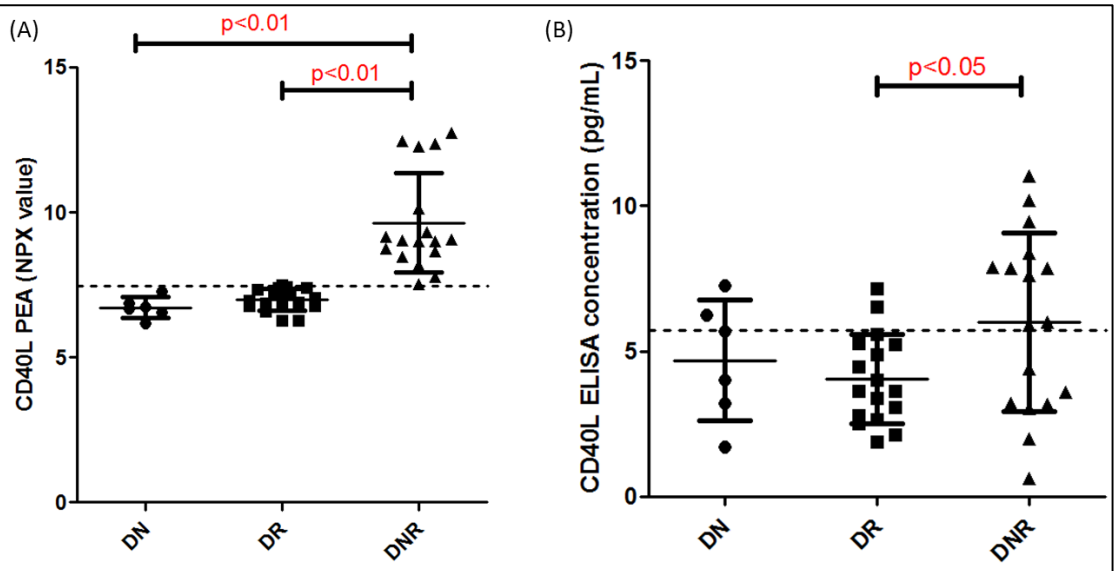

Analysis	Area	Standard error	P value	Y axis intercept	Sensitivity (%)	Specificity (%)
PEA: DR vs DNR	1.000	0.000	<0.001	7.448 NPX	100.00	94.12
ELISA: DR vs DNR	0.696	0.095	0.052	5.729 pg/mL	58.82	88.24

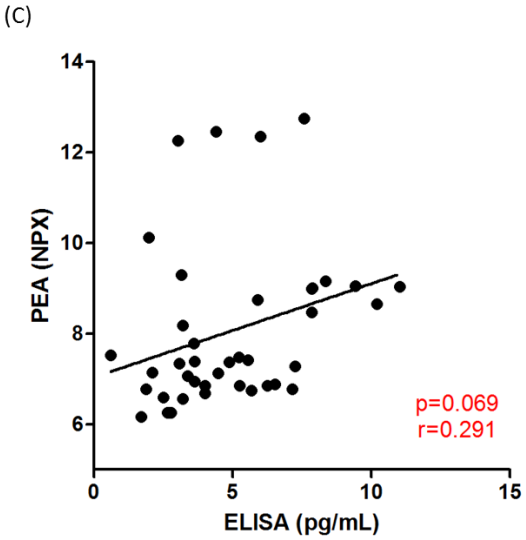

Figure 5.12: (A) CD40-L in circulating plasma was found to be increased in DMARD non-responders (n=17) compared to DMARD naïve (n=6) and DMARD responder patients (n=17) when analysed by PEA. (B) Furthermore, CD40-L was significantly increased in DMARD non-responders compared to responders when analysed by ELISA. (C) A weak positive association was observed between CASP-3 NPX values obtained by PEA and quantifications obtained by ELISA analysis of the same samples, however without significance (p>0.05). Significant difference in protein expression across patient groups was assessed by unpaired t-tests. Sensitivity/specificity values were obtained by ROC curve analysis.

CASP-3 and CD40-L NPX values were compared to ESR and CRP values recorded from the same patient on the day of sampling (**Figure 5.13**). However, no statistical significant association was observed between NPX values of either protein when compared to ESR or CRP.

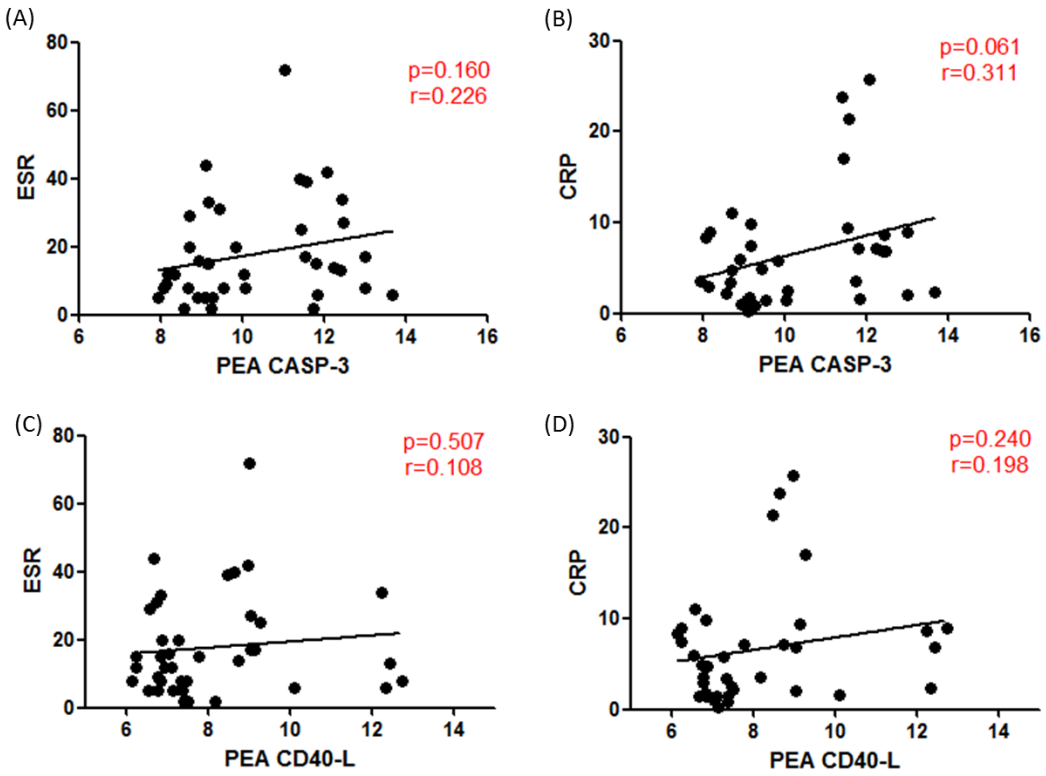

Figure 5.13: PEA CASP-3 NPX values were not statistically significantly associated with (A) ESR or (B) CRP values from the same sample. Furthermore, PEA CD40-L NPX values were not statistically significantly associated with (C) ESR or (D) CRP values from the same sample. P values were obtained using linear regression analysis. ESR = Erythrocyte sedimentation rate, CRP = C-reactive protein, PEA = Proximity extension assay.

5.2 Discussion

One of the key aims of experiments described in this chapter was to discover circulating protein biomarkers that may aid in differentiating clinical response to DMARD treatment in RA. Of the 4 protein panels tested from OLINK (total number = 384), 42 proteins were significantly differentially expressed between DMARD naïve, DMARD responder and DMARD non-responder RA patients. When classifying patients based on disease activity as determined by EULAR criteria, 10 proteins were shown to be differentially expressed between patient groups. Interestingly, these 10 proteins were also included in the 42 proteins previously shown to be differentially expressed when patients were classified by response (**Figure 5.14**). This suggests that these 10 proteins have the potential of distinguishing both disease activity and response to DMARD treatment.

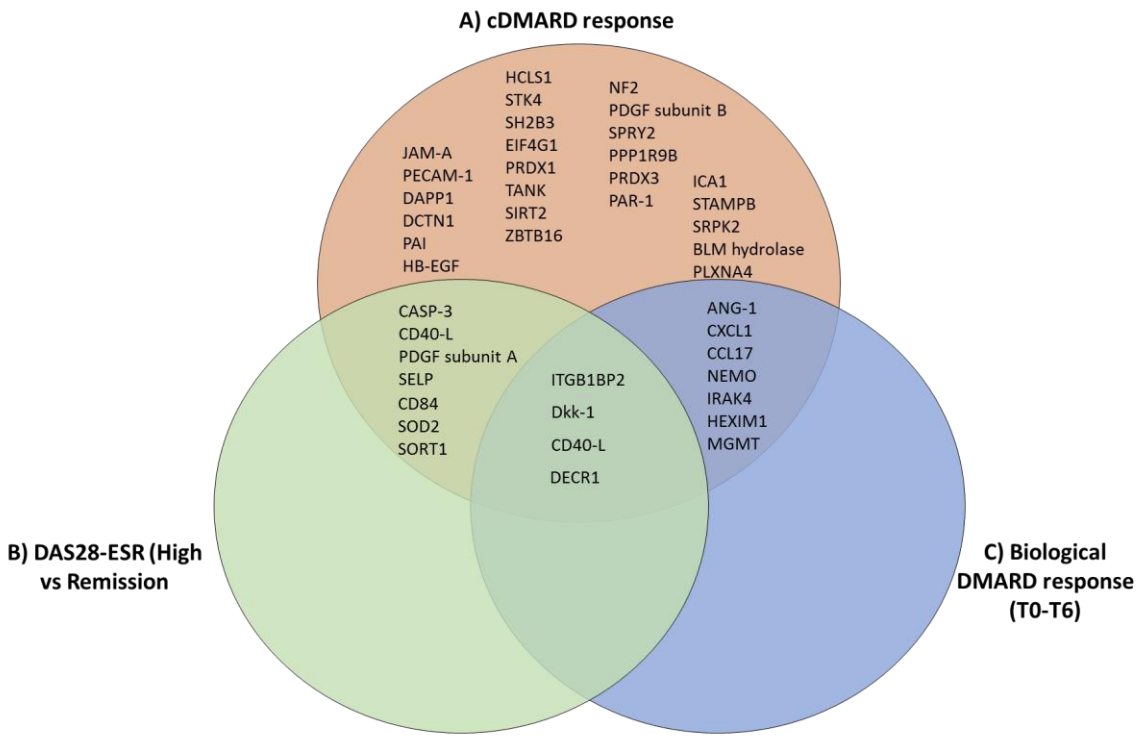

Figure 5.14: Venn diagram showing overlap between differentially expressed proteins which distinguish between RA patient subgroups: A) cDMARD responders and non-responders, B) Patients exhibiting high disease activity or remission and C) Biological DMARD responders and non-responders (where the change in protein expression was calculated as the difference between baseline (T0) and 6 month (T6) NPX values).

From the Reactome pathway table, cytokine signalling is one of the key pathways common to many of the significant proteins. For example, CASP-3, one of the 10 proteins of interest, is a regulator of cell apoptosis and has previously been associated with cleavage of pro-inflammatory cytokine IL-16 (Zhang *et al.* 1998). The findings from the current study are in agreement with previous literature. For example a recent study associated CASP-3 gene expression with DAS28 in DMARD naïve patients (Tchetina *et al.* 2017). Furthermore, CASP-3 was suggested to have potential in predicting DMARD response.

Additional proteins shown by Reactome to be associated with cytokine signalling include IRAK-1 and -4, which are linked to pro-inflammatory cytokine IL-1. Furthermore, IRAK-4 along with PDGFA and PDGFB is associated with PI3K/AKT signalling, an essential pathway involved in regulation of the cell cycle. The PI3K/AKT pathway has previously been suggested to be involved with progression of RA, and furthermore may be a potential therapeutic target (Malemud 2015).

SELP was also shown be associated with both disease activity and cDMARD treatment response. Along with other selectins, it plays a role in cell adhesion between leukocytes and endothelial cells, an important process in early inflammatory stages (de Bruijne-Admiraal *et al.* 1992). From the Reactome pathway list, SELP is associated with platelet activation in addition to PDGFA and PDGFB. Previous studies have shown an increase in serum SELP in RA patients compared to systemic sclerosis and healthy controls (Ertenli *et al.* 1998; Ates *et al.* 2004), suggesting it may be a useful marker in diagnosis. However, from current literature SELP is not known to distinguish response and non-response in RA.

The transport of antigen-bound MHCII molecules to the cell surface involves DCTN1 (Appendix N). This is an important process in T cell activation as part of the adaptive immune response. The data presented in this chapter shows that DCTN1 is significantly increased in DMARD non-responders compared to responders, however it is not associated with disease activity in RA. A previous study demonstrated an increase in DCTN1 gene expression in RA patients compared to control patients with OA (Li *et al.* 2014). However, it has not been previously associated in the literature with cDMARD treatment response. Interestingly, in the current study both CASP-3

and DCTN1 plasma concentrations are significantly decreased in patients with higher FoxP3^{+} Tregs, however increased in non-responder patients with higher disease activity. This is in agreement with previous findings presented in chapter 4, where DMARD non-responders exhibit lower levels of FoxP3 compared to responders.

Dkk-1 is also among the 10 significantly differentially expressed proteins between patients sub-grouped based on disease activity. Dkk-1 has previously been of interest in relation to RA due its association with bone formation. For example, a recent study demonstrated an increase in serum Dkk-1 levels in RA patients with increased radiographic disease progression (Seror *et al.* 2016). The observation made in the current study of increased Dkk-1 in DMARD non-responders may be linked to increased bone damage due to lack of treatment efficacy, however this suggestion would need to be confirmed with radiographic assessment.

ITGB1BP2 and CD40-L proteins appear to be associated with disease activity and response in cDMARD treated patients, and also response in patients treated with biological DMARDs. However, increased numbers of patients treated with biologic DMARDs are required confirm the latter observation. ITGB1BP2, a protein expressed by heart muscles, is not known to be associated with response in arthritis. However, reduced levels have been previously linked to cardiac impairment (Brancaccio *et al.* 1999). CD40-L is a marker of platelet activation and is present on certain T cell subsets (Datta and Kalled 1997; Otterdal *et al.* 2004). It has an inflammatory role in the immune response because via CD40 binding, it is associated with non-canonical NFκB signalling (Appendix O). CD40-L has been shown to play a role in autoimmune diseases including SLE and RA (Koshy *et al.* 1996; Wang and Liu 2003). Circulating

CD40-L secreted from activated T cells and platelets has been linked to disease activity in SLE (Kato *et al.* 1999). An increase in membrane bound CD40-L has been linked to increased RA disease activity (Berner *et al.* 2000), and furthermore soluble CD40-L was shown to be increased in the periphery of RA patients compared to healthy controls (Tamura *et al.* 2001). In summary, the current study's findings are completely novel, where ITGB1BP2 and CD40-L were found to be associated with RA disease activity in patients treated with cDMARDs and biological DMARDs.

PRDX1 was also a protein of interest because of its downregulation in cDMARD non-responders compared to responders and DMARD naïve patients. Furthermore, it is the most significantly increased protein detected in patients with above average $FOXP3^+$ Tregs, compared to those with below average levels. PRDX1 is essential in regulating reduction and oxidation within the cell, and its release from the cell has previously been associated with the induction of pro-inflammatory cytokines IL-6 and TNFα (Shichita *et al.* 2012; Liu *et al.* 2014). Thus, it is regarded as a promotor of inflammatory processes, and its reduction in DMARD non-responders is perhaps a curious result, as inflammatory pathways are generally upregulated in non-responders. Further investigation is needed to confirm and understand this finding.

Links between the previously obtained CD169 and CD43 cellular data (chapter 3) and proteomic data were also investigated in the current study. IL-5 and IgG Fc receptor-IIb were among those that were increased in patients with an above average relative number of $CD169^+$ monocytes, compared to those with below average levels. IL-5 showed the highest significant difference between patient groups, however this was only determined using a p value of 0.05 without accounting for FDR. IL-5 is an anti-

inflammatory cytokine produced by T helper and mast cells. It can be speculated whether monocytes play a role in IL-5 production as they act as antigen-presenting cells to T cells, subsequently activating T helper cells. However, whether CD169 has a specific role in IL-5 production would need to be verified. It is possible that the lack of association between specific cellular findings, and the circulating proteome to which the same cells contribute, is due to masking from the abundance and variety of circulating secreted proteins.

ELISA analysis was used to quantify a select number of proteins found to have significantly different NPX values between patient groups. The purpose of the ELISA was also to verify findings from the PEA analysis and show whether or not the more accessible ELISA method could be used to distinguish disease activity and treatment response in RA. CASP-3 and CD40-L were selected for ELISA quantification because both proteins were found to be significantly differentially expressed between cDMARD responders and non-responders, as well as between patients with high disease activity and in remission. Furthermore, as discussed CASP-3 and CD40-L have previously been associated with disease activity in RA (Berner *et al.* 2000; Tchetina *et al.* 2017), however to current knowledge this association with CASP-3 has only been made by gene expression analysis and not proteomic studies. The data from the current study shows a threshold can be set to reliably distinguish cDMARD responders from non-responders when PEA analysis is used. The sensitivity and specificity percentages with both CASP-3 and CD40-L are promising when analysed by PEA, where both values are above 90%. However, this cannot be said with regard to ELISA quantification results. This may be due to the difference in mechanism of each method used, for example PEA technology relies on a PCR readout following

extension and amplification steps after hybridisation of unique DNA sequences. ELISA on the other hand relies on an absorbance readout after TMB is oxidised in the presence of HRP, which is conjugated to a specific antibody targeting the protein of interest. Additionally, neither technology distinguishes between membrane bound and soluble proteins, however centrifugation steps can be introduced prior to ELISA in order to detect only the soluble form of the protein. However, the results of this study show a positive association between PEA and ELISA results, and with significance when analysing CASP-3. Therefore, perhaps with further method development of the ELISA, it may be possible to improve this association between the two assays. Additionally, as PEA data was shown to be associated with cDMARD treatment response when considering CD40-L and CASP-3 among others, this data was compared with ESR and CRP clinical data recorded on the same day of sampling. However, ESR or CRP values showed no significant association with CD40-L or CASP-3 PEA data, suggesting these blood-based inflammatory markers are unreliable in determining treatment response.

5.3 Conclusion

These results show the potential of using the circulating proteome to distinguish between response and non-response to cDMARDs and biological DMARDs, as well as disease activity classification before and during treatment in RA. For example, CASP-3 and SELP are among the most differentially expressed proteins between DMARD naïve, responder and non-responder RA patients, thus having the most potential in

distinguishing response in peripheral blood. However, a more accessible analysis method such as ELISA would need to be carried out to firstly quantify protein levels, and secondly to confirm that these findings can be transferred to this more commonly used platform.

This study demonstrates a lack of concordance between CD169 and CD43 cellular measures, and circulating proteomic findings. An *in vitro* model may be used in order to further understand the impact of this cellular interaction on the circulating proteome. However, it may be possible that in circulating blood any proteomic impact is masked by the vast numbers of circulating proteins from various sources.

Although higher patient numbers are required to confirm this, there was an association found between the change in CD40-L and ITGB1BP2 in individual biological DMARD-treated patients, and treatment response. Interestingly, both proteins are also significantly differentially expressed between cDMARD naïve, responder and non-responder patients, as well as those classed as having high, moderate or low disease activity. This suggests treatment response may be determined over time for individual patients. Thus, there may be opportunity to determine treatment response at an earlier time point than current measures, therefore allowing for greater treatment efficacy as treatment regimens can be adjusted in early disease.

Additionally, CASP-3 protein expression can reliably distinguish between DMARD responders and non-responders with sensitivity and specificity >94% when analysed by PEA. Furthermore, these PEA results had a significant positive association with ELISA quantification results of the same samples. Thus, CASP-3 could be a potential

biomarker of treatment response in RA, and with further optimisation, ELISA could be used as a more accessible and cost effective method of detection. However, if a protein based assay or test were developed to distinguish treatment response in order to aid clinical decisions, due to the vast range of proteomic data available it would likely be a multiplex measurement with an algorithm which discerns the patterns of expression of a limited number of markers.

Chapter 6

General Discussion and Future Work

6.0 General Discussion

6.0.1 CD169$^+$ monocytes and CD43$^+$ Tregs

The aim of chapter 3 was to determine the relationship between CD169$^+$ monocytes and CD43$^+$ Tregs in RA patients who were DMARD naïve, responders and non-responders as classified by EULAR criteria (Smolen *et al.* 2014b). One of the key findings of this chapter was the need to consider CD16$^+$ non-classical and intermediate monocytes, as well as CD16$^-$ classical monocytes. CD16$^+$ monocytes have been implicated as dendritic cell precursors (Ancuta *et al.* 2003), and furthermore are induced by inflammatory cytokine TGFβ (Yoon *et al.* 2014). In agreement with previous literature (Kawanaka *et al.* 2002; Cairns *et al.* 2002), CD16$^+$ monocytes are increased in peripheral blood of RA patients compared to healthy controls, whereas CD16$^-$ monocytes are decreased. This finding emphasised the need to consider both CD16$^-$ and CD16$^+$ monocyte subsets when analysing the relative number of CD169$^+$ monocytes. Previous studies have shown an increase in the relative number of CD169$^+$ classical monocytes in RA compared to health (Xiong *et al.* 2014), however have failed to report relative numbers of CD169$^+$ non-classical or intermediate monocytes. This chapter presents the novel finding of a statistically significant increase in CD169$^+$ non-classical monocytes in RA compared to health. Interestingly, DAS28-ESR had a strong association with the relative number of CD169$^+$ non-classical monocytes, which was more statistically significant than when compared to CD169$^+$ classical or intermediate monocytes.

The relative number of $CD43^+$ Tregs was reduced in RA compared to healthy controls. Furthermore, the ratio of $CD169^+$ monocytes and $CD43^+$ Tregs was found to be positively associated with DAS28-ESR. However, neither cell-surface marker could definitively discriminate between responders and non-responders to cDMARD treatment. This finding suggests CD169 and CD43 in combination are representative of disease activity in RA, however cannot distinguish long term response or non-response. It has previously been reported that $CD169^+$ monocytes and $CD43^+$ Tregs directly bind via these cell-surface markers (Ohnishi *et al.* 2013), and that the interaction between the two cell types may contribute to the decreased activation state of Tregs in RA (Wu *et al.* 2009). Although siglecs play an important role as inhibitory regulators of Treg activation and function, the findings of this chapter do not confirm a direct suppression of Tregs by $CD169^+$ monocytes via the CD169-CD43 interaction. Therefore, in order to address this question and understand the Treg activation state in RA, an *in vitro* model of inflammatory Tregs was used in the following chapter.

6.0.2 Treg activity in RA

The aim of chapter 4 was to investigate the activation state of Tregs in RA compared to health. Initial finding showed an increase in circulating Tregs in DMARD naïve and responder patients compared to health, in agreement with previous literature (Ehrenstein *et al.* 2004). However, a decrease in circulating Tregs was observed in DMARD non-responders compared to responders. Furthermore, not only were Tregs found to be reduced in number in DMARD non-responders, but also in activation state as measured by FoxP3. Specifically, this chapter reports differential relative

numbers of FoxP3$^+$ Tregs in CD45RA$^+$ naïve vs CD45RA$^-$ memory subsets. FoxP3$^+$ naïve Tregs were decreased in DMARD responders and non-responders compared to healthy controls. Furthermore, FoxP3$^+$ memory Tregs were increased in DMARD responders and non-responders compared to healthy controls, however DMARD non-responders exhibited significantly lower levels compared to responders. This suggests overall Treg activity may be restored with treatment response, and that Treg activity may be defective in non-responders.

In order to emulate an inflammatory Treg environment, such as that presented in RA, Tregs were stimulated with PMA *in vitro,* which increased relative numbers of NFκB$^+$ and FoxP3$^+$ Tregs, as well as TNFα, IL-10 and IFNɣ cytokine secretion. The key novel finding of this chapter was the role of Sia in reducing this cytokine secretion from Tregs as well as reducing intracellular percentages of NFκB and FoxP3. The purpose of the experiment was to mimic the effect monocyte-CD169 might have on the activation state of Tregs, because CD169 binds to Sia before binding its ligand. Previous studies have also highlighted a role of Sia in inflammation, and importantly Sia has been shown to increase in RA compared to healthy controls (Chrostek *et al.* 2014). It is clear that siglec-Sia mediated signalling plays a pivotal role in Treg activation and could therefore have significant influence on tolerance and suppression within the immune system. Monocyte-Treg co-culture was used in order to try to identify if Sia has the same effect on Tregs as monocytes. Additionally, CD169 and CD43 blocking antibodies were used to confirm or deny whether any effect observed is directly due to the binding of these two markers. However, due to the lack of concordance between biological replicates, the results of the co-culture were

inconclusive and thus further optimisation is needed in order to verify a relationship between CD169 and CD43.

Chapters 3 and 4 address the potential involvement of specific peripheral blood cells in disease activity and treatment response in RA. However, it is important to consider the protein environment in which they are bathed, as addressed in chapter 5.

6.0.3 Circulating protein biomarkers of response in RA

The aim of chapter 5 was initially to determine levels of a vast range of circulating proteins in cDMARD naïve, responder and non-responder RA patients in order to discover specific proteins that could act as a biomarker of treatment response. ITGB1BP2, Dkk-1, CD40-L and DECR1 were found to be significantly increased in i) cDMARD non-responders compared to responders, ii) RA patients with high disease activity compared to those in remission and iii) biological DMARDs non-responders compared to responders, where the change in protein levels between baseline and 6 months of therapy was assessed. However, due to low patient numbers the latter would need to be confirmed. The findings of this chapter demonstrated a lack of concordance between previous CD169 and CD43 cellular findings, and protein expression in autologous plasma samples. However, this may be due to masking by more abundant plasma proteins. An *in vitro* cell model is one option of investigating the contribution $CD169^{+}$ monocytes and $CD43^{+}$ Tregs may have to the circulating plasma proteome.

The key findings of this analysis demonstrated the role of a subset of proteins in distinguishing not only treatment response, but also disease activity in RA. One such protein is CASP-3, a regulator of cell apoptosis which has not previously been

reported to distinguish treatment response in RA. Although CASP-3 levels analysed by ELISA did not confirm PEA results of increased expression in DMARD non-responders compared to responders, the results between the 2 assays had a significant positive association. With further optimisation of the more accessible ELISA method, it may be possible to use CASP-3 among a panel of other proteins as markers of treatment response in RA.

6.0.4 Conclusions

The hypothesis of this thesis was that the interaction between circulating $CD169^+$ monocytes and $CD43^+$ Tregs, and the proteomic environment in which these cells are bathed, could act as potential biomarkers of disease activity in RA, and therefore could assist in determining treatment response. Firstly, this thesis suggests there is an interaction between CD169 and CD43 that contributes to disease activity in RA due to the finding of the ratio of $CD169^+$ monocytes to $CD43^+$ Tregs having a significant correlation with DAS28-ESR. However, whether there is a direct CD169-CD43 interaction that contributes to this result is inconclusive in the current study.

Furthermore, this thesis presents evidence of the ability to detect Treg activity in peripheral blood via measurement of intracellular FoxP3. DMARD non-responders exhibit reduced Treg activity compared to responders, suggesting defective Treg activity may contribute to or be a consequence of treatment non-response. Importantly, this data suggests Treg activity could be used as a surrogate measure of treatment response in RA.

Additionally, the association of monocytes with reduced Treg activity was addressed. It was found that Sia suppresses Tregs in an *in vitro* model of inflammation, as

measured by a reduction in inflammatory cytokines as well as a reduction in relative numbers of NFκB^{+} and FoxP3^{+} Tregs. This may mimic the action of CD169 on Tregs, however this could not be confirmed in the current study. Furthermore, the investigation of an association of the CD169-CD43 interaction with reduced Treg activity was inconclusive, and in need of further work to determine the role of this interaction.

This thesis demonstrates that specific circulating proteins in RA are representative of disease activity and cDMARD treatment response, therefore accepting the hypothesis, albeit further validation studies are required. In summary, this thesis presents findings that easily accessible circulating blood can be used to determine treatment response in RA. Furthermore, with this novel evidence there may be opportunity to determine treatment response at an earlier time point than current measures, therefore allowing for greater treatment efficacy as treatment regimens can be adjusted in early disease.

6.1 Limitations

Due to patient recruitment primarily being based in a location geographically distant from where samples were analysed, this part of the study was quite time consuming. Furthermore, DMARD naïve patients were difficult to recruit in large numbers as they needed to be sampled on the day of diagnosis prior to commencing their drug. Furthermore, patients treated with biological DMARDs were difficult to re-sample at their 6-month time point. This was due to a number of reasons including last minute

changes of appointment days, therefore there were low patient numbers with baseline and 6 month matched samples.

Often clinical data was not recorded by hospital staff on the day of sampling, which meant when comparing cellular or proteomic data to DAS28-ESR or other clinical measures, some samples had to be excluded from the analysis. Furthermore, although full blood counts could be recovered from clinical notes and used in the analysis of absolute monocytes, the same could not be done for T cell or Tregs. One option to improve this would be to use an automated cell counter to determine absolute numbers of Tregs, however this facility was not available for the study.

Overall, patient recruitment was extremely time consuming, unfortunately leaving less time for later cell culture experiments. Therefore, although rigorous cell culture experiments were carried out, further work is essential to confirm findings.

6.2 Future Work

Although this thesis suggests an interaction between $CD169^+$ monocytes and $CD43^+$ Tregs is representative of RA disease activity, further experiments are needed to confirm this finding. The cell culture experiments presented were inconclusive in determining i) whether CD169 and CD43 directly bind when cells are in an inflammatory state and ii) whether an interaction between CD169 and CD43 directly contributes to reduced Treg activity. One suggestion is repeating this experiment with increased biological replicates in order to increase reliability of results and

conclusively determine whether CD169 and CD43 contribute to Treg activity. Furthermore, immunocytochemistry could be useful in confirming that CD169 and CD43 physically bind during inflammation.

Furthermore, in addition to the ratio between $CD169^+$ monocytes and $CD43^+$ Tregs being representative of disease activity, $FoxP3^+$ Tregs were found to be associated with treatment response. It would be interesting to confirm these finding in a longitudinal study, where patients are sampled throughout treatment, and changes in these cellular markers are recorded.

This thesis also identified a range of circulating protein that were found to be representative of both disease activity and treatment response when tested using PEA analysis. Preliminary experiments showed a correlation PEA and ELISA analysis in the detection of CASP-3. However, further optimisation of the ELISA method is required to confirm that PEA findings can be translated to a more accessible and cost effective method. Additionally, only 2 of the proteins found to be significantly differentially expressed between patient groups were tested. It would be interesting to confirm PEA results with ELISA for each of the proteins of interest. This would enable a 'cut-off' quantification value to be set that would distinguish disease activity and response. Furthermore, in order to confirm these findings an independent cohort of patients could be sampled.

One of the key clinical issues in RA is the excessive time of 3-6 months after commencing treatment to determine whether a patient has responded or not. The value of the cellular and proteomic markers presented in this thesis in determining

disease activity and treatment response suggests it may be possible to classify patients as responders or non-responders at an earlier time point than currently possible. This suggestion would need to be confirmed primarily by introducing sampling points soon after treatment and up until the 3-month time point. The ability to determine treatment response by analysing these key cell types and/or specific protein signatures at an early stage would aid clinical decisions as well as improve overall patient outcome, as patients could be commenced on a more suitable treatment sooner than previously possible.

Appendices

Appendix A: TICORA Protocol

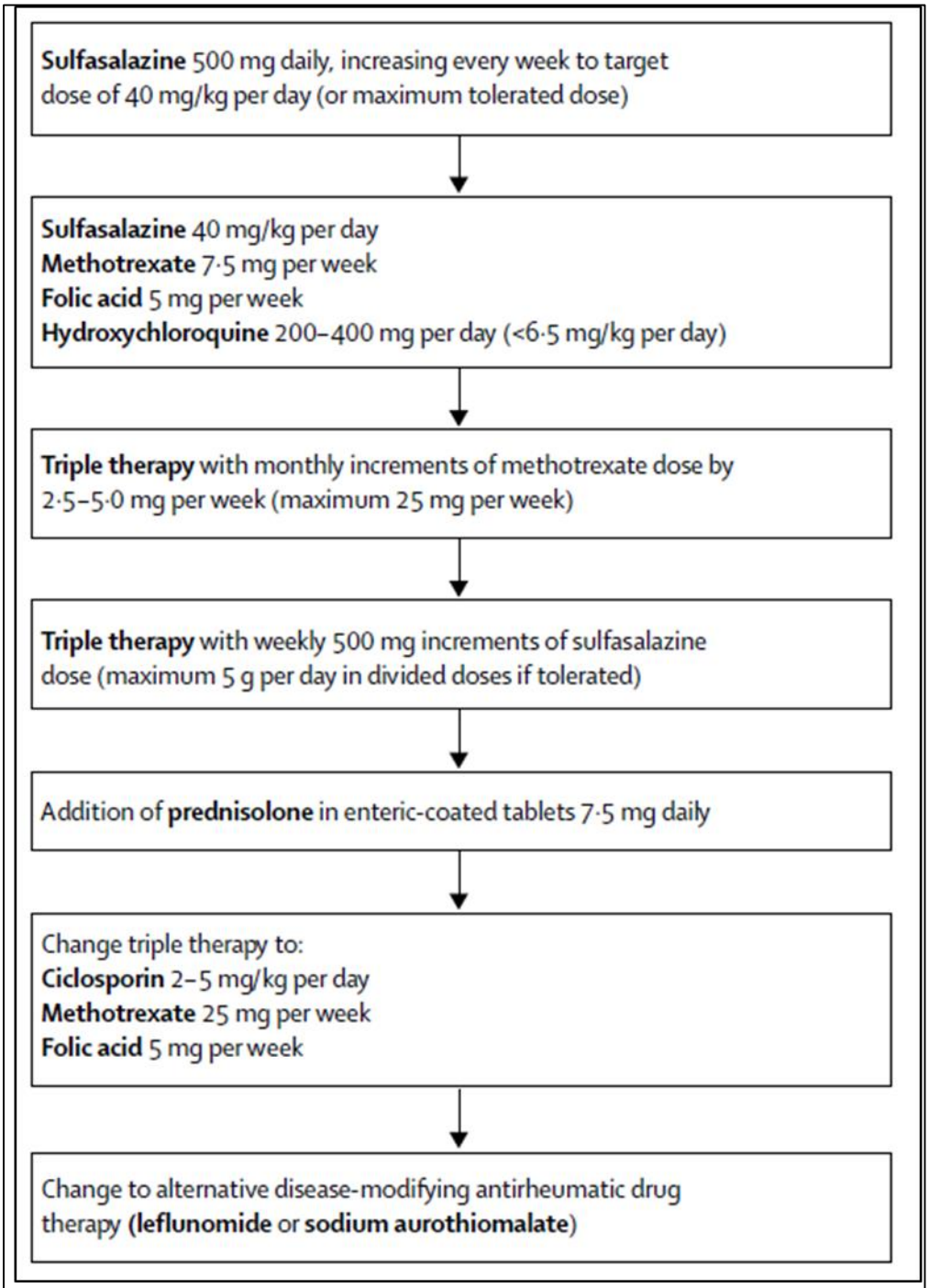

TICORA protocol using intensive DMARD treatment in order to improve clinical efficacy in RA (Grigor et al., 2004).

Appendix B: Review paper

REVIEW

Siglec-1 and -2 as potential biomarkers in autoimmune disease

Amanda J. Eakin, Michael J. Bustard, Cathy M. McGeough, Tahanver Ahmed, Anthony J. Bjourson and David S. Gibson

Northern Ireland Centre for Stratified Medicine, Altnagelvin Hospital Campus, Ulster University, Londonderry, Northern Ireland, UK

Received: June 26, 2015
Revised: November 25, 2015
Accepted: January 5, 2016

Autoimmune diseases (ADs) are currently treated with anti-inflammatory and immunosup- pressive drugs, aimed at reducing symptoms of disease in order to improve quality of life for patients. However, for a significant number of patients these therapies are ineffective, leading to an increased risk of irreversible damage and eventual disability in certain cases. Growing evidence has implicated glycosylated proteins and their cognate receptors in modulation of the autoimmune response. This review will summarize these findings with particular focus on sialic acid-binding immunoglobulin-like lectin (Siglec)-1 and Siglec-2 involvement in AD. Fluctuations in these glycosylation-dependent pathways could act as sentinels of disease activity or drug responses. If validated, protein modification and cellular response markers could help clinicians achieve remission earlier.

Keywords:
Autoimmune disease / Protein glycosylation / Sialic acid / Siglec receptor

1 Introduction

The term "autoimmune disease" (AD) is an overarching de- scription of a vast range of chronic conditions in which an abnormal immune response is established. There are over 80 ADs that range from problems in the joints in rheuma- toid arthritis (RA) and systemic lupus erythematosus (SLE) to skin conditions such as vitiligo and psoriasis [1]. The etiology of autoimmunity has been widely researched but the exact mechanisms remain elusive. Previous studies have sug- gested the role of bacterial infection [2], environmental factors [3], and genetics as potential risk factors of AD [4], however knowledge is incomplete.

The prevalence of AD is specific to each condition, for example RA affects 0.5–1% of the adult population [5].

Correspondence: Dr. David S. Gibson, Northern Ireland Centre for Stratified Medicine, C-TRIC Building, Altnagelvin Hospital Cam- pus, Ulster University, Glenshane Road, Londonderry, BT47 6SB, Northern Ireland, UK
E-mail: d.gibson@ulster.ac.uk
Fax: +44-(0)-28-7161-1422

Abbreviations: **AD**, autoimmune disease; **BCR**, B-cell receptor; **IFN**, interferon; **IgG0**, agalactosylated IgG; **IL**, interleukin; **ITIM**, immunoreceptor tyrosine-based inhibitory motif; **RA**, rheumatoid arthritis; **Siglec**, sialic acid-binding immunoglobulin-like lectin;

Epidemiological studies of AD suggest a prevalence of 7.6–9.4%, however, only covering a subset of diseases [6]. Throughout AD, there is an average female predilection of 75% according to the American Autoimmune Related Dis- eases Association [7].

Treatment of AD is aimed at relieving symptoms and limiting damage, with the ultimate aim of improving patient quality of life. Medication is often prescribed in a disease- specific regimen, for example treatment of joint-related dis- eases such as RA primarily involves anti-inflammatory and immunosuppressive drug combinations early in disease. Re- sponse rates to treatment regimens can be low, for example disease-modifying anti-rheumatic drugs used to treat RA re- port failure rates of 30% [8]. Additionally, nonresponse to glucocorticoid is common in SLE amongst other rheumatic conditions, and hence many patients experience relapse dur- ing dosage titration [9].

Sensitive biomarkers that can monitor response to treatment and subclinical disease activity are required. A reliable biomarker panel, descriptive of disease pathology could allow clinicians to determine treatment responses and switches to alternatives at an earlier time point. Furthermore, mon- itoring robust pathology descriptive biomarkers may be able to predict relapse and give the opportunity to limit damage.

This review will focus on protein glycosylation pathways, their ability to directly impact upon treatment outcomes in RA and other ADs, and their potential as biological markers of key pathological processes. The review will also discuss the cellular context of these pathways in immune response, autoimmunity, drug resistance, and disease persistence.

Two members of the sialic acid-binding immunoglobulin- like lectin (Siglec) family offer examples of key glycosylation- dependent pathways, which could contribute to AD pathology and drug resistance [10]. Siglec-1 (CD169) is a macrophage-restricted cell surface receptor that has been shown to drive proinflammatory processes and is related to disease persis- tence [11]. Siglec-2 (CD22) is a B-cell restricted molecule that negatively regulates B-cell receptor (BCR) and subsequent im- mune response and has been implicated in drug resistance [12].

2 Protein glycosylation fluctuations in AD

Glycosylation is an important post-translational modification observed in over 70% of human proteins [13] and is specific to age, gender, and environmental and biochemical factors [14]. Fluctuations in expression and activity of glycosyltransferase and glycosidase enzymes associated with the progression of disease can lead to aberrant glycosylation [15,16]. Alteration of glycans can sterically disrupt interactions between cognizant lectins and glycoproteins, which can, for example, prevent normal receptor signaling [17].

2.1 Acute-phase response proteins

The glycosylation patterns of several acute-phase plasma pro- teins differ in AD patients compared to healthy individuals, which suggests a pathogenic role. A study focused on alter- ations in sera proteins of RA patients discovered an abnor- mal elevation of fucosylation [18]. Similarly, a recent study by Higai et al. [19] found increased numbers of biantennary and alpha 1, 3-fucosylated glycans at glycosylation sites of α_1-acid glycoprotein in patients with acute inflammation compared to healthy controls.

Other sera proteins, such as Haptoglobin have been of interest in association of RA [20]. Saroha et al. [21] re- ported a unique monosaccharide pattern of Haptoglobin and acid glycoprotein to be specifically linked with RA pathogenesis.

2.2 Agalactosylated immunoglobulin

Patients with RA express a higher concentration of agalacto- sylated IgG (IgG0). This concentration positively correlates with disease severity in RA patients, suggesting a poten- tial role of IgG0 as a biomarker for disease activity [22, 23]. IgG0 also shows good correlation with biomarkers of AD in general, including inflammatory markers Interleukin-6 (IL-6) and C-reactive protein, which increase in early disease [24]. Pasek et al. [25] suggested the use of IgG0 as a marker for disease severity, as levels return to normal after anti-TNF monotherapy.

RA patients undergoing Methotrexate and Infliximab combination therapy exhibit decreased levels of IgG0 as well as clinically improved symptoms of the disease [26]. These changes in glycosylation may amplify the autoimmune re- sponse, by specific activation of macrophages, T cells, and B cells, contributing to the chronic inflammation observed in the synovium of RA patients [27].

3 Key cells in disease pathogenesis

Numerous studies have investigated molecular signatures in AD that may have the potential to distinguish response to treatment. However, despite a large volume of genetic biomarker-based studies, there remains no definitive genetic signature to differentiate response to therapy. Focusing on cellular interactions could prove to be a valuable means to differentiate responders. This section summarizes the main cells involved in inflammation, primarily monocytes, T cells, and B cells as biological indicators of disease activity or sever- ity [28].

Macrophages play a central role in AD pathogenesis, trig- gering the production of proinflammatory mediators, such as cytokines TNF-α and IL-1 [29]. The numbers of circulat- ing monocytes increase in AD patients, which highlights the importance of their role in disease pathogenesis [30–32].

Monocytes circulate in the blood stream and differen- tiate into mature macrophages on entering inflamed tis- sue. Macrophages are found in large numbers within the cartilage–pannus junction of RA patients. At this location, they display signs of activation including expression of the major histocompatibility complex, class II (MHC-II), and se- cretion of proinflammatory and regulatory cytokines [33, 34]. Macrophage activation positively correlates with progression of joint destruction, evidenced by radiological examination [35]. Synovial macrophages can differentiate into subpopula- tions that trigger the activation of T cells and proinflammatory cytokines, leading to more damage and further progression of the disease [36, 37]. Macrophages have also been investi- gated as key players in other ADs, such as Lupus Nephritis, a kidney-related complication of SLE. Lupus Nephritis

dis- ease activity positively correlates with monocyte infiltration and macrophage differentiation [32]. A subsequent section describes the macrophage-specific pathways influenced by variable glycosylation and discusses its association with dis- ease persistence in AD.

B cells orchestrate autoimmune responses in adaptive im- munity by the production of autoantibodies and antigen pre- sentation [38]. Section 4.3 will focus on how protein glyco- sylation influences the BCR and could ultimately determine immune tolerance and the development of autoimmunity.

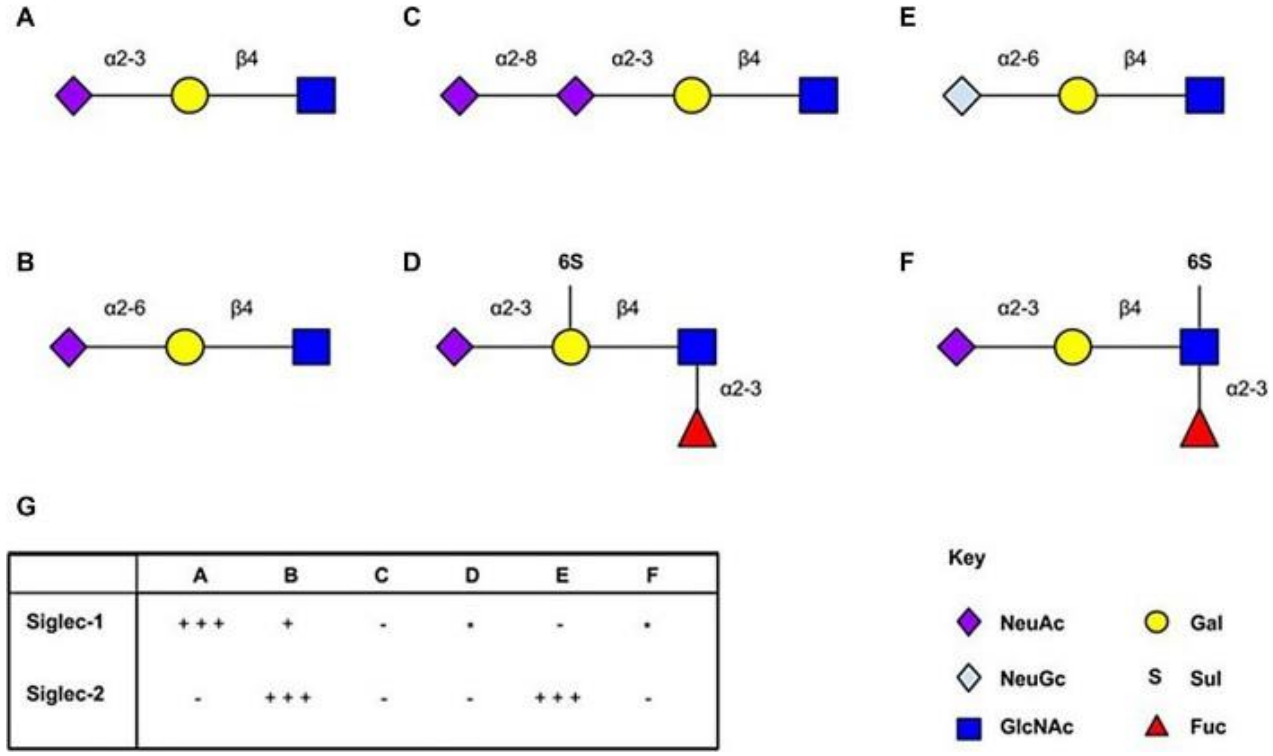

	A	B	C	D	E	F
Siglec-1	+ + +	+	-	*	-	*
Siglec-2	-	+ + +	-	-	+ + +	-

Figure 1. Selected sialic acid linkage sequences and relative affinities of Siglec-1 and Siglec-2. (A–F) represent terminal sequences of glycan structures of human (A, B, C, D, and F) and murine (E) glycoproteins and glycolipids that interact with Siglecs. (A) represents *a*.2-3 sialic acid linkage; (B) and (E) display *a*.2-6 linkage; (C) displays *a*.2-8 linkage; while both (D and F) represent sulfated *a*.2-3 sialic acid linkage. Table (G) displays the relative affinity of Siglec-1 and Siglec-2 for each glycan structure (A–F). (+++) represents greatest binding affinity, (+) represents low binding affinity, and (*) indicates binding affinity not tested. NeuAc, *N*-acetylneuraminic acid (sialic acid); NeuGc, *N*-glycolylneuraminic acid (murine sialic acid); GlcNAc, *N*-acetylglucosamine; Gal, galactose; Sul, sulfate; Fuc, fucose

T cells are also implicated in AD pathogenesis, where their activation leads to the release of cytokines such as TNF-*a*. and IL-4 [39]. $CD4^+CD25^+$ regulatory T cells, also known as sup- pressor T cells or Tregs, are a subset of T cells that play an important role in autoimmune responses. Tregs are involved in self-tolerance by suppressing the destructive functions of $CD4^+CD25^-$ effector T cells (Teffs) during the immune response [40].

Recent research has highlighted a critical relationship between Tregs and macrophages in the context of RA. In particular, Siglec-1 positive macrophages cause a negative regulation of Tregs [40]. Xiong et al. [11] demonstrated that the frequency of Siglec-1 in peripheral blood mononuclear cells was greater in RA patients, than that of healthy controls.

4 Glycosylation-dependent pathways in autoimmunity

Siglecs are sialic acid-binding immunoglobulin-like lectins that are involved in cell–cell interactions and signaling func- tions. There are several Siglec isoforms, differing in biolog- ical function and affinity for specific sialic acids [41]. There is substantial evidence that Siglec-1 and -2 in particular are involved in disease persistence and treatment resistance in RA and potentially other ADs.

4.1 Siglec-1 (CD169)

Siglec-1, also known as Sialoadhesin or CD169 is a cell surface receptor restricted to macrophages and their monocyte precursors, with high expression found in secondary lymphoid tissues. The structure of Siglec-1 comprises 17 immunoglobulin-like domains including one V-set domain through which it binds ligands, and 16 C2-set domains, which elongate the binding site away from the surface of the cell [42] (Fig. 1). Siglec-1 performs many functions, most importantly cell adhesion, accommodated by the elongation of the C2-set domains (Fig. 1) [43]. It binds to granulocytes, B cells, erythrocytes, and a subset of CD8 T cells [44]. It also acts as an endocytic receptor by internalization of sialic acid-tagged pathogens [45]. Hartnell et al. [44] also found Siglec-1 is highly conserved in the extracellular region between mouse and man, which confirms the role of Siglec-1 in cell–cell interactions.

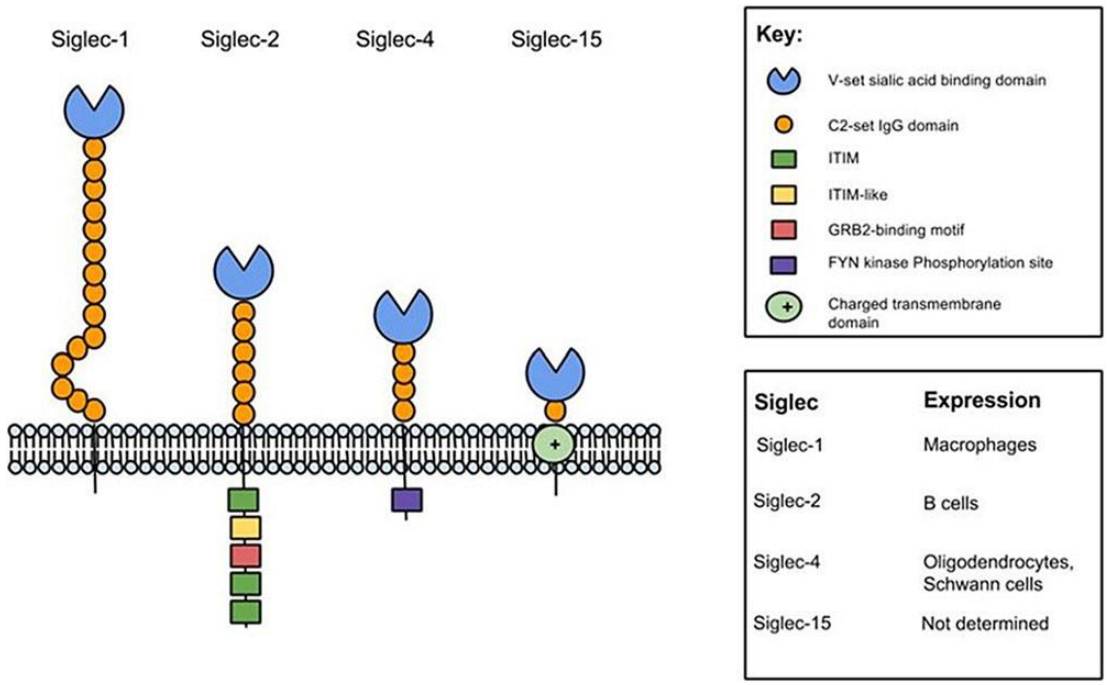

Figure 2. The structure and expression of highly conserved siglecs. Siglecs are type-I mem- brane proteins made up of a variable number (1–16) of extra- cellular C2-set immunoglobulin domains and an amino terminal V-set domain that mediates sialic acid binding. Siglec-1 lacks intracellular tyrosine-based signaling motifs and has a poorly conserved cytoplasmic tail. Siglec-2's (CD22) cytoplasmic tail consists of five tyrosine-based signaling motifs, including three ITIMs.

The lack of immunoreceptor tyrosine-based inhibitory sig- naling motif (ITIM) in the cytoplasmic domain strongly sug- gests Siglec-1 functions primarily via cell–cell and cell–matrix interactions [44]. It may also play a role in anti-viral and anti- bacterial activity as its regulation is subject to type I and type II interferon (IFN) induction [46]. Siglec-1 increases in a num- ber of ADs associated with IFN signaling, including SLE, type 1 diabetes, and systemic sclerosis [47–49]. In a study measur- ing IFN biomarkers, Siglec-1 expression was increased in 86% SLE patients [50]. These findings suggest Siglec-1 is a marker of prospective disease activity in AD.

Most Siglecs show a binding preference in either α.2,3 or α.2,6 glycosidic linkage (the numbers here indicate the spe- cific carbons with the hexose ring). Siglec-1 has a predilection for α.2,3, accommodated by glycosyltransferase and glycosi- dase enzymes (Fig. 2) [16]. It can also bind in α.2,8 linkage, but with weak affinity [51]. X-ray crystallography shows the binding of Siglec-1 is accommodated by a salt bridge formed between an arginine residue in the V-set domain and the carboxylate of the sialic acid [52].

Siglec-1 is described as a candidate biomarker for RA disease activity due to its increased expression on periph- eral blood monocytes in patients relative to healthy controls [11]. RA patients also exhibited a decrease in average Siglec-1 levels during successful treatment with DMARDs [11]. Xiong et al. also found an increased frequency of Siglec-1 mRNA within monocytes of RA patients during active dis- ease and were able to correlate their findings with other dis- ease predictors including DAS28, erythrocyte sedimentation rate, rheumatoid factor, and C-reactive protein levels. A pre- vious study demonstrated similar results, where a strong correlation was observed between levels of Siglec-1 posi- tive monocytes and clinical parameters for patients with the disease [53].

4.2 Siglec-1 interacts with Tregs

Siglec-1 positive macrophages negatively regulate Tregs [40] (Fig. 3). In vitro experiments demonstrate that Siglec-1 KO macrophages trigger the production of Tregs at a higher rate than wild-type macrophages, therefore confirming that Siglec-1 positive macrophages suppress the proliferation of Tregs. Importantly, a decrease in the number of Siglec-1 pos- itive macrophages leads to an increase in Tregs, which leads to a lower disease activity in an RA model [40].

The interaction between Siglec-1 and Tregs is believed to occur through the T-cell surface receptor, CD43. This sialy- lated glycoprotein has been identified as a counter receptor for Siglec-1 [54, 55]. In vivo experiments show a direct inter- action between the two receptors, however the mechanism through which this occurs remains unclear and warrants fur- ther investigation [56].

4.3 Siglec-2 (CD22) and BCR

BCR plays an important role in immune tolerance. BCR is negatively regulated by Siglec-2 [12] (Fig. 4). Siglec-2 is widely expressed by the majority of peripheral mature B cells [57], however its expression is lost during B-cell differentiation into plasma cells. It is expressed at high levels on B cells in the fol- licular, mantle, and marginal zones of the spleen, but weakly expressed by B cells in the germinal center [58]. In resting B cells, the majority of Siglec-2 is localized in clatherin-enriched microdomains [59].

Lanoue et al. [60] demonstrated Siglec-2 mediated sup- pression of BCR by in vitro studies of glycoconjugate ligands binding in α.2-6. The study highlighted that BCR activation by antigen-expressing target cells was reduced when the target

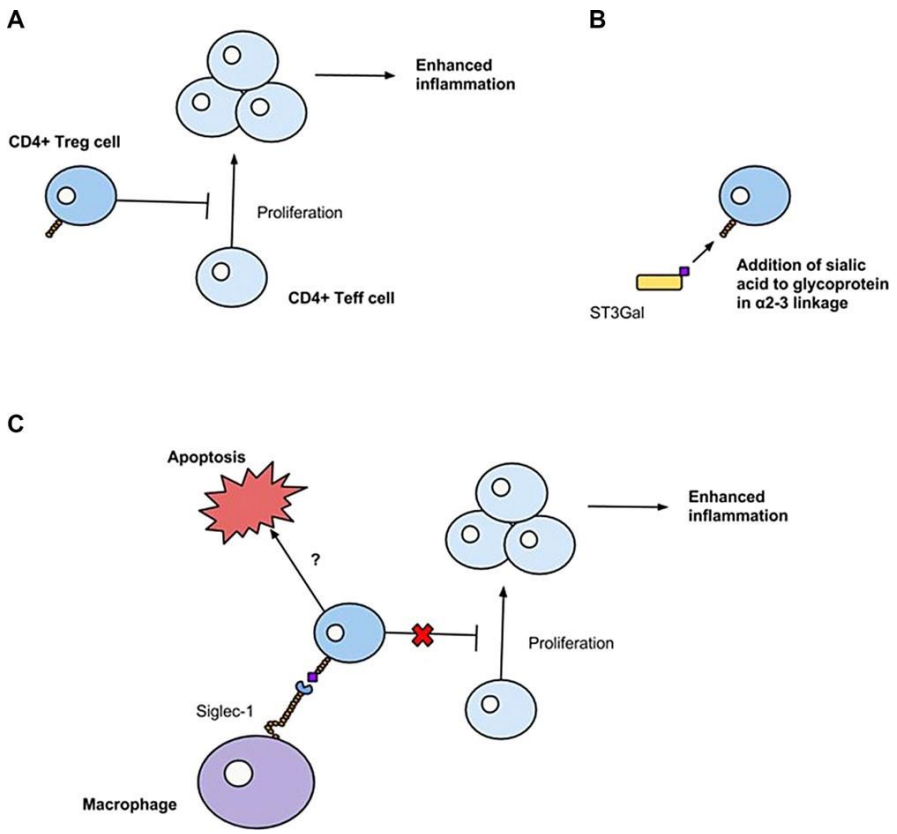

Figure 3. The inhibitory role of siglec-1 on $CD4^+$ Treg cells, subsequent increase in $CD4^+$ Teff cell proliferation, and enhanced inflammatory response. (A) demonstrates the inhibitory role $CD4^+$ Tregs on $CD4^+$ Teff proliferation and subsequent proinflammatory response. (B) Kidder et al. demonstrated an increase in *J3*-galactoside *a*.-2,3-sialyltransferase (ST3Gal) mRNA expression and *a*.2-3 sialylation of $CD4^+$ Treg cells in a murine model of SLE. (C) Kidder et al. also demonstrated siglec-1 positive macrophages induced the death of $CD4^+$ Treg cells, expressing sialic acid in *a*.2-3 linkage, by an unknown mechanism. The subsequent reduction in Treg numbers resulted in an increase in Teffs and enhanced inflammation.

cells co-expressed *a*.2-6 sialic acid glycoconjugates. This find- ing eludes to a potential role for Siglec-2 in the maintenance of tolerance and the development of autoimmunity.

The importance of ligand binding in the maintenance of B-cell homeostasis has also been investigated by Poe et al. [61]. This study showed that knock-in mice expressing one of the two Siglec-2 mutations abrogating ligand binding displayed higher rates of turnover in peripheral and recirculating bone marrow B cells in vivo.

Activation of the BCR signaling cascade leads to an increase in calcium ions (Ca^{2+}) released from intracellu- lar stores through the phosphorylation and activation of a range of signaling molecules, including BtK, BLNK/SLP65, and PLC')'2 [12]. BCR activation also initiates an influx of extracellular Ca^{2+} through the calcium release activated channel. Rapid phosphorylation of Siglec-2 ITIMs by the Src kinase, Lyn, occurs following BCR cross-linkage [62]. The tyrosine phosphatase SHP-1 is then recruited and binds to two phosphorylated ITIMs. Then, SHP-1 dampens BCR signaling through the depletion of endoplasmic reticulum Ca^{2+} stores and activation of the Ca^{2+} pump PMCA4 [12] (Fig. 5).

Siglec-2 null mice display increased intracellular Ca^{2+} sig-
naling following BCR activation [63–66], as well as a more rapid B-cell turnover, reduced numbers of circulating blood and bone marrow B cells, and enhanced BCR-induced B- cell apoptosis [61, 65–67]. The mechanisms behind decreased Ca^{2+} levels as a result of Siglec-2 binding remain unclear. However, studies suggest that therapies targeting Siglec-
2 could increase BCR activation, thus improving patient outcome [68].

Two independent Siglec-2 null mouse strains display in- creased autoantibody production against single- and double- stranded DNA and histone complexes [64, 69, 70]. These findings suggest Siglec-2 may play a key role in the antibody- mediated autoimmunity characteristic of AD. Additionally this pathway may be responsible for antidrug antibodies pro- duction, which play a causal role in secondary non-response to therapy [71].

Siglec-2 polymorphisms have been associated with au- toimmunity in a number of mouse strains [72], most of which occur within the ligand-binding domain [58]. SHP-
1 null and SHP-1 mutant mice display a similar hyperresponsive phenotype to the Siglec-2 null mouse [67, 73], and demonstrate increased levels of spontaneous au- toantibody production [74, 75]. As autoantibody produc- tion has been shown to influence treatment responses [71], this further suggests Siglec-2 may contribute to non- response to drug therapy. The findings to date indicate that

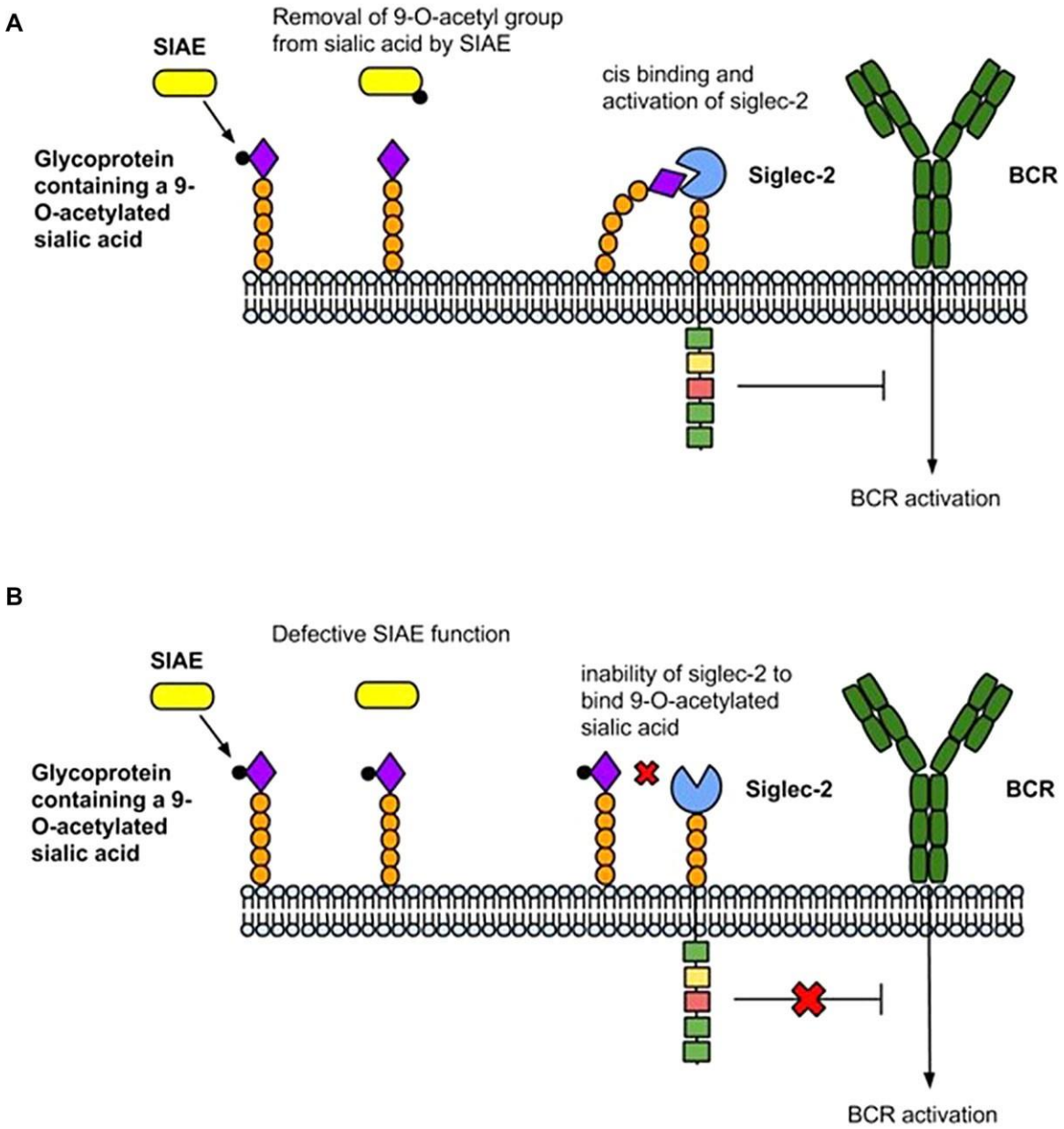

Figure 4. The effect of normal and defective SIAE function on Siglec-2 regulation of BCR activation. (A) demonstrates normal sialic acid acetylesterase (SIAE) function. SIAE is responsible for the removal of 9-*O*-acetyl groups from sialic acid molecules in sialylated glycoconju- gates. Glycoproteins containing sialic acid in *a*.2-6 linkage are capable of binding to and activating Siglec-2, both in cis-, as demonstrated, and trans- interactions. The activation of Siglec-2 inhibits BCR activation and subsequent immune response. (B) demonstrates defective SIAE function, resulting in increased 9-*O*-acetylated sialic acid. Siglec-1, -2, and -3 are incapable of binding ligands containing 9-*O*-acetylated sialic acid. A defective SIAE system will therefore result in reduced Siglec-2 suppression of BCR activation. This can result in increased autoreactive BCR signaling and immunogenicity.

polymorphisms within Siglec-2 and its ligands or down- stream intracellular pathways may increase the susceptibility of developing antidrug antibodies and subsequently subthera- peutic response to therapy. However, further research into the effects of these polymorphisms within patient populations is required.

4.4 A role for sialyltransferases in autoimmunity?

A large number of sialyltransferases are responsible for the generation of sialic acids, ligands of the Siglecs. Sialic acids are created in *a*.2-3, *a*.2-6, and *a*.2-8 linkage, depending on the underlying structure of the relevant

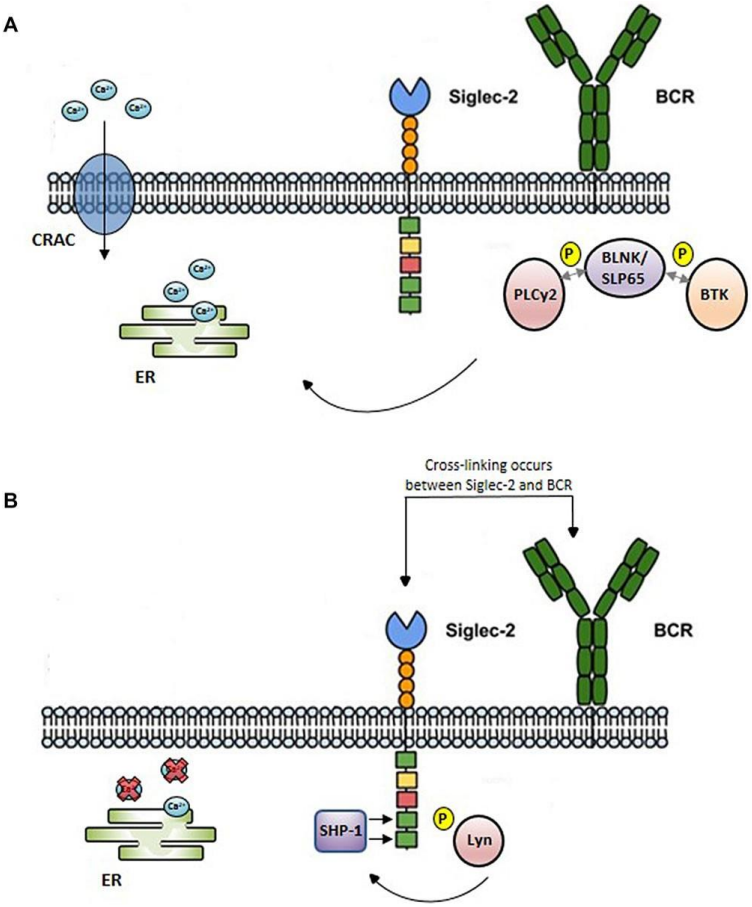

Figure 5. The downregulation of BCR signaling caused by cross-linking of Siglec-2. (A) BCR becomes phosphorylated and activated due to PLCγ2, BLNK/SLP65, and BTK signal- ing molecules. This leads to an increase in calcium ions (Ca^{2+}) from endoplasmic retic- ulum (ER). Calcium ions are also brought into the cell via the calcium release acti- vated channel (CRAC). (B) Af- ter cross-linking between BCR and Siglec-2, ITIMs of Siglec-2 become phosphorylated by the Src kinase, Lyn. This leads to the recruitment of SHP-1 tyro- sine phosphatase that subse- quently binds to two phospho- rylated ITIMs. Calcium stores are depleted within intracellular stores, causing BCR signaling to be reduced.

N-glycan, *O*-linked mucin, or glycolipid [76]. β-Galactoside α-2,6-sialyltransferase-I (ST6Gal-I) is the sialyltransferase re- sponsible for creating sialic acids in α2-6 linkage. It has been implicated in the regulation and induction of B-cell tolerance and subsequently autoimmunity through its role in creating α2-6 sialic acid ligands for Siglec-2. ST6Gal-I deficient mice do not mimic the enhanced BCR activation seen in the Siglec- 2 null mouse, but do display impaired immune responses to thymus-dependent and thymus-independent antigens [77]. Further research is required to elucidate the mechanisms behind this phenotype.

A recent study by Liu et al. [78] demonstrated that ST6Gal- I inhibits TNF-α mediated macrophage apoptosis via sialyla- tion of the TNF receptor 1 and downregulation of ST6Gal- 1 enhanced TNF-α mediated macrophage apoptosis. The evidence to date suggests that ST6Gal-I may play a key role in autoimmunity and subsequent response to TNF-α targeted biological therapy.

ST3Gal is the sialyltransferase responsible for produc- ing α2-3 linked sialic acids. In the Kidder et al. [79] study, T cells expressing the Siglec-1 ligand had increased ST3Gal- III and ST3Gal-VI transcript expression. α2-3 sialylation was also found to be essential for Siglec-1 binding and modula- tion of T-cell activation (illustrated in Fig. 3). Siglec-1 defi- cient mice display an increase in $CD8^+$ T cells within the spleen and lymph nodes [80], however ST3Gal-I null mice ex- hibit a phenotype displaying relatively reduced levels of $CD8^+$ T cells [81]. Again, further research is required to elucidate the relationship between ST3Gal, Siglec-1, and circulating T cells as well as other immune cell populations.

5 Conclusions

Existing unguided approaches to therapy result in high rates of non-response to autoimmunity treatments. The mecha- nisms behind non-response are poorly understood, limiting the ability to tightly control disease and establish remission in a timely fashion. This review summarizes evidence of two key protein glycosylation-driven pathways of the immune re- sponse in ADs. We postulate that perturbed protein glycosy- lation observed in autoimmune patients, leads to an adverse imbalance of T-cell subsets that can be measured as a sur- rogate of non-response or resistance to drug therapy. With a clearer knowledge of these pathways, it is foreseeable that novel monitoring tools could be developed for early stratifica- tion of patients onto the most suitable treatment regimen.

D.S.G. and A.J.E. wish to acknowledge the award of a Ph.D. fellowship from Department of Education and Learning, Northern Ireland, UK. This work was financed by a grant awarded to A.
J. Bjourson under the European Union Regional Development Fund (ERDF) EU Sustainable Competitiveness Programme for
N. Ireland & the Northern Ireland Public Health Agency (HSC R&D).

The authors have declared no conflict of interest.

6 References

[1] Roddick, J., Autoimmune disease, 2015 Available at: http:// www.healthline.com/health/autoimmune-disorders#Overvi ew1 (Accessed November 18, 2015).

[2] Smyk, D. S., Koutsoumpas, A. L., Mytilinaiou, M. G., Rigopoulou, E. I. et al., Helicobacter pylori and autoimmune disease: cause or bystander. *World J. Gastroenterol.* 2014, *20*, 613–629.

[3] Selgrade, M. K., Cooper, G. S., Germolec, D. R., Heindel, J. J., Linking environmental agents and autoimmune disease: an agenda for future research. *Environ. Health Perspect.* 1999, *107* (Suppl 5), 811–813.

[4] Cooper, G. S., Miller, F. W., Pandey, J. P., The role of ge- netic factors in autoimmune disease: implications for en- vironmental research. *Environ. Health Perspect.* 1999, *107* (Suppull 5), 693–700.

[5] Gabriel, S. E., Michaud, K., Epidemiological studies in incidence, prevalence, mortality, and comorbidity of the rheumatic diseases. *Arthritis Res. Ther.* 2009, *11*, 1–16.

[6] Cooper, G. S., Bynum, M. L., Somers, E. C., Recent insights in the epidemiology of autoimmune diseases: improved preva- lence estimates and understanding of clustering of diseases. *J. Autoimmun.* 2009, *33*, 197–207.

[7] AARDA, AARDA—autoimmune related disease informa- tion (Autoimmune Disease in Women), 2015, Available at: http://www.aarda.org/ (Accessed November 20, 2015).

[8] Tak, P. P., A personalized medicine approach to biologic treat- ment of rheumatoid arthritis: a preliminary treatment algo- rithm. *Rheumatology* 2012, *51*, 600–609.

[9] Melo, A. K., Melo, M. R., Saramago, A. B., Demartino,
G. et al., Persistent glucocorticoid resistance in systemic lupus erythematosus patients during clinical remission. *Genet. Mol. Res.* 2013, *12*, 2010–2019.

[10] Sperandio, M., Gleissner, C. A., Ley, K., Glycosylation in im- mune cell trafficking. *Immunol. Rev.* 2009, *230*, 97–113.

[11] Xiong, Y. S., Cheng, Y., Lin, Q. S., Wu, A. L. et al., Increased ex- pression of Siglec-1 on peripheral blood monocytes and its role in mononuclear cell reactivity to autoantigen in rheuma- toid arthritis. *Rheumatology* 2014, *53*, 250–259.

[12] Jellusova, J., Nitschke, L., Regulation of B cell functions by the sialic acid-binding receptors siglec-G and CD22. *Front. Immunol.* 2012, *2*, 1–14.

[13] Apweiler, R., Hermjakob, H., Sharon, N., On the frequency of protein glycosylation, as deduced from analysis of the Swiss-Prot database. *Biochim. Biophys. Acta* 1999, *1473*, 4–
8.

[14] Knezevic, A., Polasek, O., Gornik, O., Rudan, I. et al., Variabil- ity, heritability and environmental determinants of human plasma *N*-glycome. *J. Proteome Res.* 2009, *8*, 694–701.

[15] Parkkinen, J., Aberrant lectin-binding activity of im- munoglobulin G in serum from rheumatoid arthritis patients. *Clin. Chem.* 1989, *35*, 1638–1643.

[16] Ohtsubo, K., Marth, J. D., Glycosylation in cellular mecha- nisms of health and disease. *Cell* 2006, *126*, 855–867.

[17] Collins, E. S., Galligan, M. C., Saldova, R., Adamczyk, B. et al., Glycosylation status of serum in inflammatory arthritis in re- sponse to anti-TNF treatment. *Rheumatology* 2013, *52*, 1572–
1582.

[18] Mann, A. C., Record, C. O., Self, C. H., Turner, G. A., Monosac- charide composition of haptoglobin in liver diseases and al- cohol abuse: large changes in glycosylation associated with alcoholic liver disease. *Clin. Chim. Acta* 1994, *227*, 69–78.

[19] Higai, K., Aoki, Y., Azuma, Y., Matsumoto, K., Glycosylation of site-specific glycans of alpha1-acid glycoprotein and alter- ations in acute and chronic inflammation. *Biochim. Biophys. Acta* 2005, *1725*, 128–135.

[20] Zheng, X., Wu, S. L., Hincapie, M., Hancock, W. S., Study of the human plasma proteome of rheumatoid arthritis. *J. Chromatogr. A* 2009, *1216*, 3538–3545.

[21] Saroha, A., Biswas, S., Chatterjee, B. P., Das, H. R., Altered glycosylation and expression of plasma alpha-1-

acid gly- coprotein and haptoglobin in rheumatoid arthritis. *J. Chro- matogr. B Analyt. Technol. Biomed. Life Sci.* 2011, *879*, 1839– 1843.

[22] Alavi, A., Axford, J. S., Glyco-biomarkers: potential deter- minants of cellular physiology and pathology. *Dis. Markers* 2008, *25*, 193–205.

[23] Carson, D. A., Chen, P. P., Fox, R. I., Kipps, T. J. et al., Rheuma- toid factor and immune networks. *Annu. Rev. Immunol.* 1987, *5*, 109–126.

[24] Troelsen, L. N., Jacobsen, S., Abrahams, J. L., Royle, L. et al., IgG glycosylation changes and MBL2 polymorphisms: as- sociations with markers of systemic inflammation and joint destruction in rheumatoid arthritis. *J. Rheumatol.* 2012, *39*, 463–469.

[25] Pasek, M., Duk, M., Podbielska, M., Sokolik, R. et al., Galac- tosylation of IgG from rheumatoid arthritis (RA) patients— changes during therapy. *Glycoconj. J.* 2006, *23*, 463–471.

[26] Croce, A., Firuzi, O., Altieri, F., Eufemi, M. et al., Effect of inflix- imab on the glycosylation of IgG of patients with rheumatoid arthritis. *J. Clin. Lab. Anal.* 2007, *21*, 303–314.

[27] Firestein, G. S., Evolving concepts of rheumatoid arthritis.
Nature 2003, *423*, 356–361.

[28] Zhang, Y., Lv, K., Zhang, C. M., Jin, B. Q. et al., The role of LAIR-1 (CD305) in T cells and monocytes/macrophages in patients with rheumatoid arthritis. *Cell. Immunol.* 2014, *287*, 46–52.

[29] Kim, K. W., Cho, M. L., Lee, S. H., Oh, H. J. et al., Human rheumatoid synovial fibroblasts promote osteoclastogenic activity by activating RANKL via TLR-2 and TLR-4 activation. *Immunol. Lett.* 2007, *110*, 54–64.

[30] Chara, L., Sanchez-Atrio, A., Perez, A., Cuende, E. et al., The number of circulating monocytes as biomarkers of the clin- ical response to methotrexate in untreated patients with rheumatoid arthritis. *J. Transl. Med.* 2015, *13*, 1–10.

[31] Huang, Q., Ma, Y., Adebayo, A., Pope, R. M., Increased macrophage activation mediated through toll-like receptors in rheumatoid arthritis. *Arthritis Rheum.* 2007, *56*, 2192–
2201.

[32] Chalmers, S. A., Chitu, V., Ramanujam, M., Putterman, C., Therapeutic targeting of macrophages in lupus nephritis. *Discov. Med.* 2015, *20*, 43–49.

[33] Kinne, R. W., Brauer, R., Stuhlmuller, B., Palombo-Kinne, E., Burmester, G. R., Macrophages in rheumatoid arthritis. *Arthritis Res.* 2000, *2*, 189–202.

[34] Bresnihan, B., Pathogenesis of joint damage in rheumatoid arthritis. *J. Rheumatol.* 1999, *26*, 717–719.

[35] Mulherin, D., Fitzgerald, O., Bresnihan, B., Synovial tissue macrophage populations and articular damage in rheuma- toid arthritis. *Arthritis Rheum.* 1996, *39*, 115–124.

[36] Klareskog, L., Forsum, U., Kabelitz, D., Ploen, L. et al., Im- mune functions of human synovial cells. Phenotypic and T cell regulatory properties of macrophage-like cells that ex- press HLA-DR. *Arthritis Rheum.* 1982, *25*, 488–501.

[37] Miossec, P., van den Berg, W., Th1/Th2 cytokine balance in arthritis. *Arthritis Rheum.* 1997, *40*, 2105–2115.

[38] Silverman, G. J., Carson, D. A., Roles of B cells in rheumatoid arthritis. *Arthritis Res. Ther.* 2003, *5* (Suppl 4), S1–S6.

[39] Cope, A. P., Schulze-Koops, H., Aringer, M., The central role of T cells in rheumatoid arthritis. *Clin. Exp. Rheumatol.* 2007, *25*, S4–S11.

[40] Wu, C., Rauch, U., Korpos, E., Song, J. et al., Sialoadhesin- positive macrophages bind regulatory T cells, negatively controlling their expansion and autoimmune disease pro- gression. *J. Immunol.* 2009, *182*, 6508–6516.

[41] Crocker, P. R., Siglecs: sialic-acid-binding immunoglobulin- like lectins in cell-cell interactions and signalling. *Curr. Opin. Struct. Biol.* 2002, *12*, 609–615.

[42] Crocker, P.R., Mucklow, S., Bouckson, V., McWilliam, A. et al., Sialoadhesin, a macrophage sialic acid binding receptor for haemopoietic cells with 17 immunoglobulin-like domains. *EMBO J.* 1994, *13*, 4490–4503.

[43] Munday, J., Floyd, H., Crocker, P. R., Sialic acid binding re- ceptors (siglecs) expressed by macrophages. *J. Leukoc. Biol.* 1999, *66*, 705–711.

[44] Hartnell, A., Steel, J., Turley, H., Jones, M. et al., Characteri- zation of human sialoadhesin, a sialic acid binding receptor expressed by resident and inflammatory macrophage pop- ulations. *Blood* 2001, *97*, 288–296.

[45] Delputte, P. L., Van Gorp, H., Favoreel, H. W., Hoebeke, I. et al., Porcine sialoadhesin (CD169/Siglec-1) is an endocytic receptor that allows targeted delivery of toxins and antigens to macrophages. *PLoS One* 2011, *6*, 1–12.

[46] O'Neill, A. S., van den Berg, T. K., Mullen, G. E., Sialoadhesin—a macrophage-restricted marker of im- munoregulation and inflammation. *Immunology* 2013, *138*,
198–207.

[47] Biesen, R., Demir, C., Barkhudarova, F., Grun, J. R. et al., Sialic acid-binding Ig-like lectin 1 expression in inflammatory and resident monocytes is a potential biomarker for monitoring disease activity and success of therapy in systemic lupus erythematosus. *Arthritis Rheum.* 2008, *58*, 1136–1145.

[48] Ferreira, R. C., Guo, H., Coulson, R. M., Smyth, D. J. et al., A type I interferon transcriptional signature precedes autoim- munity in children genetically at risk for type 1 diabetes. *Diabetes* 2014, *63*, 2538–2550.

[49] York, M. R., Nagai, T., Mangini, A. J., Lemaire, R. et al., A macrophage marker, Siglec-1, is increased on circulating monocytes in patients with systemic sclerosis and induced by type I interferons and toll-like receptor agonists. *Arthritis Rheum.* 2007, *56*, 1010–1020.

[50] Rose, T., Grutzkau, A., Hirseland, H., Huscher, D. et al., IF- Nalpha and its response proteins, IP-10 and SIGLEC-1, are biomarkers of disease activity in systemic lupus erythemato- sus. *Ann. Rheum. Dis.* 2013, *72*, 1639–1645.

[51] Crocker, P. R., Paulson, J. C., Varki, A., Siglecs and their roles in the immune system. *Nat. Rev. Immunol.* 2007, *7*, 255–266.

[52] May, A. P., Robinson, R. C., Vinson, M., Crocker, P. R., Jones,
E. Y., Crystal structure of the *N*-terminal domain of siaload- hesin in complex with 3' sialyllactose at 1.85 A resolution. *Mol. Cell* 1998, *1*, 719–728.

[53] Biesen, R., Demir, C., Barkhudarova, F., Grun, J. R. et al., Sialic acid-binding Ig-like lectin 1 expression in inflammatory and resident monocytes is a potential biomarker for monitoring disease activity and success of therapy in systemic lupus erythematosus. *Arthritis Rheum.* 2008, *58*, 1136–1145.

[54] Kidder, D., Richards, H. E., Ziltener, H. J., Garden, O. A., Crocker, P. R., Sialoadhesin ligand expression identifies a subset of CD4+Foxp3- T cells with a distinct activation and glycosylation profile. *J. Immunol.* 2013, *190*, 2593–2602.

[55] van den Berg, T. K., Nath, D., Ziltener, H. J., Vestweber, D. et al., Cutting edge: CD43 functions as a T cell counter- receptor for the macrophage adhesion receptor sialoadhesin (Siglec-1). *J. Immunol.* 2001, *166*, 3637–3640.

[56] Ohnishi, K., Komohara, Y., Saito, Y., Miyamoto, Y. et al., CD169-positive macrophages in regional lymph nodes are associated with a favorable prognosis in patients with col- orectal carcinoma. *Cancer Sci.* 2013, *104*, 1237–1244.

[57] Tedder, T. F., Inaoki, M., Sato, S., The CD19-CD21 complex regulates signal transduction thresholds governing humoral immunity and autoimmunity. *Immunity* 1997, *6*, 107–118.

[58] Poe, J. C., Tedder, T. F., CD22 and Siglec-G in B cell function and tolerance. *Trends Immunol.* 2012, *33*, 413–420.

[59] Grewal, P. K., Boton, M., Ramirez, K., Collins, B. E. et al., ST6Gal-I restrains CD22-dependent antigen receptor endo- cytosis and Shp-1 recruitment in normal and pathogenic im- mune signaling. *Mol. Cell. Biol.* 2006, *26*, 4970–4981.

[60] Lanoue, A., Batista, F. D., Stewart, M., Neuberger, M. S., In- teraction of CD22 with alpha2,6-linked sialoglycoconjugates: innate recognition of self to dampen B cell autoreactivity? *Eur. J. Immunol.* 2002, *32*, 348–355.

[61] Poe, J. C., Fujimoto, Y., Hasegawa, M., Haas, K. M. et al., CD22 regulates B lymphocyte function in vivo through both ligand- dependent and ligand-independent mechanisms. *Nat. Im- munol.* 2004, *5*, 1078–1087.

[62] Smith, K. G., Tarlinton, D. M., Doody, G. M., Hibbs, M. L., Fearon, D. T., Inhibition of the B cell by CD22: a requirement for Lyn. *J. Exp. Med.* 1998, *187*, 807–811.

[63] Doody, G. M., Justement, L. B., Delibrias, C. C., Matthews, R.
J. et al., A role in B cell activation for CD22 and the protein tyrosine phosphatase SHP. *Science* 1995, *269*, 242–244.

[64] O'Keefe, T. L., Williams, G. T., Davies, S. L., Neuberger, M. S., Hyperresponsive B cells in CD22-deficient mice. *Science* 1996, *274*, 798–801.

[65] Otipoby, K. L., Andersson, K. B., Draves, K. E., Klaus, S. J. et al., CD22 regulates thymus-independent responses and the lifespan of B cells. *Nature* 1996, *384*, 634–637.

[66] Nitschke, L., Carsetti, R., Ocker, B., Kohler, G., Lamers, M. C., CD22 is a negative regulator of B-cell receptor signalling. *Curr. Biol.* 1997, *7*, 133–143.

[67] Sato, S., Miller, A. S., Inaoki, M., Bock, C. B. et al., CD22 is both a positive and negative regulator of B lymphocyte anti- gen receptor signal transduction: altered signaling in CD22- deficient mice. *Immunity* 1996, *5*, 551–562.

[68] Sieger, N., Fleischer, S. J., Mei, H. E., Reiter, K. et al., CD22 ligation inhibits downstream B cell receptor signaling and Ca(2+) flux upon activation. *Arthritis Rheum.* 2013, *65*, 770–
779.

[69] O'Keefe, T. L., Williams, G. T., Batista, F. D., Neuberger, M. S., Deficiency in CD22, a B cell-specific inhibitory receptor, is sufficient to predispose to development of high affinity autoantibodies. *J. Exp. Med.* 1999, *189*, 1307–1313.

[70] Poe, J. C., Smith, S. H., Haas, K. M., Yanaba, K. et al., Ampli- fied B lymphocyte CD40 signaling drives regulatory B10 cell expansion in mice. *PLoS One* 2011, *6*, e22464.

[71] van Schouwenburg, P. A., Rispens, T., Wolbink, G. J., Im- munogenicity of anti-TNF biologic therapies for rheumatoid arthritis. *Nat. Rev. Rheumatol.* 2013, *9*, 164–172.

[72] Lajaunias, F., Ibnou-Zekri, N., Fossati Jimack, L., Chichepor- tiche, Y. et al., Polymorphisms in the Cd22 gene of inbred mouse strains. *Immunogenetics* 1999, *49*, 991–995.

[73] Cyster, J. G., Goodnow, C. C., Protein tyrosine phosphatase 1C negatively regulates antigen receptor signaling in B lym- phocytes and determines thresholds for negative selection. *Immunity* 1995, *2*, 13–24.

[74] Shultz, L. D., Schweitzer, P. A., Rajan, T. V., Yi, T. et al., Mutations at the murine motheaten locus are within the hematopoietic cell protein-tyrosine phosphatase (Hcph) gene. *Cell* 1993, *73*, 1445–1454.

[75] Kozlowski, M., Mlinaric-Rascan, I., Feng, G. S., Shen, R. et al., Expression and catalytic activity of the tyrosine phosphatase PTP1C is severely impaired in motheaten and viable mothe- aten mice. *J. Exp. Med.* 1993, *178*, 2157–2163.

[76] Pillai, S., Netravali, I. A., Cariappa, A., Mattoo, H., Siglecs and immune regulation. *Annu. Rev. Immunol.* 2012, *30*, 357–392.

[77] Hennet, T., Chui, D., Paulson, J. C., Marth, J. D., Immune regulation by the ST6Gal sialyltransferase. *Proc. Natl. Acad. Sci. USA* 1998, *95*, 4504–4509.

[78] Liu, Z., Swindall, A. F., Kesterson, R. A., Schoeb, T. R. et al., ST6Gal-I regulates macrophage apoptosis via alpha2-6 sia- lylation of the TNFR1 death receptor. *J. Biol. Chem.* 2011, *286*, 39654–39662.

[79] Kidder, D., Richards, H. E., Ziltener, H. J., Garden, O. A., Crocker, P. R., Sialoadhesin ligand expression identifies a subset of CD4+Foxp3- T cells with a distinct activation and glycosylation profile. *J. Immunol.* 2013, *190*, 2593–2602.

[80] Oetke, C., Vinson, M. C., Jones, C., Crocker, P. R., Sialoadhesin-deficient mice exhibit subtle changes in B- and T-cell populations and reduced immunoglobulin M levels. *Mol. Cell. Biol.* 2006, *26*, 1549–1557.

[81] Priatel, J. J., Chui, D., Hiraoka, N., Simmons, C. J. et al., The ST3Gal-I sialyltransferase controls CD8+ T lymphocyte homeostasis by modulating *O*-glycan biosynthesis. *Immu- nity* 2000, *12*, 273–283

Appendix C: Raw data relevant to chapter 3

	X axis	Y axis	Number of values	Mean	Median	Standard deviation
(A)	HC	#Monocytes x10^9/L	19	0.45	0.46	0.10
	DN		6	0.55	0.47	0.22
	DR		23	0.53	0.52	0.10
	D-NR		30	0.67	0.62	0.23
(B)	HC	% Classical monocytes	19	45.03	52.00	20.33
	DN		6	26.50	28.90	15.31
	DR		24	21.37	20.65	9.68
	D-NR		32	22.09	18.15	15.03
(C)	HC	% Non-classical monocytes	19	7.60	7.20	2.61
	DN		6	10.75	10.80	3.80
	DR		24	10.93	9.80	4.98
	D-NR		32	9.91	8.85	4.79
(D)	HC	% Intermediate monocytes	19	45.83	37.10	21.31
	DN		6	61.20	57.40	17.00
	DR		24	66.37	64.45	10.31
	D-NR		32	66.90	68.80	13.90

Figure 3.3 raw data

	X axis	Y axis	Number of values	Mean	Median	Standard deviation
(A)	HC	% CD169+ classical monocytes	19	9.43	7.80	5.89
	DN		6	21.83	13.50	22.80
	DR		24	21.89	9.95	26.31
	D-NR		32	19.83	10.20	26.40
(B)	HC	% CD169+ non-classical monocytes	19	12.15	8.40	8.39
	DN		6	30.10	29.20	18.41
	DR		24	30.95	28.30	16.73
	D-NR		32	30.68	26.30	15.05
(C)	HC	% CD169+ intermediate monocytes	19	13.87	10.60	9.78
	DN		6	30.02	22.95	23.00
	DR		24	25.77	15.95	25.14
	D-NR		32	24.13	14.30	25.65
(D)	HC	MFI CD169+ classical monocytes	19	3.64	3.68	0.65
	DN		6	3.64	3.53	0.69
	DR		24	3.57	3.34	0.85
	D-NR		32	4.09	3.56	2.17
(E)	HC	MFI CD169+ non-classical monocytes	19	3.29	3.32	0.68
	DN		6	3.10	2.99	0.34
	DR		24	3.14	3.05	0.50
	D-NR		32	3.30	2.93	1.36
(F)	HC	MFI CD169+ intermediate monocytes	19	3.48	3.50	0.58
	DN		6	3.59	3.18	1.14
	DR		24	3.71	3.71	0.57
	D-NR		32	4.00	3.40	1.88

Figure 3.4 raw data

	X axis	Y axis	Number of values	Mean	Median	Standard deviation
(A)	HC	% CD43+ Tregs	19	96.94	97.30	2.43
	DN		6	96.37	97.15	2.52
	DR		24	94.37	95.40	2.70
	D-NR		32	95.41	97.50	4.65
(B)	HC	CD43 MFI	19	23.44	11.15	27.96
	DN		6	11.26	9.31	5.96
	DR		24	12.85	8.85	11.76
	D-NR		29	10.34	6.37	11.55

Figure 3.5 raw data

	X axis	Y axis	Number of values	Mean	Median	Standard deviation
(A)	HC	% CD169+ classical/ %CD43	19	0.10	0.08	0.06
	DN		6	0.23	0.14	0.25
	DR		24	0.23	0.10	0.28
	D-NR		32	0.21	0.10	0.27
(B)	HC	% CD169+ non-classical/ %CD43	19	0.13	0.09	0.09
	DN		6	0.31	0.30	0.19
	DR		24	0.33	0.31	0.18
	D-NR		32	0.32	0.27	0.15
(C)	HC	% CD169+ intermediate/ %CD43	19	0.14	0.11	0.10
	DN		6	0.32	0.24	0.26
	DR		24	0.27	0.17	0.27
	D-NR		32	0.25	0.15	0.27
(D)	HC	MFI CD169+ classical/ %CD43	19	0.30	0.30	0.19
	DN		6	0.41	0.44	0.22
	DR		24	0.40	0.36	0.19
	D-NR		32	0.57	0.45	0.43
(E)	HC	MFI CD169+ non-classical/ %CD43	19	0.26	0.24	0.16
	DN		6	0.36	0.33	0.20
	DR		24	0.36	0.33	0.19
	D-NR		32	0.46	0.42	0.32
(F)	HC	MFI CD169+ intermediate/ %CD43	19	0.28	0.26	0.18
	DN		6	0.40	0.37	0.23
	DR		24	0.43	0.39	0.22
	D-NR		32	0.57	0.48	0.38

Figure 3.8 raw data

Appendix D: i) FACS panels and ii) Treg phenotypes used in previous literature.

(i)

CD marker	Fluorophore	Marker of	Cell type
CD14	APC H7	Monocytes	Macrophage, monocyte, granulocyte
CD16	PE-Cy7	Monocyte subsets	T cell, dendritic cell, NK cell, macrophage, monocyte, granulocyte
CD32	APC	Fc receptor for IgG - II	B cell, macrophage, monocyte, granulocyte, platelet
CD64	BV510	Fc receptor for IgG - I	Dendritic cell, stem cell, macrophage, monocyte, granulocyte
CD169	PE	Siglec-1	Dendritic cell, macrophage, monocyte
CD3	BV510	T cells	T cell
CD4	FITC	T cells/Tregs	T cell, macrophage, monocyte, granulocyte
CD45	BV421	Leukocytes	T cell, B cell, Dendritic cell, NK cell, stem cell, macrophage, monocyte, granulocyte
CD45RA	AlexaFluor 700	Naïve T cells	T cell, B cell, Dendritic cell, NK cell, stem cell, macrophage, monocyte
CD127	PE-Cy7	IL-7 receptor	T cell, stem cell, macrophage, monocyte
CD25	BV421 or PE	IL-2 receptor	T cell, B cell, NK cell, macrophage, monocyte
CD43	BV605	Sialophorin	T cell, NK cell, stem cell, macrophage, monocyte, granulocyte, platelet

FACS panels and reasons for use

(ii)

Phenotype	Reference
$CD4^+CD25^+$	van Amelsfort et al., 2007
$CD4^+CD25^+FoxP3^+$	Bonelli et al., 2016
$CD4^+CD25^+CD127^-$	Pihl et al., 2013
	Wang et al., 2015
$CD4^+FoxP3^+$ or	Chien et al., 2017
$CD4^+FoxP3^-$	

Treg phenotypes used in previous literature

References for ii): (van Amelsfort *et al.* 2007; Pihl *et al.* 2013; Wang *et al.* 2015; Bonelli *et al.* 2016; Chien and Chiang 2017)

Appendix E: Raw data relevant to chapter 4.

X axis	Y axis	Number of values	Mean	Median	Standard deviation
HC	% Tregs	21	9.70	9.10	3.21
DN		6	24.17	25.00	8.77
DR		24	20.41	17.80	11.75
D-NR		31	9.97	9.50	4.98

Figure 4.4 raw data

	X axis	Y axis	Number of values	Mean	Median	Standard deviation
(A)	HC	%CD45RA+FoxP3- Tregs	13	12.42	10.90	9.47
	DN		6	7.72	6.90	3.51
	DR		24	8.16	6.50	5.54
	D-NR		31	22.56	19.90	16.39
(B)	HC	%CD45RA+FoxP3+ Tregs	17	35.74	29.60	23.27
	DN		6	20.05	20.20	10.75
	DR		24	15.84	13.60	8.81
	D-NR		27	14.61	13.20	8.33
(C)	HC	%CD45RA-FoxP3+ Tregs	13	15.96	15.40	11.44
	DN		6	40.72	42.00	10.82
	DR		24	45.94	46.70	15.42
	D-NR		31	26.85	21.60	18.66
(D)	HC	%CD45RA+FoxP3-CD43+ Tregs	13	11.66	10.30	9.36
	DN		6	9.00	8.40	4.25
	DR		24	8.69	7.75	5.79
	D-NR		31	22.79	20.50	16.40
(E)	HC	%CD45RA+FoxP3+CD43+ Tregs	13	38.86	31.00	23.23
	DN		6	19.65	19.30	11.75
	DR		24	15.54	13.75	8.65
	D-NR		31	15.47	15.50	8.41
(F)	HC	%CD45RA-FoxP3+CD43+ Tregs	13	17.74	17.30	11.50
	DN		6	38.15	42.80	11.70
	DR		24	44.79	46.40	14.87
	D-NR		31	26.54	20.50	18.16

Figure 4.6 raw data

Appendix F: OLINK Panels

OLINK CVDII panel

CVD II		CVD II		CVD II	
Protein	Uniprot ID	Protein	Uniprot ID	Protein	Uniprot ID
BMP-6	P22004	IL18	Q14116	PSGL-1	Q14242
ANG-1	Q15389	FGF-21	Q9NSA1	CCL17	Q92583
ADM	P35318	PIgR	P01833	CCL3	P10147
CD40-L	P29965	RAGE	Q15109	MMP7	P09237
SLAMF7	Q9NQ25	SOD2	P04179	IgG Fc receptor II-b	P31994
PGF	P49763	CTRC	Q99895	ITGB1BP2	Q9UKP3
ADAM-TS13	Q76LX8	FGF-23	Q9GZV9	DCN	P07585
BOC	Q9BWV1	SPON2	Q9BUD6	Dkk-1	O94907
IL-4RA	P24394	GH	P01241	LPL	P06858
SRC	P12931	FS	P19883	PRSS8	Q16651
IL-1ra	P18510	GLO1	Q04760	AGRP	O00253
IL6	P05231	CD84	Q9UIB8	HB-EGF	Q99075
TNFRSF10A	O00220	PAPPA	Q13219	GDF-2	Q9UK05
STK4	Q13043	SERPINA12	Q8IW75	FABP2	P12104
IDUA	P35475	REN	P00797	THPO	P40225
TNFRSF11A	Q9Y6Q6	DECR1	Q16698	MARCO	Q9UEW3
PAR-1	P25116	MERTK	Q12866	GT	P51161
TRAIL-R2	O14763	KIM1	Q96D42	BNP	P16860
PRSS27	Q9BQR3	THBS2	P35442	MMP12	P39900
TIE2	Q02763	TM	P07204	ACE2	Q9BYF1
TF	P13726	VSIG2	Q96IQ7	PD-L2	Q9BQ51
IL1RL2	Q9HB29	AMBP	P02760	CTSL1	P07711
PDGF subunit B	P01127	PRELP	P51888	hOSCAR	Q8IYS5
IL-27	Q8NEV9,Q14213	HO-1	P09601	TNFRSF13B	O14836
IL-17D	Q8TAD2	XCL1	P47992	TGM2	P21980
CXCL1	P09341	IL16	Q14005	LEP	P41159
LOX-1	P78380	SORT1	Q99523	CA5A	P35218
Gal-9	O00182	CEACAM8	P31997	HSP 27	P04792
GIF	P27352	PTX3	P26022	CD4	P01730
SCF	P21583			NEMO	Q9Y6K9
				VEGFD	O43915
				PARP-1	P09874
				HAOX1	Q9UJM8

OLINK CVDIII panel

CVD III		CVD III		CVD III	
Protein	**Uniprot ID**	**Protein**	**Uniprot ID**	**Protein**	**Uniprot ID**
TNFRSF14	Q92956	TR	P02786	PGLYRP1	O75594
LDL receptor	P01130	TNFRSF10C	O14798	CPA1	P15085
ITGB2	P05107	GDF-15	Q99988	JAM-A	Q9Y624
IL-17RA	Q96F46	SELE	P16581	Gal-4	P56470
TNF-R2	P20333	AZU1	P20160	IL-1RT2	P27930
MMP-9	P14780	DLK-1	P80370	SHPS-1	P78324
EPHB4	P54760	SPON1	Q9HCB6	CCL15	Q16663
IL2-RA	P01589	MPO	P05164	CASP-3	P42574
OPG	O00300	CXCL16	Q9H2A7	uPA	P00749
ALCAM	Q13740	IL-6RA	P08887	CPB1	P15086
TFF3	Q07654	RETN	Q9HD89	CHI3L1	P36222
SELP	P16109	IGFBP-1	P08833	ST2	Q01638
CSTB	P04080	CHIT1	Q13231	t-PA	P00750
MCP-1	P13500	TR-AP	P13686	SCGB3A2	Q96PL1
CD163	Q86VB7	CCL22	O00626	EGFR	P00533
Gal-3	P17931	PSP-D	P35247	IGFBP-7	Q16270
GRN	P28799	PI3	P19957	CD93	Q9NPY3
MEPE	Q9NQ76	Ep-CAM	P16422	IL-18BP	O95998
BLM hydrolase	Q13867	AP-N	P15144	COL1A1	P02452
PLC	P98160	AXL	P30530	PON3	Q15166
LTBR	P36941	IL-1RT1	P14778	CTSZ	Q9UBR2
Notch 3	Q9UM47	MMP-2	P08253	MMP-3	P08254
TIMP4	Q99727	FAS	P25445	RARRES2	Q99969
CNTN1	Q12860	MB	P02144	ICAM-2	P13598
CDH5	P33151	TNFSF13B	Q9Y275	KLK6	Q92876
TLT-2	Q5T2D2	PRTN3	P24158	PDGF subunit A	P04085
FABP4	P15090	PCSK9	Q8NBP7	TNF-R1	P19438
TFPI	P10646	U-PAR	Q03405	IGFBP-2	P18065
PAI	P05121	OPN	P10451	vWF	P04275
CCL24	O00175	CTSD	P07339	PECAM-1	P16284
				NT-proBNP	NA
				CCL16	O15467

OLINK Immune response panel

Immune response		Immune response		Immune response	
Protein	**Uniprot ID**	**Protein**	**Uniprot ID**	**Protein**	**Uniprot ID**
PPP1R9B	Q96SB3	NTF4	P34130	BACH1	O14867
GLB1	P16278	KRT19	P08727	PIK3AP1	Q6ZUJ8
PSIP1	O75475	ITM2A	O43736	SPRY2	O43597
ZBTB16	Q05516	HNMT	P50135	STC1	P52823
IRAK4	Q9NWZ3	CCL11	P51671	ARNT	P27540
TPSAB1	Q15661	MILR1	Q7Z6M3	FAM3B	P58499
HCLS1	P14317	EGLN1	Q9GZT9	SH2D1A	O60880
CNTNAP2	Q9UHC6	NFATC3	Q12968	ICA1	Q05084
CLEC4G	Q6UXB4	LY75	O60449	DFFA	O00273
IRF9	Q00978	EIF5A	P63241	DCBLD2	Q96PD2
EDAR	Q9UNE0	EIF4G1	Q04637	FCRL6	Q6DN72
IL6	P05231	CD28	P10747	NCR1	O76036
DGKZ	Q13574	PTH1R	Q03431	CXCL12	P48061
CLEC4C	Q8WTT0	BIRC2	Q13490	AREG	P15514
IRAK1	P51617	HSD11B1	P28845	IFNLR1	Q8IU57
CLEC4A	Q9UMR7	NF2	P35240	DAPP1	Q9UN19
PRDX1	Q06830	PLXNA4	Q9HCM2	PADI2	Q9Y2J8
PRDX3	P30048	SH2B3	Q9UQQ2	SIT1	Q9Y3P8
FGF2	P09038	FCRL3	Q96P31	MASP1	P48740
PRDX5	P30044	CKAP4	Q07065	LAMP3	Q9UQV4
DPP10	Q8N608	JUN	P05412	CLEC7A	Q9BXN2
TRIM5	Q9C035	HEXIM1	O94992	CLEC6A	Q6EIG7
DCTN1	Q14203	CLEC4D	Q8WXI8	DDX58	O95786
ITGA6	P23229	PRKCQ	Q04759	IL12RB1	P42701
CDSN	Q15517	MGMT	P16455	TANK	Q92844
GALNT3	Q14435	TREM1	Q9NP99	ITGA11	Q9UKX5
FXYD5	Q96DB9	CXADR	P78310	KPNA1	P52294
TRAF2	Q12933	IL10	P22301	LAG3	P18627
TRIM21	P19474	SRPK2	P78362	IL5	P05113
LILRB4	Q8NHJ6	KLRD1	Q13241	CD83	Q01151
				ITGB6	P18564
				BTN3A2	P78410

OLINK Inflammation panel

Inflammation		Inflammation		Inflammation	
Protein	**Uniprot ID**	**Protein**	**Uniprot ID**	**Protein**	**Uniprot ID**
IL8	P10145	IL18	Q14116	CD5	P06127
VEGFA	P15692	SLAMF1	Q13291	CCL3	P10147
BDNF	P23560	TGF-alpha	P01135	Flt3L	P49771
MCP-3	P80098	MCP-4	Q99616	CXCL6	P80162
GDNF	P39905	CCL11	P51671	CXCL10	P02778
CDCP1	Q9H5V8	TNFSF14	O43557	4E-BP1	Q13541
CD244	Q9BZW8	FGF-23	Q9GZV9	IL-20	Q9NYY1
IL7	P13232	IL-10RA	Q13651	SIRT2	Q8IXJ6
OPG	O00300	FGF-5	Q8NF90	CCL28	Q9NRJ3
LAP TGF-beta-1	P01137	MMP-1	P03956	DNER	Q8NFT8
uPA	P00749	LIF-R	P42702	EN-RAGE	P80511
IL6	P05231	FGF-21	Q9NSA1	CD40	P25942
IL-17C	Q9P0M4	CCL19	Q99731	IL33	O95760
MCP-1	P13500	IL-15RA	Q13261	IFN-gamma	P01579
IL-17A	Q16552	IL-10RB	Q08334	FGF-19	O95750
CXCL11	O14625	IL-22 RA1	Q8N6P7	IL4	P05112
AXIN1	O15169	IL-18R1	Q13478	LIF	P15018
TRAIL	P50591	PD-L1	Q9NZQ7	NRTN	Q99748
IL-20RA	Q9UHF4	Beta-NGF	P01138	MCP-2	P80075
CXCL9	Q07325	CXCL5	P42830	CASP-8	Q14790
CST5	P28325	TRANCE	O14788	CCL25	O15444
IL-2RB	P14784	HGF	P14210	CX3CL1	P78423
IL-1 alpha	P01583	IL-12B	P29460	TNFRSF9	Q07011
OSM	P13725	IL-24	Q13007	NT-3	P20783
IL2	P60568	IL13	P35225	TWEAK	O43508
CXCL1	P09341	ARTN	Q5T4W7	CCL20	P78556
TSLP	Q969D9	MMP-10	P09238	ST1A1	P50225
CCL4	P13236	IL10	P22301	STAMPB	O95630
CD6	Q8WWJ7	TNF	P01375	IL5	P05113
SCF	P21583	CCL23	P55773	ADA	P00813
				TNFB	P01374
				CSF-1	P09603

Appendix G: OLINK raw data

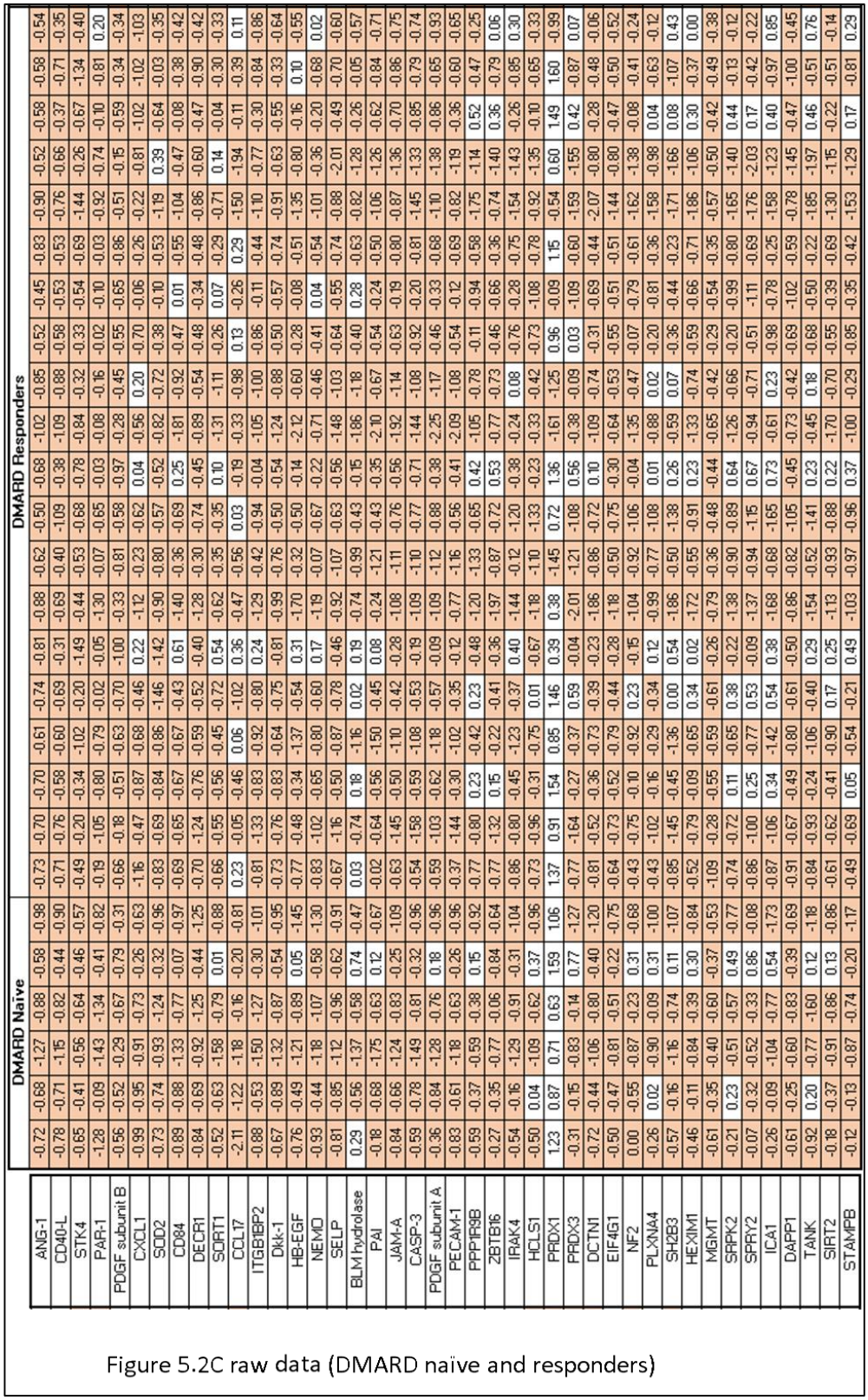

	DMARD Naïve												DMARD Responders											
ANG-1	-0.72	-0.68	-1.27	-0.88	-0.58	-0.98	-0.73	-0.70	-0.70	-0.61	-0.74	-0.81	-0.88	-0.62	-0.50	-0.68	-1.02	-0.85	-0.52	-0.45	-0.83	-0.90	-0.52	-0.58	-0.58	-0.54
CD40-L	-0.78	-0.71	-1.15	-0.82	-0.44	-0.90	-0.71	-0.76	-0.58	-0.60	-0.69	-0.31	-0.69	-0.40	-1.09	-0.38	-1.09	-0.88	-0.58	-0.53	-0.53	-0.76	-0.66	-0.37	-0.71	-0.35
STK4	-0.65	-0.41	-0.56	-0.64	-0.46	-0.57	-0.49	-0.20	-0.34	-1.02	-0.20	-1.49	-0.44	-0.53	-0.68	-0.78	-0.84	-0.32	-0.33	-0.54	-0.69	-1.44	-0.26	-0.67	-1.34	-0.40
PAR-1	-1.28	-0.09	-1.43	-1.34	-0.41	-0.82	-0.19	-1.05	-0.80	-0.79	-0.02	-0.05	-1.30	-0.07	-0.65	-0.03	-0.08	-0.16	-0.02	-0.10	-0.03	-0.92	-0.74	-0.10	-0.81	0.20
PDGF subunit B	-0.56	-0.52	-0.29	-0.67	-0.79	-0.31	-0.66	-0.18	-0.51	-0.63	-0.70	-1.00	-0.33	-0.81	-0.58	-0.97	-0.28	-0.45	-0.55	-0.65	-0.86	-0.51	-0.15	-0.59	-0.34	-0.34
CXCL1	-0.99	-0.95	-0.91	-0.73	-0.26	-0.63	-1.16	-0.47	-0.87	-0.68	-0.46	0.22	-1.12	-0.23	-0.62	0.04	-0.56	0.20	-0.70	-0.06	-0.26	-0.22	-0.81	-1.02	-1.02	-1.03
SOD2	-0.73	-0.74	-0.93	-1.24	-0.32	-0.96	-0.83	-0.69	-0.84	-0.86	-1.46	-1.42	-0.90	-0.80	-0.57	-0.52	-0.82	-0.72	-0.38	-0.10	-0.53	-1.19	0.39	-0.64	-0.03	-0.35
CD84	-0.89	-0.88	-1.33	-0.77	-0.07	-0.97	-0.69	-0.65	-0.67	-0.67	-0.43	0.61	-1.40	-0.36	-0.69	0.25	-1.81	-0.92	-0.47	0.01	-0.55	-1.04	-0.47	-0.08	-0.38	-0.42
DECR1	-0.84	-0.69	-0.92	-1.25	-0.44	-1.25	-0.70	-1.24	-0.76	-0.59	-0.52	-0.40	-1.28	-0.30	-0.74	-0.45	-0.89	-0.54	-0.48	-0.34	-0.48	-0.86	-0.60	-0.47	-0.90	-0.42
SORT1	-0.52	-0.63	-1.58	-0.79	0.01	-0.88	-0.66	-0.55	-0.56	-0.45	-0.72	0.54	-0.62	-0.35	-0.35	0.10	-1.31	-1.11	-0.26	0.07	-0.29	-0.71	0.14	-0.04	-0.30	-0.33
CCL17	-2.11	-1.22	-1.18	-1.16	-0.20	-0.81	0.23	-0.05	-0.46	0.06	-1.02	0.36	-0.47	-0.56	0.03	-0.19	-0.33	-0.98	0.13	-0.26	0.29	-1.50	-1.94	-0.11	-0.39	0.11
ITGBTBP2	-0.88	-0.53	-1.50	-1.27	-0.30	-1.01	-0.81	-1.33	-0.83	-0.92	-0.80	0.24	-1.29	-0.42	-0.94	-0.04	-1.05	-1.00	-0.86	-0.11	-0.44	-1.10	-0.77	-0.30	-0.84	-0.86
Dkk-1	-0.67	-0.89	-1.32	-0.87	-0.54	-0.95	-0.73	-0.76	-0.83	-0.64	-0.75	-0.81	-0.99	-0.76	-0.50	-0.54	-1.24	-0.88	-0.50	-0.57	-0.74	-0.91	-0.63	-0.55	-0.33	-0.64
HB-EGF	-0.76	-0.49	-1.21	-0.89	0.05	-1.45	-0.77	-0.48	-0.34	-1.37	-0.54	0.31	-1.70	-0.32	-0.50	-0.14	-2.12	-0.60	-0.28	-0.08	-0.51	-1.35	-0.80	-0.16	0.10	-0.55
NEMO	-0.93	-0.44	-1.18	-1.07	-0.58	-1.30	-0.83	-1.02	-0.65	-0.80	-0.60	0.17	-1.19	-0.07	-0.67	-0.22	-0.71	-0.46	-0.41	0.04	-0.54	-1.01	-0.36	-0.20	-0.68	0.02
SELP	-0.81	-0.85	-1.12	-0.96	-0.62	-0.91	-0.67	-1.16	-0.50	-0.87	-0.78	-0.46	-0.92	-1.07	-0.63	-0.56	-1.48	-1.03	-0.64	-0.55	-0.74	-0.88	-2.01	-0.49	-0.70	-0.60
BLM hydrolase	0.29	-0.56	-1.37	-0.58	0.74	-0.47	0.03	-0.74	0.18	-1.16	0.02	0.19	-0.74	-0.99	-0.43	-0.15	-1.86	-1.18	-0.40	0.28	-0.63	-0.82	-1.28	-0.26	-0.05	-0.57
PAI	-0.18	-0.68	-1.75	-0.63	0.12	-0.67	-0.02	-0.64	-0.56	-1.50	-0.45	0.08	-0.24	-1.21	-0.43	-0.35	-2.10	-0.67	-0.54	-0.24	-0.50	-1.06	-1.26	-0.62	-0.84	-0.71
JAM-A	-0.84	-0.66	-1.24	-0.83	-0.25	-1.09	-0.63	-1.45	-0.50	-1.10	-0.42	-0.28	-1.08	-1.11	-0.76	-0.56	-1.92	-1.14	-0.63	-0.19	-0.80	-0.87	-1.36	-0.70	-0.86	-0.75
CASP-3	-0.59	-0.78	-1.49	-0.81	-0.32	-0.96	-0.54	-1.58	-0.59	-1.08	-0.53	-0.19	-1.09	-1.10	-0.77	-0.71	-1.44	-1.08	-0.92	-0.20	-0.81	-1.45	-1.33	-0.85	-0.79	-0.74
PDGF subunit A	-0.36	-0.84	-1.28	-0.76	0.18	-0.96	-0.59	-1.03	-0.62	-1.18	-0.57	-0.09	-1.09	-1.12	-0.88	-0.38	-2.25	-1.17	-0.46	-0.33	-0.68	-1.10	-1.38	-0.86	-0.65	-0.93
PECAM-1	-0.83	-0.61	-1.18	-0.63	-0.26	-0.96	-0.37	-1.44	-0.30	-1.02	-0.35	-0.12	-0.77	-1.16	-0.56	-0.41	-2.09	-1.08	-0.54	-0.12	-0.69	-0.82	-1.19	-0.36	-0.60	-0.65
PPP1R9B	-0.59	-0.37	-0.59	-0.38	0.15	-0.92	-0.77	-0.80	0.23	-0.42	0.23	-0.48	-1.20	-1.33	-0.65	0.42	-1.05	-0.78	-0.11	-0.94	-0.58	-1.75	-1.14	0.52	-0.47	-0.25
ZBTB16	-0.27	-0.35	-0.77	-0.06	-0.84	-0.64	-0.77	-1.32	0.15	-0.22	-0.41	-0.36	-1.97	-0.87	-0.72	0.53	-0.77	-0.73	-0.46	-0.66	-0.36	-0.74	-1.40	0.36	-0.79	0.06
IRAK4	-0.54	-0.16	-1.29	-0.91	-0.31	-1.04	-0.86	-0.80	-0.45	-1.23	-0.37	0.40	-1.44	-0.12	-1.20	-0.38	-0.24	0.08	-0.76	-0.28	-0.75	-1.54	-1.43	-0.26	-0.85	0.30
HCLS1	-0.50	0.04	-1.09	-0.62	0.37	-0.96	-0.73	-0.96	-0.31	-0.75	0.01	-0.67	-1.18	-1.10	-1.33	-0.23	-0.33	-0.42	-0.73	-1.08	-0.78	-0.92	-1.35	-0.10	-0.65	-0.33
PRDX1	1.23	0.87	0.71	0.63	1.59	1.06	1.37	0.91	1.54	0.85	1.46	0.39	0.38	-1.45	0.72	1.36	-1.61	-1.25	0.96	-0.09	1.15	-0.54	0.60	1.49	1.60	-0.99
PRDX3	-0.31	-0.15	-0.83	-0.14	0.77	-1.27	-0.77	-1.64	-0.27	-0.37	0.59	-0.04	-2.01	-1.21	-1.08	0.56	-0.38	-0.09	0.03	-1.09	-0.60	-1.59	-1.55	0.42	-0.87	0.07
DCTN1	-0.72	-0.44	-1.06	-0.80	-0.40	-1.20	-0.81	-0.52	-0.36	-0.73	-0.39	-0.23	-1.86	-0.86	-0.72	0.10	-1.09	-0.74	-0.31	-0.69	-0.44	-2.07	-0.80	-0.28	-0.48	-0.06
EIF4G1	-0.50	-0.47	-0.81	-0.51	-0.22	-0.75	-0.64	-0.73	-0.52	-0.79	-0.44	-0.28	-1.18	-0.50	-0.75	-0.30	-0.64	-0.53	-0.55	-0.51	-0.51	-1.44	-0.80	-0.47	-0.50	-0.52
NF2	0.00	-0.55	-0.87	-0.23	0.31	-0.68	-0.43	-0.75	-0.10	-0.92	0.23	-0.15	-1.04	-0.92	-1.06	-0.04	-1.35	-0.47	-0.07	-0.79	-0.61	-1.62	-1.38	-0.08	-0.41	-0.24
PLXNA4	-0.26	0.02	-0.90	-0.09	0.31	-1.00	-0.43	-1.02	-0.16	-0.29	-0.34	0.12	-0.99	-0.77	-1.08	0.01	-0.88	0.02	-0.20	-0.81	-0.36	-1.58	-0.98	0.04	-0.63	-0.12
SH2B3	-0.57	-0.16	-1.16	-0.74	0.11	-1.07	-0.85	-1.45	-0.45	-1.36	0.00	0.54	-1.86	-0.50	-1.38	0.26	-0.59	0.07	-0.36	-0.44	-0.23	-1.71	-1.66	0.08	-1.07	0.43
HEXIM1	-0.46	-0.11	-0.84	-0.39	0.30	-0.84	-0.52	-0.79	-0.09	-0.65	0.34	0.02	-1.72	-0.55	-0.91	0.23	-1.33	-0.74	-0.59	-0.66	-0.71	-1.86	-1.06	0.30	-0.37	0.00
MGMT	-0.61	-0.35	-0.40	-0.60	-0.37	-0.53	-1.09	-0.28	-0.55	-0.59	-0.61	-0.26	-0.79	-0.36	-0.48	-0.44	-0.65	-0.42	-0.29	-0.54	-0.35	-0.57	-0.50	-0.42	-0.49	-0.38
SRPK2	-0.21	0.23	-0.51	-0.57	0.49	-0.77	-0.74	-0.72	0.11	-0.65	0.38	-0.22	-1.38	-0.90	-0.89	0.64	-1.26	-0.66	-0.20	-0.99	-0.80	-1.65	-1.40	0.44	-0.13	-0.12
SPRY2	-0.07	-0.32	-0.52	-0.33	0.86	-0.08	-0.86	-1.00	0.25	-0.77	0.53	-0.09	-1.37	-0.94	-1.15	0.67	-0.94	-0.71	-0.51	-1.11	-0.69	-1.76	-2.03	0.17	-0.42	-0.22
ICA1	-0.26	-0.09	-1.04	-0.77	0.54	-1.73	-0.87	-1.06	0.34	-1.42	0.54	0.38	-1.68	-0.68	-1.65	0.73	-0.61	0.23	-0.98	-0.78	-0.25	-1.58	-1.23	0.40	-0.97	0.85
DAPP1	-0.61	-0.25	-0.60	-0.83	-0.39	-0.69	-0.91	-0.67	-0.49	-0.80	-0.61	-0.50	-0.86	-0.82	-1.05	-0.45	-0.73	-0.42	-0.69	-1.02	-0.59	-0.78	-1.45	-0.47	-1.00	-0.45
TANK	-0.92	0.20	-0.77	-1.60	0.12	-1.18	-0.84	-0.93	-0.24	-1.06	-0.40	0.29	-1.54	-0.52	-1.41	0.23	-0.45	0.18	-0.68	-0.50	-0.22	-1.85	-1.97	0.46	-0.51	0.76
SIRT2	-0.18	-0.37	-0.91	-0.86	0.13	-0.86	-0.61	-0.62	-0.41	-0.90	0.17	0.25	-1.13	-0.93	-0.88	0.22	-1.70	-0.70	-0.55	-0.39	-0.69	-1.30	-1.15	-0.22	-0.51	-0.14
STAMPB	-0.12	-0.13	-0.87	-0.74	-0.20	-1.17	-0.49	-0.69	0.05	-0.54	-0.21	0.49	-1.03	-0.97	-0.96	0.37	-1.00	-0.29	-0.85	-0.35	-0.42	-1.53	-1.29	0.17	-0.81	0.29

Figure 5.2C raw data (DMARD naïve and responders)

	DMARD Non-responders																																			
ANG-1	0.45	0.48	0.30	0.63	0.71	2.80	2.58	2.67	-0.10	2.28	2.81	0.12	0.19	0.33	-0.35	0.04	0.06	-0.20	-1.24	0.57	0.19	0.58	-0.27	0.63	0.26	0.44	0.38	0.46	0.69	0.34
CD40-L	0.66	0.66	0.44	0.85	0.21	3.05	2.86	2.74	-0.29	1.37	2.80	-0.12	0.14	0.68	-0.43	0.04	0.02	-0.99	-0.61	0.43	0.50	-0.99	0.13	0.32	0.26	0.76	0.18	0.65	0.69	0.47
STK4	-0.24	-0.21	-0.10	-0.21	1.74	3.00	2.53	2.81	1.07	2.49	2.68	0.13	0.31	-0.17	0.16	0.35	0.19	-0.18	-0.22	-0.13	0.21	-0.11	0.02	0.03	-0.23	0.22	0.25	-0.25	0.25	-0.11
PAR-1	0.99	-0.86	1.03	0.62	0.89	2.38	2.51	2.69	-2.21	1.38	1.28	0.67	-0.71	-1.14	0.48	-0.28	0.94	0.69	0.19	-0.67	-0.27	-0.77	0.88	-0.09	1.02	0.42	0.66	-0.26	1.47	-0.84
PDGF subunit B	-0.43	-0.11	-0.12	-0.57	2.09	2.75	2.82	2.94	0.20	2.97	2.73	-0.19	0.05	0.05	0.02	-0.07	0.03	-0.21	-0.34	-0.15	0.19	0.10	-0.10	0.01	-0.18	0.12	-0.04	-0.33	-0.08	0.08
CXCL1	0.16	-0.17	-0.22	1.71	-0.12	2.65	2.34	2.50	-1.57	1.42	2.95	-0.33	-0.43	0.45	0.52	0.03	-0.40	0.58	-0.17	1.14	-0.14	-0.65	0.94	-0.16	0.95	0.27	-0.03	0.77	-0.65	0.94
SOD2	0.28	0.29	1.49	0.97	-0.15	2.41	2.18	2.22	-1.89	1.41	2.07	-0.04	0.68	1.22	-0.13	0.16	-0.07	-0.24	-1.11	0.88	1.19	-0.40	0.21	0.74	0.33	1.23	0.23	0.66	0.76	0.56
CD84	0.57	0.12	0.55	1.26	-0.57	2.68	2.20	2.15	-2.64	0.97	1.97	0.81	0.23	1.08	0.06	0.18	0.22	0.04	-0.36	0.87	0.48	-1.19	-0.10	0.79	0.41	0.92	-0.01	0.35	1.15	0.59
DECR1	1.02	0.31	0.83	1.14	-0.21	2.70	2.68	2.83	1.13	1.92	2.22	-0.26	0.13	0.76	-0.16	-0.19	0.06	-0.37	-0.95	0.54	0.35	-0.70	-0.08	0.22	0.46	0.53	-0.23	0.60	0.66	0.41
SORT1	0.58	0.35	0.88	1.40	-0.95	2.16	1.62	1.48	-4.21	0.67	1.95	0.20	0.48	1.17	-0.44	-0.13	-0.04	-0.45	-0.84	1.43	0.68	0.05	0.10	0.61	0.33	1.11	0.01	0.73	0.69	0.52
CCL17	0.05	0.17	-1.35	1.75	-0.41	2.20	2.21	1.70	-1.50	1.11	1.52	0.27	0.91	0.72	-1.05	-0.56	0.50	-0.22	0.01	1.02	0.62	1.69	-0.48	0.92	0.27	1.45	1.14	-0.60	-0.01	-1.31
ITGBIBP2	0.80	0.11	0.62	1.21	0.13	2.71	2.09	2.51	-0.76	1.23	2.62	0.42	0.44	0.60	0.04	0.56	0.30	-0.20	-0.40	1.03	0.57	-0.59	0.20	0.35	0.16	0.81	0.14	0.69	0.96	0.61
Dkk-1	0.64	0.70	0.78	1.06	-0.26	2.35	2.39	2.22	-1.61	1.62	2.41	0.18	0.50	0.92	-0.39	0.13	-0.17	-0.80	-0.90	0.79	0.90	0.54	0.24	0.93	0.23	1.04	0.47	0.95	0.76	0.92
HB-EGF	-0.33	0.49	0.02	1.23	-0.24	2.51	2.01	2.04	-1.44	1.35	2.30	0.47	0.08	0.96	-0.73	-0.59	0.09	-0.04	-0.66	0.70	0.48	0.14	-0.06	1.09	0.68	1.52	0.15	0.89	1.15	0.69
NEMO	0.54	-0.03	0.17	0.40	0.41	2.88	2.85	3.16	0.53	1.62	2.69	-0.31	0.13	0.17	-0.80	-0.10	0.03	-0.19	-0.97	0.61	0.24	-0.32	-0.28	0.30	0.28	0.40	-0.01	-0.27	1.12	0.44
SELP	0.59	0.58	-1.09	0.61	-0.11	1.43	1.01	0.91	-2.08	0.58	1.85	1.20	0.97	1.08	1.29	1.08	1.10	0.73	1.06	0.91	1.23	-0.27	0.67	0.76	0.59	1.11	0.70	1.32	1.51	0.70
BLM hydrolase	-0.14	0.52	-0.81	0.75	-0.53	1.06	-0.06	0.28	-3.78	0.01	1.52	1.06	0.86	2.27	0.93	0.41	0.79	0.08	0.23	0.16	1.00	-0.82	0.46	0.57	0.18	0.76	0.28	1.79	2.27	0.41
PAI	0.97	0.41	-0.79	0.65	-0.68	1.81	1.06	0.46	-2.72	0.59	2.15	0.92	1.06	1.94	0.98	0.59	0.84	0.31	0.31	0.32	1.28	0.20	0.16	0.86	0.23	0.83	-0.24	1.34	1.75	0.07
JAM-A	0.33	0.34	-1.05	0.29	-0.14	1.34	0.90	1.16	-1.34	0.24	1.43	1.28	1.02	1.67	1.25	1.12	1.48	0.71	1.29	0.56	1.31	-0.41	0.59	0.87	0.29	0.94	0.55	1.42	1.86	0.69
CASP-3	0.49	0.46	-0.87	0.72	-0.01	1.74	1.35	1.37	-1.18	0.98	2.18	0.97	0.92	1.40	0.83	0.93	1.05	0.58	0.69	0.69	1.25	-0.29	0.47	0.81	0.48	0.77	0.51	1.12	1.75	0.56
PDGF subunit A	0.48	0.47	-0.68	0.67	0.11	1.87	1.79	1.19	-1.22	1.23	2.37	1.05	0.53	1.67	0.98	0.86	0.93	0.13	0.52	0.16	1.00	0.11	0.39	0.74	-0.23	0.88	0.25	1.08	1.60	0.51
PECAM-1	0.48	0.48	-1.23	0.12	-0.68	0.79	0.49	0.59	-2.37	0.02	0.97	1.19	0.95	1.72	1.45	1.17	1.60	0.71	1.42	0.56	1.39	-0.31	0.53	0.92	0.15	1.13	0.55	1.54	1.96	0.80
PPP1R9B	-0.08	0.92	-2.32	0.78	-0.58	2.68	2.06	2.41	0.10	-0.27	2.91	0.58	0.77	0.88	0.72	0.94	-0.08	-0.13	-0.96	1.01	0.44	-0.03	-0.25	0.28	-0.58	0.50	0.02	0.77	0.51	0.02
ZBTB16	0.09	1.72	-0.87	1.11	-1.46	2.74	1.10	1.98	-0.82	0.05	2.16	0.60	0.86	0.86	0.61	0.02	0.61	-1.04	-1.34	0.80	0.67	-0.53	-0.62	0.91	0.56	0.63	-0.66	0.50	1.92	1.24
IRAK4	0.31	0.34	-1.26	0.45	0.13	2.55	2.28	3.02	-0.46	1.53	2.43	0.32	0.54	0.66	0.32	0.80	0.60	-0.32	-0.75	0.68	0.39	-0.84	-0.34	0.35	0.26	0.65	0.34	0.29	1.12	0.03
HCLS1	0.15	0.18	-0.60	0.54	0.37	2.77	2.39	2.76	-1.56	1.87	2.62	0.61	0.49	0.52	0.57	0.41	0.19	-0.42	-0.81	0.55	0.24	-0.42	0.24	0.47	0.16	0.63	0.32	0.70	0.79	-0.03
PRDX1	-1.66	0.16	-1.55	-0.22	-1.34	0.29	-0.38	-0.29	-2.62	-0.05	0.74	-0.35	-0.17	-0.03	-0.20	-1.07	-1.53	-0.87	-1.41	-0.44	-0.35	-0.42	-0.53	0.27	-0.04	0.23	-0.14	0.09	-0.66	-0.42
PRDX3	0.75	0.80	-0.87	1.06	-1.10	1.62	1.35	2.11	-0.12	1.05	2.27	0.53	0.53	0.93	1.09	0.31	-0.36	-1.14	-2.02	1.01	0.29	-0.45	0.48	0.43	0.63	1.06	-0.11	1.48	0.56	-0.36
DCTN1	-0.04	0.95	-1.18	0.49	-0.14	2.67	2.15	2.44	0.62	1.46	2.89	0.39	0.81	0.77	0.49	0.77	0.49	0.18	-0.55	1.20	0.95	-0.14	-0.34	0.05	0.16	0.23	-0.10	-0.09	0.43	-0.09
EIF4G1	0.03	0.31	-0.60	0.20	1.20	2.91	2.70	3.04	-0.77	2.49	2.88	0.16	0.18	0.34	0.27	0.09	0.14	-0.10	-0.59	0.30	0.11	-0.75	0.05	0.10	0.11	0.34	0.17	0.23	0.26	0.04
NF2	-0.15	0.61	-1.13	0.80	-0.71	2.60	2.08	2.38	-1.80	1.61	2.70	0.49	0.55	0.99	0.46	0.78	0.01	-0.42	-0.95	0.90	0.52	-1.12	0.18	0.43	0.07	0.77	0.26	0.92	0.69	-0.29
PLXNA4	0.02	0.55	-1.00	0.07	-0.05	2.46	2.49	2.74	-2.46	1.95	2.62	0.50	0.31	0.47	0.12	0.04	-0.06	-0.28	-1.27	0.69	0.19	-0.74	-0.24	0.35	0.16	0.74	0.80	0.48	0.77	0.01
SH2B3	0.37	0.14	-0.62	0.50	0.28	2.46	2.00	2.97	-0.22	1.52	2.14	0.86	0.22	0.64	0.44	0.51	0.43	-0.08	-0.86	0.24	-0.31	-0.81	0.35	0.33	0.83	0.29	0.31	0.47	1.19	-0.49
HEXIM1	0.01	0.70	-0.77	0.66	-0.61	2.62	1.93	2.73	-1.95	1.25	2.66	0.70	0.77	0.70	0.50	0.22	0.09	-0.24	-1.07	0.71	0.37	-0.92	-0.06	0.37	0.13	0.89	0.09	0.44	1.03	0.06
MGMT	0.10	0.09	-0.62	0.14	-0.29	2.83	2.75	2.99	-2.25	2.88	2.93	0.18	0.17	0.16	0.29	0.33	0.27	0.09	-0.22	0.20	-0.25	-0.45	0.14	-0.01	-0.04	0.20	0.08	0.04	0.00	0.20
SRPK2	-0.02	0.79	-0.82	0.82	-1.15	1.96	2.02	2.46	-2.04	1.27	2.57	0.50	0.30	0.93	0.37	0.05	0.09	-0.45	-1.64	1.06	0.24	-1.05	0.14	0.59	0.32	0.82	0.05	0.97	0.89	0.46
SPRY2	0.13	0.87	-0.84	0.88	-0.95	2.12	1.13	2.13	-1.30	1.07	2.44	0.55	0.46	1.11	0.60	0.42	-0.69	-0.91	-1.43	1.30	0.68	-1.24	0.23	0.61	0.32	1.02	0.49	1.43	0.44	0.35
ICA1	0.01	0.37	-1.07	1.10	-1.13	1.81	1.72	2.15	-1.35	0.65	1.76	0.42	0.55	0.85	0.89	0.77	0.25	-0.42	-1.27	1.29	0.29	-0.82	0.01	0.78	0.31	0.95	0.62	0.96	1.14	0.05
DAPP1	0.06	0.14	-0.17	0.34	0.94	2.68	2.61	2.76	-0.57	2.59	2.72	0.17	0.31	0.44	0.46	0.30	0.03	-0.22	-0.68	0.41	0.04	-0.32	0.11	0.25	0.17	0.33	0.22	1.28	0.43	0.27
TANK	-0.08	0.67	-1.65	0.77	-1.05	2.06	1.43	2.55	0.21	0.40	2.33	0.66	0.23	0.09	0.14	0.75	0.61	-0.44	-0.73	0.98	-0.02	-0.42	0.24	0.67	0.80	0.78	0.40	0.71	1.82	0.45
SIRT2	0.33	0.11	-0.84	0.52	0.07	2.52	2.02	2.20	-2.55	1.70	2.59	0.91	0.56	1.11	0.04	0.38	-0.13	-0.32	-0.58	0.79	0.44	-0.64	-0.42	0.44	0.43	0.94	0.54	0.71	0.99	0.36
STAMPB	0.29	0.46	-1.67	0.46	-0.38	2.46	2.01	2.49	-2.20	1.48	2.12	0.87	0.48	0.90	-0.13	0.22	-0.13	-0.59	-1.32	0.82	0.34	-0.56	-0.06	0.33	0.53	1.03	0.53	0.68	1.56	0.31

Figure 5.2C raw data (DMARD Non-responders)

Figure 5.10C raw data

	Remission										Low	
CD40-L	-0.68	-0.74	-0.54	-0.66	-0.67	-1.10	-1.10	-0.54	-0.74	-0.31	-0.29	-0.87	-0.63
SOD2	-0.91	-0.76	-0.92	-1.59	-0.98	-0.63	-0.90	-0.42	-1.29	-0.70	-0.40	-0.79	0.39
CD84	-0.78	-0.73	-0.75	-0.48	-1.57	-0.77	-2.04	-0.53	-1.17	-0.09	-0.47	-1.03	-0.53
DECR1	-0.66	-1.26	-0.73	-0.47	-1.30	-0.71	-0.87	-0.43	-0.84	-0.42	-0.36	-0.50	-0.56
SORT1	-0.83	-0.71	-0.72	-0.90	-0.79	-0.47	-1.60	-0.36	-0.90	-0.09	-0.45	-1.37	0.12
ITGB1BP2	-0.75	-1.28	-0.78	-0.74	-1.24	-0.89	-0.99	-0.80	-1.04	-0.23	-0.80	-0.95	-0.71
Dkk-1	-0.74	-0.77	-0.84	-0.76	-1.02	-0.50	-1.28	-0.49	-0.93	-0.54	-0.64	-0.90	-0.63
SELP	-0.70	-1.19	-0.54	-0.81	-0.95	-0.66	-1.50	-0.68	-0.91	-0.52	-0.63	-1.05	-2.03
CASP-3	-0.52	-1.54	-0.56	-0.50	-1.05	-0.75	-1.40	-0.89	-1.41	-0.82	-0.71	-1.05	-1.29
PDGF subunit A	-0.55	-0.98	-0.58	-0.53	-1.04	-0.83	-2.17	-0.42	-1.05	-0.81	-0.88	-1.11	-1.32

	Moderate																				
CD40-L	-1.16	-0.80	-0.39	-0.89	-0.57	-0.49	-0.49	-0.68	1.01	1.58	-0.04	0.24	-0.38	0.13	0.11	-0.99	-0.57	0.63	0.23	0.92	0.60
SOD2	-1.02	-1.35	-0.37	-1.05	-0.94	-0.13	-0.59	-0.06	1.02	1.48	-0.07	0.71	-0.16	0.15	-0.09	-0.28	-1.20	1.25	0.20	1.29	0.57
CD84	-1.49	-0.86	-0.08	-1.09	-0.76	0.01	-0.62	-0.43	1.41	1.09	0.90	0.25	0.06	0.20	0.24	0.04	-0.41	0.53	-0.12	1.03	0.66
DECR1	-0.91	-1.26	-0.38	-1.27	-0.55	-0.28	-0.43	-0.88	1.34	2.19	-0.19	0.24	-0.08	-0.11	0.17	-0.31	-0.94	0.47	0.01	0.68	0.54
SORT1	-1.93	-0.99	-0.04	-1.10	-0.59	0.03	-0.39	-0.41	1.62	0.75	0.18	0.52	-0.57	-0.20	-0.10	-0.58	-1.05	0.76	0.07	1.27	0.56
ITGB1BP2	-1.45	-1.21	-0.23	-0.95	-0.87	-0.04	-0.38	-0.78	1.30	1.31	0.50	0.51	0.11	0.63	0.37	-0.13	-0.33	0.65	0.27	0.89	0.69
Dkk-1	-1.36	-0.89	-0.54	-0.97	-0.64	-0.57	-0.75	-0.31	1.17	1.76	0.23	0.57	-0.38	0.18	-0.14	-0.81	-0.92	1.00	0.29	1.15	1.02
SELP	-1.15	-0.99	-0.65	-0.94	-0.90	-0.58	-0.77	-0.73	0.57	0.55	1.16	0.93	1.25	1.04	1.06	0.69	1.02	1.19	0.63	1.06	0.66
CASP-3	-1.45	-0.78	-0.30	-0.93	-1.05	-0.19	-0.78	-0.76	0.72	0.98	0.96	0.92	0.83	0.93	1.04	0.59	0.70	1.24	0.47	0.77	0.56
PDGF subunit A	-1.22	-0.71	0.21	-0.91	-1.12	-0.29	-0.63	-0.60	0.69	1.24	1.06	0.55	0.99	0.88	0.94	0.16	0.55	1.02	0.41	0.90	0.53

	High								
CD40-L	0.81	0.56	3.40	3.13	0.83	0.56	0.44	0.37	0.79
SOD2	0.27	1.56	2.55	2.19	1.28	0.92	0.77	0.33	0.68
CD84	0.63	0.61	3.00	2.21	1.21	0.98	0.88	0.46	0.39
DECR1	1.21	1.00	3.03	2.51	0.93	0.68	0.33	0.60	0.75
SORT1	0.64	1.00	2.52	2.27	1.34	1.64	0.68	0.35	0.82
ITGB1BP2	0.88	0.70	2.82	2.73	0.68	1.11	0.42	0.23	0.77
Dkk-1	0.72	0.87	2.53	2.59	1.02	0.87	1.03	0.29	1.04
SELP	0.56	-1.12	1.39	1.80	1.04	0.87	0.72	0.55	1.28
CASP-3	0.49	-0.84	1.73	2.15	1.39	0.69	0.81	0.48	1.12
PDGF subunit A	0.51	-0.63	1.86	2.35	1.67	0.19	0.75	-0.19	1.09

Appendix H: Chapter 5, Figure 5.5 - full list of associated diseases

Term	P-value	Adjusted P-value	Old P-value	Old Adjusted P-value	Z-score	Combined Score	Genes
Arthritis	0.001	0.027	0.000	0.016	-4.636	34.279	SELP;CASP3;CXCL1;DKK1
Cerebrovascular_disease	0.012	0.080	0.007	0.068	-4.357	19.388	SELP;CASP3;DECR1
Proliferative_vitreoretinopathy	0.000	0.027	0.000	0.016	-2.333	18.342	PDGFB;PDGFA
Hypertension	0.023	0.080	0.015	0.068	-3.910	14.812	SELP;CASP3;DECR1
Type_2_diabetes_mellitus	0.019	0.080	0.012	0.068	-3.709	14.743	ZBTB16;ICA1;SPRY2
Huntington's_disease	0.011	0.080	0.008	0.068	-3.100	13.947	CASP3;SIRT2
Cancer	0.025	0.080	0.016	0.068	-3.594	13.265	ZBTB16;PDGFB;NF2
Neurodegenerative_disease	0.023	0.080	0.015	0.068	-3.309	12.418	DCTN1;SIRT2;EIF4G1
Celiac_disease	0.015	0.080	0.011	0.068	-2.886	12.179	SH2B3;PLXNA4
Hyperglycemia	0.022	0.080	0.016	0.068	-2.833	10.861	CASP3;DECR1
Lung_disease	0.026	0.080	0.019	0.068	-2.722	9.947	CASP3;CXCL1
Toxic_encephalopathy	0.029	0.080	0.021	0.072	-2.592	9.196	CASP3;DECR1
Coronary_artery_disease	0.069	0.122	0.052	0.097	-2.210	5.911	SELP;SORT1
Alzheimer's_disease	0.063	0.121	0.047	0.093	-2.099	5.798	SELP;PLXNA4
Kluver-Bucy_syndrome	0.010	0.080	0.011	0.068	-1.087	4.959	SH2B3
Arthus_reaction	0.015	0.080	0.014	0.068	-1.078	4.555	SELP
Contact_dermatitis	0.010	0.080	0.011	0.068	-0.972	4.434	CCL17
Connective_tissue_cancer	0.019	0.080	0.018	0.068	-0.976	3.880	NF2
Acute_pancreatitis	0.021	0.080	0.019	0.068	-0.911	3.528	SELP
Dysgammaglobulinemia	0.015	0.080	0.014	0.068	-0.787	3.327	CD84
Benign_meningioma	0.015	0.080	0.014	0.068	-0.757	3.201	NF2
Meningioma	0.013	0.080	0.012	0.068	-0.686	3.006	NF2
Denys-Drash_syndrome	0.021	0.080	0.019	0.068	-0.759	2.939	PDGFA
Interstitial_cystitis	0.019	0.080	0.018	0.068	-0.727	2.890	HBEGF
Acquired_metabolic_disease	0.158	0.196	0.121	0.167	-1.510	2.784	SPRY2;TANK
Infectious_mononucleosis	0.027	0.080	0.025	0.072	-0.764	2.760	CD84
Antley-Bixler_syndrome	0.029	0.080	0.026	0.072	-0.747	2.645	DECR1
Intermittent_claudication	0.029	0.080	0.026	0.072	-0.723	2.560	SELP
Chromosome_17q11.2_deletion_syndrome,_1.4Mb	0.027	0.080	0.025	0.072	-0.671	2.426	BLMH
Diphtheria	0.047	0.099	0.042	0.087	-0.774	2.363	HBEGF
Basal_ganglia_calcification	0.035	0.086	0.031	0.077	-0.702	2.350	PDGFB
Hypothyroidism	0.029	0.080	0.026	0.072	-0.661	2.339	SH2B3
Familial_adenomatous_polyposis	0.051	0.102	0.045	0.090	-0.772	2.293	HBEGF
Chagas_disease	0.065	0.122	0.057	0.104	-0.789	2.156	DECR1
Brain_ischemia	0.071	0.122	0.062	0.107	-0.779	2.060	CASP3
Cutaneous_fibrous_histiocytoma	0.031	0.083	0.028	0.075	-0.567	1.968	PDGFB
Kabuki_syndrome	0.059	0.116	0.052	0.097	-0.683	1.931	DECR1
Ankylosis	0.047	0.099	0.042	0.087	-0.631	1.926	DKK1
Keratitis	0.079	0.126	0.069	0.110	-0.640	1.627	CXCL1
Smallpox	0.041	0.095	0.037	0.085	-0.508	1.621	DAPP1
Eosinophilia	0.130	0.184	0.112	0.160	-0.780	1.593	CCL17
Scabies	0.013	0.080	0.012	0.068	-0.362	1.585	CD84
Frontotemporal_dementia	0.079	0.126	0.069	0.110	-0.620	1.574	DCTN1
Brain_disease	0.150	0.196	0.130	0.167	-0.820	1.557	CASP3
Perinatal_necrotizing_enterocolitis	0.037	0.088	0.033	0.079	-0.471	1.550	HBEGF
Progressive_supranuclear_palsy	0.049	0.101	0.043	0.089	-0.502	1.512	DCTN1
Meningitis	0.088	0.139	0.077	0.121	-0.615	1.491	IRAK4
Atherosclerosis	0.104	0.157	0.090	0.136	-0.645	1.462	SELP
Peripheral_artery_disease	0.017	0.080	0.016	0.068	-0.352	1.440	SELP
Chronic_lymphocytic_leukemia	0.033	0.083	0.030	0.075	-0.419	1.428	HCLS1
Diabetes_mellitus	0.144	0.195	0.125	0.167	-0.732	1.417	SH2B3
Globe_disease	0.133	0.186	0.116	0.161	-0.694	1.398	SRPK2

Full list of associated diseases referring to Figure 5.5, where combined score is >1.4.

(List obtained from Jenson diseases via STRING)

Appendix I: Chapter 5, Figure 5.6 - full pathway list

Pathway name	#Entities found	#Entities total	Entities ratio	Entities pValue	Entities FDR	#Reactions found	#Reactions total	Submitted entities found
PI5P, PP2A and IER3 Regulate PI3K/AKT Signaling	5	112	0.008	0.000	0.016	1	7	PDGFB;PDGFA;IRAK4;HBEGF
Negative regulation of the PI3K/AKT network	5	120	0.009	0.000	0.016	1	10	PDGFB;PDGFA;IRAK4;HBEGF
Immune System	23	2643	0.196	<0.001	0.016	114	1444	CD40L;DCTN1;ZBTB16;PDGFB;DAPP1;PDGFA;CXCL1;IRAK4;SOD2;TANK;SELP;CASP3;PECAM1;BLMH;NF2;NEMO;CCL17;EIF4G1;HBEGF
Platelet degranulation	5	137	0.010	<0.001	0.016	4	11	SELP;PDGFB;PECAM1;PDGFA
Neurodegenerative Diseases	3	31	0.002	<0.001	0.016	2	22	PRDX1;SOD2
Deregulated CDK5 triggers multiple neurodegenerative pathways in Alzheimer's disease models	3	31	0.002	<0.001	0.016	2	22	PRDX1;SOD2
Response to elevated platelet cytosolic Ca2+	5	144	0.011	<0.001	0.016	4	14	SELP;PDGFB;PECAM1;PDGFA
Signaling by Interleukins	11	793	0.059	<0.001	0.016	24	468	CASP3;PDGFB;PDGFA;CXCL1;IRAK4;SOD2;NEMO;HBEGF
Downstream signal transduction	3	36	0.003	<0.001	0.017	16	16	PDGFB;PDGFA
Cytokine Signaling in Immune system	13	1108	0.082	<0.001	0.017	31	601	CD40L;CASP3;PDGFB;PDGFA;CXCL1;IRAK4;SOD2;NEMO;EIF4G1;HBE
Constitutive Signaling by Aberrant PI3K in Cancer	4	89	0.007	0.001	0.017	1	2	PDGFB;PDGFA;HBEGF
PI3K/AKT Signaling in Cancer	4	120	0.009	0.002	0.044	1	21	PDGFB;PDGFA;HBEGF
Platelet activation, signaling and aggregation	6	305	0.023	0.002	0.044	18	114	SELP;PAR1;PDGFB;PECAM1;PDGF
Detoxification of Reactive Oxygen Species	3	65	0.005	0.003	0.063	3	34	PRDX3;PRDX1;SOD2
Signaling by Receptor Tyrosine Kinases	8	585	0.043	0.003	0.063	77	625	CASP3;PDGFB;SPRY2;PDGFA;STK4;SH2B3;HBEGF
Sema3A PAK dependent Axon repulsion	2	19	0.001	0.003	0.063	3	6	STK4;PLXNA4
Signaling by PDGF	3	69	0.005	0.003	0.063	26	28	PDGFB;PDGFA
Signaling by Hippo	2	22	0.002	0.004	0.077	7	30	CASP3;STK4
Hemostasis	9	801	0.059	0.005	0.103	32	323	SELP;CD84;PAR1;PDGFB;PECAM1;PDGFA;SH2B3
RHO GTPases activate PAKs	2	27	0.002	0.006	0.103	4	15	NF2;STK4
MGMT-mediated DNA damage reversal	1	2	0.000	0.008	0.132	2	2	MGMT
PIP3 activates AKT signaling	5	303	0.022	0.008	0.132	1	87	PDGFB;PDGFA;IRAK4;HBEGF
Diseases of Immune System	2	34	0.003	0.009	0.132	9	14	IRAK4;NEMO
Diseases associated with the TLR signaling cascade	2	34	0.003	0.009	0.132	9	14	IRAK4;NEMO
MAPK family signaling cascades	5	325	0.024	0.011	0.132	3	86	PDGFB;PDGFA;STK4;HBEGF
Defective MMADHC causes methylmalonic aciduria and homocystinuria type cblD	1	3	0.000	0.012	0.132	1	1	PRDX1
IKBKB deficiency causes SCID	1	3	0.000	0.012	0.132	1	1	NEMO
Intracellular signaling by second messengers	5	341	0.025	0.013	0.132	1	106	PDGFB;PDGFA;IRAK4;HBEGF
CLEC7A (Dectin-1) signaling	3	120	0.009	0.014	0.132	4	45	NEMO;CCL17
MyD88 deficiency (TLR5)	1	4	0.000	0.016	0.132	1	1	IRAK4
Stimulation of the cell death response by PAK-2p34	1	4	0.000	0.016	0.132	1	4	CASP3
Activated TLR4 signalling	3	131	0.010	0.017	0.132	25	85	IRAK4;NEMO;TANK
IRAK4 deficiency (TLR5)	1	5	0.000	0.021	0.132	2	2	IRAK4
Defective MMACHC causes methylmalonic aciduria and homocystinuria type cblC	1	5	0.000	0.021	0.132	2	2	PRDX1
SMAC-mediated apoptotic response	1	5	0.000	0.021	0.132	2	6	CASP3
SMAC binds to IAPs	1	5	0.000	0.021	0.132	1	3	CASP3
SMAC-mediated dissociation of IAP:caspase complexes	1	5	0.000	0.021	0.132	1	3	CASP3
Cell surface interactions at the vascular wall	4	256	0.019	0.022	0.132	10	64	SELP;CD84;PECAM1
Toll Like Receptor 4 (TLR4) Cascade	3	145	0.011	0.022	0.132	25	94	IRAK4;NEMO;TANK
Misspliced LRP5 mutants have enhanced beta-catenin-dependent signaling	1	6	0.000	0.025	0.132	1	1	Dkk1
NADE modulates death signalling	1	6	0.000	0.025	0.132	1	3	CASP3
RAF/MAP kinase cascade	4	267	0.020	0.025	0.132	1	39	PDGFB;PDGFA;HBEGF
Non-integrin membrane-ECM interactions	2	61	0.005	0.027	0.132	1	22	PDGFB;PDGFA
MAPK1/MAPK3 signaling	4	274	0.020	0.027	0.132	1	46	PDGFB;PDGFA;HBEGF
Activation of caspases through apoptosome-mediated	1	7	0.001	0.029	0.132	1	2	CASP3
Cytochrome c-mediated apoptotic response	1	7	0.001	0.029	0.132	1	5	CASP3
Interleukin-20 family signaling	4	286	0.021	0.031	0.132	1	56	PDGFB;PDGFA;HBEGF
Dectin-1 mediated noncanonical NF-kB signaling	2	66	0.005	0.031	0.132	1	9	CCL17
IkBA variant leads to EDA-ID	1	8	0.001	0.033	0.132	1	1	NEMO
Activation of gene expression by SREBF (SREBP)	2	70	0.005	0.034	0.132	2	42	ANG1
PTK6 promotes HIF1A stabilization	1	9	0.001	0.037	0.132	5	5	HBEGF
IKBKG deficiency causes anhidrotic ectodermal dysplasia with immunodeficiency (EDA-ID) (via TLR)	1	9	0.001	0.037	0.132	1	1	NEMO
Apoptotic factor-mediated response	1	9	0.001	0.037	0.132	3	11	CASP3
Semaphorin interactions	2	73	0.005	0.037	0.132	15	40	STK4;PLXNA4
Gene and protein expression by JAK-STAT signaling after Interleukin-12 stimulation	2	74	0.005	0.038	0.132	1	36	SOD2
Uptake and function of diphtheria toxin	1	10	0.001	0.041	0.132	4	5	HBEGF
POU5F1 (OCT4), SOX2, NANOG repress genes related to differentiation	1	10	0.001	0.041	0.132	1	7	Dkk1
Toll-Like Receptors Cascades	3	185	0.014	0.042	0.132	53	180	IRAK4;NEMO;TANK
Disease	11	1502	0.111	0.042	0.132	20	905	PRDX1;PDGFB;PDGFA;IRAK4;SOD2;Dkk1;NEMO;HBEGF
Diseases of signal transduction	5	466	0.034	0.044	0.132	2	297	PDGFB;PDGFA;Dkk1;HBEGF
Apoptotic cleavage of cell adhesion proteins	1	11	0.001	0.045	0.132	5	10	CASP3
Extracellular matrix organization	4	329	0.024	0.048	0.132	3	318	CASP3;PDGFB;PECAM1;PDGFA
Caspase-mediated cleavage of cytoskeletal proteins	1	12	0.001	0.049	0.132	7	10	CASP3
EGFR Transactivation by Gastrin	1	12	0.001	0.049	0.132	4	6	HBEGF
Ligand-independent caspase activation via DCC	1	12	0.001	0.049	0.132	4	8	CASP3
Regulation of cholesterol biosynthesis by SREBP (SREBF)	2	86	0.006	0.050	0.132	2	52	ANG1

Full list of pathways referring to Figure 5.6, p value is <0.05 (List obtained from Reactome)

Appendix J: The regulation of PI3K/AKT signalling

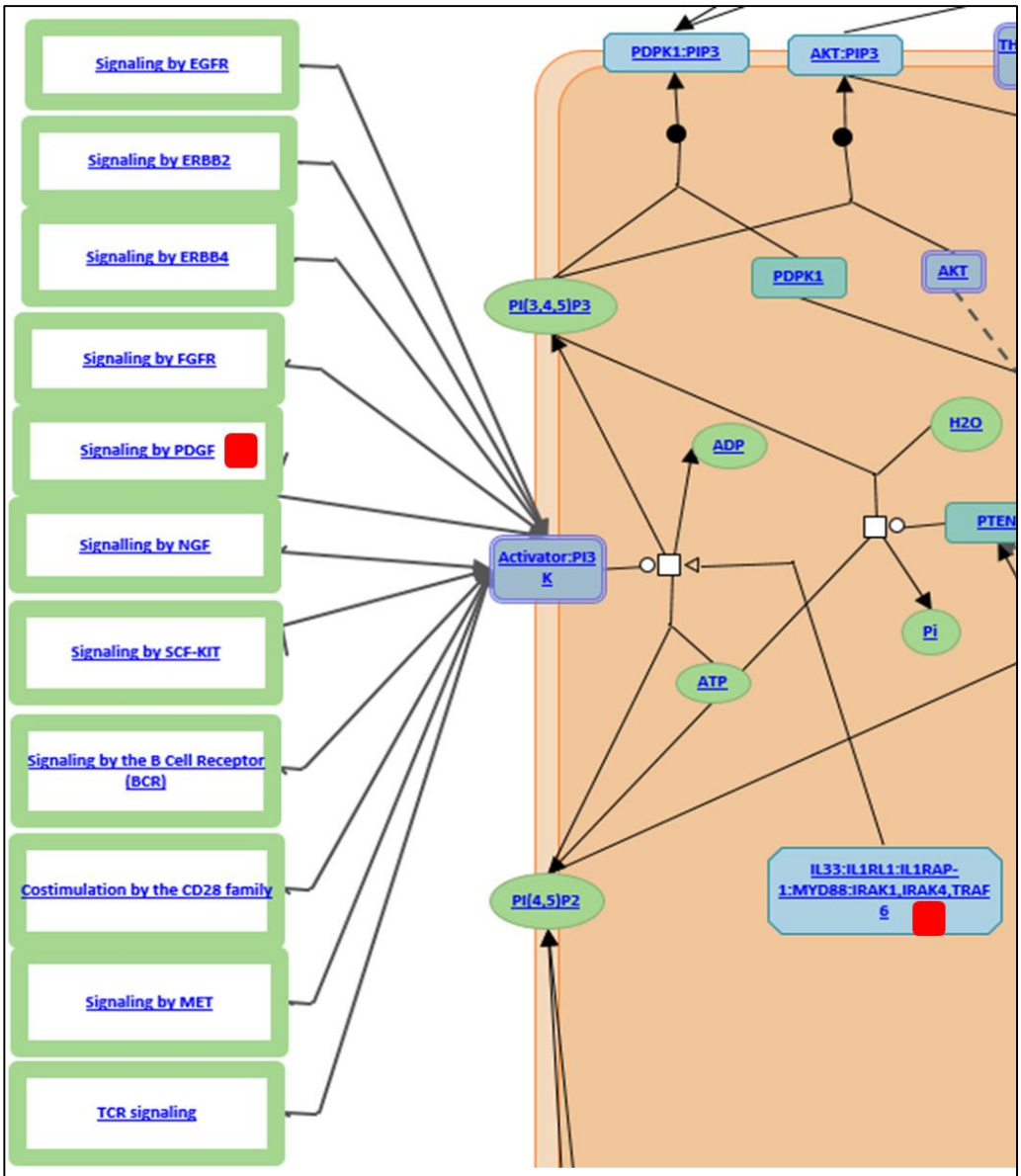

PDGFB, PDGFA and IRAK4 contribute to the PI3K signalling pathway. Red square indicates upregulation in DMARD non-responders compared to DMARD naïve and responder patients.

Appendix K: Downregulation of CXCL1 by IL-10

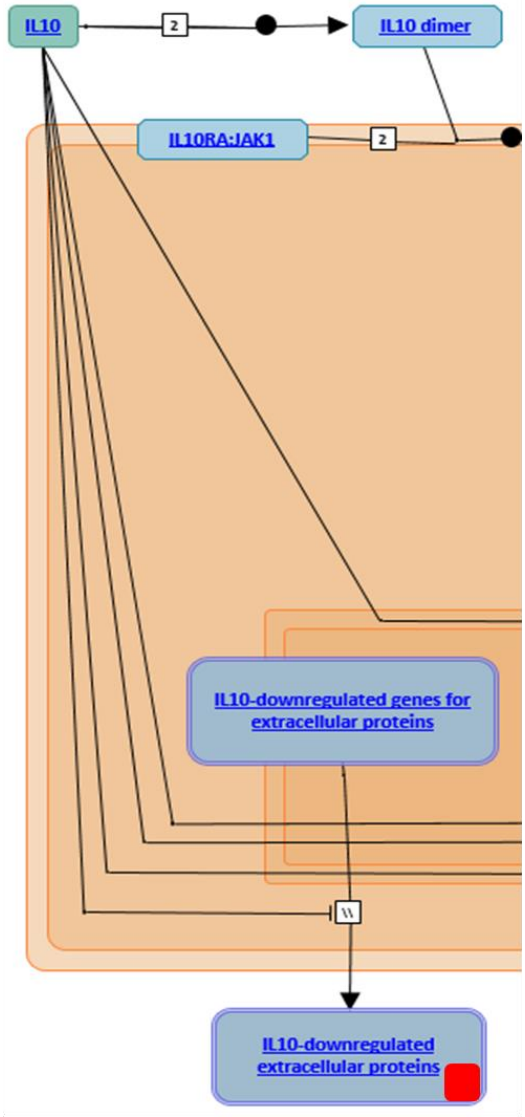

IL-10 signalling leads to the downregulation of several proteins including CXCL1. Red square indicates upregulation in DMARD non-responders compared to DMARD naïve and responder patients.

Appendix L: Involvement of NEMO in IL17RA signalling

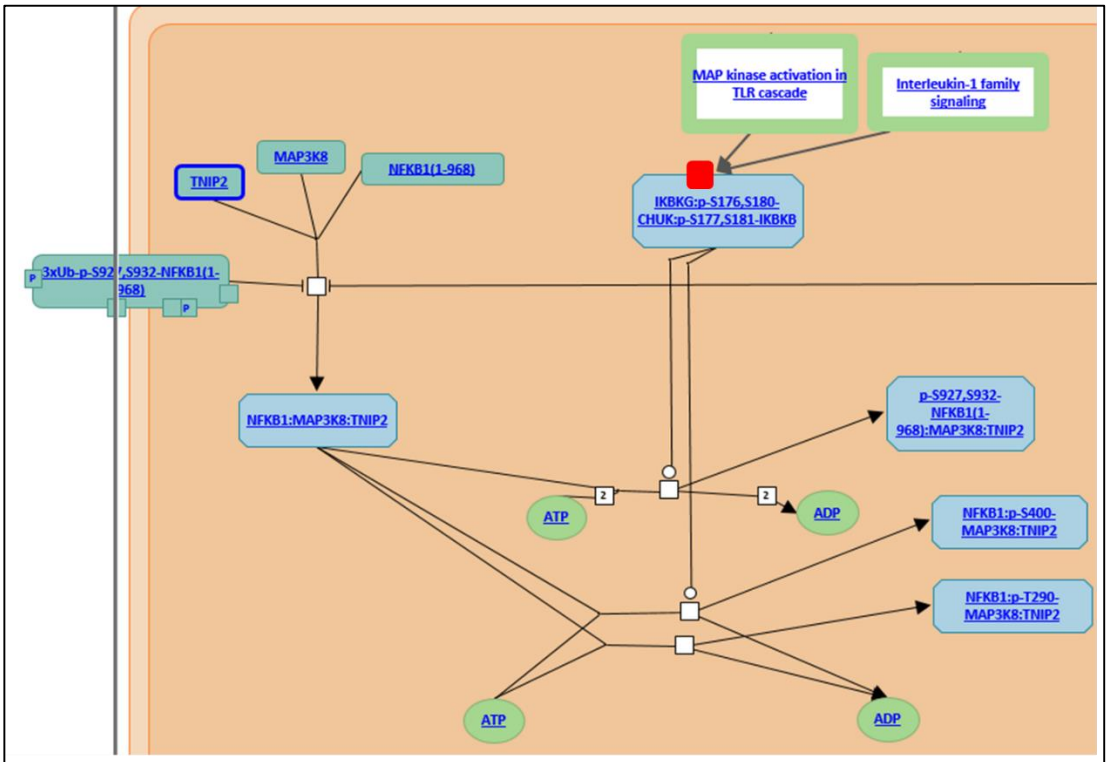

The involvement of NEMO in IL17RA signalling via the NFκB pathway. Red square indicates upregulation in DMARD non-responders compared to DMARD naïve and responder patients.

Appendix M: CASP-3/STK4 interaction

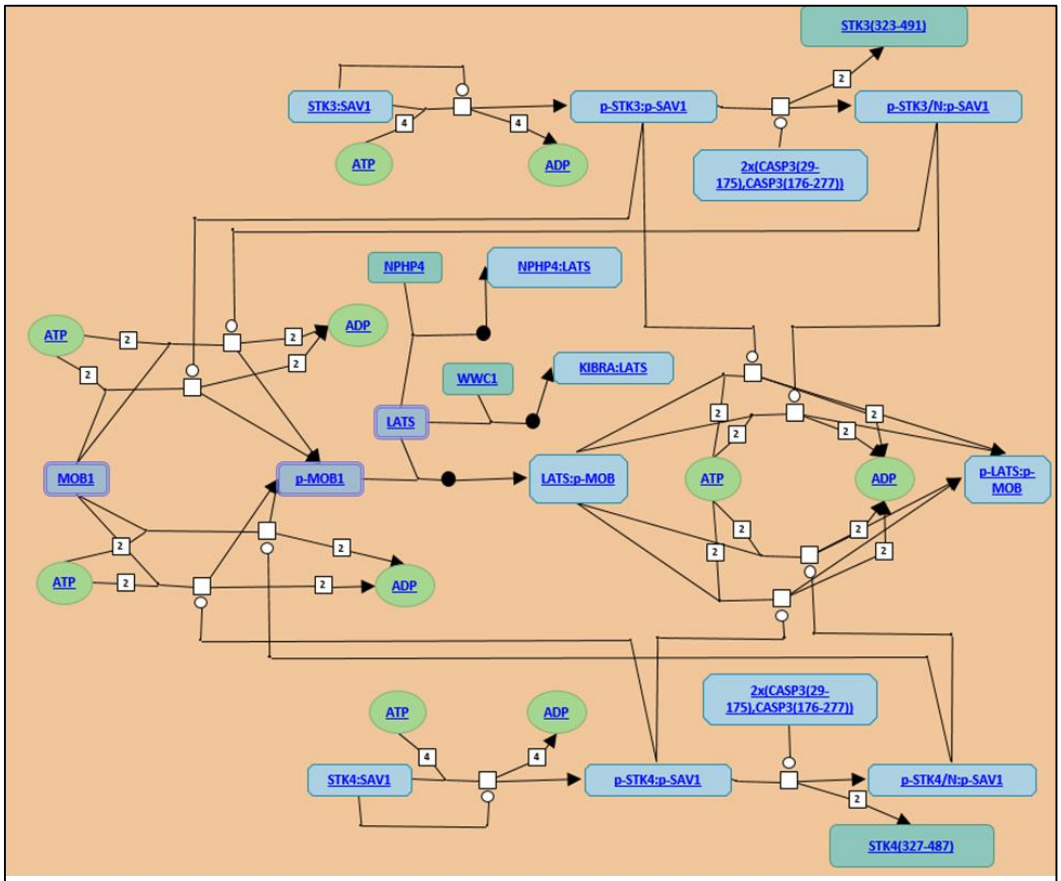

CASP-3 cleaves STK4, involved in the Hippo pathway – regulating pathway of cell proliferation and apoptosis. (Figure from Reactome).

Appendix N: Transport of MHCII by DCTN1

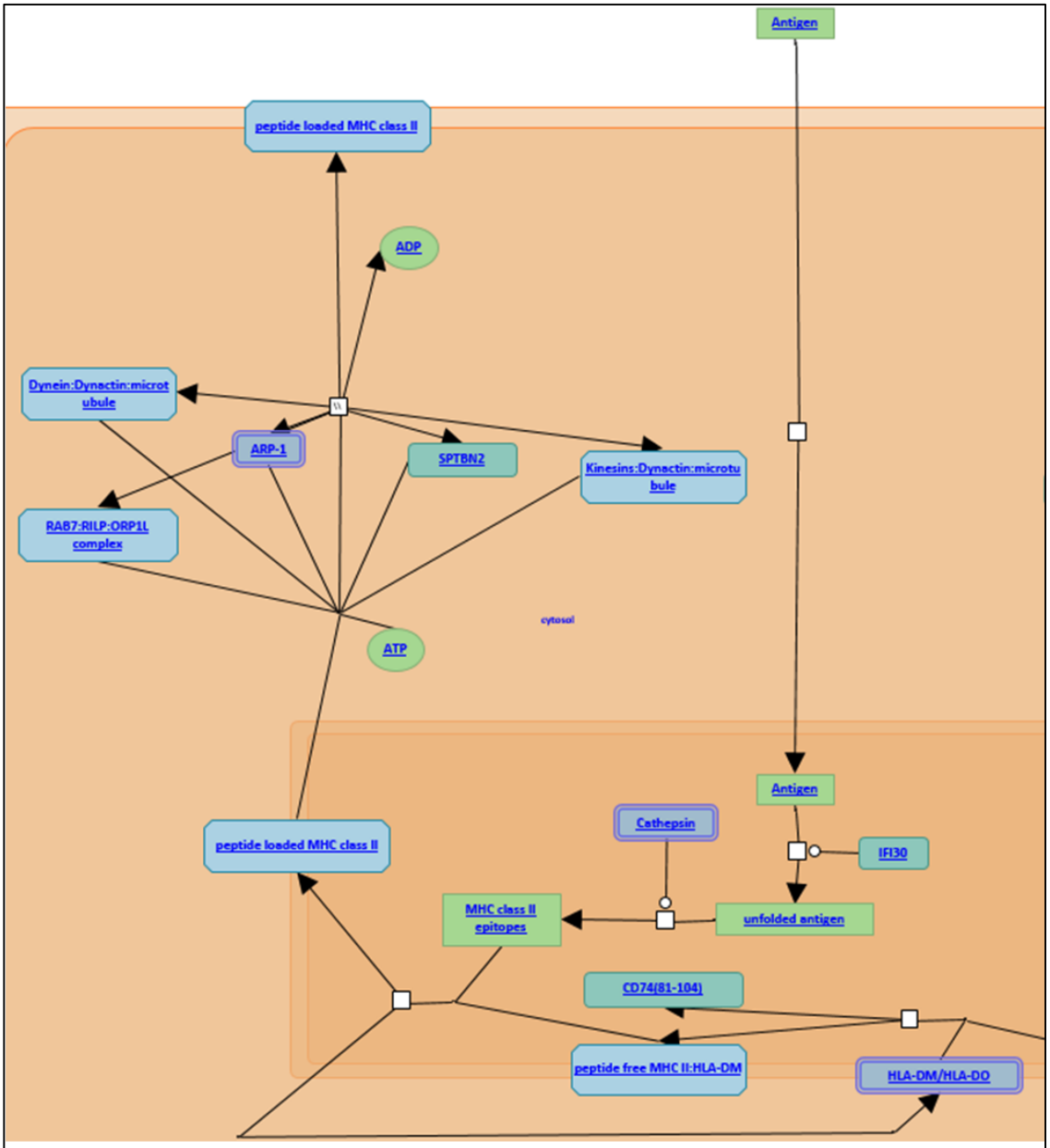

DCTN1 (Dynactin) is involved in transportation of MHC II molecules to the surface of the cell.

(Figure from Reactome).

Appendix O: Non-canonical NFκB signalling

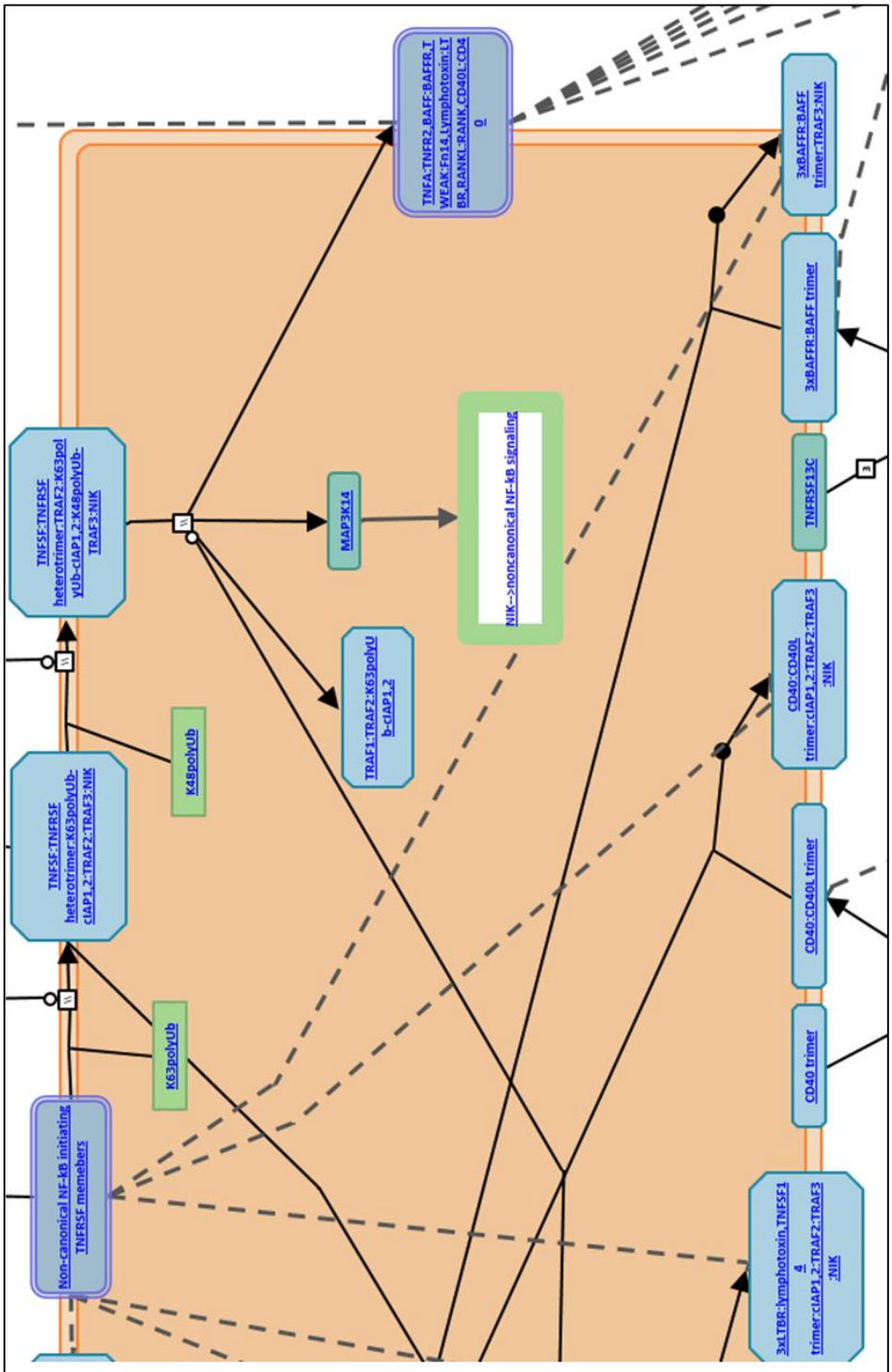

CD40 binds CD40L, which is involved in NFκB non-canonical signalling and therefore cytokine production.

Appendix P: Stability assessment of βactin housekeeping gene

Raw Ct values

βactin Ct value	Unstimulated Day 1	Unstimulated Day 2	LPS stimulated (200ng/ml) Day 2
1	18.14	17.65	18.82
2	18.13	17.65	18.76
3	17.99	18.26	18.13
4	17.87	18.09	18.1

NormFinder stability assessment

βactin	Stability value	Standard error
1	0.020	0.013
2	0.018	0.013
3	0.022	0.014
4	0.016	0.013

βactin stability was found to exhibit acceptable stability values (<0.05) which were similar across unstimulated control cells and LPS stimulated cells. Stability was assessed using NormFinder software.

References

Ai, W., Li, H., Song, N., Li, L. and Chen, H. (2013) Optimal method to stimulate cytokine production and its use in immunotoxicity assessment. *International Journal of Environmental Research and Public Health,* 10(9), 3834-3842.

Alavi, A. and Axford, J.S. (2006) The pivotal nature of sugars in normal physiology and disease. *Wiener Medizinische Wochenschrift (1946),* 156(1-2), 19-33.

Alavi, A. and Axford, J.S. (2008) Glyco-biomarkers: potential determinants of cellular physiology and pathology. *Disease Markers,* 25(4-5), 193-205.

Alberts, B. and Johnson, A. (2002) T Cells and MHC Proteins. *In:* Anon.*Biology of the Cell. 4th edition.* 4th ed. New York: Garland Science,

Aletaha, D. and Smolen, J.S. (2011) Joint damage in rheumatoid arthritis progresses in remission according to the Disease Activity Score in 28 joints and is driven by residual swollen joints. *Arthritis and Rheumatism,* 63(12), 3702-3711.

Alpizar-Rodriguez, D., Pluchino, N., Canny, G., Gabay, C. and Finckh, A. (2017) The role of female hormonal factors in the development of rheumatoid arthritis. *Rheumatology (Oxford, England),* 56(8), 1254-1263.

Alturfan, A.A., Uslu, E., Alturfan, E.E., Hatemi, G., Fresko, I. and Kokoglu, E. (2007) Increased serum sialic acid levels in primary osteoarthritis and inactive rheumatoid arthritis. *The Tohoku Journal of Experimental Medicine,* 213(3), 241-248.

Alves, J.D., Marinho, A. and Serra, M.J. (2011) Tocilizumab: is there life beyond anti-TNF blockade? *International Journal of Clinical Practice,* 65(4), 508-513.

Alzabin, S. and Williams, R.O. (2011) Effector T cells in rheumatoid arthritis: lessons from animal models. *FEBS Letters,* 585(23), 3649-3659.

American College of Rheumatology and European League Against Rheumatism. (2010) *
2010 ACR/EULAR Classification
Criteria for Rheumatoid Arthritis* Available at: https://www.eular.org/myUploadData/files/RA%20Class%20Slides%20ACR_Web.pdf

Amos, C.I., Chen, W.V., Remmers, E., Siminovitch, K.A., Seldin, M.F., Criswell, L.A., Lee, A.T., John, S., Shephard, N.D., Worthington, J., Cornelis, F., Plenge, R.M., Begovich, A.B., Dyer, T.D., Kastner, D.L. and Gregersen, P.K. (2007) Data for Genetic Analysis Workshop (GAW) 15 Problem 2, genetic causes of rheumatoid arthritis and associated traits. *BMC Proceedings,* 1 Suppl 1, S3.

Ancuta, P., Rao, R., Moses, A., Mehle, A., Shaw, S.K., Luscinskas, F.W. and Gabuzda, D. (2003) Fractalkine preferentially mediates arrest and migration of CD16+ monocytes. *The Journal of Experimental Medicine,* 197(12), 1701-1707.

Angata, T., Hayakawa, T., Yamanaka, M., Varki, A. and Nakamura, M. (2006) Discovery of Siglec-14, a novel sialic acid receptor undergoing concerted evolution with Siglec-5 in primates. *FASEB Journal : Official Publication of the Federation of American Societies for Experimental Biology,* 20(12), 1964-1973.

Antero, D.C., Parra, A.G., Miyazaki, F.H., Gehlen, M. and Skare, T.L. (2011) Secondary Sjogren's syndrome and disease activity of rheumatoid arthritis. *Revista Da Associacao Medica Brasileira (1992),* 57(3), 319-322.

Anthony, R.M., Nimmerjahn, F., Ashline, D.J., Reinhold, V.N., Paulson, J.C. and Ravetch, J.V. (2008) Recapitulation of IVIG anti-inflammatory activity with a recombinant IgG Fc. *Science (New York, N.Y.),* 320(5874), 373-376.

Appel, H., Wu, P., Scheer, R., Kedor, C., Sawitzki, B., Thiel, A., Radbruch, A., Sieper, J. and Syrbe, U. (2011) Synovial and peripheral blood CD4+FoxP3+ T cells in spondyloarthritis. *The Journal of Rheumatology,* 38(11), 2445-2451.

Apweiler, R., Hermjakob, H. and Sharon, N. (1999) On the frequency of protein glycosylation, as deduced from analysis of the SWISS-PROT database. *Biochimica Et Biophysica Acta,* 1473(1), 4-8.

Ardman, B., Sikorski, M.A., Settles, M. and Staunton, D.E. (1990) Human immunodeficiency virus type 1-infected individuals make autoantibodies that bind to CD43 on normal thymic lymphocytes. *The Journal of Experimental Medicine,* 172(4), 1151-1158.

Arend, W.P. and Firestein, G.S. (2012) Pre-rheumatoid arthritis: predisposition and transition to clinical synovitis. *Nature Reviews.Rheumatology,* 8(10), 573-586.

Artifoni, M., Rothschild, P.R., Brezin, A., Guillevin, L. and Puechal, X. (2014) Ocular inflammatory diseases associated with rheumatoid arthritis. *Nature Reviews.Rheumatology,* 10(2), 108-116.

Ates, A., Kinikli, G., Turgay, M. and Duman, M. (2004) Serum-soluble selectin levels in patients with rheumatoid arthritis and systemic sclerosis. *Scandinavian Journal of Immunology,* 59(3), 315-320.

Auffray, C., Sieweke, M.H. and Geissmann, F. (2009) Blood monocytes: development, heterogeneity, and relationship with dendritic cells. *Annual Review of Immunology,* 27, 669-692.

Avina-Zubieta, J.A., Choi, H.K., Sadatsafavi, M., Etminan, M., Esdaile, J.M. and Lacaille, D. (2008) Risk of cardiovascular mortality in patients with rheumatoid arthritis: a meta-analysis of observational studies. *Arthritis and Rheumatism,* 59(12), 1690-1697.

Axelsson, B., Youseffi-Etemad, R., Hammarstrom, S. and Perlmann, P. (1988) Induction of aggregation and enhancement of proliferation and IL-2 secretion in

human T cells by antibodies to CD43. *Journal of Immunology (Baltimore, Md.: 1950),* 141(9), 2912-2917.

Aya, K., Alhawagri, M., Hagen-Stapleton, A., Kitaura, H., Kanagawa, O. and Novack, D.V. (2005) NF-(kappa)B-inducing kinase controls lymphocyte and osteoclast activities in inflammatory arthritis. *The Journal of Clinical Investigation,* 115(7), 1848-1854.

Bakker, M.F., Jacobs, J.W., Verstappen, S.M. and Bijlsma, J.W. (2007) Tight control in the treatment of rheumatoid arthritis: efficacy and feasibility. *Annals of the Rheumatic Diseases,* 66 Suppl 3, iii56-60.

Balakrishnan, L., Bhattacharjee, M., Ahmad, S., Nirujogi, R.S., Renuse, S., Subbannayya, Y., Marimuthu, A., Srikanth, S.M., Raju, R., Dhillon, M., Kaur, N., Jois, R., Vasudev, V., Ramachandra, Y., Sahasrabuddhe, N.A., Prasad, T., Mohan, S., Gowda, H., Shankar, S. and Pandey, A. (2014) Differential proteomic analysis of synovial fluid from rheumatoid arthritis and osteoarthritis patients. *Clinical Proteomics,* 11(1), 1-0275-11-1.

Barr, T.A., Shen, P., Brown, S., Lampropoulou, V., Roch, T., Lawrie, S., Fan, B., O'Connor, R.A., Anderton, S.M., Bar-Or, A., Fillatreau, S. and Gray, D. (2012) B cell depletion therapy ameliorates autoimmune disease through ablation of IL-6-producing B cells. *The Journal of Experimental Medicine,* 209(5), 1001-1010.

Baud, V. and Karin, M. (2001) Signal transduction by tumor necrosis factor and its relatives. *Trends in Cell Biology,* 11(9), 372-377.

Baum, M.K., Rafie, C., Sales, S., Lai, S., Duan, R., Jayaweera, D.T., Page, J.B. and Campa, A. (2008) C-reactive protein: a poor marker of cardiovascular disease risk in HIV+ populations with a high prevalence of elevated serum transaminases. *International Journal of STD & AIDS,* 19(6), 410-413.

Bax, M., Huizinga, T.W. and Toes, R.E. (2014) The pathogenic potential of autoreactive antibodies in rheumatoid arthritis. *Seminars in Immunopathology,* 36(3), 313-325.

Beaulieu, A.D. and McColl, S.R. (1994) Differential expression of two major cytokines produced by neutrophils, interleukin-8 and the interleukin-1 receptor antagonist, in neutrophils isolated from the synovial fluid and peripheral blood of patients with rheumatoid arthritis. *Arthritis and Rheumatism,* 37(6), 855-859.

Begovich, A.B., Carlton, V.E., Honigberg, L.A., Schrodi, S.J., Chokkalingam, A.P., Alexander, H.C., Ardlie, K.G., Huang, Q., Smith, A.M., Spoerke, J.M., Conn, M.T., Chang, M., Chang, S.Y., Saiki, R.K., Catanese, J.J., Leong, D.U., Garcia, V.E., McAllister, L.B., Jeffery, D.A., Lee, A.T., Batliwalla, F., Remmers, E., Criswell, L.A., Seldin, M.F., Kastner, D.L., Amos, C.I., Sninsky, J.J. and Gregersen, P.K. (2004) A missense single-nucleotide polymorphism in a gene encoding a protein tyrosine phosphatase

(PTPN22) is associated with rheumatoid arthritis. *American Journal of Human Genetics,* 75(2), 330-337.

Berk, M., Williams, L.J., Jacka, F.N., O'Neil, A., Pasco, J.A., Moylan, S., Allen, N.B., Stuart, A.L., Hayley, A.C., Byrne, M.L. and Maes, M. (2013) So depression is an inflammatory disease, but where does the inflammation come from? *BMC Medicine,* 11, 200-7015-11-200.

Berner, B., Wolf, G., Hummel, K.M., Muller, G.A. and Reuss-Borst, M.A. (2000) Increased expression of CD40 ligand (CD154) on CD4+ T cells as a marker of disease activity in rheumatoid arthritis. *Annals of the Rheumatic Diseases,* 59(3), 190-195.

Bettelli, E., Dastrange, M. and Oukka, M. (2005) Foxp3 interacts with nuclear factor of activated T cells and NF-kappa B to repress cytokine gene expression and effector functions of T helper cells. *Proceedings of the National Academy of Sciences of the United States of America,* 102(14), 5138-5143.

Beydoun, H.A., el-Amin, R., McNeal, M., Perry, C. and Archer, D.F. (2013) Reproductive history and postmenopausal rheumatoid arthritis among women 60 years or older: Third National Health and Nutrition Examination Survey. *Menopause (New York, N.Y.),* 20(9), 930-935.

Biesen, R., Demir, C., Barkhudarova, F., Grun, J.R., Steinbrich-Zollner, M., Backhaus, M., Haupl, T., Rudwaleit, M., Riemekasten, G., Radbruch, A., Hiepe, F., Burmester, G.R. and Grutzkau, A. (2008) Sialic acid-binding Ig-like lectin 1 expression in inflammatory and resident monocytes is a potential biomarker for monitoring disease activity and success of therapy in systemic lupus erythematosus. *Arthritis and Rheumatism,* 58(4), 1136-1145.

Bjornadal, L., Baecklund, E., Yin, L., Granath, F., Klareskog, L. and Ekbom, A. (2002) Decreasing mortality in patients with rheumatoid arthritis: results from a large population based cohort in Sweden, 1964-95. *The Journal of Rheumatology,* 29(5), 906-912.

Blackburn, W.D.,Jr. (1994) Validity of acute phase proteins as markers of disease activity. *The Journal of Rheumatology.Supplement,* 42, 9-13.

Boechat Nde, O., Ogusku, M.M., Boechat, A.L. and Sadahiro, A. (2012) Interaction between smoking and HLA-DRB1*04 gene is associated with a high cardiovascular risk in Brazilian Amazon patients with rheumatoid arthritis. *PloS One,* 7(8), e41588.

Bonelli, M., Goschl, L., Bluml, S., Karonitsch, T., Hirahara, K., Ferner, E., Steiner, C.W., Steiner, G., Smolen, J.S. and Scheinecker, C. (2016) Abatacept (CTLA-4Ig) treatment reduces T cell apoptosis and regulatory T cell suppression in patients with rheumatoid arthritis. *Rheumatology (Oxford, England),* 55(4), 710-720.

Brancaccio, M., Guazzone, S., Menini, N., Sibona, E., Hirsch, E., De Andrea, M., Rocchi, M., Altruda, F., Tarone, G. and Silengo, L. (1999) Melusin is a new muscle-specific

interactor for beta(1) integrin cytoplasmic domain. *The Journal of Biological Chemistry,* 274(41), 29282-29288.

Bresnihan, B. (1999) Pathogenesis of joint damage in rheumatoid arthritis. *The Journal of Rheumatology,* 26(3), 717-719.

Bugatti, S., Vitolo, B., Caporali, R., Montecucco, C. and Manzo, A. (2014) B cells in rheumatoid arthritis: from pathogenic players to disease biomarkers. *BioMed Research International,* 2014, 681678.

Cabrera-Marroquin, R., Contreras-Yanez, I., Alcocer-Castillejos, N. and Pascual-Ramos, V. (2014) Major depressive episodes are associated with poor concordance with therapy in rheumatoid arthritis patients: the impact on disease outcomes. *Clinical and Experimental Rheumatology,* 32(6), 904-913.

Cairns, A.P., Crockard, A.D. and Bell, A.L. (2002) The CD14+ CD16+ monocyte subset in rheumatoid arthritis and systemic lupus erythematosus. *Rheumatology International,* 21(5), 189-192.

Cao, D., Malmstrom, V., Baecher-Allan, C., Hafler, D., Klareskog, L. and Trollmo, C. (2003) Isolation and functional characterization of regulatory CD25brightCD4+ T cells from the target organ of patients with rheumatoid arthritis. *European Journal of Immunology,* 33(1), 215-223.

Caporali, R., Caprioli, M., Bobbio-Pallavicini, F., Bugatti, S. and Montecucco, C. (2009) Long term treatment of rheumatoid arthritis with rituximab. *Autoimmunity Reviews,* 8(7), 591-594.

Caramalho, I., Lopes-Carvalho, T., Ostler, D., Zelenay, S., Haury, M. and Demengeot, J. (2003) Regulatory T cells selectively express toll-like receptors and are activated by lipopolysaccharide. *The Journal of Experimental Medicine,* 197(4), 403-411.

Caramelo, J.J. and Parodi, A.J. (2007) How sugars convey information on protein conformation in the endoplasmic reticulum. *Seminars in Cell & Developmental Biology,* 18(6), 732-742.

Carson, D.A., Chen, P.P., Fox, R.I., Kipps, T.J., Jirik, F., Goldfien, R.D., Silverman, G., Radoux, V. and Fong, S. (1987) Rheumatoid factor and immune networks. *Annual Review of Immunology,* 5, 109-126.

Chabaud, M., Garnero, P., Dayer, J.M., Guerne, P.A., Fossiez, F. and Miossec, P. (2000) Contribution of interleukin 17 to synovium matrix destruction in rheumatoid arthritis. *Cytokine,* 12(7), 1092-1099.

Chambers, R.E., MacFarlane, D.G., Whicher, J.T. and Dieppe, P.A. (1983) Serum amyloid-A protein concentration in rheumatoid arthritis and its role in monitoring disease activity. *Annals of the Rheumatic Diseases,* 42(6), 665-667.

Chara, L., Sanchez-Atrio, A., Perez, A., Cuende, E., Albarran, F., Turrion, A., Chevarria, J., Del Barco, A., Sanchez, M.A., Monserrat, J., Prieto, A., de la Hera, A., Sanz, I., Diaz, D. and Alvarez-Mon, M. (2015) The number of circulating monocytes as biomarkers of the clinical response to methotrexate in untreated patients with rheumatoid arthritis. *Journal of Translational Medicine,* 13(1), 2.

Chara, L., Sanchez-Atrio, A., Perez, A., Cuende, E., Albarran, F., Turrion, A., Chevarria, J., Sanchez, M.A., Monserrat, J., de la Hera, A., Prieto, A., Sanz, I., Diaz, D. and Alvarez-Mon, M. (2012) Monocyte populations as markers of response to adalimumab plus MTX in rheumatoid arthritis. *Arthritis Research & Therapy,* 14(4), R175.

Charpin, C., Arnoux, F., Martin, M., Toussirot, E., Lambert, N., Balandraud, N., Wendling, D., Diot, E., Roudier, J. and Auger, I. (2013) New autoantibodies in early rheumatoid arthritis. *Arthritis Research & Therapy,* 15(4), R78.

Chen, M.H., Chen, M.H., Liu, C.Y., Tsai, C.Y., Huang, D.F., Lin, H.Y., Lee, M.H. and Huang, Y.H. (2017) Hepatitis B Virus Reactivation in Rheumatoid Arthritis Patients Undergoing Biologics Treatment. *The Journal of Infectious Diseases,* 215(4), 566-573.

Chen, Y.S., Yan, W., Geczy, C.L., Brown, M.A. and Thomas, R. (2009) Serum levels of soluble receptor for advanced glycation end products and of S100 proteins are associated with inflammatory, autoantibody, and classical risk markers of joint and vascular damage in rheumatoid arthritis. *Arthritis Research & Therapy,* 11(2), R39.

Chien, C.H. and Chiang, B.L. (2017) Regulatory T cells induced by B cells: a novel subpopulation of regulatory T cells. *Journal of Biomedical Science,* 24(1), 86-017-0391-3.

Chrostek, L., Cylwik, B., Gindzienska-Sieskiewicz, E., Gruszewska, E., Szmitkowski, M. and Sierakowski, S. (2014) Sialic acid level reflects the disturbances of glycosylation and acute-phase reaction in rheumatic diseases. *Rheumatology International,* 34(3), 393-399.

Collins, B.E., Blixt, O., Han, S., Duong, B., Li, H., Nathan, J.K., Bovin, N. and Paulson, J.C. (2006) High-affinity ligand probes of CD22 overcome the threshold set by cis ligands to allow for binding, endocytosis, and killing of B cells. *Journal of Immunology (Baltimore, Md.: 1950),* 177(5), 2994-3003.

Collins, E.S., Galligan, M.C., Saldova, R., Adamczyk, B., Abrahams, J.L., Campbell, M.P., Ng, C.T., Veale, D.J., Murphy, T.B., Rudd, P.M. and Fitzgerald, O. (2013) Glycosylation status of serum in inflammatory arthritis in response to anti-TNF treatment. *Rheumatology (Oxford, England),* 52(9), 1572-1582.

Conway, R., Low, C., Coughlan, R.J., O'Donnell, M.J. and Carey, J.J. (2015) Methotrexate use and risk of lung disease in psoriasis, psoriatic arthritis, and inflammatory bowel disease: systematic literature review and meta-analysis of randomised controlled trials. *BMJ (Clinical Research Ed.),* 350, h1269.

Cribbs, A.P., Kennedy, A., Penn, H., Amjadi, P., Green, P., Read, J.E., Brennan, F., Gregory, B. and Williams, R.O. (2015) Methotrexate Restores Regulatory T Cell Function Through Demethylation of the FoxP3 Upstream Enhancer in Patients With Rheumatoid Arthritis. *Arthritis & Rheumatology (Hoboken, N.J.),* 67(5), 1182-1192.

Cribbs, A.P., Kennedy, A., Penn, H., Read, J.E., Amjadi, P., Green, P., Syed, K., Manka, S.W., Brennan, F.M., Gregory, B. and Williams, R.O. (2014) Treg cell function in rheumatoid arthritis is compromised by ctla-4 promoter methylation resulting in a failure to activate the indoleamine 2,3-dioxygenase pathway. *Arthritis & Rheumatology (Hoboken, N.J.),* 66(9), 2344-2354.

Croce, A., Firuzi, O., Altieri, F., Eufemi, M., Agostino, R., Priori, R., Bombardieri, M., Alessandri, C., Valesini, G. and Saso, L. (2007) Effect of infliximab on the glycosylation of IgG of patients with rheumatoid arthritis. *Journal of Clinical Laboratory Analysis,* 21(5), 303-314.

Crocker, P.R. (2002) Siglecs: sialic-acid-binding immunoglobulin-like lectins in cell-cell interactions and signalling. *Current Opinion in Structural Biology,* 12(5), 609-615.

Crocker, P.R., Mucklow, S., Bouckson, V., McWilliam, A., Willis, A.C., Gordon, S., Milon, G., Kelm, S. and Bradfield, P. (1994) Sialoadhesin, a macrophage sialic acid binding receptor for haemopoietic cells with 17 immunoglobulin-like domains. *The EMBO Journal,* 13(19), 4490-4503.

Crocker, P.R., Paulson, J.C. and Varki, A. (2007) Siglecs and their roles in the immune system. *Nature Reviews.Immunology,* 7(4), 255-266.

Crofford, L.J. (2013) Use of NSAIDs in treating patients with arthritis. *Arthritis Research & Therapy,* 15 Suppl 3, S2.

Crofford, L.J., Lipsky, P.E., Brooks, P., Abramson, S.B., Simon, L.S. and van de Putte, L.B. (2000) Basic biology and clinical application of specific cyclooxygenase-2 inhibitors. *Arthritis and Rheumatism,* 43(1), 4-13.

Cronstein, B.N. (2005) Low-dose methotrexate: a mainstay in the treatment of rheumatoid arthritis. *Pharmacological Reviews,* 57(2), 163-172.

Cruz-Munoz, M.E., Salas-Vidal, E., Salaiza-Suazo, N., Becker, I., Pedraza-Alva, G. and Rosenstein, Y. (2003) The CD43 coreceptor molecule recruits the zeta-chain as part of its signaling pathway. *Journal of Immunology (Baltimore, Md.: 1950),* 171(4), 1901-1908.

Curtis, J.R., Westfall, A.O., Allison, J., Bijlsma, J.W., Freeman, A., George, V., Kovac, S.H., Spettell, C.M. and Saag, K.G. (2006) Population-based assessment of adverse events associated with long-term glucocorticoid use. *Arthritis and Rheumatism,* 55(3), 420-426.

Curtis, J.R., Xie, F., Yun, H., Saag, K.G., Chen, L. and Delzell, E. (2015) Risk of hospitalized infection among rheumatoid arthritis patients concurrently treated with a biologic agent and denosumab. *Arthritis & Rheumatology (Hoboken, N.J.),* 67(6), 1456-1464.

Cylwik, B., Chrostek, L., Gindzienska-Sieskiewicz, E., Sierakowski, S. and Szmitkowski, M. (2010) Relationship between serum acute-phase proteins and high disease activity in patients with rheumatoid arthritis. *Advances in Medical Sciences,* 55(1), 80-85.

Dahl, M.G., Gregory, M.M. and Scheuer, P.J. (1971) Liver damage due to methotrexate in patients with psoriasis. *British Medical Journal,* 1(5750), 625-630.

Dai, S., Hirayama, T., Abbas, S. and Abu-Amer, Y. (2004) The IkappaB kinase (IKK) inhibitor, NEMO-binding domain peptide, blocks osteoclastogenesis and bone erosion in inflammatory arthritis. *The Journal of Biological Chemistry,* 279(36), 37219-37222.

Darwich, L., Coma, G., PeÃ±a, R., Bellido, R., Blanco, E.J.J., Este, J.A., Borras, F.E., Clotet, B., Ruiz, L., Rosell, A., Andreo, F., Parkhouse, R.M.E. and Bofill, M. (2009) Secretion of interferon-Î³ by human macrophages demonstrated at the single-cell level after costimulation with interleukin (IL)-12 plus IL-18. *Immunology,* 126(3), 386-393.

Dasuri, K., Antonovici, M., Chen, K., Wong, K., Standing, K., Ens, W., El-Gabalawy, H. and Wilkins, J.A. (2004) The synovial proteome: analysis of fibroblast-like synoviocytes. *Arthritis Research & Therapy,* 6(2), R161-8.

Datta, S.K. and Kalled, S.L. (1997) CD40-CD40 ligand interaction in autoimmune disease. *Arthritis and Rheumatism,* 40(10), 1735-1745.

Davis, J.M. and Matteson, E.L. (2012) My Treatment Approach to Rheumatoid Arthritis. *Mayo Clinic Proceedings,* 87(7), 659-673.

de Bruijne-Admiraal, L.G., Modderman, P.W., Von dem Borne, A.E. and Sonnenberg, A. (1992) P-selectin mediates Ca(2+)-dependent adhesion of activated platelets to many different types of leukocytes: detection by flow cytometry. *Blood,* 80(1), 134-142.

de Pablo, P., Dietrich, T. and McAlindon, T.E. (2008) Association of periodontal disease and tooth loss with rheumatoid arthritis in the US population. *The Journal of Rheumatology,* 35(1), 70-76.

de Vries, R. (2011) Genetics of rheumatoid arthritis: time for a change! *Current Opinion in Rheumatology,* 23(3), 227-232.

Delputte, P.L., Van Gorp, H., Favoreel, H.W., Hoebeke, I., Delrue, I., Dewerchin, H., Verdonck, F., Verhasselt, B., Cox, E. and Nauwynck, H.J. (2011) Porcine Sialoadhesin

(CD169/Siglec-1) Is an Endocytic Receptor that Allows Targeted Delivery of Toxins and Antigens to Macrophages. *PLoS ONE,* 6(2), . doi:10.1371/journal.pone.0016827.

Dissick, A., Redman, R.S., Jones, M., Rangan, B.V., Reimold, A., Griffiths, G.R., Mikuls, T.R., Amdur, R.L., Richards, J.S. and Kerr, G.S. (2010) Association of periodontitis with rheumatoid arthritis: a pilot study. *Journal of Periodontology,* 81(2), 223-230.

Doran, M.F., Crowson, C.S., Pond, G.R., O'Fallon, W.M. and Gabriel, S.E. (2002) Frequency of infection in patients with rheumatoid arthritis compared with controls: a population-based study. *Arthritis and Rheumatism,* 46(9), 2287-2293.

Dougados, M., Soubrier, M., Antunez, A., Balint, P., Balsa, A., Buch, M.H., Casado, G., Detert, J., El-Zorkany, B., Emery, P., Hajjaj-Hassouni, N., Harigai, M., Luo, S.F., Kurucz, R., Maciel, G., Mola, E.M., Montecucco, C.M., McInnes, I., Radner, H., Smolen, J.S., Song, Y.W., Vonkeman, H.E., Winthrop, K. and Kay, J. (2014) Prevalence of comorbidities in rheumatoid arthritis and evaluation of their monitoring: results of an international, cross-sectional study (COMORA). *Annals of the Rheumatic Diseases,* 73(1), 62-68.

Doyle, M.K., Rahman, M.U., Frederick, B., Birbara, C.A., de Vries, D., Toedter, G., Wu, X., Chen, D., Ranganath, V.K., Westerman, M.E. and Furst, D.E. (2013) Effects of subcutaneous and intravenous golimumab on inflammatory biomarkers in patients with rheumatoid arthritis: results of a phase 1, randomized, open-label trial. *Rheumatology (Oxford, England),* 52(7), 1214-1219.

Dubreuil, M., Rho, Y.H., Man, A., Zhu, Y., Zhang, Y., Love, T.J., Ogdie, A., Gelfand, J.M. and Choi, H.K. (2014) Diabetes incidence in psoriatic arthritis, psoriasis and rheumatoid arthritis: a UK population-based cohort study. *Rheumatology (Oxford, England),* 53(2), 346-352.

Duhen, T., Duhen, R., Lanzavecchia, A., Sallusto, F. and Campbell, D.J. (2012) Functionally distinct subsets of human FOXP3+ Treg cells that phenotypically mirror effector Th cells. *Blood,* 119(19), 4430-4440.

Eakin, A.J., Bustard, M.J., McGeough, C.M., Ahmed, T., Bjourson, A.J. and Gibson, D.S. (2016) Siglec-1 and -2 as potential biomarkers in autoimmune disease. *Proteomics.Clinical Applications,* 10(6), 635-644.

Edwards, J.C., Szczepanski, L., Szechinski, J., Filipowicz-Sosnowska, A., Emery, P., Close, D.R., Stevens, R.M. and Shaw, T. (2004) Efficacy of B-cell-targeted therapy with rituximab in patients with rheumatoid arthritis. *The New England Journal of Medicine,* 350(25), 2572-2581.

Ehrenstein, M.R., Evans, J.G., Singh, A., Moore, S., Warnes, G., Isenberg, D.A. and Mauri, C. (2004) Compromised function of regulatory T cells in rheumatoid arthritis and reversal by anti-TNFalpha therapy. *The Journal of Experimental Medicine,* 200(3), 277-285.

Eleff, M., Franks, P.E., Wampler, G.L., Collins, J.M. and Goldmad, I.D. (1985) Analysis of "early" thymidine/inosine protection as an adjunct to methotrexate therapy. *Cancer Treat Rep,* 69(7-8), 867.

Ertenli, I., Kiraz, S., Arici, M., Haznedaroglu, I.C., Calguneri, M., Celik, I. and Kirazli, S. (1998) P-selectin as a circulating molecular marker in rheumatoid arthritis with thrombocytosis. *The Journal of Rheumatology,* 25(6), 1054-1058.

Estrada-Capetillo, L., Hernandez-Castro, B., Monsivais-Urenda, A., Alvarez-Quiroga, C., Layseca-Espinosa, E., Abud-Mendoza, C., Baranda, L., Urzainqui, A., Sanchez-Madrid, F. and Gonzalez-Amaro, R. (2013) Induction of Th17 lymphocytes and Treg cells by monocyte-derived dendritic cells in patients with rheumatoid arthritis and systemic lupus erythematosus. *Clinical & Developmental Immunology,* 2013, 584303.

Eudy, A.M., Vines, A.I., Dooley, M.A., Cooper, G.S. and Parks, C.G. (2014) Elevated C-reactive protein and self-reported disease activity in systemic lupus erythematosus. *Lupus,* 23(14), 1460-1467.

Fabregat, A., Jupe, S., Matthews, L., Sidiropoulos, K., Gillespie, M., Garapati, P., Haw, R., Jassal, B., Korninger, F., May, B., Milacic, M., Roca, C.D., Rothfels, K., Sevilla, C., Shamovsky, V., Shorser, S., Varusai, T., Viteri, G., Weiser, J., Wu, G., Stein, L., Hermjakob, H. and D'Eustachio, P. (2017) The Reactome Pathway Knowledgebase. *Nucleic Acids Research,*

Feelders, R.A., Vreugdenhil, G., de Jong, G., Swaak, A.J. and van Eijk, H.G. (1992) Transferrin microheterogeneity in rheumatoid arthritis. Relation with disease activity and anemia of chronic disease. *Rheumatology International,* 12(5), 195-199.

Fisher, B.A., Bang, S.Y., Chowdhury, M., Lee, H.S., Kim, J.H., Charles, P., Venables, P. and Bae, S.C. (2014) Smoking, the HLA-DRB1 shared epitope and ACPA fine-specificity in Koreans with rheumatoid arthritis: evidence for more than one pathogenic pathway linking smoking to disease. *Annals of the Rheumatic Diseases,* 73(4), 741-747.

Fonseca, J.E., Edwards, J.C., Blades, S. and Goulding, N.J. (2002) Macrophage subpopulations in rheumatoid synovium: reduced CD163 expression in CD4+ T lymphocyte-rich microenvironments. *Arthritis and Rheumatism,* 46(5), 1210-1216.

Fontenot, J.D., Rasmussen, J.P., Williams, L.M., Dooley, J.L., Farr, A.G. and Rudensky, A.Y. (2005) Regulatory T cell lineage specification by the forkhead transcription factor foxp3. *Immunity,* 22(3), 329-341.

Frosch, M., Strey, A., Vogl, T., Wulffraat, N.M., Kuis, W., Sunderkotter, C., Harms, E., Sorg, C. and Roth, J. (2000) Myeloid-related proteins 8 and 14 are specifically secreted during interaction of phagocytes and activated endothelium and are useful markers for monitoring disease activity in pauciarticular-onset juvenile rheumatoid arthritis. *Arthritis and Rheumatism,* 43(3), 628-637.

Fujishima, S., Hoffman, A.R., Vu, T., Kim, K.J., Zheng, H., Daniel, D., Kim, Y., Wallace, E.F., Larrick, J.W. and Raffin, T.A. (1993) Regulation of neutrophil interleukin 8 gene expression and protein secretion by LPS, TNF-alpha, and IL-1 beta. *Journal of Cellular Physiology,* 154(3), 478-485.

Furusawa, Y., Obata, Y., Fukuda, S., Endo, T.A., Nakato, G., Takahashi, D., Nakanishi, Y., Uetake, C., Kato, K., Kato, T., Takahashi, M., Fukuda, N.N., Murakami, S., Miyauchi, E., Hino, S., Atarashi, K., Onawa, S., Fujimura, Y., Lockett, T., Clarke, J.M., Topping, D.L., Tomita, M., Hori, S., Ohara, O., Morita, T., Koseki, H., Kikuchi, J., Honda, K., Hase, K. and Ohno, H. (2013) Commensal microbe-derived butyrate induces the differentiation of colonic regulatory T cells. *Nature,* 504(7480), 446-450.

Gabriel, S.E. and Michaud, K. (2009) Epidemiological studies in incidence, prevalence, mortality, and comorbidity of the rheumatic diseases. *Arthritis Research & Therapy,* 11(3), 229.

Garip, Y., Eser, F. and Bodur, H. (2016) Comorbidities in Turkish patients with rheumatoid arthritis: association with the health-related quality of life in terms of disease activity, functional and radiological status, severity of pain, and social and emotional functioning. *Acta Reumatologica Portuguesa,* 41(4), 344-349.

Gavin, M.A., Rasmussen, J.P., Fontenot, J.D., Vasta, V., Manganiello, V.C., Beavo, J.A. and Rudensky, A.Y. (2007) Foxp3-dependent programme of regulatory T-cell differentiation. *Nature,* 445(7129), 771-775.

Goekoop-Ruiterman, Y.P., de Vries-Bouwstra, J.K., Allaart, C.F., van Zeben, D., Kerstens, P.J., Hazes, J.M., Zwinderman, A.H., Ronday, H.K., Han, K.H., Westedt, M.L., Gerards, A.H., van Groenendael, J.H., Lems, W.F., van Krugten, M.V., Breedveld, F.C. and Dijkmans, B.A. (2008) Clinical and radiographic outcomes of four different treatment strategies in patients with early rheumatoid arthritis (the BeSt study): A randomized, controlled trial. *Arthritis and Rheumatism,* 58(2 Suppl), S126-35.

Greene, S., Watanabe, K., Braatz-Trulson, J. and Lou, L. (1995) Inhibition of dihydroorotate dehydrogenase by the immunosuppressive agent leflunomide. *Biochem Pharmacol,* 50(6), 861.

Gregersen, P.K., Silver, J. and Winchester, R.J. (1987) The shared epitope hypothesis. An approach to understanding the molecular genetics of susceptibility to rheumatoid arthritis. *Arthritis and Rheumatism,* 30(11), 1205-1213.

Grigor, C., Capell, H., Stirling, A., McMahon, A.D., Lock, P., Vallance, R., Kincaid, W. and Porter, D. (2004) Effect of a treatment strategy of tight control for rheumatoid arthritis (the TICORA study): a single-blind randomised controlled trial. *Lancet (London, England),* 364(9430), 263-269.

Grove, M.L., Hassell, A.B., Hay, E.M. and Shadforth, M.F. (2000) Adverse reactions to disease-modifying anti-rheumatic drugs in clinical practice. *Q J Med,* 94(6), 309.

Gruys, E., Toussaint, M.J., Niewold, T.A. and Koopmans, S.J. (2005) Acute phase reaction and acute phase proteins. *Journal of Zhejiang University.Science.B,* 6(11), 1045-1056.

Guo, W., Zhao, Y., Zhang, Z., Tan, N., Zhao, F., Ge, C., Liang, L., Jia, D., Chen, T., Yao, M., Li, J. and He, X. (2011) Disruption of xCT inhibits cell growth via the ROS/autophagy pathway in hepatocellular carcinoma. *Cancer Lett,* 312(1), 55.

Guo, H., Zheng, M., Zhang, K., Yang, F., Zhang, X., Han, Q., Chen, Z.N. and Zhu, P. (2016) Functional defects in CD4(+) CD25(high) FoxP3(+) regulatory cells in ankylosing spondylitis. *Scientific Reports,* 6, 37559.

Haas, C.S., Creighton, C.J., Pi, X., Maine, I., Koch, A.E., Haines, G.K., Ling, S., Chinnaiyan, A.M. and Holoshitz, J. (2006) Identification of genes modulated in rheumatoid arthritis using complementary DNA microarray analysis of lymphoblastoid B cell lines from disease-discordant monozygotic twins. *Arthritis and Rheumatism,* 54(7), 2047-2060.

Hamerman, J.A. and Lanier, L.L. (2006) Inhibition of immune responses by ITAM-bearing receptors. *Science's STKE : Signal Transduction Knowledge Environment,* 2006(320), re1.

Hartnell, A., Steel, J., Turley, H., Jones, M., Jackson, D.G. and Crocker, P.R. (2001) Characterization of human sialoadhesin, a sialic acid binding receptor expressed by resident and inflammatory macrophage populations. *Blood,* 97(1), 288-296.

Heinrich, P.C., Behrmann, I., Muller-Newen, G., Schaper, F. and Graeve, L. (1998) Interleukin-6-type cytokine signalling through the gp130/Jak/STAT pathway. *The Biochemical Journal,* 334 (Pt 2)(Pt 2), 297-314.

Heinrich, P.C., Castell, J.V. and Andus, T. (1990) Interleukin-6 and the acute phase response. *The Biochemical Journal,* 265(3), 621-636.

Heo, Y.J., Joo, Y.B., Oh, H.J., Park, M.K., Heo, Y.M., Cho, M.L., Kwok, S.K., Ju, J.H., Park, K.S., Cho, S.G., Park, S.H., Kim, H.Y. and Min, J.K. (2010) IL-10 suppresses Th17 cells and promotes regulatory T cells in the CD4+ T cell population of rheumatoid arthritis patients. *Immunology Letters,* 127(2), 150-156.

Hessian, P.A. and Fisher, L. (2001) The heterodimeric complex of MRP-8 (S100A8) and MRP-14 (S100A9). Antibody recognition, epitope definition and the implications for structure. *European Journal of Biochemistry / FEBS,* 268(2), 353-363.

Higai, K., Aoki, Y., Azuma, Y. and Matsumoto, K. (2005) Glycosylation of site-specific glycans of alpha1-acid glycoprotein and alterations in acute and chronic inflammation. *Biochimica Et Biophysica Acta,* 1725(1), 128-135.

Higashi, N., Wu, K., Gronhoj Larsen, C., Deleuran, M., Kawana, S., Yamamoto, K. and Thestrup-Pedersen, K. (2001) Expression and function of CD43 and CDw60 on T cells from patients with atopic dermatitis. *Acta Dermato-Venereologica,* 81(4), 263-267.

Hirabara, S., Takahashi, N., Fukaya, N., Miyake, H., Yabe, Y., Kaneko, A., Ito, T., Oguchi, T., Kida, D., Hirano, Y., Fujibayashi, T., Sugiura, F., Hayashi, M., Funahashi, K., Hanabayashi, M., Asai, S., Ishiguro, N. and Kojima, T. (2014) Clinical efficacy of abatacept, tocilizumab, and etanercept in Japanese rheumatoid arthritis patients with inadequate response to anti-TNF monoclonal antibodies. *Clinical Rheumatology,* 33(9), 1247-1254.

Hoffmeister, R.T. (1983) Methotrexate therapy in rheumatoid arthritis: 15 years experience. *Am.J.Med.,* 75(6A), 69.

Hori, S., Nomura, T. and Sakaguchi, S. (2003) Control of regulatory T cell development by the transcription factor Foxp3. *Science (New York, N.Y.),* 299(5609), 1057-1061.

Hrycaj, P., Sobieska, M., Mackiewicz, S. and Muller, W. (1993) Microheterogeneity of alpha 1-acid glycoprotein in early and established rheumatoid arthritis. *The Journal of Rheumatology,* 20(12), 2020-2024.

Huang, Q., Ma, Y., Adebayo, A. and Pope, R.M. (2007) Increased macrophage activation mediated through toll-like receptors in rheumatoid arthritis. *Arthritis and Rheumatism,* 56(7), 2192-2201.

Humbria, A., Diaz-Gonzalez, F., Campanero, M.R., Arroyo, A.G., Laffon, A., Gonzalez-Amaro, R. and Sanchez-Madrid, F. (1994) Expression of L-selectin, CD43, and CD44 in synovial fluid neutrophils from patients with inflammatory joint diseases. Evidence for a soluble form of L-selectin in synovial fluid. *Arthritis and Rheumatism,* 37(3), 342-348.

Ilic, V., Milosevic-Jovcic, N., Petrovic, S., Markovic, D., Stefanovic, G. and Ristic, T. (2008) Glycosylation of IgG B cell receptor (IgG BCR) in multiple myeloma: relationship between sialylation and the signal activity of IgG BCR. *Glycoconjugate Journal,* 25(4), 383-392.

Ingenbleek, Y. and Young, V. (1994) Transthyretin (prealbumin) in health and disease: nutritional implications. *Annual Review of Nutrition,* 14, 495-533.

Ip, S.C., Lin, S.W. and Lai, K.M. (2015) An evaluation of the performance of five extraction methods: Chelex(R) 100, QIAamp(R) DNA Blood Mini Kit, QIAamp(R) DNA Investigator Kit, QIAsymphony(R) DNA Investigator(R) Kit and DNA IQ. *Science & Justice : Journal of the Forensic Science Society,* 55(3), 200-208.

Isomura, I., Palmer, S., Grumont, R.J., Bunting, K., Hoyne, G., Wilkinson, N., Banerjee, A., Proietto, A., Gugasyan, R., Wu, L., McNally, A., Steptoe, R.J., Thomas, R., Shannon, M.F. and Gerondakis, S. (2009) c-Rel is required for the development of thymic

Foxp3+ CD4 regulatory T cells. *The Journal of Experimental Medicine,* 206(13), 3001-3014.

Jacobsson, L.T., Hanson, R.L., Knowler, W.C., Pillemer, S., Pettitt, D.J., McCance, D.R. and Bennett, P.H. (1994) Decreasing incidence and prevalence of rheumatoid arthritis in Pima Indians over a twenty-five-year period. *Arthritis and Rheumatism,* 37(8), 1158-1165.

Jensen Hansen, I.M., Asmussen Andreasen, R., van Bui Hansen, M.N. and Emamifar, A. (2017) The Reliability of Disease Activity Score in 28 Joints-C-Reactive Protein Might Be Overestimated in a Subgroup of Rheumatoid Arthritis Patients, When the Score Is Solely Based on Subjective Parameters: A Cross-sectional, Exploratory Study. *Journal of Clinical Rheumatology : Practical Reports on Rheumatic & Musculoskeletal Diseases,* 23(2), 102-106.

Jiang, H.R., Hwenda, L., Makinen, K., Oetke, C., Crocker, P.R. and Forrester, J.V. (2006) Sialoadhesin promotes the inflammatory response in experimental autoimmune uveoretinitis. *Journal of Immunology (Baltimore, Md.: 1950),* 177(4), 2258-2264.

Jin, J., Chang, Y. and Wei, W. (2010) Clinical application and evaluation of anti-TNF-alpha agents for the treatment of rheumatoid arthritis. *Acta Pharmacologica Sinica,* 31(9), 1133-1140.

Johnston, J.A., Johnson, E.S., Waller, P.R. and Varshavsky, A. (1995) Methotrexate inhibits proteolysis of dihydrofolate reductase by the N-end rule pathway. *The Journal of Biological Chemistry,* 270(14), 8172-8178.

Jovanovic, D.V., Di Battista, J.A., Martel-Pelletier, J., Jolicoeur, F.C., He, Y., Zhang, M., Mineau, F. and Pelletier, J.P. (1998) IL-17 stimulates the production and expression of proinflammatory cytokines, IL-beta and TNF-alpha, by human macrophages. *Journal of Immunology (Baltimore, Md.: 1950),* 160(7), 3513-3521.

Jung, S.M., Kim, K.W., Yang, C.W., Park, S.H. and Ju, J.H. (2014) Cytokine-mediated bone destruction in rheumatoid arthritis. *Journal of Immunology Research,* 2014, 263625.

Kadowaki, K.M., Matsuno, H., Tsuji, H. and Tunru, I. (1994) CD4+ T cells from collagen-induced arthritic mice are essential to transfer arthritis into severe combined immunodeficient mice. *Clinical and Experimental Immunology,* 97(2), 212-218.

Kagan, J.C. and Medzhitov, R. (2006) Phosphoinositide-mediated adaptor recruitment controls Toll-like receptor signaling. *Cell,* 125(5), 943-955.

Kaneko, Y., Nimmerjahn, F. and Ravetch, J.V. (2006) Anti-inflammatory activity of immunoglobulin G resulting from Fc sialylation. *Science (New York, N.Y.),* 313(5787), 670-673.

Kang, M.J., Park, Y.J., You, S., Yoo, S.A., Choi, S., Kim, D.H., Cho, C.S., Yi, E.C., Hwang, D. and Kim, W.U. (2014) Urinary proteome profile predictive of disease activity in rheumatoid arthritis. *Journal of Proteome Research,* 13(11), 5206-5217.

Karlson, E.W. and Deane, K. (2012) Environmental and gene-environment interactions and risk of rheumatoid arthritis. *Rheumatic Diseases Clinics of North America,* 38(2), 405-426.

Kato, K., Santana-Sahagun, E., Rassenti, L.Z., Weisman, M.H., Tamura, N., Kobayashi, S., Hashimoto, H. and Kipps, T.J. (1999) The soluble CD40 ligand sCD154 in systemic lupus erythematosus. *The Journal of Clinical Investigation,* 104(7), 947-955.

Kawai, T. and Akira, S. (2006) TLR signaling. *Cell Death and Differentiation,* 13(5), 816-825.

Kawanaka, N., Yamamura, M., Aita, T., Morita, Y., Okamoto, A., Kawashima, M., Iwahashi, M., Ueno, A., Ohmoto, Y. and Makino, H. (2002) CD14+,CD16+ blood monocytes and joint inflammation in rheumatoid arthritis. *Arthritis and Rheumatism,* 46(10), 2578-2586.

Keane, J., Gershon, S., Wise, R.P., Mirabile-Levens, E., Kasznica, J., Schwieterman, W.D., Siegel, J.N. and Braun, M.M. (2001) Tuberculosis associated with infliximab, a tumor necrosis factor alpha-neutralizing agent. *The New England Journal of Medicine,* 345(15), 1098-1104.

Kelm, S., Schauer, R., Manuguerra, J.C., Gross, H.J. and Crocker, P.R. (1994) Modifications of cell surface sialic acids modulate cell adhesion mediated by sialoadhesin and CD22. *Glycoconjugate Journal,* 11(6), 576-585.

Kennedy, A., Schmidt, E.M., Cribbs, A.P., Penn, H., Amjadi, P., Syed, K., Read, J.E., Green, P., Gregory, B. and Brennan, F.M. (2014) A novel upstream enhancer of FOXP3, sensitive to methylation-induced silencing, exhibits dysregulated methylation in rheumatoid arthritis Treg cells. *European Journal of Immunology,* 44(10), 2968-2978.

Keystone, E., Landewe, R., van Vollenhoven, R., Combe, B., Strand, V., Mease, P., Shaughnessy, L., VanLunen, B. and van der Heijde, D. (2014) Long-term safety and efficacy of certolizumab pegol in combination with methotrexate in the treatment of rheumatoid arthritis: 5-year results from the RAPID 1 trial and open-label extension. *Annals of the Rheumatic Diseases,* 73(12), 2094-2100.

Khan, S., Greenberg, J.D. and Bhardwaj, N. (2009) Dendritic cells as targets for therapy in rheumatoid arthritis. *Nature Reviews.Rheumatology,* 5(10), 566-571.

Kidder, D., Richards, H.E., Ziltener, H.J., Garden, O.A. and Crocker, P.R. (2013) Sialoadhesin ligand expression identifies a subset of CD4+Foxp3- T cells with a distinct activation and glycosylation profile. *Journal of Immunology (Baltimore, Md.: 1950),* 190(6), 2593-2602.

Kiecolt-Glaser, J.K., Derry, H.M. and Fagundes, C.P. (2015) Inflammation: depression fans the flames and feasts on the heat. *The American Journal of Psychiatry,* 172(11), 1075-1091.

Kinne, R.W., Brauer, R., Stuhlmuller, B., Palombo-Kinne, E. and Burmester, G.R. (2000) Macrophages in rheumatoid arthritis. *Arthritis Research,* 2(3), 189-202.

Klak, A., Paradowska-Gorycka, A., Kwiatkowska, B. and Raciborski, F. (2016) Personalized medicine in rheumatology. *Reumatologia,* 54(4), 177-186.

Klareskog, L., Forsum, U., Kabelitz, D., Ploen, L., Sundstrom, C., Nilsson, K., Wigren, A. and Wigzell, H. (1982) Immune functions of human synovial cells. Phenotypic and T cell regulatory properties of macrophage-like cells that express HLA-DR. *Arthritis and Rheumatism,* 25(5), 488-501.

Kojima, T., Yabe, Y., Kaneko, A., Hirano, Y., Ishikawa, H., Hayashi, M., Miyake, H., Takagi, H., Kato, T., Terabe, K., Wanatabe, T., Tsuchiya, H., Kida, D., Shioura, T., Funahashi, K., Kato, D., Matsubara, H., Takahashi, N., Hattori, Y., Asai, N. and Ishiguro, N. (2013) Monitoring C-reactive protein levels to predict favourable clinical outcomes from tocilizumab treatment in patients with rheumatoid arthritis. *Modern Rheumatology / the Japan Rheumatism Association,* 23(5), 977-985.

Koshy, M., Berger, D. and Crow, M.K. (1996) Increased expression of CD40 ligand on systemic lupus erythematosus lymphocytes. *The Journal of Clinical Investigation,* 98(3), 826-837.

Kremer, J.M., Dougados, M., Emery, P., Durez, P., Sibilia, J., Shergy, W., Steinfeld, S., Tindall, E., Becker, J.C., Li, T., Nuamah, I.F., Aranda, R. and Moreland, L.W. (2005) Treatment of rheumatoid arthritis with the selective costimulation modulator abatacept: twelve-month results of a phase iib, double-blind, randomized, placebo-controlled trial. *Arthritis and Rheumatism,* 52(8), 2263-2271.

Kuleshov, M.V., Jones, M.R., Rouillard, A.D., Fernandez, N.F., Duan, Q., Wang, Z., Koplev, S., Jenkins, S.L., Jagodnik, K.M., Lachmann, A., McDermott, M.G., Monteiro, C.D., Gundersen, G.W. and Ma'ayan, A. (2016) Enrichr: a comprehensive gene set enrichment analysis web server 2016 update. *Nucleic Acids Research,* 44(W1), W90-7.

Kumar, M., Putzki, N., Limmroth, V., Remus, R., Lindemann, M., Knop, D., Mueller, N., Hardt, C., Kreuzfelder, E. and Grosse-Wilde, H. (2006) CD4+CD25+FoxP3+ T lymphocytes fail to suppress myelin basic protein-induced proliferation in patients with multiple sclerosis. *Journal of Neuroimmunology,* 180(1-2), 178-184.

Kushner, I., Gewurz, H. and Benson, M.D. (1981) C-reactive protein and the acute-phase response. *The Journal of Laboratory and Clinical Medicine,* 97(6), 739-749.

Kushner, I., Rzewnicki, D. and Samols, D. (2006) What does minor elevation of C-reactive protein signify? *The American Journal of Medicine,* 119(2), 166.e17-166.e28.

Kushner, I., Samols, D. and Magrey, M. (2010) A unifying biologic explanation for "high-sensitivity" C-reactive protein and "low-grade" inflammation. *Arthritis Care & Research,* 62(4), 442-446.

Kyburz, D., Brentano, F. and Gay, S. (2006) Mode of action of hydroxychloroquine in RA-evidence of an inhibitory effect on toll-like receptor signaling. *Nat Clin Pract Rheumatol,* 2(9), 458.

Lacerte, P., Brunet, A., Egarnes, B., Duchene, B., Brown, J.P. and Gosselin, J. (2016) Overexpression of TLR2 and TLR9 on monocyte subsets of active rheumatoid arthritis patients contributes to enhance responsiveness to TLR agonists. *Arthritis Research & Therapy,* 18, 10-015-0901-1.

Lanas, A. (2009) Nonsteroidal antiinflammatory drugs and cyclooxygenase inhibition in the gastrointestinal tract: a trip from peptic ulcer to colon cancer. *The American Journal of the Medical Sciences,* 338(2), 96-106.

Le Bras, S. and Geha, R.S. (2006) IPEX and the role of Foxp3 in the development and function of human Tregs. *The Journal of Clinical Investigation,* 116(6), 1473-1475.

Lee, S.E., West, K.P.,Jr, Cole, R.N., Schulze, K.J., Christian, P., Wu, L.S., Yager, J.D., Groopman, J. and Ruczinski, I. (2015) Plasma Proteome Biomarkers of Inflammation in School Aged Children in Nepal. *PloS One,* 10(12), e0144279.

Lee, S.W., Park, H.J., Kim, B.K., Han, K.H., Lee, S.K., Kim, S.U. and Park, Y.B. (2012) Leflunomide increases the risk of silent liver fibrosis in patients with rheumatoid arthritis receiving methotrexate. *Arthritis Research & Therapy,* 14(5), R232.

Lefebvre, J.C., Giordanengo, V., Limouse, M., Doglio, A., Cucchiarini, M., Monpoux, F., Mariani, R. and Peyron, J.F. (1994) Altered glycosylation of leukosialin, CD43, in HIV-1-infected cells of the CEM line. *The Journal of Experimental Medicine,* 180(5), 1609-1617.

Lewkowicz, N., Mycko, M.P., Przygodzka, P., Cwiklinska, H., Cichalewska, M., Matysiak, M., Selmaj, K. and Lewkowicz, P. (2016) Induction of human IL-10-producing neutrophils by LPS-stimulated Treg cells and IL-10. *Mucosal Immunology,* 9(2), 364-378.

Lewkowicz, P., Lewkowicz, N., Sasiak, A. and Tchorzewski, H. (2006) Lipopolysaccharide-activated CD4+CD25+ T regulatory cells inhibit neutrophil function and promote their apoptosis and death. *Journal of Immunology (Baltimore, Md.: 1950),* 177(10), 7155-7163.

Li, Q. and Verma, I.M. (2002) NF-kappaB regulation in the immune system. *Nature Reviews.Immunology,* 2(10), 725-734.

Li, X.J., Xu, M., Zhao, X.Q., Zhao, J.N., Chen, F.F., Yu, W., Gao, D.Y. and Luo, B. (2013) Proteomic analysis of synovial fibroblast-like synoviocytes from rheumatoid arthritis. *Clinical and Experimental Rheumatology,* 31(4), 552-558.

Li, Y., Cleveland, B., Klots, I., Travis, B., Richardson, B.A., Anderson, D., Montefiori, D., Polacino, P. and Hu, S.L. (2008) Removal of a single N-linked glycan in human immunodeficiency virus type 1 gp120 results in an enhanced ability to induce neutralizing antibody responses. *Journal of Virology,* 82(2), 638-651.

Li, Y. and Kurlander, R.J. (2010) Comparison of anti-CD3 and anti-CD28-coated beads with soluble anti-CD3 for expanding human T cells: differing impact on CD8 T cell phenotype and responsiveness to restimulation. *Journal of Translational Medicine,* 8, 104-5876-8-104.

Li, Z.C., Xiao, J., Peng, J.L., Chen, J.W., Ma, T., Cheng, G.Q., Dong, Y.Q., Wang, W.L. and Liu, Z.D. (2014) Functional annotation of rheumatoid arthritis and osteoarthritis associated genes by integrative genome-wide gene expression profiling analysis. *PloS One,* 9(2), e85784.

Liao, H., Wu, J., Kuhn, E., Chin, W., Chang, B., Jones, M.D., O'Neil, S., Clauser, K.R., Karl, J., Hasler, F., Roubenoff, R., Zolg, W. and Guild, B.C. (2004) Use of mass spectrometry to identify protein biomarkers of disease severity in the synovial fluid and serum of patients with rheumatoid arthritis. *Arthritis and Rheumatism,* 50(12), 3792-3803.

Liao, K.P., Gunnarsson, M., KÃ¤llberg, H., Ding, B., Plenge, R.M., Padyukov, L., Karlson, E.W., Klareskog, L., Askling, J. and Alfredsson, L. (2009) A specific association exists between type 1 diabetes and anti-CCP positive rheumatoid arthritis. *Arthritis and Rheumatism,* 60(3), 653-660.

Liu, D., Mao, P., Huang, Y., Liu, Y., Liu, X., Pang, X. and Li, Y. (2014) Proteomic analysis of lung tissue in a rat acute lung injury model: identification of PRDX1 as a promoter of inflammation. *Mediators of Inflammation,* 2014, 469358.

Lopez, S., Halbwachs-Mecarelli, L., Ravaud, P., Bessou, G., Dougados, M. and Porteu, F. (1995) Neutrophil expression of tumour necrosis factor receptors (TNF-R) and of activation markers (CD11b, CD43, CD63) in rheumatoid arthritis. *Clinical and Experimental Immunology,* 101(1), 25-32.

Lortat-Jacob, H., Baltzer, F. and Grimaud, J.A. (1996) Heparin decreases the blood clearance of interferon-gamma and increases its activity by limiting the processing of its carboxyl-terminal sequence. *The Journal of Biological Chemistry,* 271(27), 16139-16143.

Lundy, S.K., Sarkar, S., Tesmer, L.A. and Fox, D.A. (2007) Cells of the synovium in rheumatoid arthritis. T lymphocytes. *Arthritis Research & Therapy,* 9(1), 202.

Macian, F., Garcia-Cozar, F., Im, S.H., Horton, H.F., Byrne, M.C. and Rao, A. (2002) Transcriptional mechanisms underlying lymphocyte tolerance. *Cell,* 109(6), 719-731.

Malemud, C.J. (2015) The PI3K/Akt/PTEN/mTOR pathway: a fruitful target for inducing cell death in rheumatoid arthritis? *Future Medicinal Chemistry,* 7(9), 1137-1147.

Malik, P. and Clements, J.B. (2004) Protein kinase CK2 phosphorylation regulates the interaction of Kaposi's sarcoma-associated herpesvirus regulatory protein ORF57 with its multifunctional partner hnRNP K. *Nucleic Acids Research,* 32(18), 5553-5569.

Malottki, K., Barton, P., Tsourapas, A., Uthman, A.O., Liu, Z., Routh, K., Connock, M., Jobanputra, P., Moore, D., Fry-Smith, A. and Chen, Y.F. (2011) Adalimumab, etanercept, infliximab, rituximab and abatacept for the treatment of rheumatoid arthritis after the failure of a tumour necrosis factor inhibitor: a systematic review and economic evaluation. *Health Technology Assessment (Winchester, England),* 15(14), 1-278.

Mann, A.C., Record, C.O., Self, C.H. and Turner, G.A. (1994) Monosaccharide composition of haptoglobin in liver diseases and alcohol abuse: large changes in glycosylation associated with alcoholic liver disease. *Clinica Chimica Acta; International Journal of Clinical Chemistry,* 227(1-2), 69-78.

Marston, B., Palanichamy, A. and Anolik, J.H. (2010) B cells in the pathogenesis and treatment of rheumatoid arthritis. *Current Opinion in Rheumatology,* 22(3), 307-315.

Mathay, C., Ammerlaan, W. and Betsou, F. (2012) Automatic buffy coat extraction: methodology, feasibility, optimization and validation study. *Biopreservation and Biobanking,* 10(6), 543-547.

Matsuki, F., Saegusa, J., Miyamoto, Y., Misaki, K., Kumagai, S. and Morinobu, A. (2013) CD45RA-Foxp3(high) activated/effector regulatory T cells in the CCR7 + CD45RA-CD27 + CD28+central memory subset are decreased in peripheral blood from patients with rheumatoid arthritis. *Biochemical and Biophysical Research Communications,* 438(4), 778-783.

May, M.J., D'Acquisto, F., Madge, L.A., Glockner, J., Pober, J.S. and Ghosh, S. (2000) Selective inhibition of NF-kappaB activation by a peptide that blocks the interaction of NEMO with the IkappaB kinase complex. *Science (New York, N.Y.),* 289(5484), 1550-1554.

McAleer, J.P. and Vella, A.T. (2008) Understanding how lipopolysaccharide impacts CD4 T-cell immunity. *Critical Reviews in Immunology,* 28(4), 281-299.

McWilliams, D.F., Kiely, P.D., Young, A. and Walsh, D.A. (2013) Baseline factors predicting change from the initial DMARD treatment during the first 2 years of rheumatoid arthritis: experience in the ERAN inception cohort. *BMC Musculoskeletal Disorders,* 14, 153-2474-14-153.

Mellado, M., Martinez-Munoz, L., Cascio, G., Lucas, P., Pablos, J.L. and Rodriguez-Frade, J.M. (2015) T Cell Migration in Rheumatoid Arthritis. *Frontiers in Immunology,* 6, 384.

Meng, J., Parroche, P., Golenbock, D.T. and McKnight, C.J. (2008) The differential impact of disulfide bonds and N-linked glycosylation on the stability and function of CD14. *The Journal of Biological Chemistry,* 283(6), 3376-3384.

Milkova, L., Voelcker, V., Forstreuter, I., Sack, U., Anderegg, U., Simon, J.C. and Maier-Simon, C. (2010) The NF-kappaB signalling pathway is involved in the LPS/IL-2-induced upregulation of FoxP3 expression in human CD4+CD25high regulatory T cells. *Experimental Dermatology,* 19(1), 29-37.

Miller, M.C., Manning, H.B., Jain, A., Troeberg, L., Dudhia, J., Essex, D., Sandison, A., Seiki, M., Nanchahal, J., Nagase, H. and Itoh, Y. (2009) Membrane type 1 matrix metalloproteinase is a crucial promoter of synovial invasion in human rheumatoid arthritis. *Arthritis and Rheumatism,* 60(3), 686-697.

Min, S.Y., Yan, M., Du, Y., Wu, T., Khobahy, E., Kwon, S.R., Taneja, V., Bashmakov, A., Nukala, S., Ye, Y., Orme, J., Sajitharan, D., Kim, H.Y. and Mohan, C. (2013) Intra-articular nuclear factor-kappaB blockade ameliorates collagen-induced arthritis in mice by eliciting regulatory T cells and macrophages. *Clinical and Experimental Immunology,* 172(2), 217-227.

Miossec, P. and van den Berg, W. (1997) Th1/Th2 cytokine balance in arthritis. *Arthritis and Rheumatism,* 40(12), 2105-2115.

Mobini, M., Maboudi, A. and Ali Mohammadpour, R. (2017) Periodontitis in rheumatoid arthritis patients, abundance and association with disease activity. *Medical Journal of the Islamic Republic of Iran,* 31, 44.

Mohan, V.K., Ganesan, N. and Gopalakrishnan, R. (2014) Association of susceptible genetic markers and autoantibodies in rheumatoid arthritis. *Journal of Genetics,* 93(2), 597-605.

Moreland, L.W., Alten, R., Van den Bosch, F., Appelboom, T., Leon, M., Emery, P., Cohen, S., Luggen, M., Shergy, W., Nuamah, I. and Becker, J.C. (2002) Costimulatory blockade in patients with rheumatoid arthritis: a pilot, dose-finding, double-blind, placebo-controlled clinical trial evaluating CTLA-4Ig and LEA29Y eighty-five days after the first infusion. *Arthritis and Rheumatism,* 46(6), 1470-1479.

Morita, K., Okamura, T., Inoue, M., Komai, T., Teruya, S., Iwasaki, Y., Sumitomo, S., Shoda, H., Yamamoto, K. and Fujio, K. (2016) Egr2 and Egr3 in regulatory T cells cooperatively control systemic autoimmunity through Ltbp3-mediated TGF-beta3 production. *Proceedings of the National Academy of Sciences of the United States of America,* 113(50), E8131-E8140.

Mottonen, M., Heikkinen, J., Mustonen, L., Isomaki, P., Luukkainen, R. and Lassila, O. (2005) CD4+ CD25+ T cells with the phenotypic and functional characteristics of regulatory T cells are enriched in the synovial fluid of patients with rheumatoid arthritis. *Clinical and Experimental Immunology,* 140(2), 360-367.

Mukherjee, D., Nissen, S.E. and Topol, E.J. (2001) Risk of cardiovascular events associated with selective COX-2 inhibitors. *Jama,* 286(8), 954-959.

Mulherin, D., Fitzgerald, O. and Bresnihan, B. (1996) Synovial tissue macrophage populations and articular damage in rheumatoid arthritis. *Arthritis and Rheumatism,* 39(1), 115-124.

Munday, J., Floyd, H. and Crocker, P.R. (1999) Sialic acid binding receptors (siglecs) expressed by macrophages. *Journal of Leukocyte Biology,* 66(5), 705-711.

Murphy, G. and Nagase, H. (2008) Reappraising metalloproteinases in rheumatoid arthritis and osteoarthritis: destruction or repair? *Nature Clinical Practice.Rheumatology,* 4(3), 128-135.

Nagar, M., Jacob-Hirsch, J., Vernitsky, H., Berkun, Y., Ben-Horin, S., Amariglio, N., Bank, I., Kloog, Y., Rechavi, G. and Goldstein, I. (2010) TNF activates a NF-kappaB-regulated cellular program in human CD45RA- regulatory T cells that modulates their suppressive function. *Journal of Immunology (Baltimore, Md.: 1950),* 184(7), 3570-3581.

Naito-Matsui, Y., Takada, S., Kano, Y., Iyoda, T., Sugai, M., Shimizu, A., Inaba, K., Nitschke, L., Tsubata, T., Oka, S., Kozutsumi, Y. and Takematsu, H. (2014) Functional evaluation of activation-dependent alterations in the sialoglycan composition of T cells. *The Journal of Biological Chemistry,* 289(3), 1564-1579.

Nakano, K., Whitaker, J.W., Boyle, D.L., Wang, W. and Firestein, G.S. (2013) DNA methylome signature in rheumatoid arthritis. *Annals of the Rheumatic Diseases,* 72(1), 110-117.

National rheumatoid arthritis society (NRAS). (2013) Available at: http://www.nras.org.uk/data/files/Publications/Biologics-.pdf

Newton, R. (2014) Anti-inflammatory glucocorticoids: changing concepts. *European Journal of Pharmacology,* 724, 231-236.

NICE. (2009) *Rheumatoid arthritis: The management of rheumatoid arthritis in adults.* Available at: https://www.nice.org.uk/guidance/cg79

Nie, H., Zheng, Y., Li, R., Guo, T.B., He, D., Fang, L., Liu, X., Xiao, L., Chen, X., Wan, B., Chin, Y.E. and Zhang, J.Z. (2013) Phosphorylation of FOXP3 controls regulatory T cell function and is inhibited by TNF-alpha in rheumatoid arthritis. *Nature Medicine,* 19(3), 322-328.

Nielen, M.M., van Schaardenburg, D., Reesink, H.W., Twisk, J.W., van de Stadt, R.J., van der Horst-Bruinsma, I.E., de Koning, M.H., Habibuw, M.R. and Dijkmans, B.A. (2006) Simultaneous development of acute phase response and autoantibodies in preclinical rheumatoid arthritis. *Annals of the Rheumatic Diseases,* 65(4), 535-537.

Nile, C.J., Read, R.C., Akil, M., Duff, G.W. and Wilson, A.G. (2008) Methylation status of a single CpG site in the IL6 promoter is related to IL6 messenger RNA levels and rheumatoid arthritis. *Arthritis and Rheumatism,* 58(9), 2686-2693.

Nitschke, L. (2005) The role of CD22 and other inhibitory co-receptors in B-cell activation. *Current Opinion in Immunology,* 17(3), 290-297.

Nong, Y.H., Remold-O'Donnell, E., LeBien, T.W. and Remold, H.G. (1989) A monoclonal antibody to sialophorin (CD43) induces homotypic adhesion and activation of human monocytes. *The Journal of Experimental Medicine,* 170(1), 259-267.

Ogata, A., Tanimura, K., Sugimoto, T., Inoue, H., Urata, Y., Matsubara, T., Kondo, M., Ueki, Y., Iwahashi, M., Tohma, S., Ohta, S., Saeki, Y., Tanaka, T. and Musashi Study Investigators. (2014) Phase III study of the efficacy and safety of subcutaneous versus intravenous tocilizumab monotherapy in patients with rheumatoid arthritis. *Arthritis Care & Research,* 66(3), 344-354.

Ogrendik, M. (2013) Antibiotics for the treatment of rheumatoid arthritis. *International Journal of General Medicine,* 7, 43-47.

O'Hara, R., Murphy, E.P., Whitehead, A.S., FitzGerald, O. and Bresnihan, B. (2000) Acute-phase serum amyloid A production by rheumatoid arthritis synovial tissue. *Arthritis Research,* 2(2), 142-144.

Ohnishi, K., Komohara, Y., Saito, Y., Miyamoto, Y., Watanabe, M., Baba, H. and Takeya, M. (2013) CD169-positive macrophages in regional lymph nodes are associated with a favorable prognosis in patients with colorectal carcinoma. *Cancer Science,* 104(9), 1237-1244.

Ohtsubo, K. and Marth, J.D. (2006) Glycosylation in cellular mechanisms of health and disease. *Cell,* 126(5), 855-867.

O'Neill, A.S., van den Berg, T.K. and Mullen, G.E. (2013) Sialoadhesin - a macrophage-restricted marker of immunoregulation and inflammation. *Immunology,* 138(3), 198-207.

Onishi, R.M. and Gaffen, S.L. (2010) Interleukin-17 and its target genes: mechanisms of interleukin-17 function in disease. *Immunology,* 129(3), 311-321.

Ormseth, M.J., Chung, C.P., Oeser, A.M., Connelly, M.A., Sokka, T., Raggi, P., Solus, J.F., Otvos, J.D. and Stein, C.M. (2015) Utility of a novel inflammatory marker, GlycA,

for assessment of rheumatoid arthritis disease activity and coronary atherosclerosis. *Arthritis Research & Therapy,* 17, 117-015-0646-x.

Ortea, I., Roschitzki, B., Ovalles, J.G., Longo, J.L., de la Torre, I., Gonzalez, I., Gomez-Reino, J.J. and Gonzalez, A. (2012) Discovery of serum proteomic biomarkers for prediction of response to infliximab (a monoclonal anti-TNF antibody) treatment in rheumatoid arthritis: an exploratory analysis. *Journal of Proteomics,* 77, 372-382.

Otterdal, K., Pedersen, T.M. and Solum, N.O. (2004) Release of soluble CD40 ligand after platelet activation: studies on the solubilization phase. *Thrombosis Research,* 114(3), 167-177.

Pai, S., Pai, L. and Birkenfeldt, R. (1998) Correlation of serum IgA rheumatoid factor levels with disease severity in rheumatoid arthritis. *Scandinavian Journal of Rheumatology,* 27(4), 252-256.

Park, J.K., Rosenstein, Y.J., Remold-O'Donnell, E., Bierer, B.E., Rosen, F.S. and Burakoff, S.J. (1991) Enhancement of T-cell activation by the CD43 molecule whose expression is defective in Wiskott-Aldrich syndrome. *Nature,* 350(6320), 706-709.

Parkkinen, J. (1989) Aberrant lectin-binding activity of immunoglobulin G in serum from rheumatoid arthritis patients. *Clinical Chemistry,* 35(8), 1638-1643.

Pasek, M., Duk, M., Podbielska, M., Sokolik, R., Szechinski, J., Lisowska, E. and Krotkiewski, H. (2006) Galactosylation of IgG from rheumatoid arthritis (RA) patients--changes during therapy. *Glycoconjugate Journal,* 23(7-8), 463-471.

Passlick, B., Flieger, D. and Ziegler-Heitbrock, H.W. (1989) Identification and characterization of a novel monocyte subpopulation in human peripheral blood. *Blood,* 74(7), 2527-2534.

Patil, P., Parker, R.A., Rawcliffe, C., Olaleye, A., Moore, S., Daly, N., Sen, D. and Ioannou, Y. (2014) Methotrexate-induced nausea and vomiting in adolescent and young adult patients. *Clinical Rheumatology,* 33(3), 403-407.

Paul, R. and Rotzsch, W. (1989) The diagnostic significance of mucoproteins, sialic acid and cortisol in assessing the activity of rheumatic diseases. *Zeitschrift Fur Die Gesamte Innere Medizin Und Ihre Grenzgebiete,* 44(14), 410-413.

Perez-Sola, M.J., Torre-Cisneros, J., Perez-Zafrilla, B., Carmona, L., Descalzo, M.A., Gomez-Reino, J.J. and BIOBADASER Study Group. (2011) Infections in patients treated with tumor necrosis factor antagonists: incidence, etiology and mortality in the BIOBADASER registry. *Medicina Clinica,* 137(12), 533-540.

Peters, M.J., Symmons, D.P., McCarey, D., Dijkmans, B.A., Nicola, P., Kvien, T.K., McInnes, I.B., Haentzschel, H., Gonzalez-Gay, M.A., Provan, S., Semb, A., Sidiropoulos, P., Kitas, G., Smulders, Y.M., Soubrier, M., Szekanecz, Z., Sattar, N. and Nurmohamed, M.T. (2010) EULAR evidence-based recommendations for

cardiovascular risk management in patients with rheumatoid arthritis and other forms of inflammatory arthritis. *Annals of the Rheumatic Diseases,* 69(2), 325-331.

Petrow, P.K., Thoss, K., Katenkamp, D. and Brauer, R. (1996) Adoptive transfer of susceptibility to antigen-induced arthritis into severe combined immunodeficient (SCID) mice: role of CD4+ and CD8+ T cells. *Immunological Investigations,* 25(4), 341-353.

Pihl, M., Akerman, L., Axelsson, S., Cheramy, M., Hjorth, M., Mallone, R., Ludvigsson, J. and Casas, R. (2013) Regulatory T cell phenotype and function 4 years after GAD-alum treatment in children with type 1 diabetes. *Clinical and Experimental Immunology,* 172(3), 394-402.

Pikwer, M., Bergstrom, U., Nilsson, J.A., Jacobsson, L. and Turesson, C. (2012) Early menopause is an independent predictor of rheumatoid arthritis. *Annals of the Rheumatic Diseases,* 71(3), 378-381.

Pillai, S., Netravali, I.A., Cariappa, A. and Mattoo, H. (2012) Siglecs and immune regulation. *Annual Review of Immunology,* 30, 357-392.

Piller, V., Piller, F. and Fukuda, M. (1989) Phosphorylation of the major leukocyte surface sialoglycoprotein, leukosialin, is increased by phorbol 12-myristate 13-acetate. *The Journal of Biological Chemistry,* 264(31), 18824-18831.

Polansky, J.K., Kretschmer, K., Freyer, J., Floess, S., Garbe, A., Baron, U., Olek, S., Hamann, A., von Boehmer, H. and Huehn, J. (2008) DNA methylation controls Foxp3 gene expression. *European Journal of Immunology,* 38(6), 1654-1663.

Pouliot, P., Plante, I., Raquil, M.A., Tessier, P.A. and Olivier, M. (2008) Myeloid-related proteins rapidly modulate macrophage nitric oxide production during innate immune response. *Journal of Immunology (Baltimore, Md.: 1950),* 181(5), 3595-3601.

Powell, L.D., Sgroi, D., Sjoberg, E.R., Stamenkovic, I. and Varki, A. (1993) Natural ligands of the B cell adhesion molecule CD22 beta carry N-linked oligosaccharides with alpha-2,6-linked sialic acids that are required for recognition. *The Journal of Biological Chemistry,* 268(10), 7019-7027.

Pratt, A.G., Isaacs, J.D. and Mattey, D.L. (2009) Current concepts in the pathogenesis of early rheumatoid arthritis. *Best Practice & Research.Clinical Rheumatology,* 23(1), 37-48.

Przybysz, M., Maszczak, D., Borysewicz, K., Szechinski, J. and Katnik-Prastowska, I. (2007) Relative sialylation and fucosylation of synovial and plasma fibronectins in relation to the progression and activity of rheumatoid arthritis. *Glycoconjugate Journal,* 24(9), 543-550.

Radwan, W.M., Khalifa, K.A., Esaily, H.A. and Lashin, N.,A. (2015) $CD14^{++}CD16^{+}$ monocyte subset expansion in rheumatoid arthritis patients: Relation to disease activity and interleukin-17. *The Egyptian Rhaumatologist,* 38(3), 161.

Raghav, S.K., Gupta, B., Agrawal, C., Saroha, A., Das, R.H., Chaturvedi, V.P. and Das, H.R. (2006) Altered expression and glycosylation of plasma proteins in rheumatoid arthritis. *Glycoconjugate Journal,* 23(3-4), 167-173.

Ramachandran, G. (2014) Gram-positive and gram-negative bacterial toxins in sepsis: a brief review. *Virulence,* 5(1), 213-218.

Ravetch, J.V. and Lanier, L.L. (2000) Immune inhibitory receptors. *Science (New York, N.Y.),* 290(5489), 84-89.

Razi, N. and Varki, A. (1999) Cryptic sialic acid binding lectins on human blood leukocytes can be unmasked by sialidase treatment or cellular activation. *Glycobiology,* 9(11), 1225-1234.

Remold-O'Donnell, E., Kenney, D.M., Parkman, R., Cairns, L., Savage, B. and Rosen, F.S. (1984) Characterization of a human lymphocyte surface sialoglycoprotein that is defective in Wiskott-Aldrich syndrome. *The Journal of Experimental Medicine,* 159(6), 1705-1723.

Richardson, B., Scheinbart, L., Strahler, J., Gross, L., Hanash, S. and Johnson, M. (1990) Evidence for impaired T cell DNA methylation in systemic lupus erythematosus and rheumatoid arthritis. *Arthritis and Rheumatism,* 33(11), 1665-1673.

Rodenburg, R.J., Ganga, A., van Lent, P.L., van de Putte, L.B. and van Venrooij, W.J. (2000) The antiinflammatory drug sulfasalazine inhibits tumor necrosis factor alpha expression in macrophages by inducing apoptosis. *Arthritis and Rheumatism,* 43(9), 1941-1950.

Ruof, J. and Stucki, G. (1999) Validity aspects of erythrocyte sedimentation rate and C-reactive protein in ankylosing spondylitis: a literature review. *The Journal of Rheumatology,* 26(4), 966-970.

Sabeh, F., Fox, D. and Weiss, S.J. (2010) Membrane-type I matrix metalloproteinase-dependent regulation of rheumatoid arthritis synoviocyte function. *Journal of Immunology (Baltimore, Md.: 1950),* 184(11), 6396-6406.

Sakaguchi, S., Ono, M., Setoguchi, R., Yagi, H., Hori, S., Fehervari, Z., Shimizu, J., Takahashi, T. and Nomura, T. (2006) Foxp3+ CD25+ CD4+ natural regulatory T cells in dominant self-tolerance and autoimmune disease. *Immunological Reviews,* 212, 8-27.

Sakaguchi, S., Yamaguchi, T., Nomura, T. and Ono, M. (2008) Regulatory T cells and immune tolerance. *Cell,* 133(5), 775-787.

Salliot, C. and van der Heijde, D. (2009) Long-term safety of methotrexate monotherapy in patients with rheumatoid arthritis: a systematic literature research. *Annals of the Rheumatic Diseases,* 68(7), 1100-1104.

Samuels, J., Ng, Y.S., Coupillaud, C., Paget, D. and Meffre, E. (2005) Impaired early B cell tolerance in patients with rheumatoid arthritis. *The Journal of Experimental Medicine,* 201(10), 1659-1667.

Saroha, A., Biswas, S., Chatterjee, B.P. and Das, H.R. (2011) Altered glycosylation and expression of plasma alpha-1-acid glycoprotein and haptoglobin in rheumatoid arthritis. *Journal of Chromatography.B, Analytical Technologies in the Biomedical and Life Sciences,* 879(20), 1839-1843.

Sbong, S. and Feldman, M. (2014) Frequency and causes of C-reactive protein and erythrocyte sedimentation rate disagreements in adults. *International Journal of Rheumatic Diseases,*

Scher, J.U., Ubeda, C., Equinda, M., Khanin, R., Buischi, Y., Viale, A., Lipuma, L., Attur, M., Pillinger, M.H., Weissmann, G., Littman, D.R., Pamer, E.G., Bretz, W.A. and Abramson, S.B. (2012) Periodontal disease and the oral microbiota in new-onset rheumatoid arthritis. *Arthritis and Rheumatism,* 64(10), 3083-3094.

Schildberger, A., Rossmanith, E., Eichhorn, T., Strassl, K. and Weber, V. (2013) Monocytes, Peripheral Blood Mononuclear Cells, and THP-1 Cells Exhibit Different Cytokine Expression Patterns following Stimulation with Lipopolysaccharide. *Mediators of Inflammation,* 2013, 10.1155/2013/697972.

Schlegel, P.M., Steiert, I., Kotter, I. and Muller, C.A. (2013) B cells contribute to heterogeneity of IL-17 producing cells in rheumatoid arthritis and healthy controls. *PloS One,* 8(12), e82580.

Schloder, J., Berges, C., Luessi, F. and Jonuleit, H. (2017) Dimethyl Fumarate Therapy Significantly Improves the Responsiveness of T Cells in Multiple Sclerosis Patients for Immunoregulation by Regulatory T Cells. *International Journal of Molecular Sciences,* 18(2), 10.3390/ijms18020271.

Schwartz, R.H. (1996) Models of T cell anergy: is there a common molecular mechanism? *The Journal of Experimental Medicine,* 184(1), 1-8.

Sekigawa, I., Yanagida, M., Iwabuchi, K., Kaneda, K., Kaneko, H., Takasaki, Y., Jung, G., Sone, S., Tanaka, Y., Ogawa, H. and Takamori, K. (2008) Protein biomarker analysis by mass spectrometry in patients with rheumatoid arthritis receiving anti-tumor necrosis factor-alpha antibody therapy. *Clinical and Experimental Rheumatology,* 26(2), 261-267.

Seror, R., Boudaoud, S., Pavy, S., Nocturne, G., Schaeverbeke, T., Saraux, A., Chanson, P., Gottenberg, J.E., Devauchelle-Pensec, V., Tobon, G.J., Mariette, X. and Miceli-Richard, C. (2016) Increased Dickkopf-1 in Recent-onset Rheumatoid Arthritis is a

New Biomarker of Structural Severity. Data from the ESPOIR Cohort. *Scientific Reports,* 6, 18421.

Shalini P., U., Debnath, T., JVS, V., Kona, L.K., Kamaraju, S.R., Kancherla, R. and Chelluri, L.K. (2015) A study on FoxP3 and Tregs in paired samples of peripheral blood and synovium in rheumatoid arthritis. *Central-European Journal of Immunology,* 40(4), 431-436.

Sheehan, N.J., Slavin, B.M., Donovan, M.P., Mount, J.N. and Mathews, J.A. (1986) Lack of correlation between clinical disease activity and erythrocyte sedimentation rate, acute phase proteins or protease inhibitors in ankylosing spondylitis. *British Journal of Rheumatology,* 25(2), 171-174.

Shichikawa, K., Inoue, K., Hirota, S., Maeda, A., Ota, H., Kimura, M., Ushiyama, T. and Tsujimoto, M. (1999) Changes in the incidence and prevalence of rheumatoid arthritis in Kamitonda, Wakayama, Japan, 1965-1996. *Annals of the Rheumatic Diseases,* 58(12), 751-756.

Shichita, T., Hasegawa, E., Kimura, A., Morita, R., Sakaguchi, R., Takada, I., Sekiya, T., Ooboshi, H., Kitazono, T., Yanagawa, T., Ishii, T., Takahashi, H., Mori, S., Nishibori, M., Kuroda, K., Akira, S., Miyake, K. and Yoshimura, A. (2012) Peroxiredoxin family proteins are key initiators of post-ischemic inflammation in the brain. *Nature Medicine,* 18(6), 911-917.

Silman, A.J., MacGregor, A.J., Thomson, W., Holligan, S., Carthy, D., Farhan, A. and Ollier, W.E. (1993) Twin concordance rates for rheumatoid arthritis: results from a nationwide study. *British Journal of Rheumatology,* 32(10), 903-907.

Singh, J.A., Cameron, C., Noorbaloochi, S., Cullis, T., Tucker, M., Christensen, R., Ghogomu, E.T., Coyle, D., Clifford, T., Tugwell, P. and Wells, G.A. (2015) Risk of serious infection in biological treatment of patients with rheumatoid arthritis: a systematic review and meta-analysis. *Lancet (London, England),* 386(9990), 258-265.

Smeets, T.J., Kraan, M.C., Galjaard, S., Youssef, P.P., Smith, M.D. and Tak, P.P. (2001) Analysis of the cell infiltrate and expression of matrix metalloproteinases and granzyme B in paired synovial biopsy specimens from the cartilage-pannus junction in patients with RA. *Annals of the Rheumatic Diseases,* 60(6), 561-565.

Smolen, J.S., Aletaha, D., Bijlsma, J.W., Breedveld, F.C., Boumpas, D., Burmester, G., Combe, B., Cutolo, M., de Wit, M., Dougados, M., Emery, P., Gibofsky, A., Gomez-Reino, J.J., Haraoui, B., Kalden, J., Keystone, E.C., Kvien, T.K., McInnes, I., Martin-Mola, E., Montecucco, C., Schoels, M., van der Heijde, D. and T2T Expert Committee. (2010a) Treating rheumatoid arthritis to target: recommendations of an international task force. *Annals of the Rheumatic Diseases,* 69(4), 631-637.

Smolen, J.S., Han, C., van der Heijde, D.M., Emery, P., Bathon, J.M., Keystone, E., Maini, R.N., Kalden, J.R., Aletaha, D., Baker, D., Han, J., Bala, M., St Clair, E.W. and Active-Controlled Study of Patients Receiving Infliximab for the Treatment of

Rheumatoid Arthritis of Early Onset (ASPIRE) Study Group. (2009) Radiographic changes in rheumatoid arthritis patients attaining different disease activity states with methotrexate monotherapy and infliximab plus methotrexate: the impacts of remission and tumour necrosis factor blockade. *Annals of the Rheumatic Diseases,* 68(6), 823-827.

Smolen, J.S., Kay, J., Matteson, E.L., Landewe, R., Hsia, E.C., Xu, S., Zhou, Y. and Doyle, M.K. (2014a) Insights into the efficacy of golimumab plus methotrexate in patients with active rheumatoid arthritis who discontinued prior anti-tumour necrosis factor therapy: post-hoc analyses from the GO-AFTER study. *Annals of the Rheumatic Diseases,* 73(10), 1811-1818.

Smolen, J.S., Landewe, R., Breedveld, F.C., Buch, M., Burmester, G., Dougados, M., Emery, P., Gaujoux-Viala, C., Gossec, L., Nam, J., Ramiro, S., Winthrop, K., de Wit, M., Aletaha, D., Betteridge, N., Bijlsma, J.W., Boers, M., Buttgereit, F., Combe, B., Cutolo, M., Damjanov, N., Hazes, J.M., Kouloumas, M., Kvien, T.K., Mariette, X., Pavelka, K., van Riel, P.L., Rubbert-Roth, A., Scholte-Voshaar, M., Scott, D.L., Sokka-Isler, T., Wong, J.B. and van der Heijde, D. (2014b) EULAR recommendations for the management of rheumatoid arthritis with synthetic and biological disease-modifying antirheumatic drugs: 2013 update. *Annals of the Rheumatic Diseases,* 73(3), 492-509.

Smolen, J.S., Landewe, R., Breedveld, F.C., Dougados, M., Emery, P., Gaujoux-Viala, C., Gorter, S., Knevel, R., Nam, J., Schoels, M., Aletaha, D., Buch, M., Gossec, L., Huizinga, T., Bijlsma, J.W., Burmester, G., Combe, B., Cutolo, M., Gabay, C., Gomez-Reino, J., Kouloumas, M., Kvien, T.K., Martin-Mola, E., McInnes, I., Pavelka, K., van Riel, P., Scholte, M., Scott, D.L., Sokka, T., Valesini, G., van Vollenhoven, R., Winthrop, K.L., Wong, J., Zink, A. and van der Heijde, D. (2010b) EULAR recommendations for the management of rheumatoid arthritis with synthetic and biological disease-modifying antirheumatic drugs. *Annals of the Rheumatic Diseases,* 69(6), 964-975.

Sokka, T. and Pincus, T. (2009) Erythrocyte sedimentation rate, C-reactive protein, or rheumatoid factor are normal at presentation in 35%-45% of patients with rheumatoid arthritis seen between 1980 and 2004: analyses from Finland and the United States. *The Journal of Rheumatology,* 36(7), 1387-1390.

Solomon, D.H., Kremer, J., Curtis, J.R., Hochberg, M.C., Reed, G., Tsao, P., Farkouh, M.E., Setoguchi, S. and Greenberg, J.D. (2010) Explaining the cardiovascular risk associated with rheumatoid arthritis: traditional risk factors versus markers of rheumatoid arthritis severity. *Annals of the Rheumatic Diseases,* 69(11), 1920-1925.

Sperling, A.I., Green, J.M., Mosley, R.L., Smith, P.L., DiPaolo, R.J., Klein, J.R., Bluestone, J.A. and Thompson, C.B. (1995) CD43 is a murine T cell costimulatory receptor that functions independently of CD28. *The Journal of Experimental Medicine,* 182(1), 139-146.

Stastny, P. (1976) Mixed lymphocyte cultures in rheumatoid arthritis. *The Journal of Clinical Investigation,* 57(5), 1148-1157.

Stastny, P. (1978) Association of the B-cell alloantigen DRw4 with rheumatoid arthritis. *The New England Journal of Medicine,* 298(16), 869-871.

Suzuki, A., Yamada, R., Chang, X., Tokuhiro, S., Sawada, T., Suzuki, M., Nagasaki, M., Nakayama-Hamada, M., Kawaida, R., Ono, M., Ohtsuki, M., Furukawa, H., Yoshino, S., Yukioka, M., Tohma, S., Matsubara, T., Wakitani, S., Teshima, R., Nishioka, Y., Sekine, A., Iida, A., Takahashi, A., Tsunoda, T., Nakamura, Y. and Yamamoto, K. (2003) Functional haplotypes of PADI4, encoding citrullinating enzyme peptidylarginine deiminase 4, are associated with rheumatoid arthritis. *Nature Genetics,* 34(4), 395-402.

Svensson, B., Boonen, A., Albertsson, K., van der Heijde, D., Keller, C. and Hafstrom, I. (2005) Low-dose prednisolone in addition to the initial disease-modifying antirheumatic drug in patients with early active rheumatoid arthritis reduces joint destruction and increases the remission rate: a two-year randomized trial. *Arthritis and Rheumatism,* 52(11), 3360-3370.

Szklarczyk, D., Morris, J.H., Cook, H., Kuhn, M., Wyder, S., Simonovic, M., Santos, A., Doncheva, N.T., Roth, A., Bork, P., Jensen, L.J. and von Mering, C. (2017) The STRING database in 2017: quality-controlled protein-protein association networks, made broadly accessible. *Nucleic Acids Research,* 45(D1), D362-D368.

Takemura, S., Klimiuk, P.A., Braun, A., Goronzy, J.J. and Weyand, C.M. (2001) T cell activation in rheumatoid synovium is B cell dependent. *Journal of Immunology (Baltimore, Md.: 1950),* 167(8), 4710-4718.

Takeuchi, T., Yamanaka, H., Ishiguro, N., Miyasaka, N., Mukai, M., Matsubara, T., Uchida, S., Akama, H., Kupper, H., Arora, V. and Tanaka, Y. (2014) Adalimumab, a human anti-TNF monoclonal antibody, outcome study for the prevention of joint damage in Japanese patients with early rheumatoid arthritis: the HOPEFUL 1 study. *Annals of the Rheumatic Diseases,* 73(3), 536-543.

Tamura, N., Kobayashi, S., Kato, K., Bando, H., Haruta, K., Oyanagi, M., Kuriyama, M., Kipps, T.J. and Hashimoto, H. (2001) Soluble CD154 in rheumatoid arthritis: elevated plasma levels in cases with vasculitis. *The Journal of Rheumatology,* 28(12), 2583-2590.

Tchetina, E.V., Demidova, N.V., Markova, G.A., Taskina, E.A., Glukhova, S.I. and Karateev, D.E. (2017) Increased baseline RUNX2, caspase 3 and p21 gene expressions in the peripheral blood of disease-modifying anti-rheumatic drug-naive rheumatoid arthritis patients are associated with improved clinical response to methotrexate therapy. *International Journal of Rheumatic Diseases,* 20(10), 1468-1480.

ter Kuile, F., White, N.J., Holloway, P., Pasvol, G. and Krishna, S. (1993) Plasmodium falciparum: in vitro studies of the pharmacodynamic properties of drugs used for the treatment of severe malaria. *Exp Parasitol,* 76(1), 85.

The Arthritis Foundation. (2015) *Rheumatoid Arthritis.* Available at: http://www.arthritis.org/arthritis-facts/disease-center/rheumatoid-arthritis.php

Tian, H. and Cronstein, B.N. (2007) Understanding the mechanisms of action of methotrexate: implications for the treatment of rheumatoid arthritis. *Bulletin of the NYU Hospital for Joint Diseases,* 65(3), 168-173.

Tilleman, K., Van Beneden, K., Dhondt, A., Hoffman, I., De Keyser, F., Veys, E., Elewaut, D. and Deforce, D. (2005) Chronically inflamed synovium from spondyloarthropathy and rheumatoid arthritis investigated by protein expression profiling followed by tandem mass spectrometry. *Proteomics,* 5(8), 2247-2257.

Toscano, M.A., Bianco, G.A., Ilarregui, J.M., Croci, D.O., Correale, J., Hernandez, J.D., Zwirner, N.W., Poirier, F., Riley, E.M., Baum, L.G. and Rabinovich, G.A. (2007) Differential glycosylation of TH1, TH2 and TH-17 effector cells selectively regulates susceptibility to cell death. *Nature Immunology,* 8(8), 825-834.

Troelsen, L.N., Jacobsen, S., Abrahams, J.L., Royle, L., Rudd, P.M., Narvestad, E., Heegaard, N.H. and Garred, P. (2012) IgG glycosylation changes and MBL2 polymorphisms: associations with markers of systemic inflammation and joint destruction in rheumatoid arthritis. *The Journal of Rheumatology,* 39(3), 463-469.

Tyanova, S., Temu, T., Sinitcyn, P., Carlson, A., Hein, M.Y., Geiger, T., Mann, M. and Cox, J. (2016) The Perseus computational platform for comprehensive analysis of (prote)omics data. *Nature Methods,* 13(9), 731-740.

Ulmanen, I., Halonen, M., Ilmarinen, T. and Peltonen, L. (2005) Monogenic autoimmune diseases - lessons of self-tolerance. *Current Opinion in Immunology,* 17(6), 609-615.

Vaahtovuo, J., Munukka, E., Korkeamaki, M., Luukkainen, R. and Toivanen, P. (2008) Fecal microbiota in early rheumatoid arthritis. *The Journal of Rheumatology,* 35(8), 1500-1505.

van Amelsfort, J.M., Jacobs, K.M., Bijlsma, J.W., Lafeber, F.P. and Taams, L.S. (2004) CD4(+)CD25(+) regulatory T cells in rheumatoid arthritis: differences in the presence, phenotype, and function between peripheral blood and synovial fluid. *Arthritis and Rheumatism,* 50(9), 2775-2785.

van Amelsfort, J.M., van Roon, J.A., Noordegraaf, M., Jacobs, K.M., Bijlsma, J.W., Lafeber, F.P. and Taams, L.S. (2007) Proinflammatory mediator-induced reversal of CD4+,CD25+ regulatory T cell-mediated suppression in rheumatoid arthritis. *Arthritis and Rheumatism,* 56(3), 732-742.

Van Beneden, K., Coppieters, K., Laroy, W., De Keyser, F., Hoffman, I.E., Van den Bosch, F., Vander Cruyssen, B., Drennan, M., Jacques, P., Rottiers, P., Verbruggen, G., Contreras, R., Callewaert, N. and Elewaut, D. (2009) Reversible changes in serum immunoglobulin galactosylation during the immune response and treatment of

inflammatory autoimmune arthritis. *Annals of the Rheumatic Diseases,* 68(8), 1360-1365.

van den Berg, T.K., Nath, D., Ziltener, H.J., Vestweber, D., Fukuda, M., van Die, I. and Crocker, P.R. (2001) Cutting edge: CD43 functions as a T cell counterreceptor for the macrophage adhesion receptor sialoadhesin (Siglec-1). *Journal of Immunology (Baltimore, Md.: 1950),* 166(6), 3637-3640.

van den Berg, W.B. and Miossec, P. (2009) IL-17 as a future therapeutic target for rheumatoid arthritis. *Nature Reviews.Rheumatology,* 5(10), 549-553.

van Miert, A.S. (1995) Pro-inflammatory cytokines in a ruminant model: pathophysiological, pharmacological, and therapeutic aspects. *The Veterinary Quarterly,* 17(2), 41-50.

Vane, J.R. (1971) Inhibition of prostaglandin synthesis as a mechanism of action for aspirin-like drugs. *Nature: New Biology,* 231(25), 232-235.

Varki, A. and Angata, T. (2006) Siglecs--the major subfamily of I-type lectins. *Glycobiology,* 16(1), 1R-27R.

Venken, K., Hellings, N., Broekmans, T., Hensen, K., Rummens, J.L. and Stinissen, P. (2008) Natural naive CD4+CD25+CD127low regulatory T cell (Treg) development and function are disturbed in multiple sclerosis patients: recovery of memory Treg homeostasis during disease progression. *Journal of Immunology (Baltimore, Md.: 1950),* 180(9), 6411-6420.

Viatte, S., Plant, D. and Raychaudhuri, S. (2013) Genetics and epigenetics of rheumatoid arthritis. *Nature Reviews.Rheumatology,* 9(3), 141-153.

Volin, M.V., Szekanecz, Z., Halloran, M.M., Woods, J.M., Magua, J., Damergis, J.A.,Jr, Haines, K.G.,3rd, Crocker, P.R. and Koch, A.E. (1999) PECAM-1 and leukosialin (CD43) expression correlate with heightened inflammation in rat adjuvant-induced arthritis. *Experimental and Molecular Pathology,* 66(3), 211-219.

Walter, G.J., Evans, H.G., Menon, B., Gullick, N.J., Kirkham, B.W., Cope, A.P., Geissmann, F. and Taams, L.S. (2013) Interaction with activated monocytes enhances cytokine expression and suppressive activity of human CD4+CD45RO+CD25+CD127low regulatory T cells. *Arthritis and Rheumatism,* 65(3), 627-638.

Walter, G.J., Fleskens, V., Frederiksen, K.S., Rajasekhar, M., Menon, B., Gerwien, J.G., Evans, H.G. and Taams, L.S. (2016) Phenotypic, Functional, and Gene Expression Profiling of Peripheral CD45RA+ and CD45RO+ CD4+CD25+CD127(low) Treg Cells in Patients With Chronic Rheumatoid Arthritis. *Arthritis & Rheumatology (Hoboken, N.J.),* 68(1), 103-116.

Wang, C.R. and Liu, M.F. (2003) Regulation of CCR5 expression and MIP-1alpha production in CD4+ T cells from patients with rheumatoid arthritis. *Clinical and Experimental Immunology,* 132(2), 371-378.

Wang, H., Daniel, V., Sadeghi, M. and Opelz, G. (2013) Differences in the induction of induced human CD4(+) CD25(+) FoxP3(+) T-regulatory cells and CD3(+) CD8(+) CD28(-) T-suppressor cells subset phenotypes in vitro: comparison of phorbol 12-myristate 13-acetate/ionomycin and phytohemagglutinin stimulation. *Transplantation Proceedings,* 45(5), 1822-1831.

Wang, H., Li, L., Zhang, Y., Pan, S.C., Chen, A.Q. and Qian, W.D. (2015) Expression and significance of CD4(+)CD25(+)CD127(-) regulatory T cells in peripheral blood of patients with different phenotypes of Guillain-Barre syndrome. *International Journal of Clinical and Experimental Medicine,* 8(10), 19126-19131.

Ward, M.M. (2004) Relative sensitivity to change of the erythrocyte sedimentation rate and serum C-reactive protein concentration in rheumatoid arthritis. *The Journal of Rheumatology,* 31(5), 884-895.

Wehrens, E.J., Prakken, B.J. and van Wijk, F. (2013) T cells out of control--impaired immune regulation in the inflamed joint. *Nature Reviews.Rheumatology,* 9(1), 34-42.

Wells, G., Becker, J.C., Teng, J., Dougados, M., Schiff, M., Smolen, J., Aletaha, D. and van Riel, P.L. (2009) Validation of the 28-joint Disease Activity Score (DAS28) and European League Against Rheumatism response criteria based on C-reactive protein against disease progression in patients with rheumatoid arthritis, and comparison with the DAS28 based on erythrocyte sedimentation rate. *Annals of the Rheumatic Diseases,* 68(6), 954-960.

Wendler, J., Burmester, G.R., Sorensen, H., Krause, A., Richter, C., Tony, H.P., Rubbert-Roth, A., Bartz-Bazzanella, P., Wassenberg, S., Haug-Rost, I. and Dorner, T. (2014) Rituximab in patients with rheumatoid arthritis in routine practice (GERINIS): six-year results from a prospective, multicentre, non-interventional study in 2,484 patients. *Arthritis Research & Therapy,* 16(2), R80.

Westlake, S.L., Colebatch, A.N., Baird, J., Kiely, P., Quinn, M., Choy, E., Ostor, A.J. and Edwards, C.J. (2010) The effect of methotrexate on cardiovascular disease in patients with rheumatoid arthritis: a systematic literature review. *Rheumatology (Oxford, England),* 49(2), 295-307.

White, J.C. and Goldman, I.D. (1976) Mechanism of action of methotrexate. IV. Free intracellular methotrexate required to suppress dihydrofolate reduction to tetrahydrofolate by Ehrlich ascites tumor cells in vitro. *Mol Pharmacol,* 12(5), 711.

Wiacek, R., Kolossa, K., Jankowski, T., Jeka, S., Karmowski, A., Karmowski, M. and Gworys, B. (2012) The efficacy and safety of leflunomide in patients with active rheumatoid arthritis. *Advances in Clinical and Experimental Medicine : Official Organ Wroclaw Medical University,* 21(3), 337-342.

Wilkins, M.R., Pasquali, C., Appel, R.D., Ou, K., Golaz, O., Sanchez, J.C., Yan, J.X., Gooley, A.A., Hughes, G., Humphery-Smith, I., Williams, K.L. and Hochstrasser, D.F. (1996) From proteins to proteomes: large scale protein identification by two-dimensional electrophoresis and amino acid analysis. *Bio/Technology (Nature Publishing Company),* 14(1), 61-65.

Willkens, R.F. and Watson, M.,A. (1982) Methotrexate: a perspective of its use in the treatment of rheumatic diseases. *J Lab Clin Med,* 100(3), 314.

Willkens, R.F., Watson, M.A. and Paxson, C.S. (1980) Low dose pulse methotrexate therapy in rheumatoid arthritis. *J.Rheumatol.,* 7(4), 501.

Wolfe, F., Mitchell, D.M., Sibley, J.T., Fries, J.F., Bloch, D.A., Williams, C.A., Spitz, P.W., Haga, M., Kleinheksel, S.M. and Cathey, M.A. (1994) The mortality of rheumatoid arthritis. *Arthritis and Rheumatism,* 37(4), 481-494.

Wong, P.K., Quinn, J.M., Sims, N.A., van Nieuwenhuijze, A., Campbell, I.K. and Wicks, I.P. (2006) Interleukin-6 modulates production of T lymphocyte-derived cytokines in antigen-induced arthritis and drives inflammation-induced osteoclastogenesis. *Arthritis and Rheumatism,* 54(1), 158-168.

Wozniacka, A., Lesiak, A., Boncela, J., Smolarczyk, K., McCauliffe, D.P. and Sysa-Jedrzejowska, A. (2008) The influence of antimalarial treatment on IL-1beta, IL-6 and TNF-alpha mRNA expression on UVB-irradiated skin in systemic lupus erythematosus. 159(5), 1124.

Wright, H.L., Moots, R.J. and Edwards, S.W. (2014) The multifactorial role of neutrophils in rheumatoid arthritis. *Nature Reviews.Rheumatology,* 10(10), 593-601.

Wright, H.L., Thomas, H.B., Moots, R.J. and Edwards, S.W. (2013) RNA-seq reveals activation of both common and cytokine-specific pathways following neutrophil priming. *PloS One,* 8(3), e58598.

Wu, C., Rauch, U., Korpos, E., Song, J., Loser, K., Crocker, P.R. and Sorokin, L.M. (2009) Sialoadhesin-positive macrophages bind regulatory T cells, negatively controlling their expansion and autoimmune disease progression. *Journal of Immunology (Baltimore, Md.: 1950),* 182(10), 6508-6516.

Xiong, Y.S., Cheng, Y., Lin, Q.S., Wu, A.L., Yu, J., Li, C., Sun, Y., Zhong, R.Q. and Wu, L.J. (2014) Increased expression of Siglec-1 on peripheral blood monocytes and its role in mononuclear cell reactivity to autoantigen in rheumatoid arthritis. *Rheumatology (Oxford, England),* 53(2), 250-259.

Yamaji, T., Teranishi, T., Alphey, M.S., Crocker, P.R. and Hashimoto, Y. (2002) A small region of the natural killer cell receptor, Siglec-7, is responsible for its preferred binding to alpha 2,8-disialyl and branched alpha 2,6-sialyl residues. A comparison with Siglec-9. *The Journal of Biological Chemistry,* 277(8), 6324-6332.

Yang, L., Froio, R.M., Sciuto, T.E., Dvorak, A.M., Alon, R. and Luscinskas, F.W. (2005) ICAM-1 regulates neutrophil adhesion and transcellular migration of TNF-alpha-activated vascular endothelium under flow. *Blood,* 106(2), 584-592.

Yoon, B.R., Yoo, S.J., Choi, Y., Chung, Y.H., Kim, J., Yoo, I.S., Kang, S.W. and Lee, W.W. (2014) Functional phenotype of synovial monocytes modulating inflammatory T-cell responses in rheumatoid arthritis (RA). *PloS One,* 9(10), e109775.

York, M.R., Nagai, T., Mangini, A.J., Lemaire, R., van Seventer, J.M. and Lafyatis, R. (2007) A macrophage marker, Siglec-1, is increased on circulating monocytes in patients with systemic sclerosis and induced by type I interferons and toll-like receptor agonists. *Arthritis and Rheumatism,* 56(3), 1010-1020.

Yu, N., Li, X., Song, W., Li, D., Yu, D., Zeng, X., Li, M., Leng, X. and Li, X. (2012) CD4(+)CD25 (+)CD127 (low/-) T cells: a more specific Treg population in human peripheral blood. *Inflammation,* 35(6), 1773-1780.

Yun, H., Xie, F., Delzell, E., Chen, L., Levitan, E.B., Lewis, J.D., Saag, K.G., Beukelman, T., Winthrop, K., Baddley, J.W. and Curtis, J.R. (2015) Risk of hospitalised infection in rheumatoid arthritis patients receiving biologics following a previous infection while on treatment with anti-TNF therapy. *Annals of the Rheumatic Diseases,* 74(6), 1065-1071.

Zhang, Y., Center, D.M., Wu, D.M., Cruikshank, W.W., Yuan, J., Andrews, D.W. and Kornfeld, H. (1998) Processing and activation of pro-interleukin-16 by caspase-3. *The Journal of Biological Chemistry,* 273(2), 1144-1149.

Ziegler, H.K. and Unanue, E.R. (1982) Decrease in macrophage antigen catabolism caused by ammonia and chloroquine is associated with inhibition of antigen presentation to T cells. *Proceedings of the National Academy of Sciences of the United States of America,* 79(1), 175-178.

Ziegler-Heitbrock, H.W. (2000) Definition of human blood monocytes. *Journal of Leukocyte Biology,* 67(5), 603-606.